THE UNIVERSITY
of EDINBURGH

In Situ Diazomethane Generation and the Palladium-Catalysed Cyclopropanation of Alkenes

THE UNIVERSITY *of* EDINBURGH

Carl Poree

Doctor of Philosophy

University of Edinburgh

2015

Declaration

I declare that the work in this thesis was carried out by me between October 2010 and April 2015 under the supervision of Professor Guy C. Lloyd-Jones FRS in the School of Chemistry, University of Bristol, and the School of Chemistry, University of Edinburgh, and has not been submitted for any other degree or professional qualification.

Carl Poree 22nd May 2015

Abstract

Since the discovery that diazomethane, CH_2N_2, can effect the cyclopropanation of alkenes under palladium catalysis in the 1960s, this reaction has been used to great effect in synthesis. However, the necessity of preparing and handling diazomethane, a toxic and explosive reagent, is unappealing. The substitution of diazomethane for a commercially-available and thermally-stable silylated congener, namely trimethylsilyldiazomethane (TMSDAM), has been investigated. Under optimised conditions, designed to promote protodesilylation, use of this reagent affords the same products as would be obtained with the more hazardous diazomethane, with no trace of the corresponding silylated cyclopropanes.

NMR spectroscopy has revealed that the protodesilylating agent employed in the reaction, tetrabutylammonium bifluoride (n-Bu_4N^+ HF_2^-, TBABF), reacts cleanly with TMSDAM to generate diazomethane. Under catalytic conditions, the consumption of the desilylated diazo reagent by palladium is sufficiently rapid to prevent the accumulation of this hazardous reagent in solution. Spectroscopic titration studies also revealed a "hidden" mode of TBABF catalysis, whereby adventitious water drives the regeneration of the bifluoride salt. This observation was exploited by the development of an EtOH-driven reaction variant in which catalytic amounts (20 mol%) of TBABF could be employed.

The ability to effect the *in situ* generation of diazomethane has allowed for mechanistic studies into the course of the cyclopropanation reaction to be undertaken. These reveal a partitioning in the consumption of nascent diazomethane between the desired cyclopropanation reaction and a side reaction. The product of the side reaction was identified as cyclopropane (C_3H_6), the product of formal methylene cyclotrimerisation, by employing EtOD in TBABF-catalysed deuterodesilylative cyclopropanation. The partitioning between the two pathways is dependent on the nature of the substrate, with efficient cyclopropanation dominating with electron-deficient alkenes. For an electronically-varied range of styrenes, the relative rate of productive diazomethane consumption correlates well with the energy of the frontier molecular orbitals (as determined by DFT calculations). These results are consistent with an initial, substrate-dependent partitioning of the palladium pre-catalyst between species able to effect alkene cyclopropanation, and those (likely higher-order) species which promote only the cyclotrimerisation of diazomethane.

Lay Summary

Cyclopropanes are rings containing three carbon atoms, and can be found in a number of chemical compounds important to society. Examples include Efavirenz, developed by Merck and used in the treatment of HIV, the pyrethins, which are used in herbicides, and 1-aminocyclopropanecarboxylic acid, which is found in green plants and is responsible for the generation of the gaseous plant hormone ethylene, which controls the ripening of fruit.

One method for the preparation of cyclopropanes which is used in the laboratory and in large-scale chemical manufacturing uses catalysts based on the metal palladium to promote the reaction between alkenes (which contain carbon atoms joined to each other by two bonds) and diazomethane. Although this reaction works well, diazomethane is explosive and highly toxic.

In this thesis is described a process by which the same products can be obtained without the need to make diazomethane. A non-explosive compound which is related to diazomethane, but which bears a group containing silicon, can be used in its place. By using a source of fluoride, which has a very strong affinity for silicon, diazomethane can be generated in a controlled manner in the reaction mixture. The palladium catalyst reacts with this sufficiently quickly that the hazardous diazomethane does not accumulate.

This method for making diazomethane in the reaction mixture also allowed the mechanism of the reaction to be studied. Experiments revealed that not all of the diazomethane reacted in the manner expected – with the alkene – but rather that some of it reacted with itself. This was determined using a heavier type of hydrogen atom called deuterium. This behaves differently to the more familiar, lighter hydrogen in a number of ways. By exploiting the different behaviour of its nucleus in a strong magnetic field, compounds which had been "labelled" with this heavier atom could be distinguished from all other components in the reaction mixture, allowing the previously elusive side product to be found.

The extent to which the unexpected reaction occurred is dependent upon the nature of the alkene. The relative proportions of expected and unexpected products was found to depend on the spatial distribution and energy of the electrons – determined by quantum mechanical calculations – which bind the atoms of the alkene together.

Acknowledgments

Firstly, I would like to thank my supervisor, Professor Guy Lloyd-Jones FRS. His unremitting encouragement and enthusiasm have been inspiring. Under his guidance, this project has gone in directions that I would not originally have envisaged; this is in part due to his thoughtful suggestions, as well as the freedom he gives members of the group to go about their studies in their own way. I am incredibly grateful for having had the opportunity to work in this group.

I've had the privilege of working with some fantastic people during the last few years in the Lloyd-Jones group. Between them, they've provided valuable intellectual support and much-needed comic relief. In vaguely chronological order, I'd like to thank Dr Gareth Owen-Smith, Dr Louise Evans, Dr Sophie Purser, Dr Waldemar Czaplik, Dr Alvaro Gordillo, Dr Vincent Brunet, Dr Alastair Lennox, Dr Bertram Ong, Dr Liam Ball, Dr Tomas Racys, Joe Tate, Ruth Dooley, Rob Cox, Paul Cox, Nick Taylor, Jorge Gonzalez, Chris Newcombe, Tom Corrie, Dr Alex Cresswell, Katherine Geogheghan, Matt Robinson and Marc Reid.

My thanks also go to Dr Craig Butts (School of Chemistry, University of Bristol) for answering my occasionally ridiculous questions about NMR spectroscopy, and, with the capable assistance of Paul Lawrence and Rose Silvester, for keeping the Bristol NMR lab running smoothly. At Edinburgh, I must thank Juraj Bella and Dr Lorna Murray for their assistance with NMR.

I would also like to thank Dr Jules Camp (formerly of the Department of Chemical Engineering, University of Cambridge), erstwhile tutorial partner, and more recently my principal dealer in otherwise inaccessible journal articles. I must also thank Tom Williams for many excellent pints and enjoyable concerts during the Bristol years.

Finally, I must thank my family – particularly my mother and my grandparents. I can't express in words just how grateful I am for all that they've done for me, but I think they know that already.

Abbreviations

acac	acetylacetonate
B3LYP	Becke 3 parameter Lee-Yang-Parr functional
BP86	Becke-Perdew functional
Boc	*tert*-butyloxycarbonyl
cod	1,5-cyclooctadiene
DCM	dichloromethane
DFT	density functional theory
DIAD	di-*iso*-propyl azodicarboxylate
DME	dimethoxyethane
DMSO	dimethylsulphoxide
DVTMS	divinyltetramethyldisiloxane
EI	electron impact
ESI	electrospray ionisation
EWG	electron-withdrawing group
FMO	frontier molecular orbital
FT-IR	Fourier-transform infrared spectroscopy
HMBC	heteronuclear multiple-bond correlation
HMDS	hexamethyldisilazide, $(Me_3Si)_2N^-$
HOMO	highest occupied molecular orbital
HSQC	heteronuclear single quantum coherence
LA	Lewis acid

LUMO	lowest unoccupied molecular orbital
MS	mass spectrometry
NHC	*N*-heterocyclic carbene
NMR	nuclear magnetic resonance
NMU	*N*-methyl-*N*-nitrosourea
R_f	retention factor
TBABF	tetra-*n*-butylammonium bifluoride
TBAF	tetra-*n*-butylammonium fluoride
TBDMS	*tert*-butyldimethylsilyl
THF	tetrahydrofuran
TMEDA	*N,N,N',N'*-tetramethylethylenediamine
TMS	trimethylsilyl
TMSDAM	trimethylsilyldiazomethane
TPP	5,10,15,20-tetraphenylporphyrinato

Contents

1 Introduction

1.1 Diazomethane

1.1.1 Discovery and Applications

Diazomethane (CH_2N_2, **1**), first prepared by von Pechmann in the late 1890s by the action of alkalis on various nitroso derivatives of methylamine,[1,2] is undoubtedly a useful component of the synthetic chemist's toolbox. Four distinct reaction roles can be identified for diazomethane (Scheme 1.1)[3]

- CH_3^+ synthon (e.g. methyl esterification of carboxylic acids);
- $:CH_2$ synthon (e.g. cyclopropanation of alkenes);
- $[CHN_2]^-$ synthon (e.g. Arndt-Eistert homologation of carboxylic acids);
- 1,3-dipole in 1,3-dipolar cycloaddition reactions.

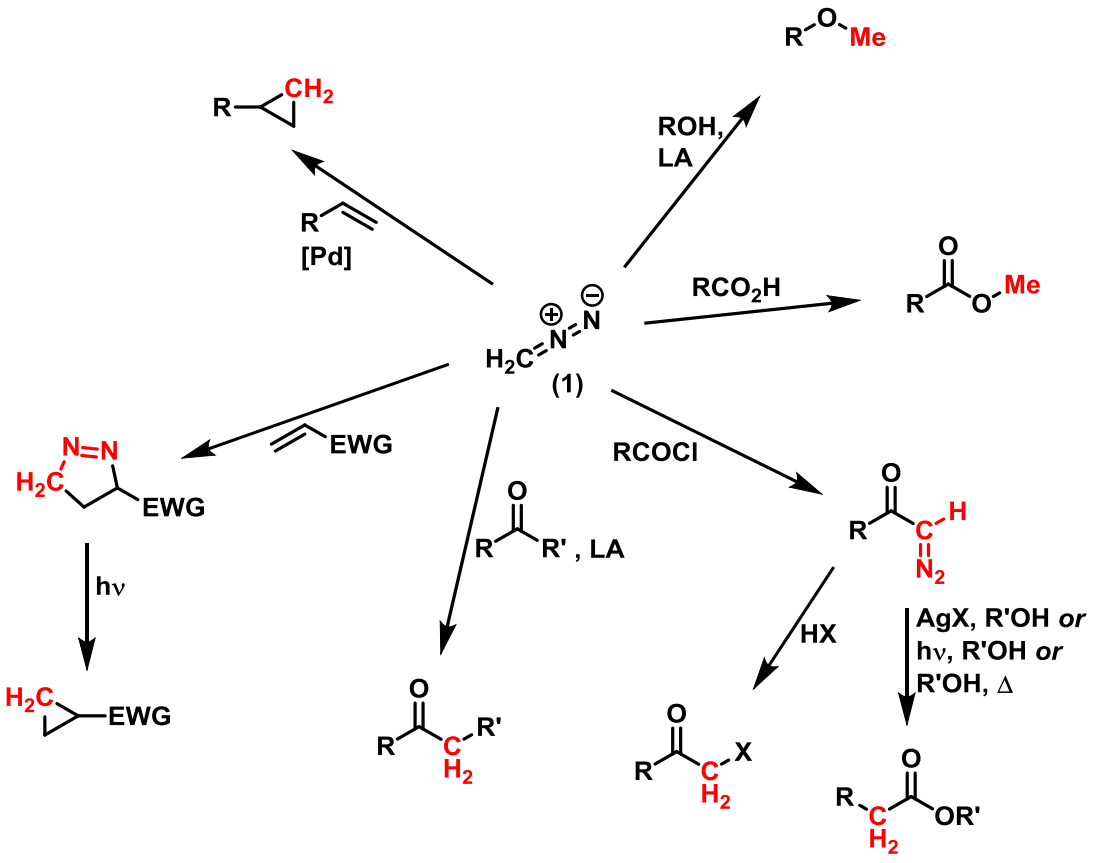

Scheme 1.1 Selected roles of diazomethane in organic synthesis.

1.1.2 Toxicity

The synthetic versatility of diazomethane is hampered by the considerable practical difficulties encountered in its preparation. The toxicity of the compound was noted first by von Pechmann, who found that inhalation of diazomethane fumes led to dyspnoea, chest pain and exhaustion. LeWinn reported a fatal case of diazomethane poisoning in the 1940s;[4] this followed a number of earlier reports from both chemists and physicians of ill effects encountered on working with the compound.

1.1.3 Diazomethane Preparation at Laboratory and Industrial Scales

Methods for the preparation of diazomethane on the laboratory scale are largely unchanged since the original reports by von Pechmann (*vide supra*).[1] The alkaline decomposition of *N*-methyl-*N*-nitroso compounds remains by far the most popular method (Scheme 1.2). Although a number of these precursors have been found to be explosive, acutely toxic and carcinogenic, *N*-methyl-*N*-nitroso-*p*-toluenesulphonamide (marketed by Sigma-Aldrich® as Diazald®, **2**) has been widely adopted as a convenient diazomethane precursor, despite its severe irritant properties and relatively limited shelf life.[5] Although this does represent a considerably safer precursor relative to those used before, both careful experimental technique and the use of specially-designed apparatus are advisable for diazomethane preparation regardless of precursor; the propensity of diazomethane to undergo violent decomposition in contact with rough surfaces necessitates the use of glassware devoid of surface imperfections (e.g. scratches) and ground glass joints. Sharp edges and exposure to bright light sources are also known to cause diazomethane to detonate. A range of specifically-designed kits for diazomethane preparation and purification on scales between *ca*. 1-300 mmol are commercially available.[6]

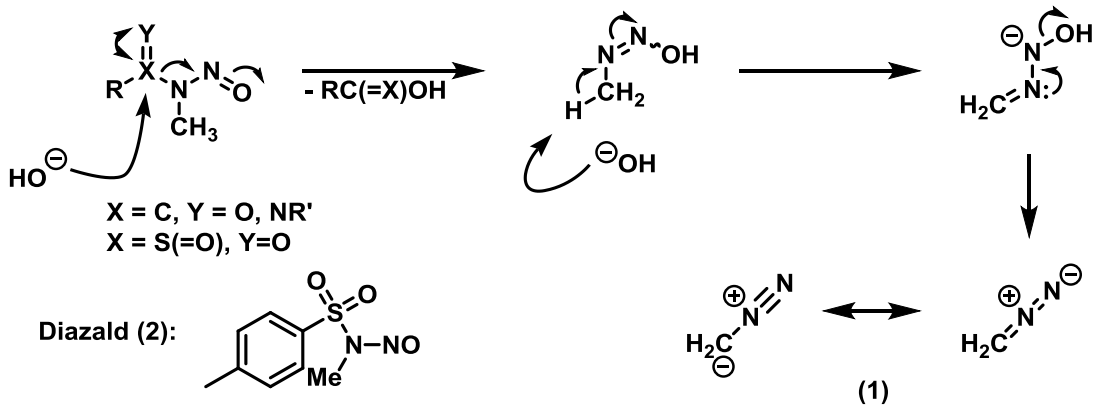

Scheme 1.2 Alkaline hydrolysis of *N*-methyl-*N*-nitroso compounds affords diazomethane (**1**).

A number of industrial groups have reported methods for continuous and batch diazomethane production on large scale. Aerojet-General Corporation reported a continuous process whereby *N*-methylurea is nitrosated with *in situ* generated nitrous acid (HNO_2) to generate *N*-methyl-*N*-nitrosourea. Subsequent treatment with aqueous KOH and phase separation affords diazomethane in a mixture of solvents, with a typical diazomethane output of 61.0 mol h^{-1} (Scheme 1.3).[7] Somewhat later, Phoenix Chemicals disclosed a process for the generation of diazomethane diluted in an inert gas.[8,9] The authors claim that use of inert gas increases the explosive limit of diazomethane to 14.7%, compared to 3.9% in air, and obviates the isolation of product in flammable and volatile organic solvents. The dilute gas stream is intended to be continuously fed into a reactor further downstream. Careful matching of the rate of diazomethane production and that of the downstream reaction allows for a minimal volume of diazomethane to be held within the system. The Phoenix process employs pre-formed Diazald, and claims an output rate of 90-93 g CH_2N_2 per hour (corresponding to a maximum of *ca.* 2.2 mol h^{-1}). While the output of this process is significantly less than that developed by Aerojet, and the starting materials more expensive, generation of diazomethane in an inert gas stream is arguably of greater utility, allowing for its use in aprotic reaction media.

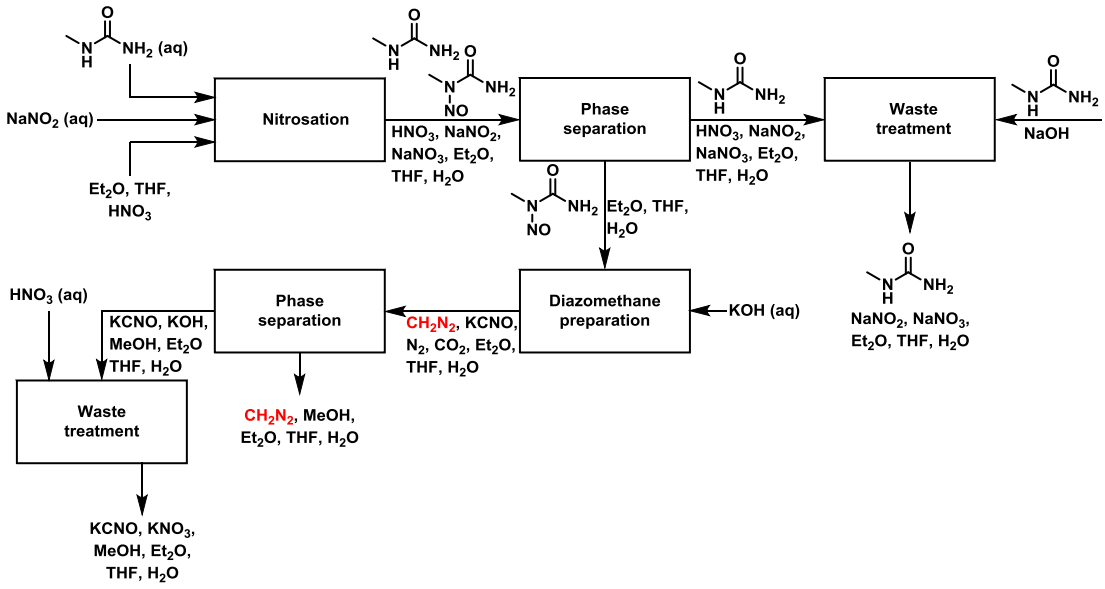

Scheme 1.3 Process flow diagram for continuous diazomethane production developed by Aerojet-General Corporation, adapted from (7).

1.2 Transition Metal-Catalysed Cyclopropanation with Diazomethane

The reactivity of diazomethane with a wide range of transition metals and their complexes has been reported in the literature.[10] However, only a select few are known to effect cyclopropanation in the presence of suitable substrates. Indeed, palladium is the only metal for which more than a handful of examples have been reported. In contrast, cyclopropanation reactions with electron-deficient diazo compounds such as ethyl diazoacetate, particularly under the influence of rhodium-based catalysts, have been the subject of intense investigations, particularly by the groups of Doyle and Davies.[11,12]

1.2.1 Discovery, Development and Applications

The first reported example of palladium-catalysed cyclopropanation with diazomethane was reported in the late 1960s by Kirmse and Kapps. Following the lead of Armstrong, who had employed allylpalladium chloride dimer in the decomposition of ethyl diazoacetate,[13] they discovered that the same complex was active in the cyclopropanation of diallyl ether, although the reaction was low-yielding. In contrast to many of the copper salts which were the main focus of the work, the palladium complex effected clean monocyclopropanation of the substrate. The copper(II) salts investigated were found to give competing homologation of an allyl group, affording allyl 3-butenyl ethers.[14] Later investigations into the cyclopropanation of vinyloxirane further demonstrated the effectiveness of this system, with cyclopropyloxirane the main product of the reaction.[15]

Three years later, Hubert and co-workers first demonstrated the ability of $Pd(OAc)_2$ to effect the cyclopropanation of styrene (**3a**) with both diazomethane (affording phenylcyclopropane, **4a**, Scheme 1.4) and ethyl diazoacetate.[16]

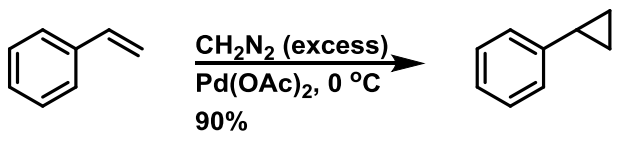

(3a) **(4a)**

Scheme 1.4 Cyclopropanation of styrene (Hubert and co-workers). Ratio of diazomethane to $Pd(OAc)_2$ reported as 250:1.

Vorbrüggen and co-workers further explored the reactivity of this catalytic system, discovering its efficacy in the cyclopropanation of strained alkenes,[17] and α,β-unsaturated carbonyl compounds (Scheme 1.5),[18] the latter having been discovered during the total synthesis of a prostaglandin analogue in which Corey-Chaykovsky and Simmons-Smith cyclopropanations had proven ineffective (**3d→4d-1,2**, Scheme 1.6).[19]

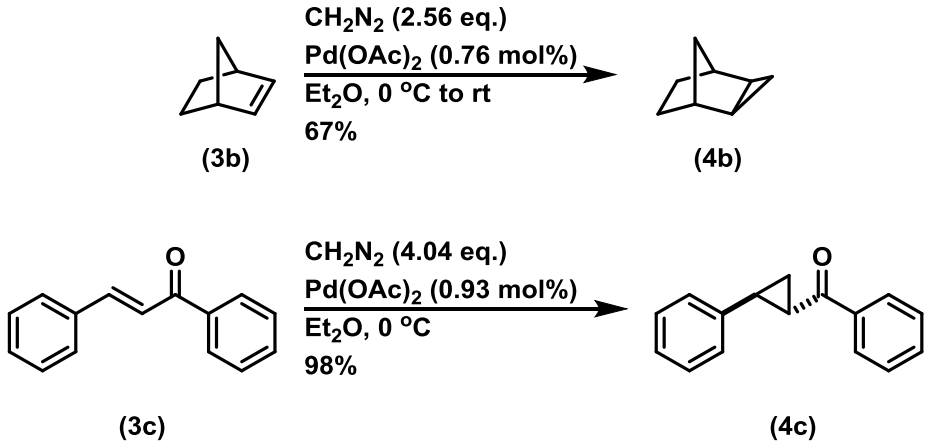

Scheme 1.5 Cyclopropanation of strained and electron-deficient alkenes (Vorbrüggen and co-workers).

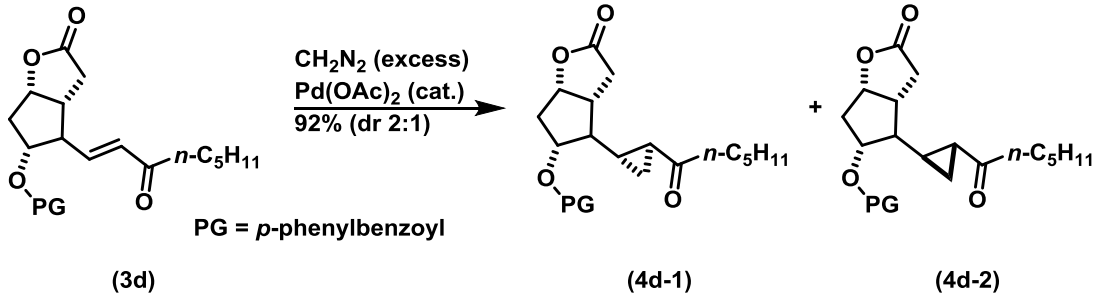

Scheme 1.6 Application of Hubert's conditions to the synthesis of the prostaglandin analogue 13,14-dihydro-13,14-methylene-PGF$_{2\alpha}$ (Vorbruggen and co-workers).

Vorbrüggen's group were also the first to note a number of the limitations of Hubert's system, finding that trisubstituted α,β-unsaturated carbonyls did not react, as well as noting the necessity of using large excesses of diazomethane to achieve satisfactory yields of cyclopropanes from some substrate classes (namely allylic alcohols). It is also noteworthy that particularly electron-deficient alkenes, such as dimethyl fumarate (**3e**), failed to give cyclopropanes, with this reaction affording the pyrazoline (**5e**) instead, the product of thermal [3+2] diazomethane cycloaddition (Scheme 1.7), as reported by von Pechmann.[1]

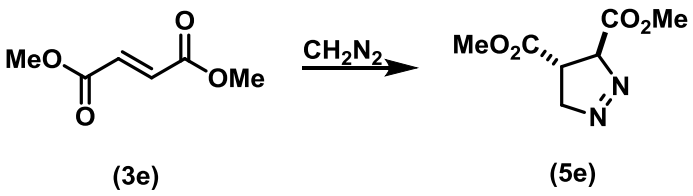

(3e) (5e)

Scheme 1.7 [3+2] dipolar cycloaddition of diazomethane to dimethyl fumarate (reported by von Pechmann) outcompetes the palladium-catalysed cyclopropanation (Vorbrüggen and co-workers).

Unactivated terminal alkenes were also shown to be good substrates for the palladium-catalysed reaction by Suda under identical conditions.[20] The clear preference of the palladium/diazomethane system for the terminal alkene in 4-vinylcyclohexene is in stark contrast to the relatively non-regioselective reactivity observed under Simmons-Smith conditions.

Regioselectivity was also observed by Markó and co-workers in the cyclopropanation of α,β,γ,δ-unsaturated carbonyl compounds, with varying levels of selectivity for the α,β-double bond (Scheme 1.8).[21]

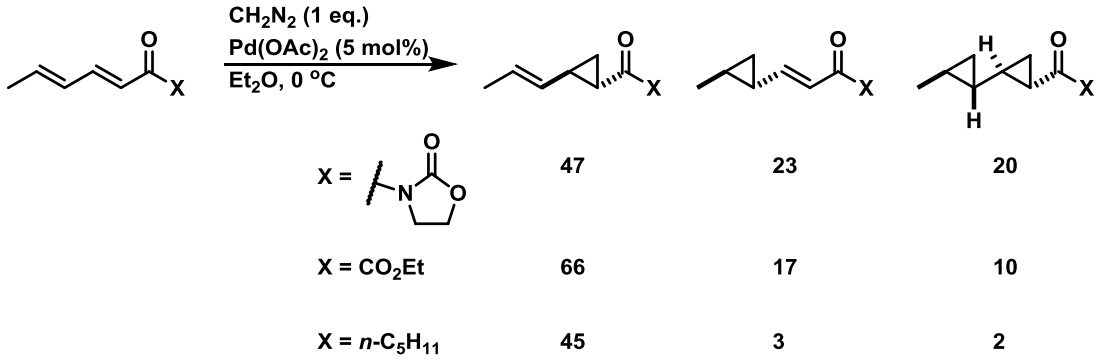

Scheme 1.8 Cyclopropanation of α,β,γ,δ-unsaturated dienes showing percentage conversions to α,β- and γ,δ-cyclopropanes, and α,β,γ,δ-bis(cyclopropanes) (Markó and co-workers).

The diazomethane/palladium system has also been employed in the synthesis of functionalised cyclopropane building blocks, such as cyclopropylstannanes, -silanes and -boronate esters, primed for use in transition-metal catalysed cross-couplings and other key C-C and C-X forming processes.

The synthesis of cyclopropylstannanes with diazomethane is largely unexplored, although a number of syntheses have been reported using the Simmons-Smith conditions for cyclopropanation. The relative lack of reports for this class of reaction is likely due in part to limited interest in the products; the resulting cyclopropylstannanes are relatively unreactive in

Stille cross-coupling.[22] However, the synthesis of doubly-stannylated cyclopropane (**4f**) and its reactivity has been explored by Markó and co-workers.[23] Given the considerable steric bulk of tributylstannyl groups, and the apparent sensitivity of the palladium-catalysed cyclopropanation to such (*vide supra*), the synthesis of *trans*-1,2-bis(tributylstannyl)cyclopropane proceeds in surprisingly good yield. Subsequent reactions allow for the synthesis of a diverse range of potentially useful cyclopropane-containing building blocks (Scheme 1.9).

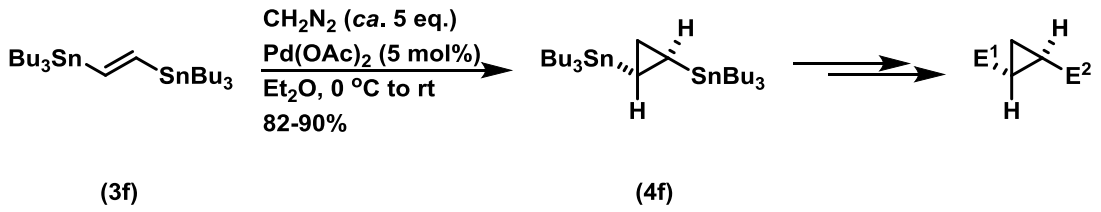

Scheme 1.9 Cyclopropanation of (*E*)-1,2-bis(tributylstannyl)ethylene, and subsequent stereoretentive elaboration *via* sequential Sn-Li exchange and trapping with electrophiles E^1, E^2 (Markó and co-workers).

Carboni and co-workers demonstrated that Hubert's conditions could be applied to the cyclopropanation of vinyl pinacolboronates (such as **3g**), with yields of up to 92% using 7 eq. CH_2N_2.[24] As was found previously by Vorbrüggen, trisubstituted alkenes are not good substrates for this reaction, with the formation of trace amounts of product, at best, being observed. Subsequent oxidation of a number of the cyclopropylboronic ester products (**4g**) to afford the corresponding cyclopropanols (**6g**) was effected with sodium perborate tetrahydrate ($NaBO_3 \cdot 4H_2O$) (Scheme 1.10).[25] Marsden and Hildebrand have shown that vinyl (1,3-propanediol)boronic esters are also good substrates for the cyclopropanation reaction, and that the products are effective substrates in Suzuki-Miyaura couplings.[26] Markó and co-workers have also demonstrated that the cyclopropanation of terminal dienylboronates proceeds with almost perfect selectivity for the double bond proximal to boron.[21]

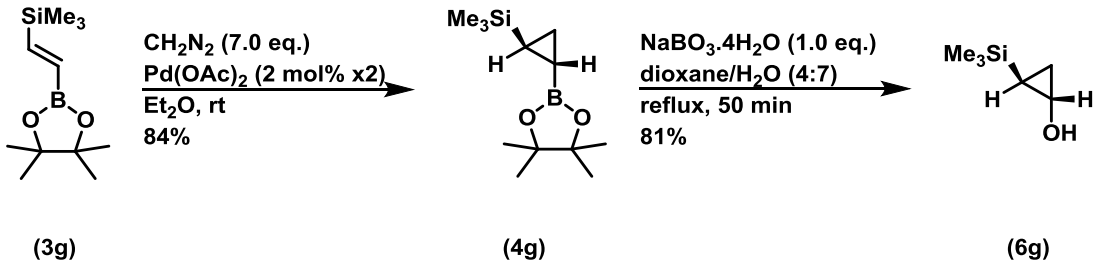

Scheme 1.10 Cyclopropanation-oxidation sequence to afford cyclopropanols (Carboni and co-workers).

The cyclopropanation of vinyl silanes has also been shown to be a synthetically useful process, with both vinyl silanes and *trans*-alkenyl silanes proving effective substrates for the palladium-catalysed reaction with diazoalkanes.[27]

As can be seen from the examples presented above, to date, the conditions generally employed for the palladium-catalysed cyclopropanation of alkenes with diazomethane are largely unchanged from those reported in 1972 by Hubert, with the exception of those methods that employ *in situ*-generated diazomethane (*vide infra*, Section 1.3). The nature of the palladium (pre)catalyst has been found to have little effect on the course of the reaction. Research by the group of Nefedov found that $PdCl_2$, $Pd(OAc)_2$, $[(\eta^3\text{-}C_3H_5)PdCl]_2$, and $(PhCN)_2PdCl_2$ gave rise to almost identical reaction outcomes in reactions with norbornene and norbornadiene.[28] A later report from the same group, however, advocated the use of palladium(II) acetylacetonate ($Pd(acac)_2$), having discovered that this complex, under directly comparable (but non-optimal) conditions, gave the highest conversion of norbornadiene to the corresponding cyclopropane(s), relative to a number of other palladium salts. Furthermore, the addition of a number of *N*-, *S*- and *P*-donor ligands were also found to lead to diminished yields of the cyclopropane products.[29] Consequently, the field has not seen benefit from the huge expansion in the number of available phosphine ligands, and their ability to tune reactivity at the metal centre, in the same way that cross-coupling chemistry under palladium catalysis has.

1.2.2 Stereoselectivity

Stereoselective Cyclopropanation under Substrate Control

A small number of reports have been published in which stereoselective cyclopropanation with diazomethane under palladium catalysis has been achieved by virtue of pre-existing substrate stereochemistry. Ohfune and co-workers demonstrated that useful levels of stereocontrol could be achieved in the cyclopropanation of an α,β-unsaturated-γ-lactam (**3h**) bearing a bulky pendant group; cyclopropanation occurred selectively on the opposite face (affording **4h**, Scheme 1.11).[30]

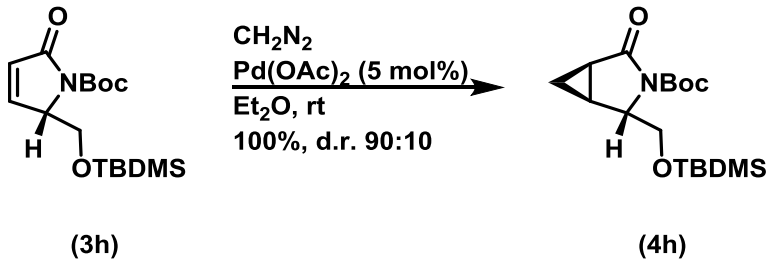

(3h) (4h)

Scheme 1.11 Cyclopropanation of an unsaturated lactam (Ohfune and co-workers).

Attempts to diastereoselectively cyclopropanate non-racemic, chiral, acyclic *N*-protected allyl amines met with less success, however.

More recently, Pietruszka and Witt have demonstrated modest levels of stereocontrol in the cyclopropanation of alkenylboronic esters bearing adjacent stereocenters (**3i**-**j**), with cyclopropanation occurring preferentially on the less hindered face of the alkene (Scheme 1.12).[31]

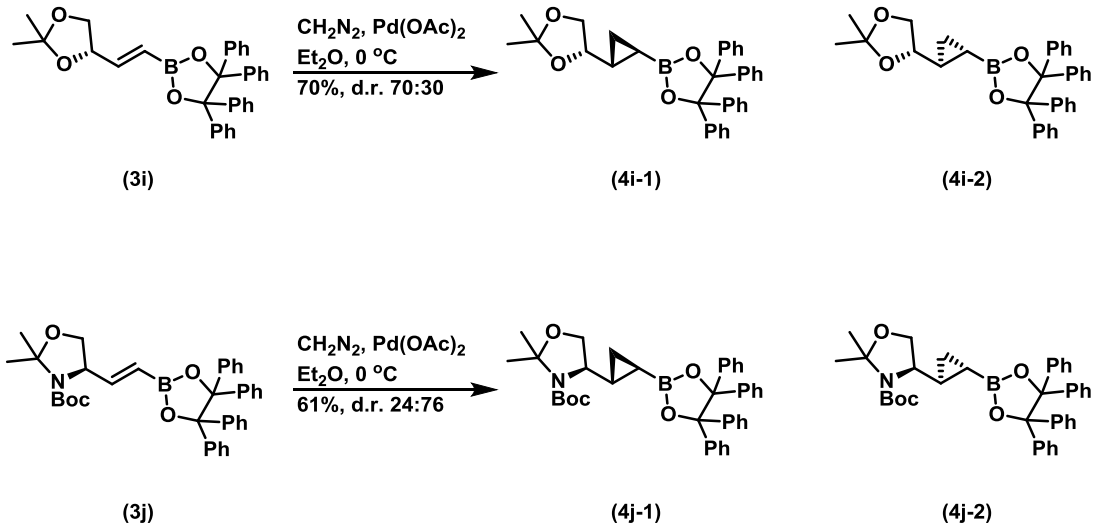

(3i) (4i-1) (4i-2)

(3j) (4j-1) (4j-2)

Scheme 1.12 Reaction of alkenylboronic acid benzpinacol esters with palladium/diazomethane (Pietruszka and Witt).

Stereoselective Cyclopropanation with Chiral Auxiliaries

In 1982, Carrié and co-workers demonstrated the use of ephedrine (**7**) as a chiral auxiliary for the asymmetric cyclopropanation of cinnamaldehyde (**3k**).[32] On the basis of NMR measurements, the enantiomeric excess was determined to be in excess of 90% (Scheme 1.13).

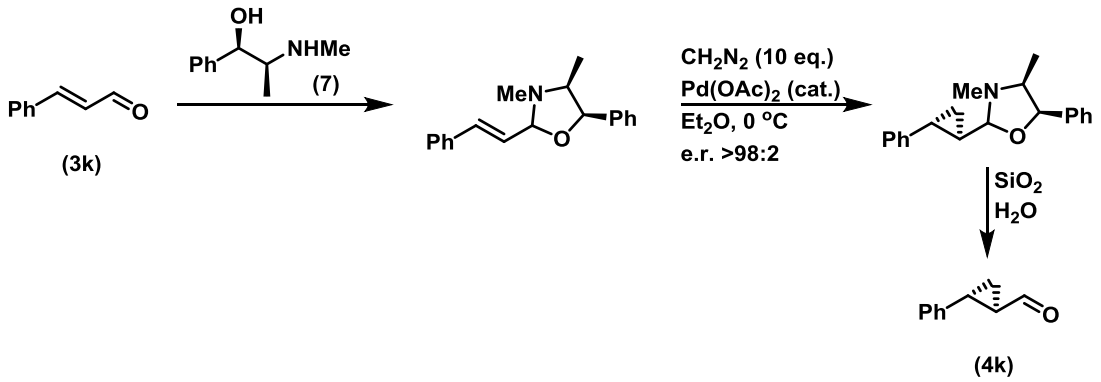

Scheme 1.13 Enantioselective cyclopropanation of cinnamaldehyde (**3k**) *via* (-)-ephedrine-derived aminal (Carrié and co-workers).

Despite this promising initial result, no demonstration of further substrate scope has been reported since. In contrast, the use of Oppolzer's sultam (**8**), pioneered by Hacksell (Scheme 1.14),[33,34] has proven moderately popular in the stereoselective cyclopropanation of α,β-unsaturated carbonyl derivatives (**3l**), finding application in the synthesis of melatoninergic agents, for example.[35]

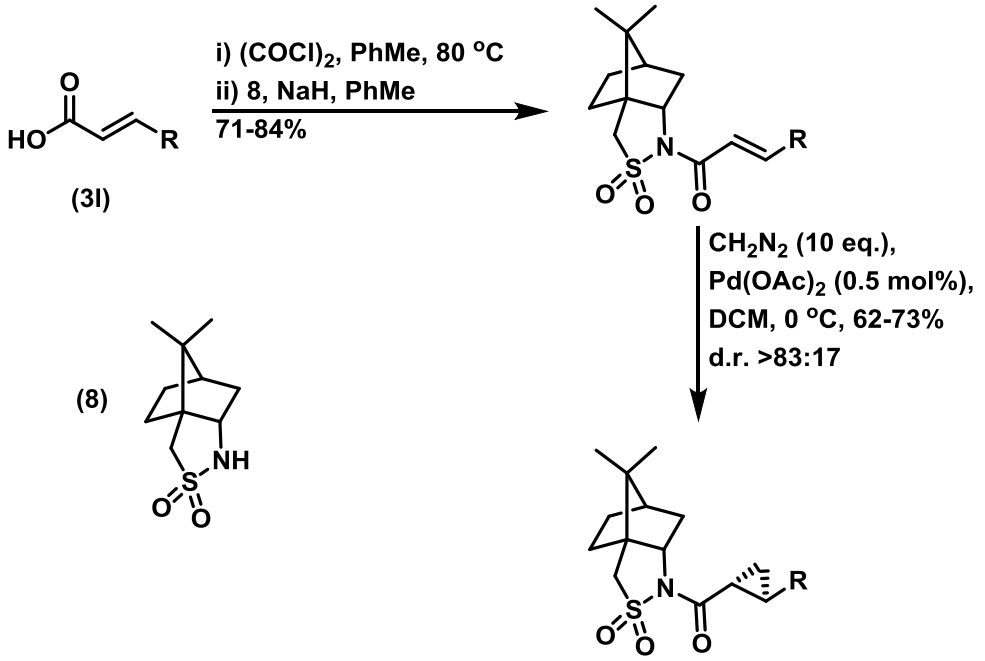

Scheme 1.14 Cyclopropanation reactions using Oppolzer's sultam (**8**) as a chiral auxiliary (Hacksell and co-workers).

Pietruszka and co-workers have extensively explored the cyclopropanation of alkenylboronic esters derived from enantiomerically pure chiral diols from the chiral pool (tartrate esters or derivatives thereof).[36,37] Careful optimisation of reaction conditions and boron ligand allowed

for diastereomeric ratios as high as 97:3.[38] The cyclopropylboronic ester products were subjected to oxidation (NaOH, H_2O_2) to afford cyclopropanols, as well as Suzuki-Miyaura cross-couplings with aryl bromides. This methodology has found use in the synthesis of cyclopropyl analogues of the vascular disrupting agent combretastatin A4.[39]

Asymmetric Catalysis in Cyclopropanation with Diazomethane

In spite of the long history of enantioselective cyclopropanation catalysis, the first example having been reported in the late 1960s,[40] the catalytic asymmetric cyclopropanation of achiral alkenes with diazomethane has not, to date, been realised. Denmark and co-workers reported their efforts to effect such a reaction with palladium bis(oxazoline) complexes in 1997.[41] Cyclopropanation of electron-deficient alkenes with a range of such catalysts gave essentially racemic products in all cases. Following extensive studies to determine the reason for the ineffectiveness of these complexes in catalysing cyclopropanation in an asymmetric sense, it was concluded that partial or complete dissociation of the ligands during catalysis was responsible for the lack of enantioinduction.

1.2.3 Mechanism

The underpinning details of the mechanism of the palladium-catalysed cyclopropanation of olefins with diazomethane remain, to date, unclear. Although a number of important insights can be gleaned from the synthetic studies reported in the literature (*vide supra*), the absence of well-established benchmark systems and genuinely comparable, quantitative data leaves many of these insights open to interpretation.

Oxidation States

First amongst the unaddressed problems with regard to the mechanism of this reaction is that of the oxidation states of catalytically-implicated species. Although the vast majority of these cyclopropanation reactions employ palladium(II) salts, most commonly palladium(II) acetate, the obvious question is whether these are themselves active in cyclopropanation, or if *in situ* reduction to Pd(0) is required for cyclopropanation to commence. Certainly, there are a great many reports of palladium black precipitation in reactions with diazomethane, but this alone does not constitute evidence for any particular oxidation state being responsible for catalysis. The efficacy of the zerovalent $Pd_2(dba)_3$ in cyclopropanation with diazomethane has been noted

by Charette.[11] However, this does not necessarily mean that Pd(0) is the sole catalytically-competent oxidation state.

Possibly the most convincing argument for implicating Pd(0) as the catalytically-active species is the substrate scope and regioselectivity discussed above. Although, as stated previously, quantitative data is scarce, the clear preference of the reaction system is for terminal, strained, and electron-deficient alkenes. Assuming a mechanism in which the alkene is bound to the palladium is operative, the preference for electron-deficient substrates is consistent with their relatively strong binding to zerovalent palladium due to the enhancement of π-backdonation from the electron-rich metal centre to the lowered LUMO of the organic fragment.[42]

Stoichiometric studies into the synthesis of (chloromethyl)palladium chloride complexes undertaken by McCrindle and co-workers have probed the reactivity of diazomethane with (cod)$PdCl_2$ (**9**).[43] The reaction was found to afford two identifiable organometallic products (Scheme 1.15), as well as metallic palladium. Although the chloromethyl complex **10** was found to be stable, the methyl complex **11** was observed to decompose, forming Pd(0). The deposition of palladium metal was found to be even more significant on the reaction of diazomethane with (hexa-1,5-diene)palladium(II) chloride.

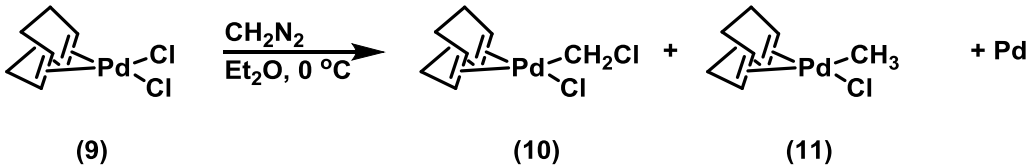

Scheme 1.15 Reaction of diazomethane with (cod)$PdCl_2$ (McCrindle and co-workers).

Subsequently, Illa *et al*. detected the formation of nanoparticulate palladium in the cyclopropanation reaction of cyclohexenone by means of transmission electron microscopy.[44] The formation of a number of organic side-products resulting from the reduction of $Pd(OAc)_2$ were observed by ESI-MS and ^{1}H NMR spectroscopy. Electrochemical studies of the reaction mixture following diazomethane consumption provided further evidence for the presence of Pd(0) in solution. However, no clear conclusions regarding the oxidation state of the active species can be drawn from this study.

The work from McCrindle's group clearly provides the required missing link between what could be considered Pd(II) precatalysts to potentially active Pd(0) species. However, the report from Illa *et al*. fails to present a convincing argument in favour of either oxidation state.

Intriguingly, Denmark and co-workers found that they were able to recover significant amounts of the (bis(oxazoline))palladium(II) chloride complex following cyclopropanation.[41] They also noted specifically that palladium black formation was not observed with the bis(oxazoline) complexes, in contrast to reactions carried out with $Pd(OAc)_2$ and $(PhCN)_2PdCl_2$ in the same study. While a different mode of reactivity with the bis(oxazoline) complexes cannot be ruled out, this does cast some doubt on the involvement of Pd(0) in cyclopropanation catalysis.

Computational Studies

The question of the course of the palladium-catalysed reaction has been addressed computationally by three groups. Bernardi, Bottoni and Miscione performed calculations in order to ascertain the likelihood that a carbenoid mechanism (with chloromethylpalladium(II) species similar to **10**, as reported by McCrindle), akin to the Simmons-Smith reaction, operates in the palladium/diazomethane system.[45] The pathway calculated (using $(H_3P)_2PdCl_2 + CH_2N_2 + CH_2CH_2$ as a model system) is prohibitively high in energy (activation energies greater than 28.4 kcal mol^{-1}, 118.8 kJ mol^{-1}). Furthermore, given the ineffectiveness of palladium phosphine complexes in the cyclopropanation reaction, their inclusion in the model system is puzzling.

In 2001, Branchadell and co-workers published a study relating to the reaction of diazomethane with palladium formate (**12**) and ethylene (**3m**) (as a model system for palladium acetate and more synthetically-relevant alkenes).[46] It was assumed that palladium(II) was the catalytically-competent species; the proposed mechanism (Scheme 1.16), based on DFT calculations, involves the sequential addition of methylene into one Pd-O bond of each carboxylate ligand. Attack of diazomethane and subsequent nitrogen extrusion forms palladium(II) methylidene **13**, which is then attacked by ethylene to form a loosely bound palladium(II)-cyclopropane adduct **14**. Intramolecular attack of the labile carbonyl oxygen drives the loss of cyclopropane and closes the catalytic cycle.

The calculated activation energies for the formation of the active catalyst (10.0 kcal mol^{-1}, 41.8 kJ mol^{-1}) and for the rate-determining on-cycle step (extrusion of nitrogen, 23.7 kcal mol^{-1}, 99.2 kJ mol^{-1}) are prohibitively high for this mechanism to be valid, on the basis of experimental temperatures and reaction times.

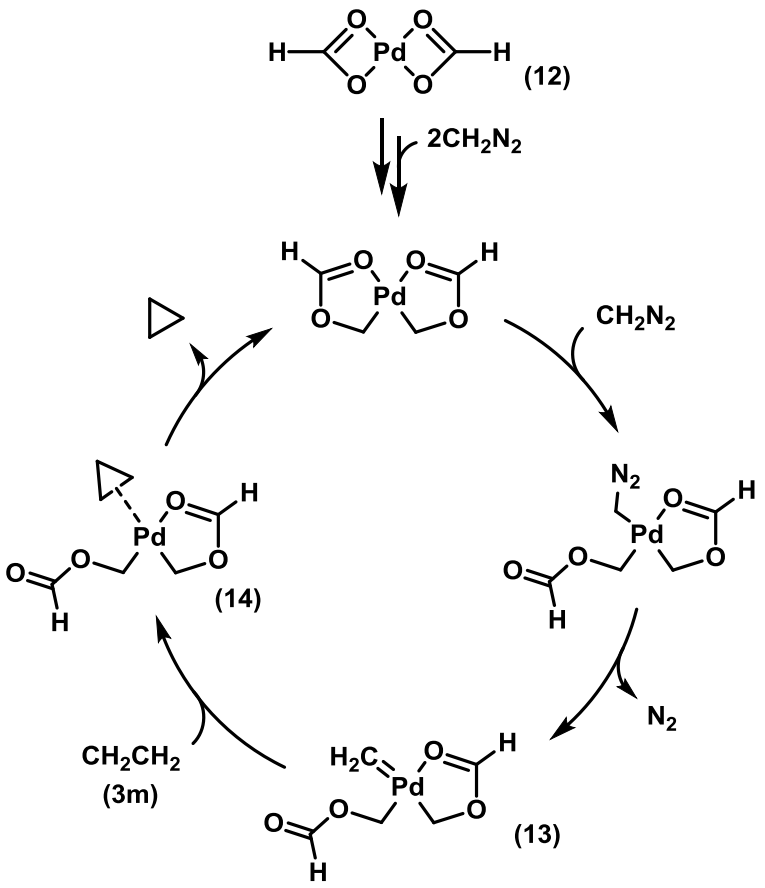

Scheme 1.16 Mechanism for Pd-catalysed cyclopropanation with palladium carboxylates proposed by Branchadell and co-workers.

The next year, Straub published an alternative computational mechanism.[47] Instead of assuming Pd(0) was not involved, however, this work was predicated on the reduction of Pd(II) precatalysts to a catalytically-active zerovalent state. The mechanism proposed involves the reaction of diazomethane with homoleptic palladium(ethylene) complexes **15**, followed by the extrusion of nitrogen resulting in palladium methylidene complexes **16**. These undergo [2+2] cycloaddition with ethylene (inner- or outer-sphere mechanisms, depending on the ligation state of palladium) to afford palladacyclobutane **17**, which reductively eliminates cyclopropane, *via* a transient cyclopropane complex **18**, and the cycle is closed by the coordination of a further equivalent of ethylene (Scheme 1.17).

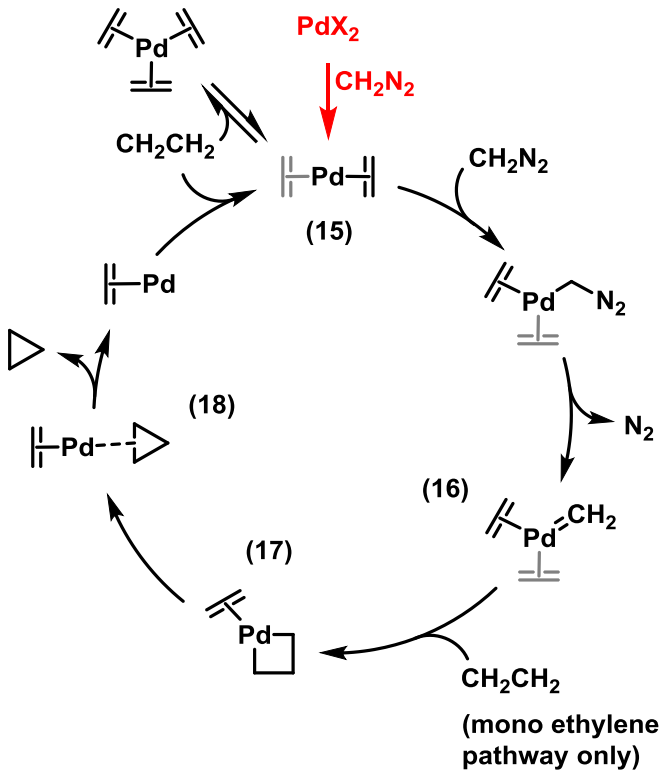

Scheme 1.17 Alkene cyclopropanation by Pd(0) proposed by Straub. The reduction step highlighted in red was assumed to occur on the basis of experimental observations by McCrindle (*43*) and Hacksell (*34*). Both mono- and bis(ethylene) species are predicted to be reactive, with the reactive manifolds converging on the common ethylene-bound palladacyclobutane intermediate.

A slight dependence of the overall calculated potential energy surface on the functional employed (B3LYP *vs*. BP86) was noted by Straub, but the magnitude of the functional dependence is sufficiently small that the broad conclusions of the study are not affected. As in Branchadell's study, extrusion of nitrogen was found to be rate-determining, albeit with a considerably lower total activation energy (17.1 kcal mol^{-1}, 71.7 kJ mol^{-1}).

1.3 *In Situ* Generation and Reaction of Diazomethane

The problems relating to toxicity and thermal instability noted above (Sections 1.1.2-1.1.3) render the employment of diazomethane in a chemical reaction something of a last resort. It was recognised by Meerwein as early as 1933 that the generation and consumption of diazomethane in a single reaction vessel could alleviate these concerns.[48]

1.3.1 *In Situ* Diazomethane Generation from *N*-Methyl-*N*-Nitroso Precursors

The one-pot generation and reaction of diazomethane was first reported by Meerwein in a 1933 patent which disclosed the liberation of diazomethane from *N*-methyl-*N*-nitrosourethane (**19**) with insoluble inorganic bases (typically K_2CO_3) in alcoholic solvents, and its reaction with both ketones and phenol (Scheme 1.18). The insoluble nature of the base employed ensures slow diazomethane generation, which prevents the build-up of hazardous amounts of the reagent, but also results in long reaction times.[48]

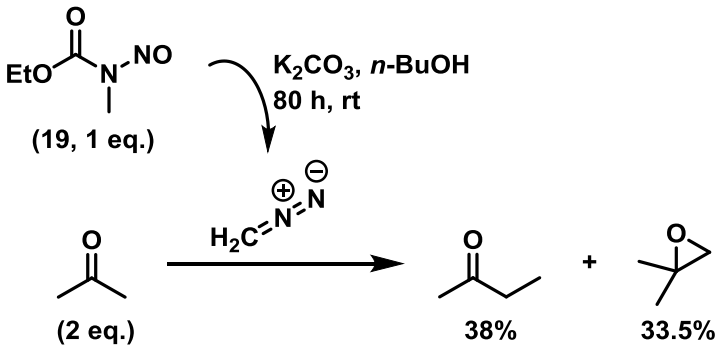

Scheme 1.18 Reaction of acetone with *in situ*-generated diazomethane (from *N*-methyl-*N*-nitrosourethane, **19**) affords the products of ketone homologation and methylene addition across the C=O double bond.

Hecht and Kozarich demonstrated that sufficiently basic substrates could promote the liberation of diazomethane from suitable precursors, finding that sodium *p*-nitrophenoxide was readily *O*-methylated on stirring with *N*-methyl-*N*-nitrosourea in DME. For less basic substrates, addition of exogenous base (Et_3N or aqueous potassium hydroxide) was required for the reaction to proceed efficiently.[49]

Successful attempts to combine transition-metal catalysed reactions with *in situ* diazomethane generation were not reported until the early 1990s. The markedly different media required for the two reactions – palladium catalysed cyclopropanations are generally performed in Et_2O or DCM, while liberation of diazomethane from *N*-methyl-*N*-nitroso compounds commonly employs aqueous potassium hydroxide – presented an opportunity for a phase-separated process, first realised by Nefedov and co-workers.[50] Slow addition of *N*-methyl-*N*-nitrosourea (NMU, **20**) *via* powder addition funnel to a mixture of (pre)catalyst and alkene in DCM/aqueous KOH afforded the corresponding cyclopropane in good yields. Alkaline degradation of NMU in the aqueous phase affords diazomethane, which is subsequently consumed by catalysis, presumably in the organic phase (Scheme 1.19). Although this biphasic approach appears to protect the active catalytic species from degradation (albeit within an optimised range of temperatures and addition rates), it is of note that the substrates reported are comparatively robust; no examples of substrates bearing base-sensitive functionality (e.g. esters) were disclosed. Consequently, this methodology for simultaneous *in situ* diazomethane generation – cyclopropanation has found relatively limited use in synthesis.[51-56]

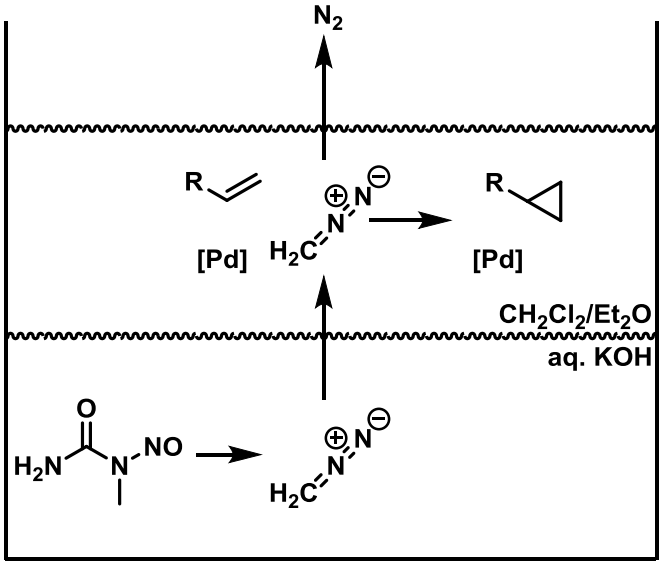

Scheme 1.19 *In situ* diazomethane generation and cyclopropanation (Nefedov and co-workers).

This approach towards cyclopropanation with *in situ*-generated diazomethane has recently been re-examined by Morandi and Carreira, who found that slow addition of a water-soluble diazomethane precursor developed by Moody (**21**)[57] to a mixture of 6 M aqueous KOH, alkene substrate and an iron porphyrin catalyst (**22**) resulted in the cyclopropanation of a range of styrenes, butadienes and enynes.[58]

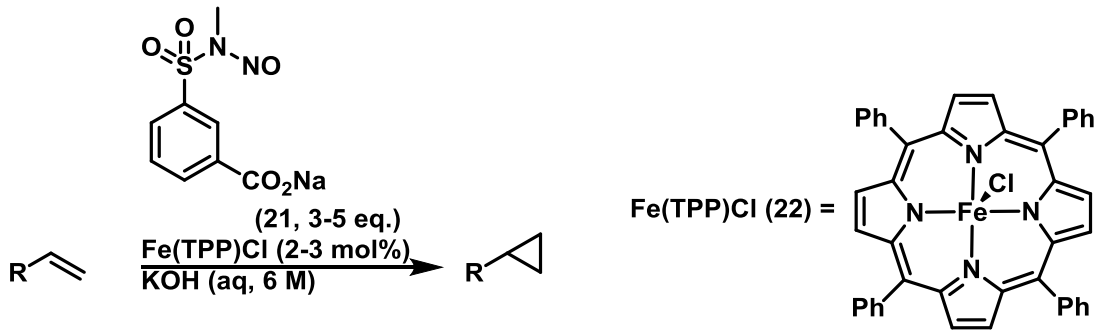

Scheme 1.20 Iron-catalysed cyclopropanation of alkenes with *in situ*-generated diazomethane (Morandi and Carreira).

In the course of this study, a number of transition metal catalysts known to promote carbene transfer were examined for their efficacy in effecting the desired transformation. While the iron(III) porphyrin proved the most effective in screening,[59] (tpp)RuCO also proved a competent catalyst, while $Pd(OAc)_2$ – the most commonly-employed catalyst in such reactions – was much less effective. The authors attributed this to the solubility of the metal salt in the bulk aqueous medium, in preference to the minor organic phase. Aqueous-soluble substrates also resisted cyclopropanation, and presumably base-sensitive substrates are unsuitable for the same reasons as in the Nefedov system.

1.3.2 Other Methods for *In Situ* Diazomethane Generation

The methyl esterification of carboxylic acids (**23**) can be achieved with trimethylsilyldiazomethane (TMSDAM, **24**) in benzene/methanol mixtures, as has been demonstrated by Shioiri and co-workers.[60] In the absence of methanol, a mixture of the (trimethylsilyl)methyl ester (**25**), the acyl silane (**26**) and the methyl ester (**27**) are formed (Scheme 1.21).[61]

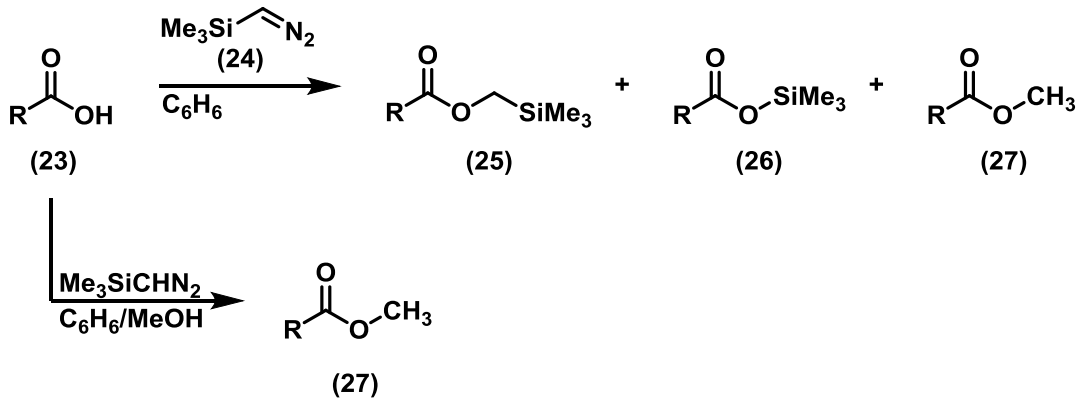

Scheme 1.21 Reaction of acetic acid with TMSDAM results in a complex mixture of products (Seyferth and co-workers). Addition of methanol to the reaction mixture gives clean formation of the methyl ester (Shioiri and co-workers).

The mechanism of the methyl esterification reaction under Shioiri's conditions has been studied by Lloyd-Jones and co-workers.[62] Kinetic partitioning between methyl ester (**27**) and (trimethylsilyl)methyl ester (**25**) was linearly correlated with methanol concentration, and exchange between the two products was ruled out. In combination with 'proton inventory' studies, the observation of a small, normal kinetic isotope effect, and the isotopic distribution of products when CH_3OH/CD_3OD mixtures were employed, these data are consistent with the *in situ* generation of diazomethane under the reaction conditions, by methanolytic protodesilylation of (trimethylsilyl)methyldiazonium carboxylate (**28**) (Scheme 1.22).

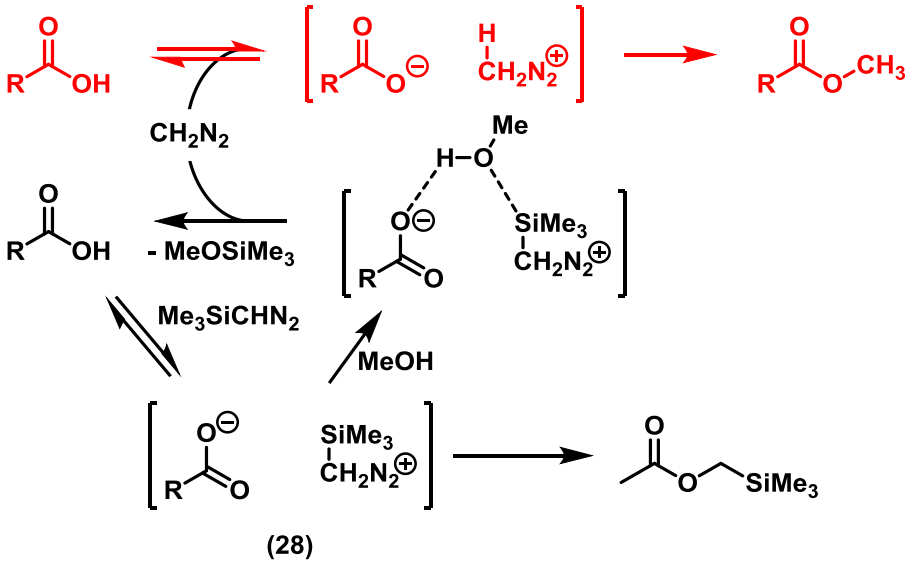

Scheme 1.22 Lloyd-Jones mechanism for Shioiri methyl esterification. *In situ* diazomethane generation *via* desilylation of the silylated diazonium intermediate intercepts the reaction manifold for the direct reaction of carboxylic acids with diazomethane (highlighted in red).

1.4 Aims

The palladium-catalysed cyclopropanation of alkenes is a reaction whose scope has been relatively well-explored, and for a number of classes of alkenes it is uniquely effective. However, the necessity of preparing and using multiple equivalents of diazomethane – a reagent well-known to be acutely toxic and prone to explosion – represents a considerable barrier to its use. Although a number of studies, by the groups of Nefedov and Carreira, have demonstrated the possibility of generating the required reagent *in situ*, these methods are not amenable to the cyclopropanation of base-sensitive substrates, and cannot, therefore, be considered wholly effective replacements for the original method, employing *ex situ*-prepared diazomethane.

The discovery by Lloyd-Jones and co-workers that the methyl esterification of carboxylic acids with TMSDAM under Shioiri's conditions proceeds *via* diazomethane generation provides a conceptually interesting, and potentially practical, alternative to the alkaline hydrolysis of *N*-methyl-*N*-nitroso compounds for diazomethane preparation. TMSDAM is a bench-stable, commercially-available reagent; the sensitivity to sharp edges, shocks and light which is well-documented for diazomethane is absent in the silylated congener. Although it too is toxic, exposure to it is minimised due to its relatively involatile nature.

Although promoted by the carboxylic acid substrate in the case of the methylation reaction, under metal-catalysed conditions, other mechanisms for protodesilylation can be envisaged. For example, Lebel and co-workers have employed TMSDAM in the synthesis of alkenes from aldehydes by *in situ* generation of methylenetriphenylphosphorane (**29**) (Scheme 1.23).[63] Their proposed mechanism does not involve diazomethane generation, instead it is suggested that the rhodium(I) catalyst employed promotes protonation of Rh-bound TMSDAM.[64] As such, TMSDAM is best considered a diazomethane surrogate in the proposed mechanism for this reaction.

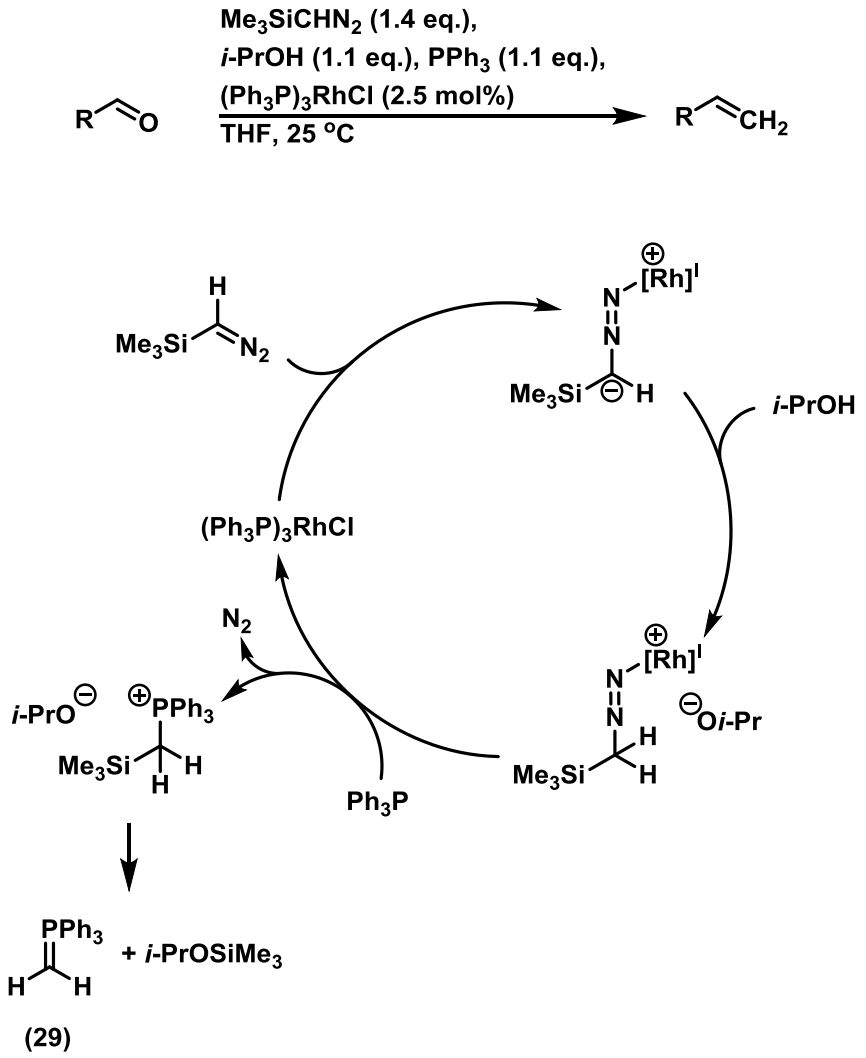

Scheme 1.23 Synthesis of terminal alkenes with TMSDAM under rhodium catalysis, and proposed mechanism (Lebel and co-workers).

TMSDAM is known to effect the cyclopropanation of electron-deficient alkenes under palladium catalysis, affording the corresponding trimethylsilyl-substituted cyclopropanes.[65] If an intermediate on the catalytic cycle to these products could be intercepted by a protodesilylating agent (HX), then the products of formal diazomethane cyclopropanation would result (Scheme 1.24). Alternatively, the direct protodesilylation of TMSDAM by HX to afford diazomethane could occur, permitting access to the established reaction manifold.

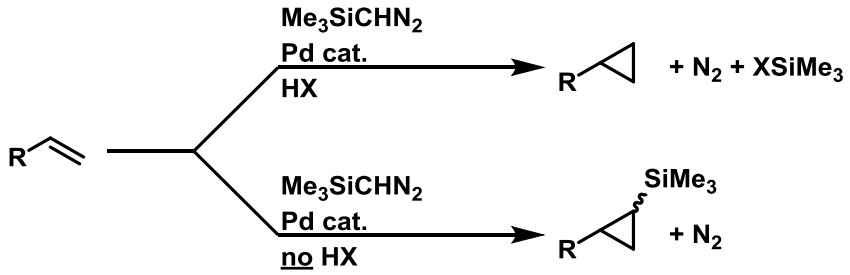

Scheme 1.24 Proposed cyclopropanation reaction (top arrow) *via* protodesilylative reaction of trimethylsilyldiazomethane under palladium catalysis.

Hereafter, these two rather different mechanistic possibilities (Scheme 1.25) will be distinguished by reference to TMSDAM as either a diazomethane *surrogate*, in the first case, or a diazomethane *precursor*, in the second. The surrogate pathway is characterised by the reaction of a catalytic intermediate in a desilylative sense so as to intercept an analogous intermediate on the non-silylated reaction manifold ($Z^{TMS} \rightarrow Z^{H}$) as in the reaction pathway identified by Lebel and co-workers. In contrast, the precursor pathway involves the formation of diazomethane ($Me_3SiCHN_2 \rightarrow CH_2N_2$) as in the Lloyd-Jones mechanism for the methyl esterification developed by Shioiri and co-workers.

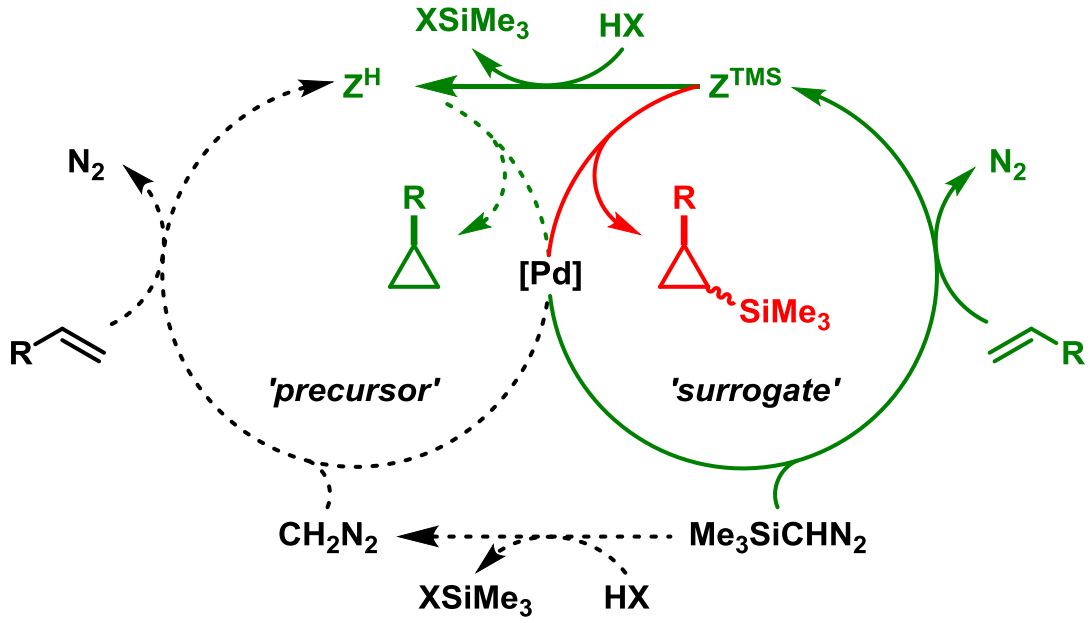

Scheme 1.25 TMSDAM as a diazomethane surrogate (green arrows), intercepting a catalytic intermediate on the CH_2N_2 manifold; or as a diazomethane precursor, by direct protodesilylation (dashed arrows).

Regardless of the nature of the desilylation event, the mechanism of the overall process is of interest; the development of synthetic methodology benefits from mechanistic understanding,

and experimental studies into the palladium-catalysed cyclopropanation of alkenes are lacking. The nature of the active catalytic species and the identity of possible competing side reactions in the diazomethane reaction are both unknown, and would be of considerable interest in designing improved protocols for this synthetically-valuable process.

2 Results and Discussion

2.1 Alcohols in Protodesilylative Cyclopropanation with TMSDAM

Initial studies into the possibility of effecting protodesilylative cyclopropanation of alkenes with TMSDAM were based on the studies of Shioiri and co-workers, who had separately established the ability of TMSDAM to effect cyclopropanation (resulting in formal :$CHSiMe_3$ addition across the double bond, Scheme 2.1)[65] and the desilylative methyl esterification of carboxylic acids with the same reagent (*vide supra*, Section 1.3.2).[60] Consequently, experiments were undertaken with the aim of reconciling the two sets of reaction conditions.

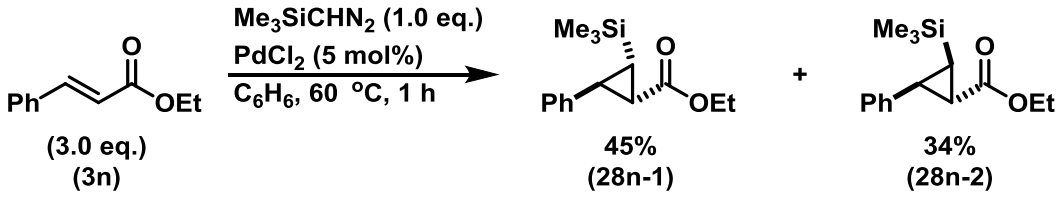

Scheme 2.1 Silylcyclopropanation of ethyl cinnamate (**3n**) with TMSDAM (Shioiri and co-workers).

2.1.1 Initial Studies in Methanolytic Cyclopropanation

The cyclopropanation of ethyl cinnamate with TMSDAM as reported by Shioiri and co-workers is effected by the addition of the diazo compound to a solution of the alkene and a palladium catalyst in benzene at 60 °C. Neither substitution of benzene for toluene nor variation in the catalyst and its loading (**29**·$PdCl_2$, 1 mol%) had an effect on the outcome of the reaction relative to that reported in the literature, while the use of a 7:3 mixture of toluene and methanol – i.e. the conditions used in the protodesilylative methyl esterification reaction – resulted in extremely vigorous effervescence of nitrogen, in contrast to the more sedate nitrogen evolution observed under alcohol-free conditions. Pleasingly, the addition of methanol resulted in the formation of 36% of the desired non-silylated product (**4n**), as well as the two diastereomers of the silylated cyclopropane (**28n-1** and **28n-2**) (Scheme 2.2).

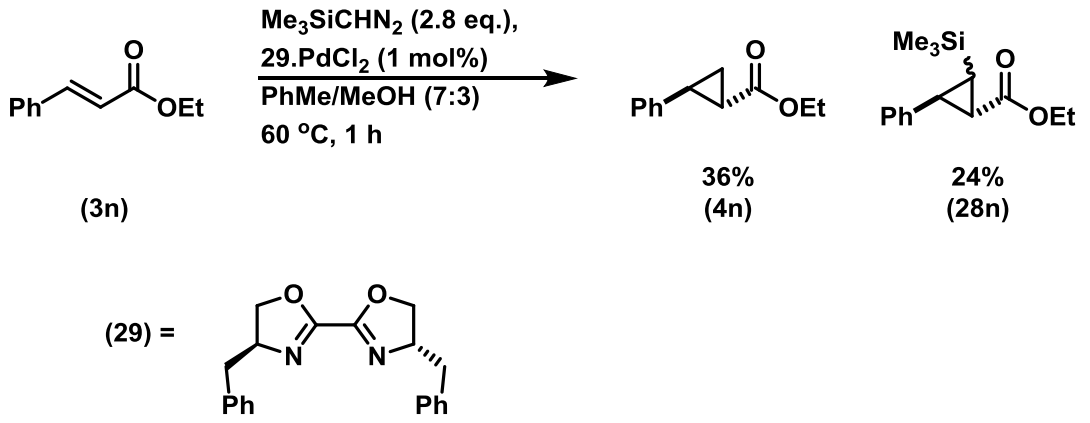

Scheme 2.2 First observation of desilylated products in Pd-catalysed cyclopropanation with TMSDAM.

Encouraged by this positive result, the reaction was repeated at room temperature in the hope of suppressing the violent nitrogen evolution. Although this led to a slightly diminished conversion (47% total, *vs*. 60%), the selectivity for the desired product was enhanced. Efforts to increase the selectivity for the non-silylated product **4n** further by increasing the methanol concentration were met with limited success. Although the selectivity did increase to synthetically useful levels (Figure 2.1), the stability of the catalyst to the reaction conditions decreased in concert, with precipitation of palladium black becoming progressively faster. It was further demonstrated (by the addition of further TMSDAM) that the palladium black formation resulted in the termination of any useful catalysis; although TMSDAM consumption continued, no additional cyclopropanation of the cinnamate **3n** was observed.

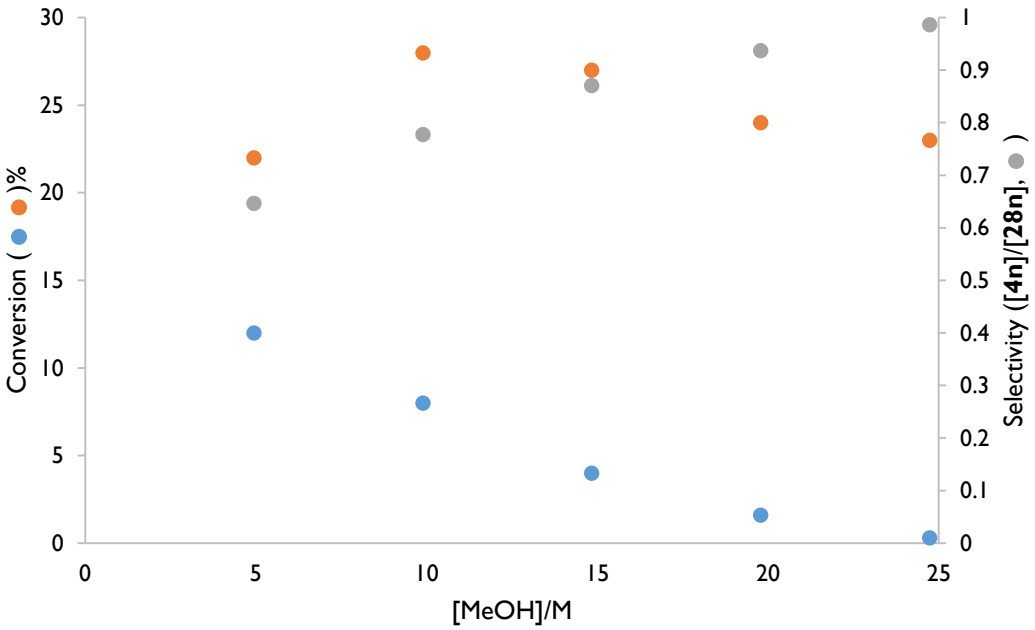

Figure 2.1 Increasing [MeOH] improves selectivity (grey circles, right-hand axis) for conversion to non-silylated cyclopropane (orange circles, left-hand axis) over the silylated product (both diastereomers, blue circles, left-hand axis).

Furthermore, little effect was found on changing the identity of the palladium (pre-)catalyst; all of those tested had previously been used in cyclopropanations with diazomethane. Under the conditions employed, all were effective, but decomposed with formation of palladium black (Table 2.1, *vide infra*). A number of catalysts based on other transition metals were tested (entries 14-17); Morandi and Carreira have demonstrated the efficacy of the iron porphyrin catalyst (entry 14), Cu(I) salts have been shown to be effective in the cyclopropanation of electron-rich alkenes (e.g. enamines), and TMSDAM is known to engage in M-Cl insertion with L_2PtCl_2 in a manner analogous to that with L_2PdCl_2 complexes.[43,66] However, all proved wholly ineffective in promoting cyclopropanation, although in all cases, TMSDAM consumption was evident.

Table 2.1 Catalyst dependence of desilylative cyclopropanation with MeOH. In the case of dinuclear catalysts, the catalyst loading reported in the table reflects that of the metal rather than the complex.

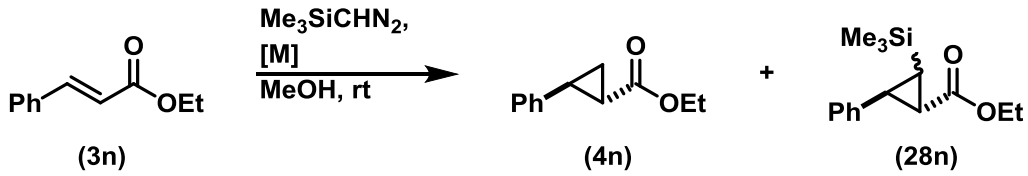

(3n) (4n) (28n)

Entry	Catalyst, [M]	Catalyst loading, mol%	TMSDAM eq.	% conversion	% selectivity (**4n**/**28n**)
1	$PdCl_2$	1	1.1	17	97
2	***29***·$PdCl_2$	1	1.1	13	94
3	***29***·$PdCl_2$	1	4.5	45	92
4	$Pd(OAc)_2$	1	1.1	25	93
5	$(PhCN)_2PdCl_2$	1	1.1	26	93
6	$(PhCN)_2PdCl_2$	1	4.5	47	92
7	$[(\eta^3\text{-allyl})PdCl]_2$	1	1.1	27	85
8	$[(\eta^3\text{-allyl})PdCl]_2$	1	4.5	67	79
9	$[(\eta^3\text{-allyl})PdCl]_2$	0.25	4.5	33	95
10	$Pd_2(dba)_3$·dba	1	1.1	19	90
11	$Pd_2(dba)_3$·dba + PPh_3	1	1.1	3	n.d.
12	$Pd_2(dba)_3$·dba + ***29***	1	1.1	25	96
13	$Pd_2(DVTMS)_3$	1	1.1	8	79
14	(TPP)FeCl (**22**)	1	1.1	-	-
15	CuCl	10	1.1	-	-
16	CuI	10	1.1	-	-
17	$PtCl_2$	1	1.1	-	-

2.1.2 Alcoholysis: Efficiency and Selectivity

Lloyd-Jones and co-workers had found methanol capable of effecting protodesilylative reaction in the methyl esterification reaction, with *t*-butanol acting only as a reservoir of exchangeable protons. However, the results of Lebel and co-workers, who employed *i*-PrOH in the methylenation reaction of aldehydes with TMSDAM (*vide supra*, Scheme 1.23), provided some precedent for protodesilylative reaction under metal catalysis with higher alcohols. Given the lack of mechanistic data in both the Lebel reaction and in the cyclopropanation with regard to the nature of the intermediates undergoing protodesilylation, it seemed foolhardy to rule out the possibility that co-solvents other than methanol might prove effective in protodesilylation without having a deleterious effect on the catalyst stability, for example by modulation of acidity.

While the catalyst stability did improve markedly on moving to use of higher alcohols as the solvent, with almost no palladium black formation in *t*-BuOH, the selectivity for non-silylated cyclopropane diminished considerably, in line with Lloyd-Jones' observations (Table 2.2).

Table 2.2 Solvent effects on the protodesilylative cyclopropanation reaction. * - reaction performed at 40 °C.

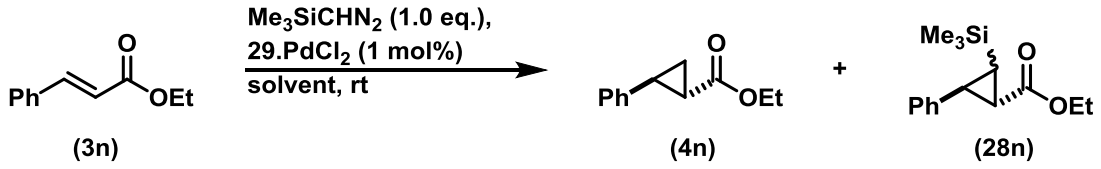

(3n) (4n) (28n)

Entry	Solvent	% conversion	% selectivity (**4n**/**28n**)
1	MeOH	13	94
2	EtOH	28	89
3	*i*-PrOH	32	74
4	*t*-BuOH	16	6
5	$HOCH_2CH_2OH$	30	84
6	CF_3CH_2OH	0	-
7*	PhOH	0	-

Ethylene glycol (entry 6) also proved moderately effective as a solvent for the reaction, albeit with lower selectivity for the desired product (**4n**). More acidic alcohols, such as trifluoroethanol and phenol, gave rise to no detectable cyclopropanes. One possible explanation for this is that the acidity of the medium favours *O*-methylation reactions, however no methyl ethers were detected – while this is not unexpected in the case of trifluoroethanol (due to the volatility of the corresponding ether), the absence of anisole in the reaction employing phenol is surprising.

Cumulatively, these results argue conclusively against the use of alcohols as the protodesilylating agent in the context of palladium catalysis, with a clear dichotomy between those conditions that engender high selectivity for the desired, non-silylated products, and those that promote catalyst stability. However, an interesting, if unlikely, possibility remained unexplored. If the cyclopropanation reaction proceeded in a non-desilylative sense, affording solely the silylated cyclopropanes, and these nascent products were subject to post-catalytic, off-metal, alcoholytic protodesilylation, the instability of the catalyst to alcohol need not prove problematic. The silylcyclopropanes could be generated *via* the catalytic silylcyclopropanation manifold, and subsequently subjected to stoichiometric protodesilylation with methanol (Scheme 2.3).

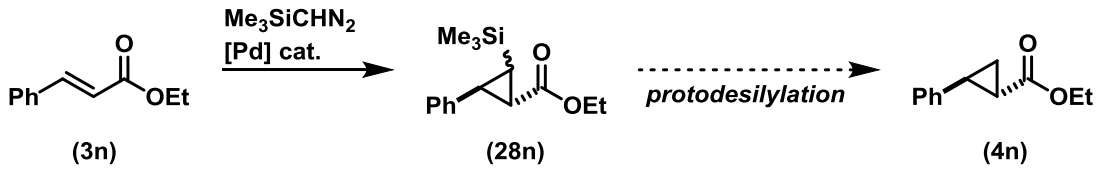

Scheme 2.3 Off-metal desilylation would allow ROH-free cyclopropanation, avoiding the problem of catalyst deactivation.

In order to probe the possibility of post-cyclisation protodesilylation, the cyclopropanes resulting from the silylcyclopropanation of ethyl cinnamate (**28n**) were added to a cyclopropanation reaction of methyl cinnamate (**3o**). Although non-silylated methyl esters were observed, no desilylation of the ethyl esters was observed (Scheme 2.4), demonstrating that the desilylation event is on-cycle and prior to an irreversible step.

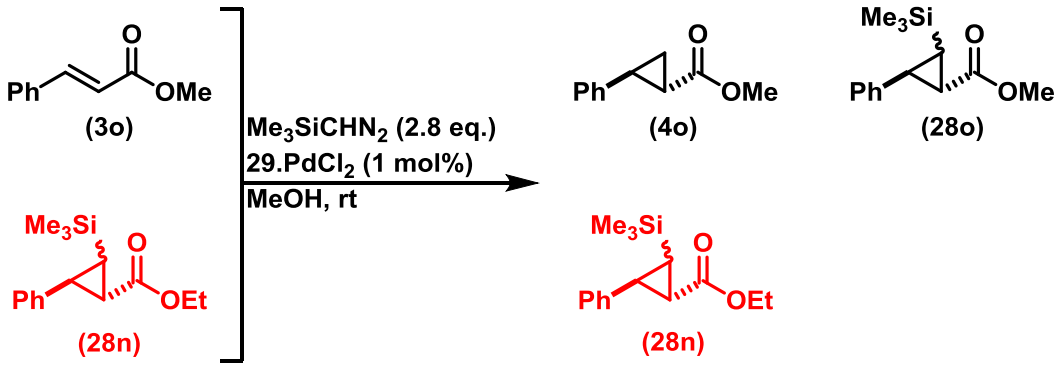

Scheme 2.4 Off-metal desilylation does not operate under the catalytic reaction conditions, with silylcyclopropanes **28n** remaining unchanged.

This outcome was not wholly unsurprising. C-Si protodesilylation is viable at sp^2- and sp-hybridised carbon centres, *via* a protonation-desilylation mechanism, in which the intermediate carbocation β- to silicon is stabilised by a hyperconjugative interaction between the C-Si σ-bond and the vacant p-orbital. Achieving this in a cyclopropane, however, would necessarily involve the cleavage of a C-C bond (Scheme 2.5A). The alternative desilylation-protonation mechanism would lead to the generation of a non-stabilised secondary cyclopropyl anion (Scheme 2.5B). Both mechanisms involve high-energy intermediates, liable to undergo undesired reactions to acyclic products (thus relieving ring strain). Furthermore, both pathways could result in the loss of stereochemical integrity – which is not observed – even if the cyclopropane remained intact.

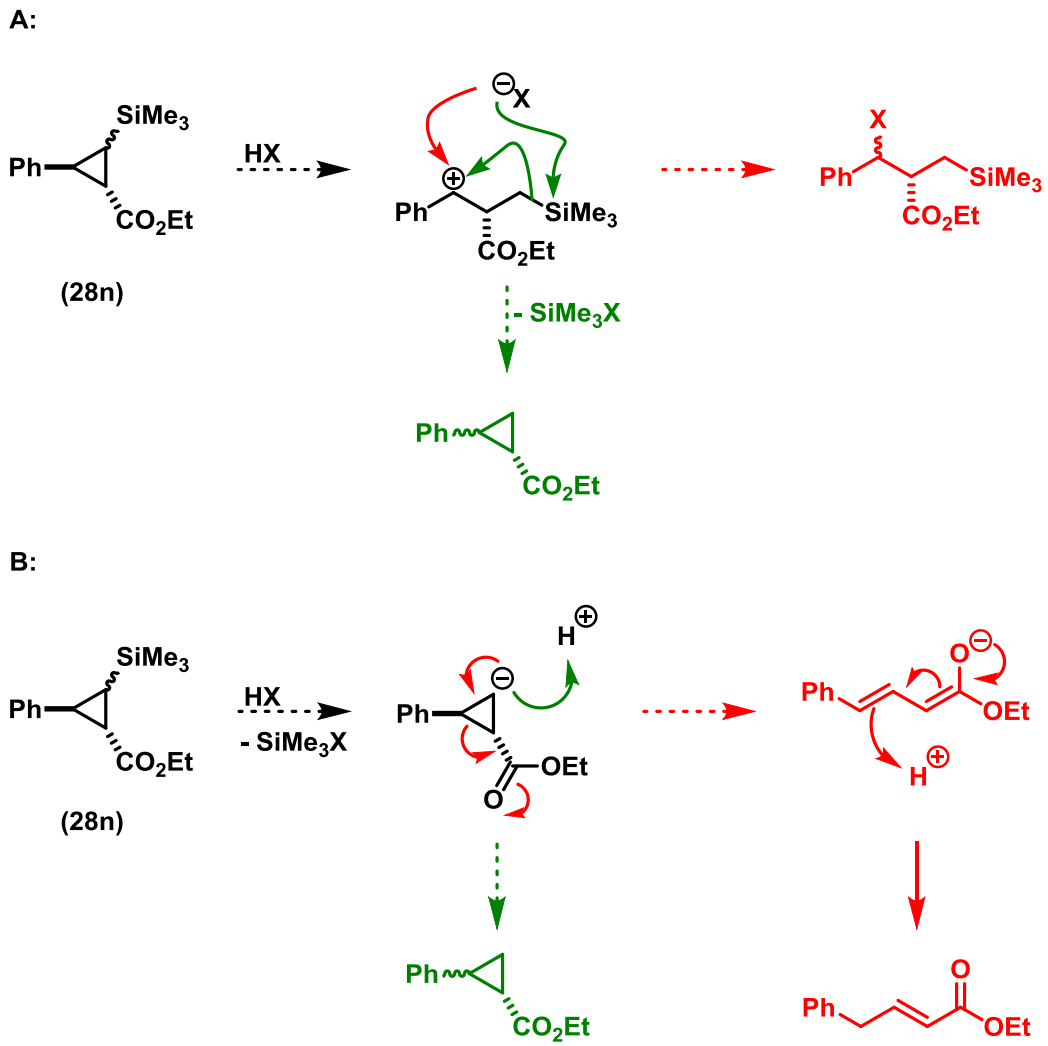

Scheme 2.5 Potential off-cycle mechanisms for cyclopropane desilylation *via* protonation-desilylation (A) or desilylation-protonation (B) result in unstable intermediates which would be liable to undergo side reactions (*via* mechanisms highlighted in red) to afford rearranged products.

These results are consistent with the protodesilylation of a catalytic intermediate being selectivity-determining in this system. Assuming the mechanism analogous to that proposed by Straub is a good model for the reaction under study,[47] likely candidates for the intermediate undergoing desilylation are κ^1*C*-trimethylsilyldiazomethane complex **30** (Scheme 2.6A), or silylated palladium methylidene **31** (Scheme 2.6B).

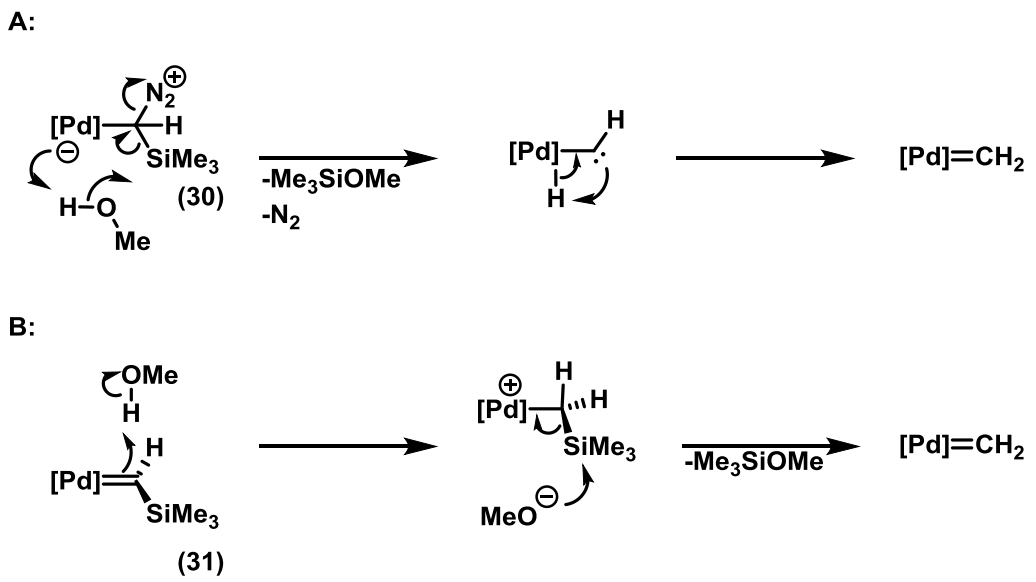

Scheme 2.6 Possible pathways for on-cycle desilylation.

Two effects were obvious from the earliest studies in the methanolytic reaction. As desired – and discussed above – the addition of methanol facilitates a desilylative pathway, although perfect selectivity for this pathway is not observed. Consequently, a selectivity-determining partitioning is implicated in the catalytic manifold. Intriguingly, however, some acceleration of the reaction is suggested by the relative vigour with which nitrogen was generated in the reaction with methanol at high temperature. Straub's study identifies the extrusion of nitrogen as rate-determining.[47] Assuming an analogous mechanism operates with TMSDAM, the observed acceleration of N_2 generation on the addition of MeOH suggests a lowering of this activation barrier, relative to the non-desilylative reaction with TMSDAM. This would be consistent with desilylation prior to the loss of N_2, catalysis of N_2-extrusion by methanol, or acceleration due to the increased polarity of the solvent medium.

2.1.3 The Fate of TMSDAM

In the reactions described above, stoichiometric excesses of TMSDAM relative to the alkene substrate were employed. However, despite clear evidence that the TMSDAM had been fully consumed (disappearance of the vivid yellow colour characteristic of the diazo compound, lack of effervescence on the addition of a carboxylic acid, measurement of the volume of gas evolved), the only products derived from it observed by ^{1}H NMR spectroscopy following work-up of the reaction were the aforementioned cyclopropanes and silylcyclopropanes. The formal

dimerization of TMSDAM-derived carbenes, affording the corresponding *trans*-alkene, is precedented under ruthenium catalysis (Scheme 2.7).[67] Although this byproduct was not observed in the alcoholytic palladium-catalysed process, the desilylated nature of the cyclopropane products suggests that any dimer-forming processes ought to be at least partially desilylative.

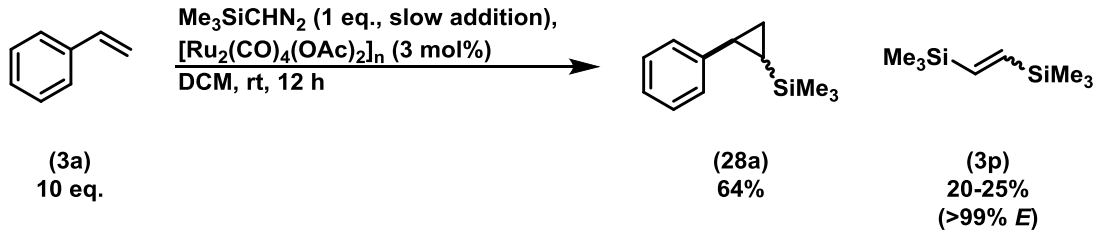

Scheme 2.7 (Trimethylsilyl)carbene dimerization in Ru-catalysed alkene cyclopropanation (Maas and Seitz).

Consequently, the formation of (trimethylsilyl)ethylene (**3q**) under catalytic conditions was considered. All efforts to observe this species by ^{1}H NMR spectroscopy following complete consumption of TMSDAM failed, but it was realised that the nitrogen generation inherent in the reaction provided an efficient means of purging volatile species (such as the mono-silylated alkene) from solution, rendering their detection challenging. In order to minimise the potential for any loss of material by this process, a small aliquot was removed from a reaction mixture as soon as possible after TMSDAM addition (*ca.* 5 s), and immediately subjected to gas chromatography. Spiking with an authentic sample of (trimethylsilyl)ethylene, prepared by the silylation of vinylmagnesium bromide with chlorotrimethylsilane, confirmed its presence in solution. However, this species could not be detected in aliquots withdrawn later in the course of the reaction, suggesting that it is efficiently purged by the nitrogen flux from the reaction.

The formation of this species, effectively a "mixed carbene dimer", is most likely due to the reaction between TMSDAM and a desilylated catalytic intermediate, in competition with the desired process. However, due to its fleeting nature in solution, quantification of its concentration in solution proved impossible. Consequently, it cannot be said with complete confidence that this is the sole product of TMSDAM side reactions.

2.2 Fluoride in Protodesilylative Cyclopropanation with TMSDAM

2.2.1 Fluoride/Alcohol Mixtures

Although reactions employing methanol ultimately proved unworkable from a synthetic perspective due to the obvious instability of the catalysts to conditions of high methanol concentration, they did at least provide good evidence that a sufficiently nucleophilic species could promote the desired reactivity. A better candidate nucleophile for silicon is fluoride anion. Fluoride reagents are used extensively in the deprotection of silyl ethers in synthesis, as well as in the cleavage of labile C-Si bonds. Tetrabutylammonium fluoride (TBAF) is probably the most commonly used source of organic-soluble F^-, but obtaining this compound in anhydrous form is challenging, with only one effective method reported in the literature. Sun and DiMagno reported in 2004 that the reaction of tetrabutylammonium cyanide with hexafluorobenzene generates anhydrous TBAF (Scheme 2.8).[68] However, the fluoride salt that results is highly basic, such that the compound is unstable with respect to E2 elimination in THF solution and the solid state.

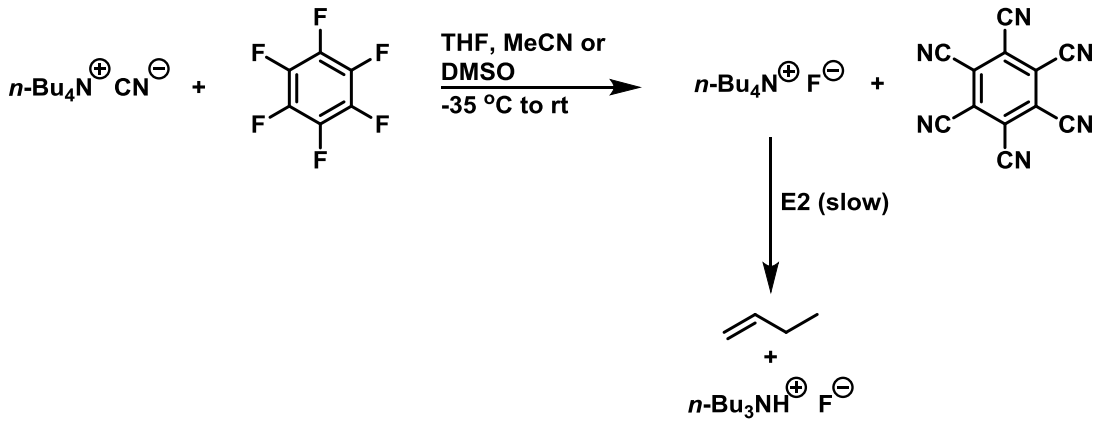

Scheme 2.8 Synthesis of anhydrous TBAF (Sun and DiMagno).

Despite concerns with regard to the hydration state of commercially-available TBAF sources, the ability of TBAF in THF to effect the desired reaction was tested in a range of alcohols (Table 2.2, entries 1-5). Although the formation of silylated cyclopropanes was almost completely suppressed, palladium black formation remained problematic, resulting in conversions below 15% in the best case.

In 2008, Kim and co-workers reported a *tert*-butanol coordinated TBAF complex which exhibited low hygroscopicity and basicity.[69] Initial experiments employing this reagent in alcoholic solvents resulted in low conversions to cyclopropanes (Table 2.3, entries 6-8). Furthermore, the mass of TBAF(*t*-BuOH)$_4$ required to satisfy the reaction stoichiometry resulted in viscous reaction mixtures, which in turn made mixing inefficient. Moreover, significant transesterification of the substrate (*ca*. 40%) was observed in one case (entry 8). KF in MeOH and EtOH (entries 9-10) gave highly-selective, but poorly yielding reactions, while *t*-BuOH (entry 11) was unable to solubilise the salt, leading to exclusive silylcyclopropanation.

Table 2.3 Desilylative cyclopropanation with fluoride sources gives low conversions to cyclopropanes. Entries marked with an asterisk (*) refer to reactions which resulted in some degree of transesterification of starting material (for all other entries, R = Et). The extent of transesterification in the products was not determined.

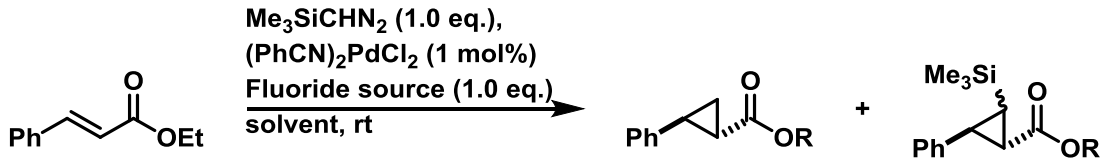

Entry	Solvent	Fluoride source	% conversion	% selectivity
1	MeOH	TBAF/THF	13	>98
2	EtOH	TBAF/THF	11	97
3	*i*-PrOH	TBAF/THF	7	>98
4*	*t*-BuOH	TBAF/THF	11	>98
5	$HOCH_2CH_2OH$	TBAF/THF	13	95
6	EtOH	TBAF(*t*-BuOH)$_4$	13	>98
7	*i*-PrOH	TBAF(*t*-BuOH)$_4$	20	>98
8*	*t*-BuOH	TBAF(*t*-BuOH)$_4$	22	>98
9*	MeOH	KF	14	>98
10	EtOH	KF	8	>98
11	*t*-BuOH	KF	25	0
12	*t*-BuOH:H_2O (3:2)	KF	14	91
13*	$HOCH_2CH_2OH$	KF	16	89

2.2.2 Metal Bifluoride Salts and Organotrifluoroborates

Contemporaneous work in the group relating to the hydrolysis of potassium organotrifluoroborates under conditions relevant to Suzuki-Miyaura cross-coupling, as well as their preparation, prompted the investigation of potassium bifluoride, KHF_2, as a potentially useful desilylating agent.[70] Despite the immediacy with which palladium black precipitation was evident, this system proved surprisingly successful in achieving the desired transformation, in contrast to an otherwise identical reaction employing potassium fluoride (Scheme 2.9).

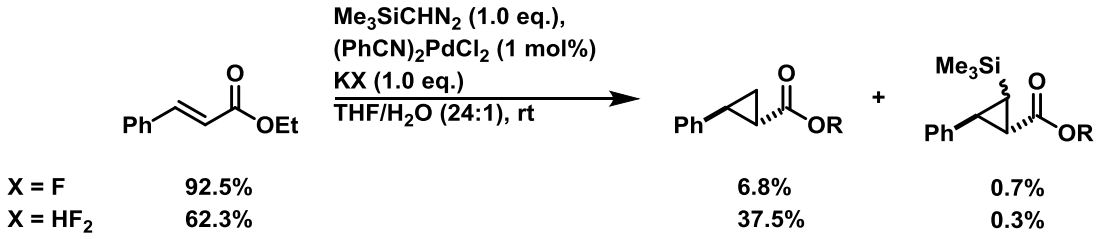

Scheme 2.9 Comparison of the efficacy of KF and KHF_2 in desilylative cyclopropanation.

Given the previously-demonstrated sensitivity of the catalyst to high methanol concentrations, that the reaction worked at all in a system employing water as a co-solvent was somewhat surprising. In line with expectations from earlier alcoholysis studies (*vide supra*), increasing the water concentration led to lower conversions, however conversions also dropped on reducing the amount of water employed. The reason for this last effect is unknown, but may be due to the diminished solubility of the bifluoride salt in the reaction mixture.

Despite extensive screening of (pre-)catalysts, water-miscible organic co-solvents, ligands and additives, no other conditions employing KHF_2 were found to be more effective than those above (Scheme 2.9).

Furthermore, the use of potassium organotrifluoroborate salts as HF/HF_2^- precursors was explored. These air- and moisture-stable salts have been used to great effect in synthesis, and the rates of their hydrolysis are well-characterised. It was thought that this hydrolysis pathway might provide a convenient method for the slow *in situ* generation of HF/HF_2^-. If the reaction were to proceed *via* direct protodesilylation of TMSDAM, forming diazomethane, this would allow a controlled, slow-release of the reagent, possibly preventing side reactions involving multiple equivalents of the diazo compound. Given the range of hydrolytic half-lives reported for potassium organotrifluoroborates in organic/aqueous conditions (these span *ca.* five orders of magnitude),[71] considerable control over the rate of reaction would be feasible.

The concept of trifluoroborate hydrolysis was proven effective in a number of reactions; reactions employing potassium cyclopropyltrifluoroborate and potassium vinyltrifluoroborate (two of the fastest salts to hydrolyse) engendered high selectivity for desilylated products, but with conversions to products no better than with KHF_2. Consequently, their use was not explored further.

2.2.3 Tetrabutylammonium Bifluoride (TBABF)

The identification of potassium bifluoride as an effective reagent for promoting protodesilylative reaction prompted a reconsideration of the approaches considered thus far. All reactions examined up to this point have employed protic solvents, as was thought to be necessary to achieve the desired reactivity. However, the literature reports of palladium-catalysed cyclopropanation with diazomethane all employ considerably less polar, and aprotic, solvents – generally dichloromethane or diethyl ether. As a consequence, it was decided to seek conditions which would effect protodesilylation in these solvents. The obvious lead to follow was the unsurpassed reactivity and selectivity engendered by the use of bifluoride salts. Examination of the literature revealed some promising precedent for the existence and synthesis of organic-soluble bifluoride salts. Tetrabutylammonium bifluoride (TBABF) was identified by Sharma and Fry as the principal fluorine-containing product arising from attempts to dry the corresponding fluoride (TBAF) by heating *in vacuo*.[72] Guerrero and co-workers later reported the synthesis of this reagent using an anion-exchange resin, and demonstrated its efficacy in the nucleophilic fluorination of aliphatic and aromatic halides.[73] Landini and co-workers identified a more practical approach to these compounds, as well as the tetraphenylphosphonium analogues developed by Clark,[74,75] by anion exchange in biphasic chloroform/water mixtures.[76]

Despite being synthetically accessible and commercially available, TBABF has found very few applications in synthesis, particularly in comparison to TBAF. The few examples that do exist serve to exemplify the advantages of this reagent. Huang and co-workers employed TBABF to promote the nucleophilic trifluoromethylation of nitriles with the Ruppert-Prakash reagent (Me_3SiCF_3), having discovered this to be the principal component of the "anhydrous TBAF" they had previously employed.[77] Lee, Shin and co-workers found TBABF to be effective in the nucleophilic displacement of alkyl triflates; the modulation of reagent basicity in comparison to TBAF was found to substantially reduce the extent of competing elimination processes.[78] They

also examined the reactivity of the even less basic tetrabutylammonium dihydrogentrifluoride (n-Bu_4N^+ $H_2F_3^-$), which gave similarly low levels of elimination, albeit with significant amounts of unidentified side products. Surya Prakash, Pertusati and Olah employed TBABF in the synthesis of tetrabutylammonium organotrifluoroborates from the corresponding boronic acids,[79] thus avoiding the use of HF as previously advocated by Batey and Quach.[80]

Synthesis of TBABF according to the procedure reported by Landini proceeded in good yield (Scheme 2.10) and afforded the product as a viscous, colourless oil.

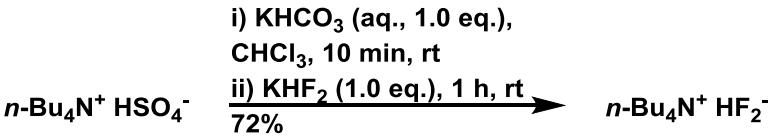

Scheme 2.10 Synthesis of TBABF by Landini's method.

Employing this reagent in a reaction with ethyl cinnamate resulted in the formation of a dark red solution; however in contrast to previous experiments no precipitation of palladium black was evident – the solution remained homogeneous. Analysis by ^{1}H NMR showed that 30% conversion to the non-silylated cyclopropane had taken place, with no trace of the corresponding silylcyclopropanes. Encouraged by the persistent homogeneity of the catalyst, the addition of further equivalents of TMSDAM gave rise to further conversion of the substrate (Table 2.4).

Table 2.4 Cyclopropanation of ethyl cinnamate employing TBABF as protodesilylation reagent.

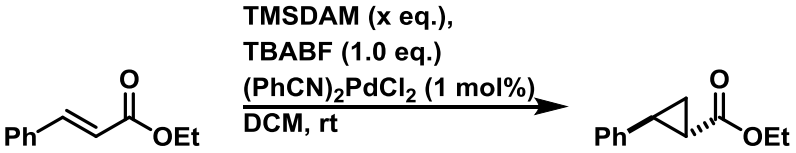

Equiv TBABF, x	% conversion	% selectivity (**4n**/**28n**)
1.1	30	>98
2.2	50	>98
3.3	70	>98

2.3 The Bifluoride-Promoted Cyclopropanation Reaction

With effective conditions for the protodesilylative cyclopropanation of alkenes with TMSDAM in hand, the rational optimisation of the process was pursued. Although the reactions with TBABF (*vide supra*) are clearly markedly more efficient than previously explored iterations of the methodology – in large part, it is assumed, due to the stabilisation of the catalytically-active species – a number of obvious questions remained unanswered. The first amongst these is the stoichiometry of TMSDAM; with multiple equivalents required to achieve good conversions to substrate, and the balance of the reagent unaccounted for, it was assumed that dimerisation processes were responsible for the incomplete mass balance, by analogy to the formation of vinyltrimethylsilane fleetingly observed in the methanolytic reaction (*vide supra*, Section 2.1.3).

In the original diazomethane process, the use of multiple equivalents of the reagent is routine – this in part due to the nature of its preparation, which does not readily allow for accurate addition of defined stoichiometric quantities. Furthermore, the nature of the addition of the reagent varies from one preparation to another; some workers distil the nascent reagent directly into the reaction mixture, others opt for addition by pipette from a previously-distilled solution, addition in a stream of inert gas (the Gaspar-Roth method), or by dropping funnel. In all cases, the rate of addition is not well-characterised, and only two of these approaches allow for the determination of reaction stoichiometry by titration of the diazomethane solution. Reactions employing TMSDAM, in contrast, allow for precise addition rates (by use of a syringe pump), and the molarity of the reagent is readily determined by titration or NMR methods.

Given that no cinnamate-derived side products were observed in reactions with TBABF, it seems reasonable to assume, as speculated above, that all TMSDAM-consuming side reactions involve the reagent alone. If this is the case, then the formation of these side products ought to be minimised by the slow addition of the reagent to the reaction mixture, such that the substrate is constantly in excess of the diazo compound.

2.3.1 Addition Rate and Mixing Effects

The slow addition of TMSDAM was found to improve the overall conversions markedly; once again, no degradation of the catalyst to form palladium black was visibly evident, nor were any traces of the silylated cyclopropanes (Scheme 2.11).

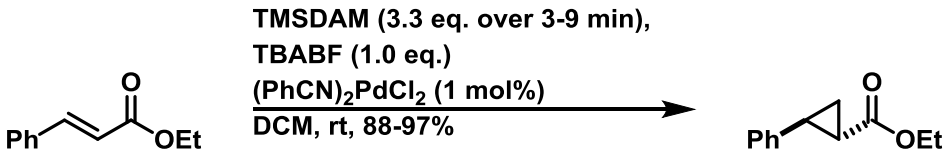

Scheme 2.11 Slow addition of TMSDAM results in higher conversions to cyclopropane.

These conversions are clearly synthetically useful, but the apparent need to use such considerable excesses of TMSDAM is not wholly satisfying. Furthermore, these experiments left some ambiguity with regards to the efficiency of the process (Figure 2.2). It remained possible that under the reaction conditions, the conversions stated were achieved prior to the complete addition of TMSDAM, and that the reaction simply stalled at high conversion, with subsequent TMSDAM addition leading to (unobserved) oligomerisation products. Alternatively, it could be that the reaction suffered competing inefficient processes from the very start, which would result in the necessity of employing a stoichiometric excess.

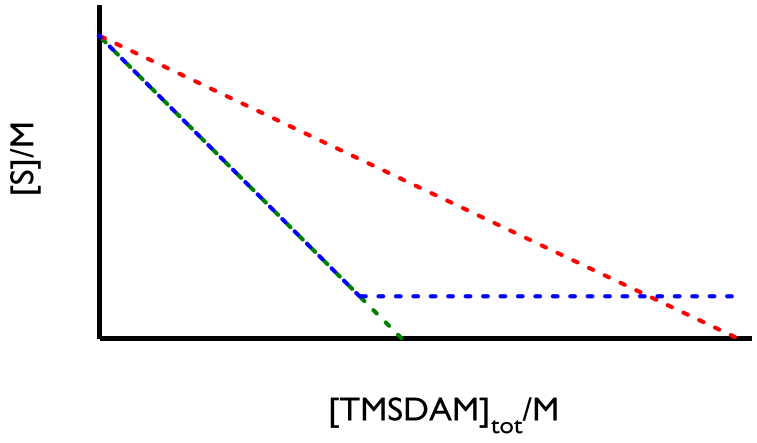

Figure 2.2 The apparent inefficiency in TMSDAM consumption can be explained by the reaction stalling at high conversion (blue line), or a competing side reaction, resulting in a constant inefficient consumption of TMSDAM (red line). The green line represents perfect efficiency, i.e. all TMSDAM is converted to product. $[TMSDAM]_{tot}$ denotes the total solution concentration of trimethylsilyl groups – assuming no loss of volatile TMS-derived species, and is a proxy for the total amount of TMSDAM added.

In order to distinguish the two possibilities, the conversion of substrate was monitored as a function of TMSDAM addition. It had been hoped to accomplish this by carrying the reaction

out directly in an NMR tube. However, this approach was abandoned following the observation of a localised region of dark red solution (as noted in preparative reactions, *vide supra*, in contrast to the pale yellow bulk untouched by TMSDAM) on the addition of small amounts of TMSDAM to a solution of $(PhCN)_2PdCl_2$, ethyl cinnamate and TBABF. Although this dissipates on mixing, it was suggestive of localised reaction on TMSDAM addition, and the loss of true homogeneity. As progressively more TMSDAM is added, the dark red colour was seen to persist throughout the sample, as before. Although the source of the colouration is not clear, it is presumably due to reactions occurring in an area of high local TMSDAM concentration

Given the initial localisation of this colour change, and the associated effervescence, this was taken as good evidence for the importance of efficient mixing, thus precluding the use of NMR tubes as reaction vessels. Although hexane and dichloromethane (the TMSDAM and reaction solvents, respectively) are miscible, it is assumed that the addition of the bifluoride salt promotes phase separation.

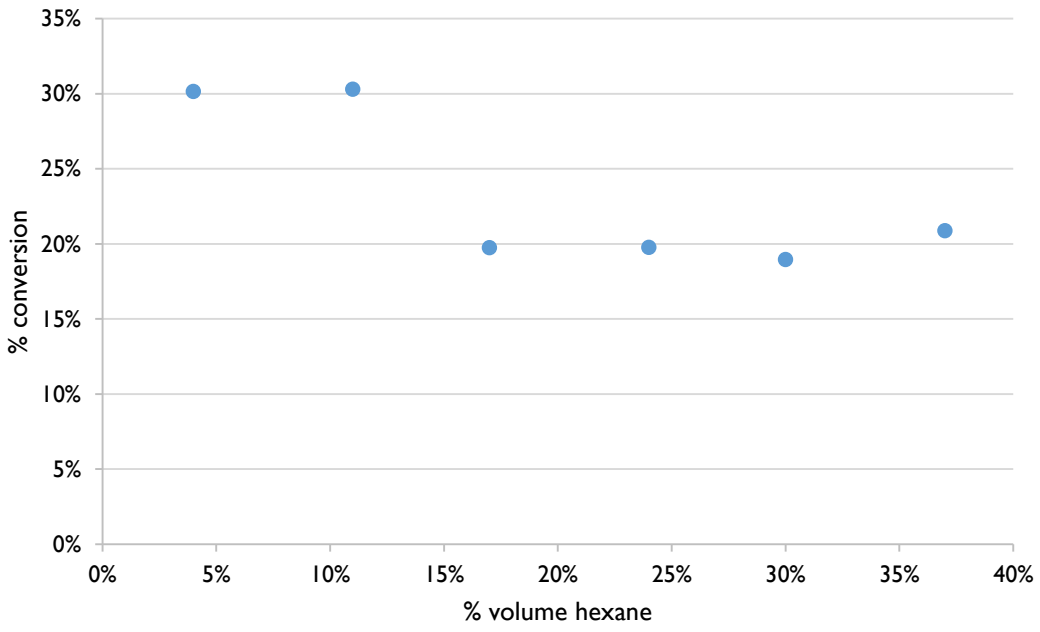

Figure 2.3 The ratio of solvents has an impact on the efficiency of reaction. Demixing is visible with > 15% v/v hexane. Addition of 1.1 eq. TMSDAM in a single injection, conditions otherwise as per Scheme 2.11 above.

Pleasingly, the potential problems raised by this inhomogeneity were simply solved by increasing the volume of DCM in the reaction mixture, which afforded monophasic reaction mixtures (Figure 2.3). The generation of high local concentrations of TMSDAM was avoided by efficient

stirring (1100 rpm) and by maintaining relatively low TMSDAM addition rates (lower addition rate set on syringe pump, fine gauge needle submerged in reaction mixture).

Under these conditions, the reaction proved amenable to monitoring by sequential portionwise addition of TMSDAM by syringe pump and sampling. Once withdrawn from the bulk solution, the samples were evaporated, redissolved in deuterated solvent and analysed by NMR spectroscopy.

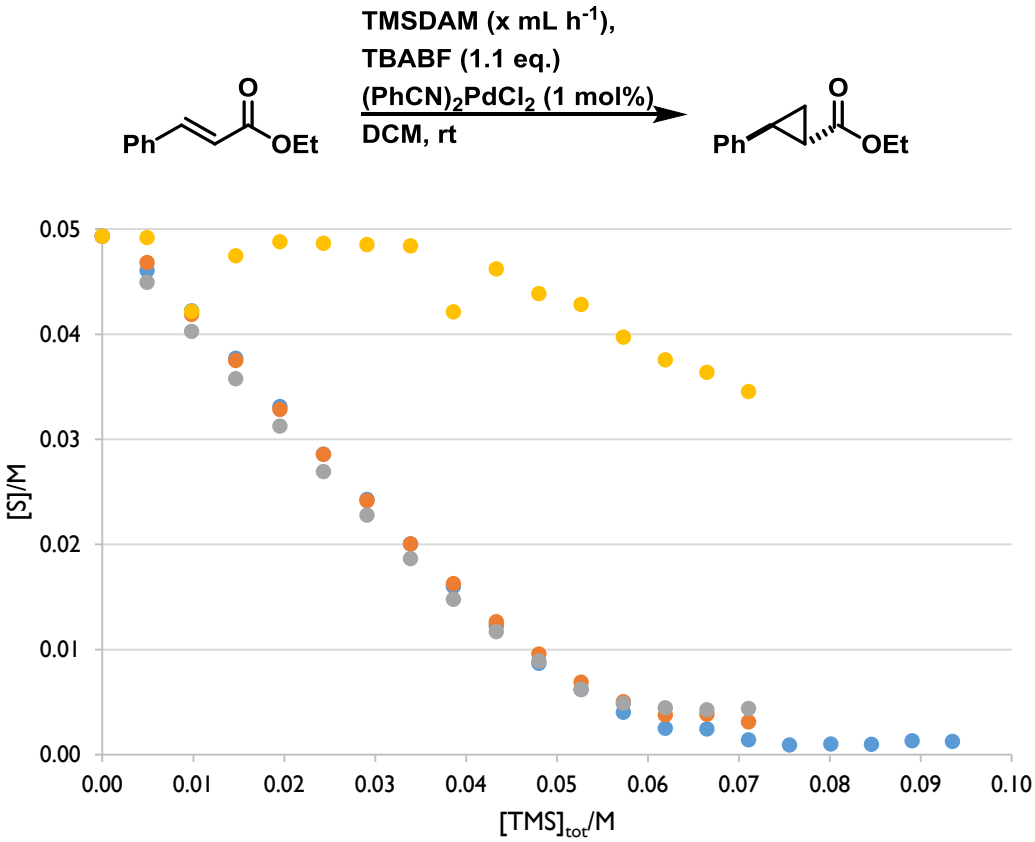

Figure 2.4 The impact of TMSDAM addition rate on substrate conversion is relatively limited (0.15 mL h^{-1}, orange circles; 1.2 mL h^{-1}, blue circles; 3.6 mL h^{-1}, grey circles – all stirred at 1100 rpm), but the impact of not stirring (yellow circles, addition rate 1.2 mL h^{-1}) is considerable. The scatter in the data from the unstirred reaction is likely due to perturbation of the biphasic system while sampling.

As can be seen in Figure 2.4, the reaction is largely insensitive to the rate of TMSDAM addition, with almost identical reaction profiles observed for addition rates between 0.15 and 3.6 mL h^{-1}, corresponding to addition times for 1.5 eq. TMSDAM between five minutes and two hours (Figure 2.4). Failure to stir the reaction leads to considerably less efficient cyclopropanation. Although formation of two discrete liquid phases was not evident, there was clear stratification in the reaction mixture; a red, hexane-rich upper phase increased in volume with TMSDAM

addition. Obtaining samples representative of the bulk reaction mixture in this case is clearly problematic, resulting in the scatter evident in Figure 2.4 above.

Most interesting, however, was the insight that this technique provided with respect to quantifying the partitioning of TMSDAM between productive and unproductive reaction manifolds. Two distinct phases of reaction can be identified. Initially, between approximately zero and eighty percent conversion ([S] > 0.01 M), there is a constant partitioning of TMSDAM between productive catalysis, affording the desired cyclopropane product, and a side reaction (or side reactions) generating side product(s), at this stage unidentified. In this phase of the reaction, the efficiency of productive consumption of TMSDAM is approximately 85%. Beyond *ca*. 80% conversion of substrate, a substantial reduction in this efficiency is evident (Figure 2.5).

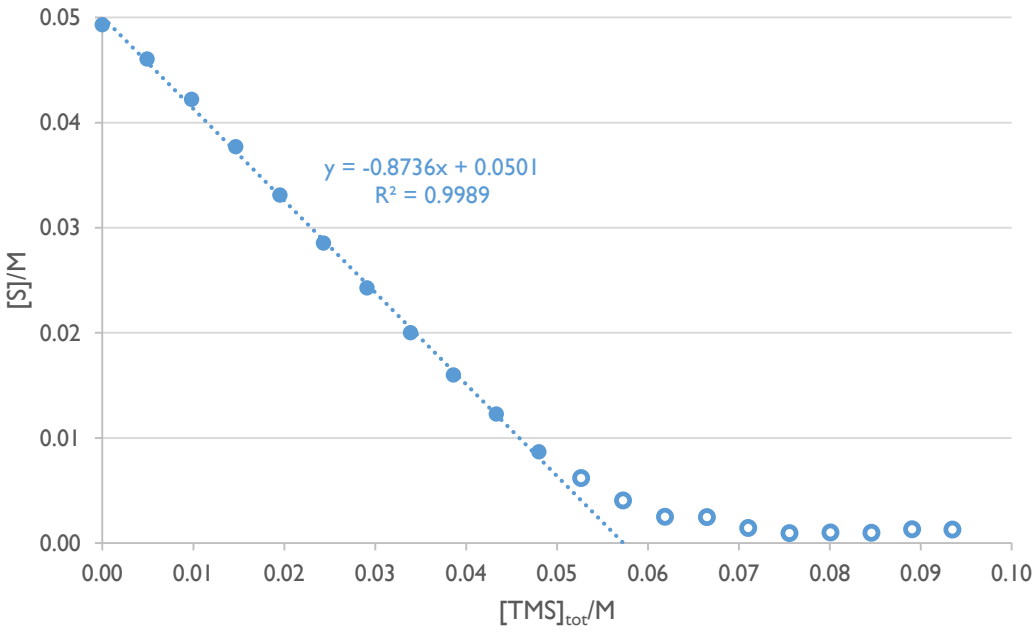

Figure 2.5 The efficiency of TMSDAM consumption as the cyclopropanation reaction reaches completion decreases substantially. The line of best fit, showing the efficiency in the earlier stages of reaction, is derived from the data marked by solid blue circles.

If the efficient linear regime persisted, extrapolation of the linear trend predicts that full conversion of alkene to cyclopropane would be achieved following the addition of 1.15 eq. TMSDAM.

One obvious reason for the decrease in reaction efficiency would be exhaustion of TBABF which, although in excess over substrate, is limiting with respect to added TMSDAM in the later stages

of the reaction. Increasing the TBABF loading, however, led to no improvement in the efficiency of TMSDAM consumption (Figure 2.6).

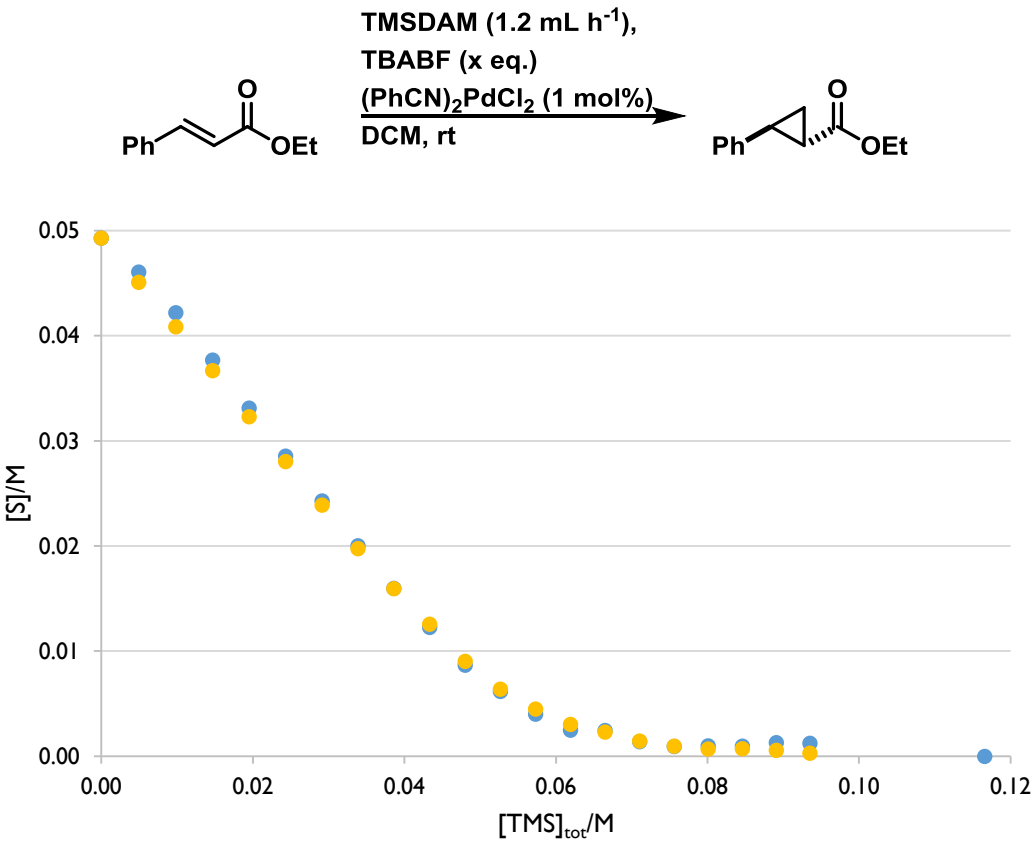

Figure 2.6 Increasing TBABF stoichiometry has no effect on the efficiency of TMSDAM consumption in the latter stages of reaction ($[TBABF]_0$ = 0.55 M, 1.1 eq., blue circles; $[TBABF]_0$ = 0.91 M, 1.5 eq., yellow circles).

This somewhat curious result prompted further investigation. Increasing the amount of substrate demonstrated that the exhaustion of TBABF can ultimately result in productive catalysis shutting down, but this only manifested itself after 1.6 turnovers of the protodesilylating agent, suggesting that this is not the only factor in play.

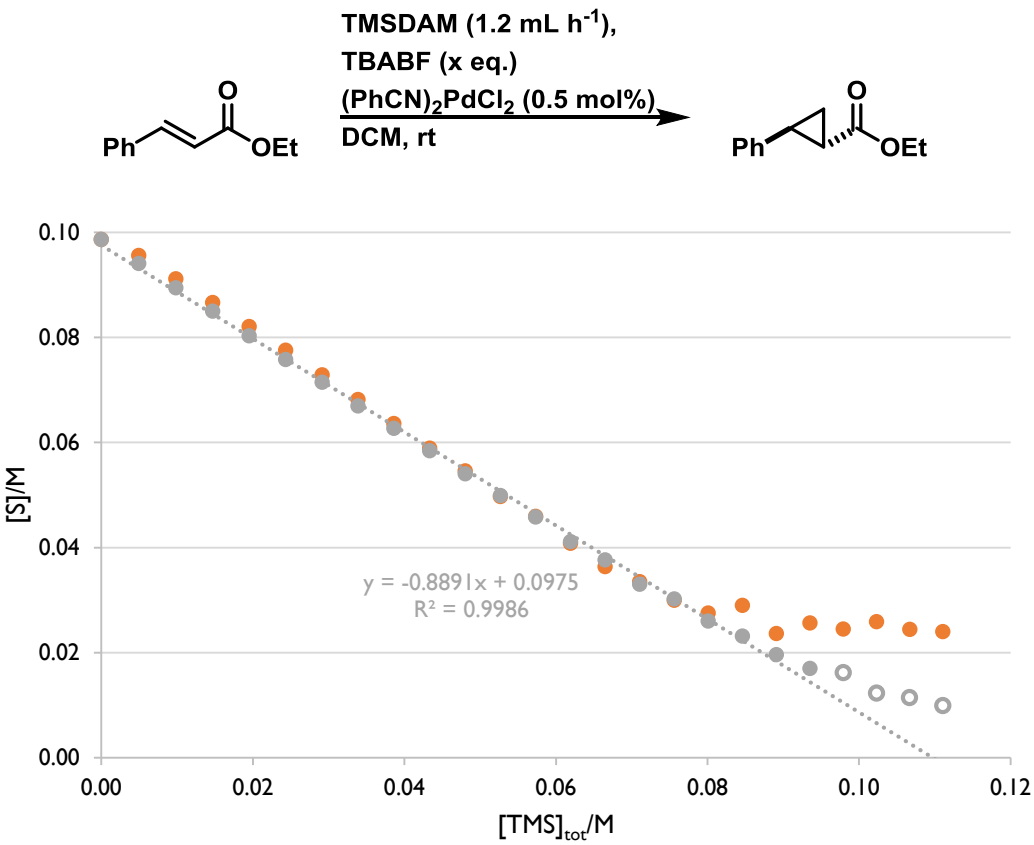

Figure 2.7 TBABF exhaustion proves important only after the point at which decreasing reaction efficiency is apparent ([TBABF]$_0$ = 0.055 M, 0.55 eq., orange circles; [TBABF]$_0$ = 0.11 M, 1.1 eq., grey circles). The line of best fit, showing the efficiency in the earlier stages of reaction, is derived from the data marked by solid grey circles.

The rationale for the surprisingly late onset of TBABF concentration-dependence and the mechanistic implications of such are discussed below (Section 2.3.3, p.54).

2.3.2 Cycle Partitioning: Productive and Unproductive Catalysis

Having ruled out the most obvious explanation for the late-stage change in TMSDAM partitioning in the cyclopropanation of ethyl cinnamate, namely the exhaustion of the desilylating agent, alternative explanations were sought for this unexpected effect. Although earlier studies had demonstrated that precipitated palladium black would turn over TMSDAM unproductively, no palladium black was evident in any reactions employing TBABF.

In a study of the cyclopropanation of styrenes by ethyl diazoacetate under Pd^0 catalysis, Belderrain and co-workers found that the addition of diethyl fumarate (the principal product of diazo coupling) led to a significant inhibition of the cyclopropanation, as determined by nitrogen

evolution.[81] This was attributed to strong binding of fumarate to the zerovalent (NHC)Pd^0 fragment.

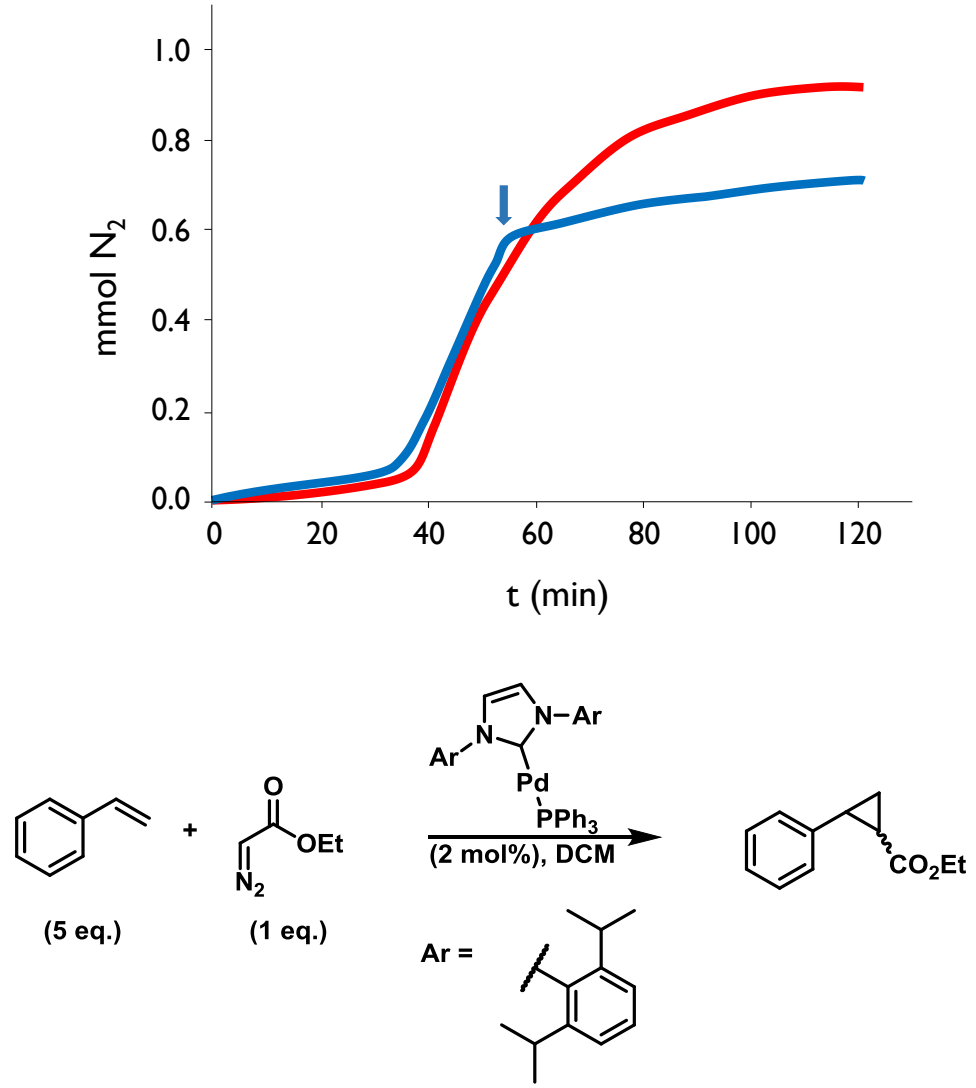

Figure 2.8 - Cyclopropanation of styrene by EDA is inhibited by fumarate, the product of diazo-coupling (Belderrain and co-workers). Graph adapted from reference (*81*). The blue arrow denotes the addition of diethyl fumarate to the reaction mixture.

This led us to consider the possibility that carbene coupling in this system could be responsible for the breakdown in productive catalysis. If the formation of ethylene were the sole side reaction during the initial, efficient, phase of the cyclopropanation reaction, its concentration would be almost equal to that of the remaining substrate at *ca*. 90% conversion (Figure 2.9).

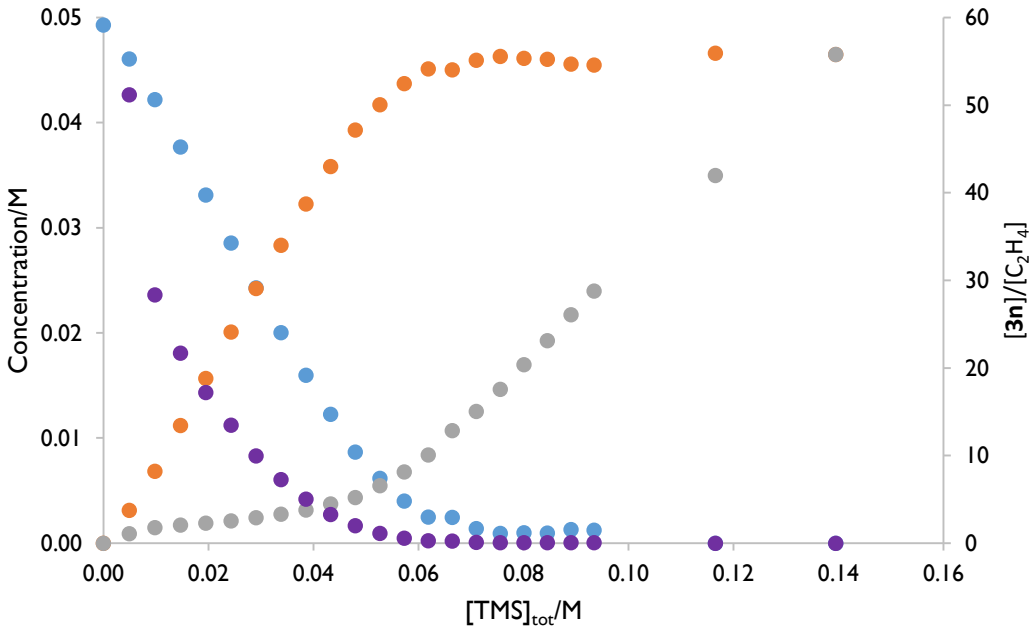

Figure 2.9 TMSDAM partitioning if the inefficient ('unproductive') process produced ethylene. Concentrations: ethyl cinnamate, X – blue circles; product, Y – orange circles; ethylene (calculated, assuming all non-productive TMSDAM consumption generates ethylene) – grey circles. The substrate/ethylene ratio (purple circles) is shown on the right-hand axis.

In Belderrain's system, the generation of the diazo-coupling product led to a significant decrease in the rate of cyclopropanation. As this was monitored by the evolution of nitrogen, it is clear that this rate decrease is due to nitrogen extrusion from the diazo reagent having stalled, rather than diversion of the diazoacetate onto another reaction manifold in the presence of diethyl fumarate. However, we did not find any accumulation of diazo reagent in the reactions with TMSDAM – addition of acetic acid did not result in effervescence – and so a different explanation is required. Assuming ethylene generation to be the unobserved side reaction, the results appeared consistent with an autocatalytic runaway, whereby the ethylene generated in the first phase of reaction leads to a diversion of catalysis into a predominantly ethylene-generating regime (*vide infra*, Scheme 2.12).

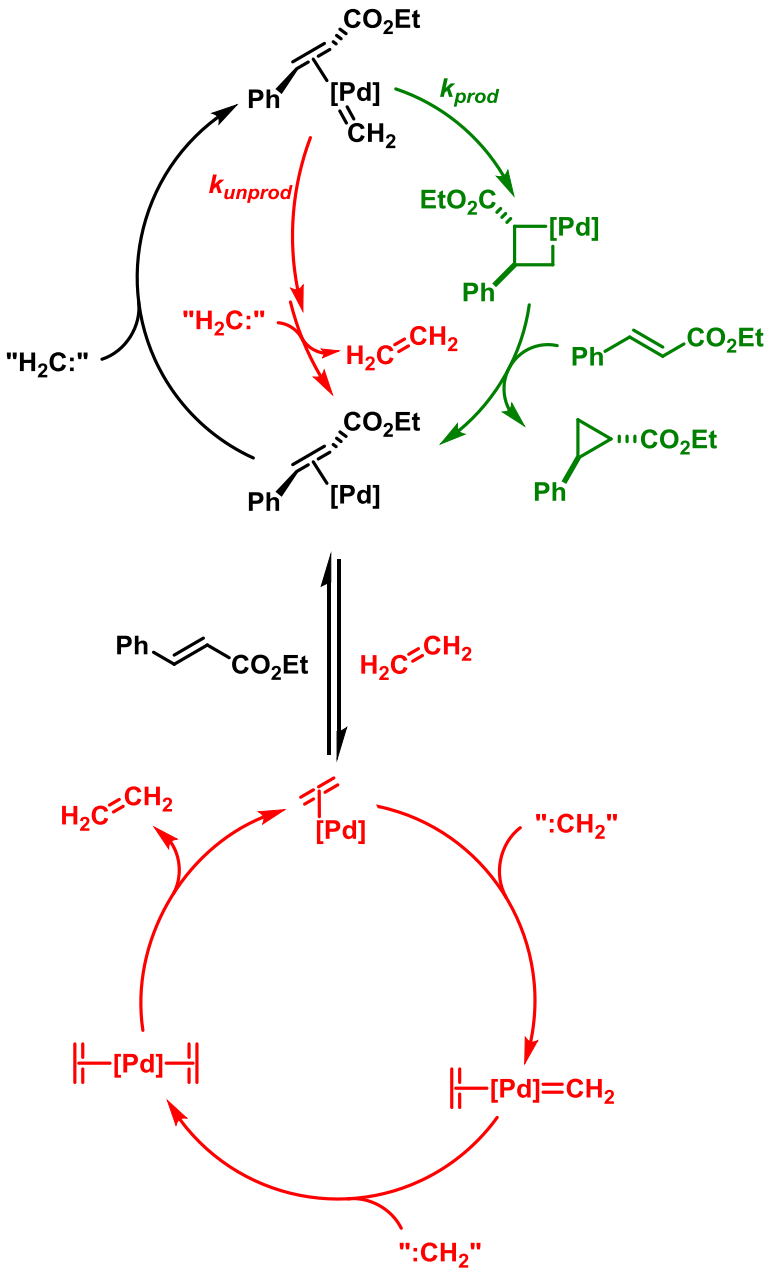

Scheme 2.12 Proposed catalytic cycles for the cyclopropanation of ethyl cinnamate. "H_2C:" denotes a source of methylene. The nature of the carbene fragment delivered to the catalytic cycle – i.e whether protodesilylation occurs on- or off-cycle (i.e. TMSDAM as diazomethane surrogate or precursor, respectively), is addressed below (Section 2.3.3).

The good linear fit obtained between the residual substrate concentration and $[TMS]_{tot}$, the concentration of TMSDAM added, in the initial stages of the reaction (*vide supra*, Figure 2.5) is consistent with a unimolecular partitioning of some substrate-bound intermediate species. The kinetically-favoured pathway (k_{prod}, towards cyclopropanation) represents one pathway from the intermediate; the other (k_{unprod}) generates a species which presumably engages in reaction with another source of $:CH_2$ to ultimately afford ethylene.

If ethylene and ethyl cinnamate are in competition for binding to the catalyst, and ethylene-bound catalyst serves only to generate more ethylene, we arrive at a system where the substrate:ethylene ratio dictates the selectivity for the upper cycle – which has a small inherent inefficiency given by $k_{unprod}/(k_{prod}+k_{unprod})$ – over the lower cycle, which is wholly inefficient. Close examination of Figure 2.9 shows that this critical ratio is approximately 2:1, which is also consistent with results employing additional substrate (Figure 2.7 above, data in grey – the onset of curvature corresponds to $[S]/[C_2H_4]_{calc} = 2$).

The cyclopropanation of two additional substrates, cyclohexenone and *p-tert*-butylstyrene was investigated. It was thought that the styrene would prove a less effective substrate for catalysis, and that cyclohexenone might prove similarly reactive to cinnamate. However, these assumptions were based solely on existing experimental data from the literature, for which adequate quantification was not available – only yields were provided. Given the probable sensitivity of the efficiency of reaction to the diazomethane addition rate, as well as different reaction conditions, over-interpretation of these values is unwise. On the basis of the proposed cycle above, we reasoned that substrates characterised by less efficient catalysis in the early stages of reaction would enter inefficient, ethylene-induced autocatalysis earlier (i.e. at a lower value of $[TMS]_{tot}$).

The cyclopropanation of the styrene was characterised by an initial phase less efficient than with ethyl cinnamate (Figure 2.10). Furthermore, the transition to the inefficient regime was evident at a lower conversion of styrene to product. The calculated ratio of substrate to (assumed) ethylene at this point is approximately 1.5 – that this ratio is lower than for cinnamate is surprising, given the greater π-acidity of the latter substrate.

The effect of slower TMSDAM addition was unexpected; as with cinnamate, no significant change to the efficiency in the first phase of reaction was apparent, but this phase continued to a higher conversion (lower substrate concentration). However, in all cases, less good linear fits were obtained than with cinnamate.

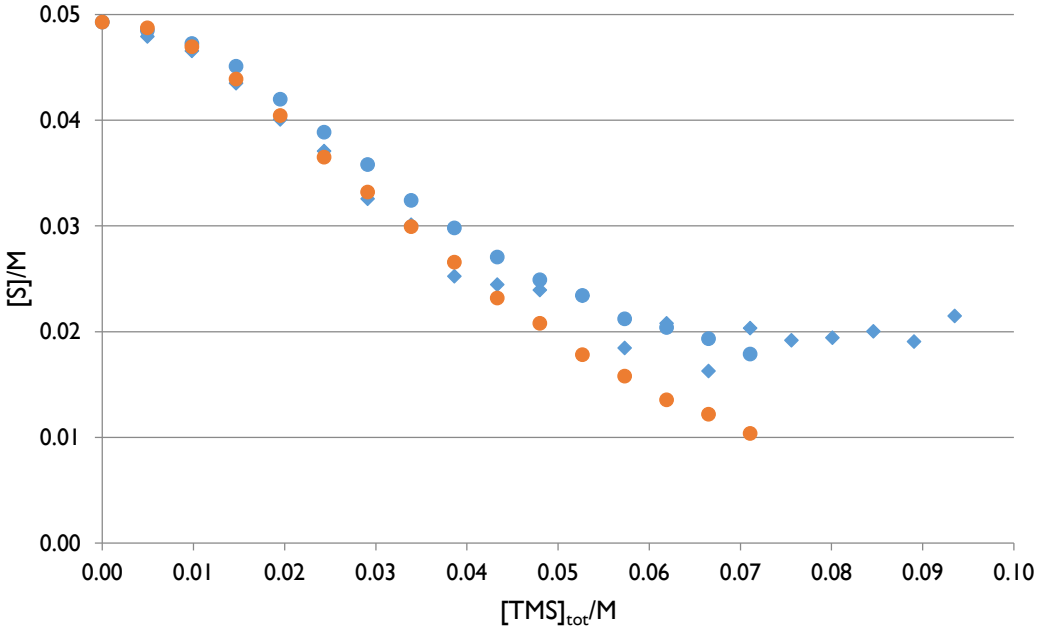

Figure 2.10 Cyclopropanation of *para*-*t*-butylstyrene with TMSDAM addition rates of 1.2 mL h^{-1} (blue circles and diamonds, two separate runs) and 0.15 mL h^{-1} (orange circles).

The results obtained with cyclohexenone were less consistent, with two apparently identical experiments giving substantially different partitioning between productive and unproductive catalysis (Figure 2.11). Considerable scatter is also evident in the reaction profile in one case, suggestive of localised reaction or phase-splitting. However, this was not visibly apparent in the reaction mixture.

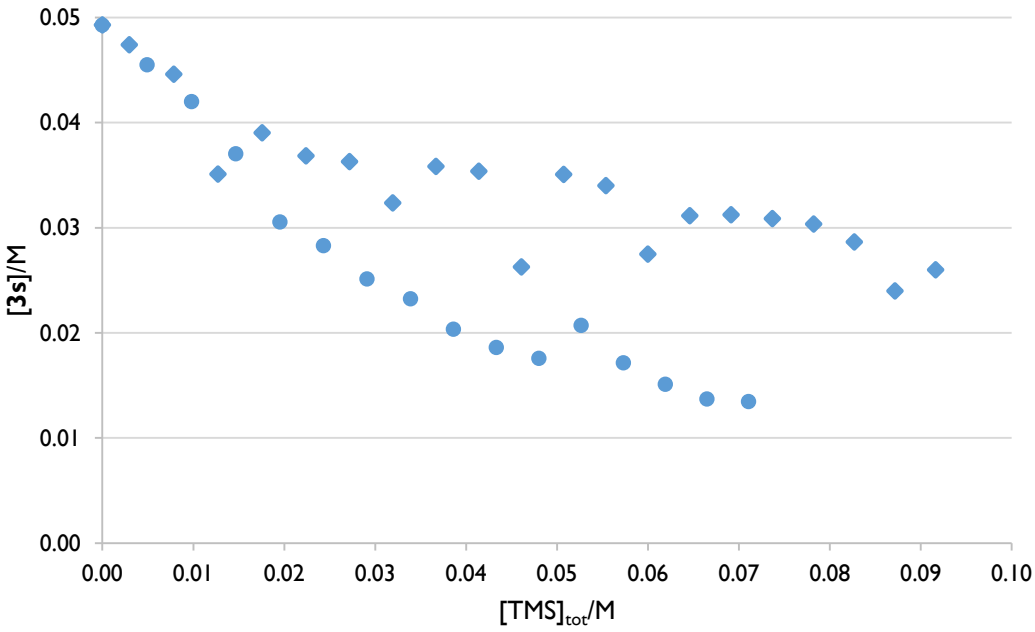

Figure 2.11 Cyclopropanation reactions of cyclohexenone (**3s**) under nominally identical conditions (blue circles and diamonds, two separate runs) give rise to significantly different conversions and apparent partitioning.

2.3.3 Bifluoride Catalysis and the Desilylation Event

The reaction design as presented thus far has been predicated on the stoichiometric protodesilylation of some intermediary species, thereby allowing TMSDAM to act as a diazomethane surrogate. The catalytic cycles presented to this point have reflected this paradigm. However, while it has been demonstrated that superstoichiometric amounts of TMSDAM are required to reach full conversion of substrate alkene to the desired cyclopropane, equally large excesses of TBABF – the species implicated in the proposed stoichiometric protodesilylation – have not been employed.

Mechanistic Proposals

The incongruity between the proposed mechanisms and the observed reactivity could be explained if only productive catalysis (i.e. that which consumes both the alkene substrate and TMSDAM to generate cyclopropane) consumed bifluoride. Given literature precedent from TMSDAM and diazoacetate chemistry (*vide supra*), we would expect the principal side product of cyclopropanation with diazo compounds to be the product of formal carbene coupling. In this reaction, this would lead us to predict that 1,2-bis(trimethylsilyl)ethylene would be formed.

This would consume TMSDAM exclusively, without depleting TBABF. However, this product has never been observed in any reaction carried out under the reaction conditions described herein. Furthermore, neither cyclopropanes derived from this alkene, nor higher oligomeric products of :$CHSiMe_3$ coupling, have been observed (Scheme 2.13).

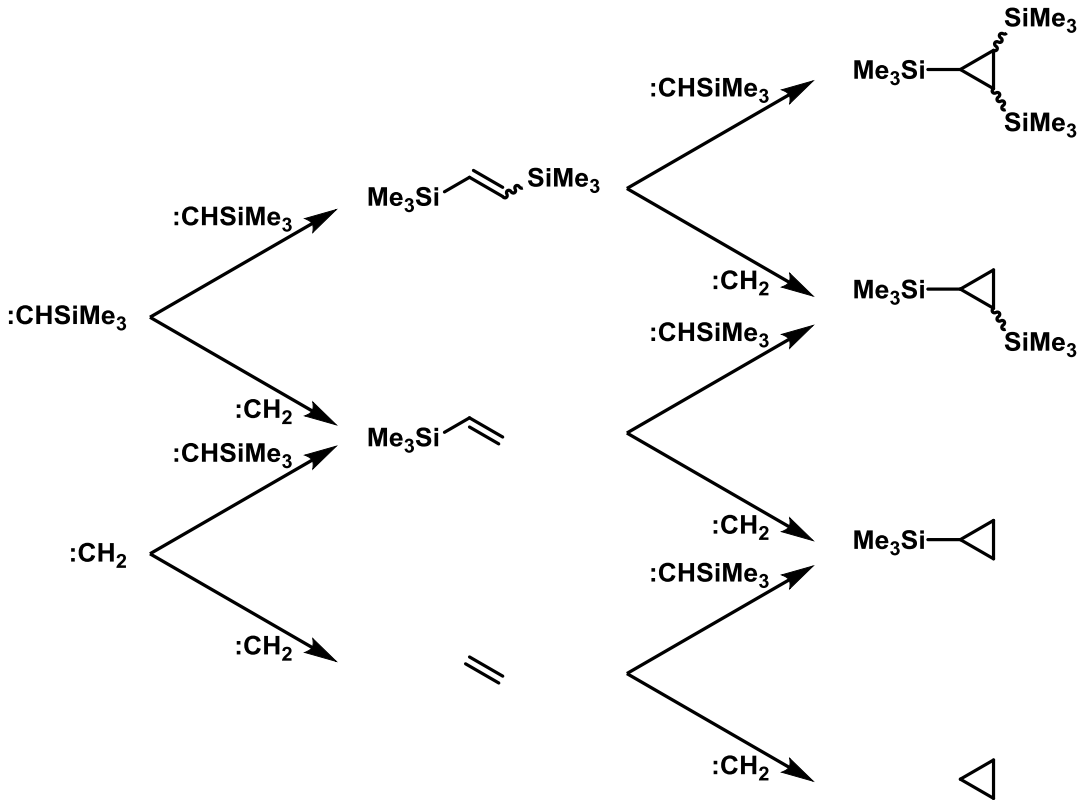

Scheme 2.13 Possible alkene and cyclopropane products resulting from the coupling of silylated and non-silylated carbene moieties.

Furthermore, control experiments employing substoichiometric TBABF (with respect to the alkene substrate) lead to conversions to cyclopropane higher than the TBABF loading (Figure 2.12). As such, this proposal can be dismissed.

A more credible explanation is that all TMSDAM consumption (productive and unproductive) is desilylative in nature, but that the desilylation is either merely catalytic in TBABF, or that another species present is capable of effecting the same transformation. However, there would appear to be no obvious candidates for the second reagent, at least not amongst the reagents deliberately added in the course of setting up the reaction. These cyclopropanation reactions are, though, set up open to air, without using anhydrous solvents, and without any particular attempt to dry the reagents employed. This is undoubtedly convenient from a practical

perspective, but does not allow us to rule out the possibility that water from incompletely dried reagents, solvents or glassware is having an impact on the system under study.

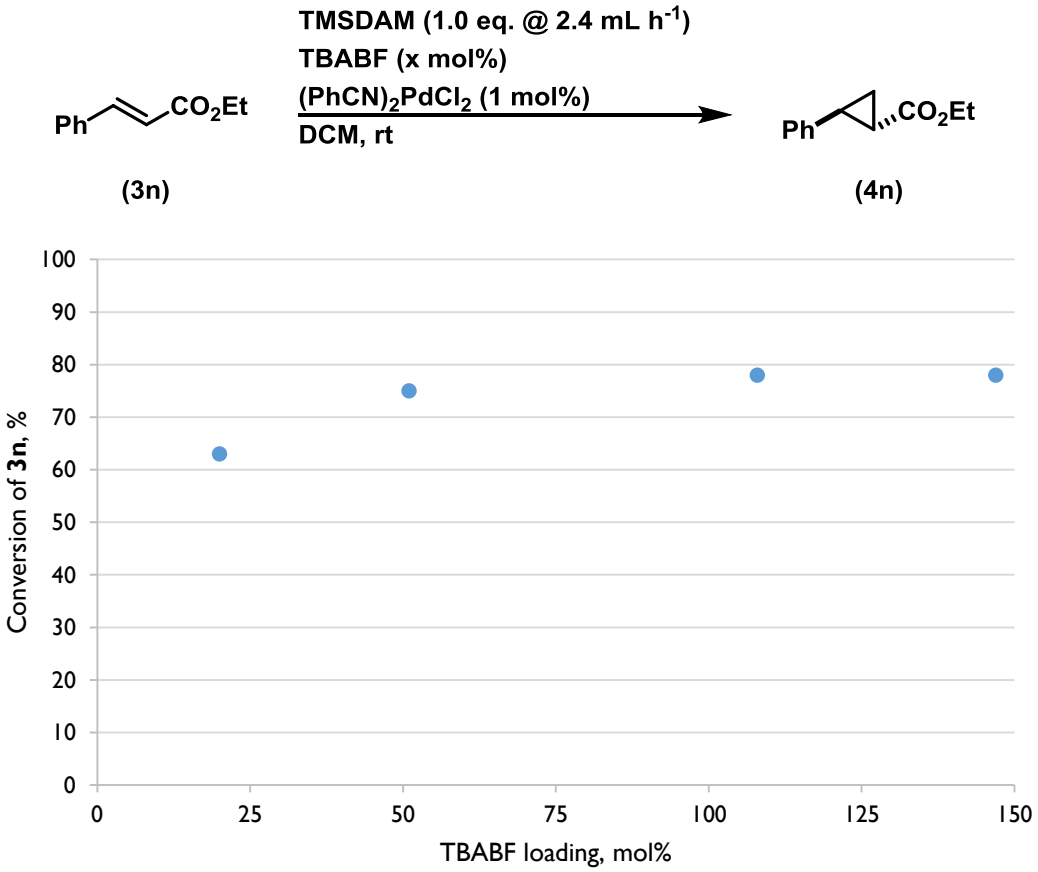

Figure 2.12 TBABF promotes desilylative cyclopropanation to an extent higher than its apparent loading.

In the second mechanistic hypothesis advanced above, the generation of non-silylated side products must also be addressed. As stated previously, fully silylated side products (derived formally from :$CHSiMe_3$ oligomerisation) were not observed. However, side products bearing fewer silyl groups (Scheme 2.13) were also not evident in NMR spectra of reaction mixture aliquots, providing further evidence that all TMSDAM added is desilylated *en route* to side product formation.[1] Although these observations alone do not allow any mechanisms to be ruled out, they can be seen as suggestive of a rapid and complete liberation of diazomethane from TMSDAM on contact with TBABF. In order to probe the plausibility of this *in situ* diazomethane

[1] This does not rule out the possibility that nascent silylated side products are themselves subject to protodesilylation. However, this would also consume TBABF, resulting in the same apparent stoichiometric deficiency of the desilylating agent.

release, and the proposed bifluoride catalysis, the direct reaction of TMSDAM with TBABF was studied by NMR spectroscopy.

In Situ Diazomethane Generation and Unintentional Catalysis

Substoichiometric aliquots of TMSDAM solution were added to a solution of TBABF in CD_2Cl_2, resulting in an orange-yellow solution. ^{1}H NMR spectra acquired immediately after the addition (<3 minutes) clearly demonstrated the absence of TMSDAM in solution. However, the appearance and growth of a singlet at approximately 3.30 ppm was evident (Figure 2.13). This chemical shift is consistent with that reported for diazomethane by Steyn and co-workers,[82] lending credence to the hypothesis that the cyclopropanation reaction proceeds *via* direct protodesilylation of TMSDAM to afford diazomethane.

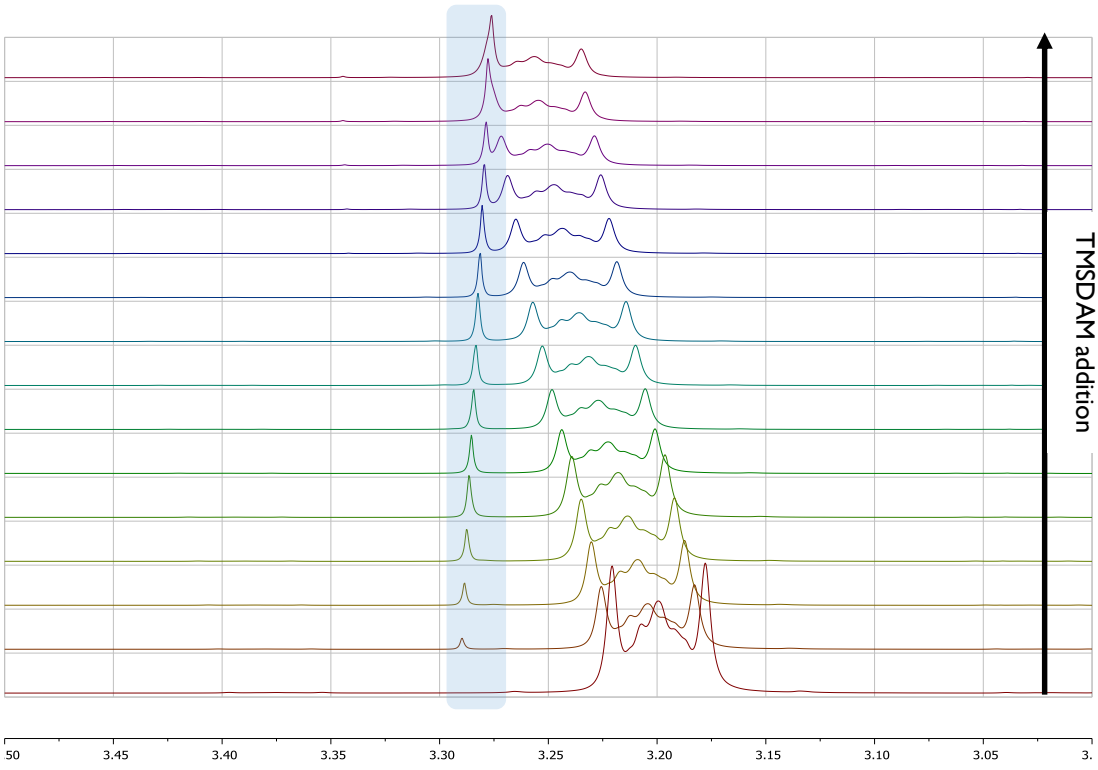

Figure 2.13 Partial ^{1}H NMR spectra following sequential additions of TMSDAM to TBABF in CD_2Cl_2, showing the generation of diazomethane (shaded blue). The multiplet at ~3.20 ppm is from the tetrabutylammonium cation.

Significantly downfield, at ~16 ppm, the typically broad resonance due to HF_2^- (often overlooked due to overzealous baseline correction) was observed to resolve into a binomial triplet, with a coupling constant of 121.5 Hz. This was matched in the ^{19}F NMR, where the typical broad singlet due to bifluoride became a well-resolved doublet with successive TMSDAM

additions (Figure 2.14). Closer inspection of the ^{19}F NMR also reveals a small 1:1:1 triplet slightly upfield of the HF_2^- resonance, with a coupling constant of 18.3 Hz ($=^1J_{H\text{-}F}(HF_2^-)\gamma_D/\gamma_H$), ascribed to DF_2^-.

The final two aliquots of TMSDAM added in this experiment were superstoichiometric with respect to TBABF, and so the diazomethane generation observed is formally due to TBABF catalysis. The incorporation of trace deuterium in bifluoride (*ca*. 2% of the total), presumably from D_2O present in the CD_2Cl_2 reaction solvent, suggests a role for water in the recycling mechanism as previously postulated. However the limited extent of DF_2^- formation (relative to HF_2^- re-formation) points to another source of water being present. Although apparently less hygroscopic than the corresponding fluoride, it must be assumed that tetrabutylammonium bifluoride contains at least enough water to be responsible for the modest catalysis evident both in this experiment (1.15 turnovers) as well as in numerous cyclopropanations. The formation of trace monodeuterated diazomethane ($CHDN_2$), although not observed, cannot be conclusively ruled out – its resonance in the ^1H NMR spectrum would be broadened due to $^2J_{H\text{-}D}$ coupling, and all too easily obscured by the much more intense shifting multiplet arising due to tetrabutylammonium methylene protons (Figure 2.13).

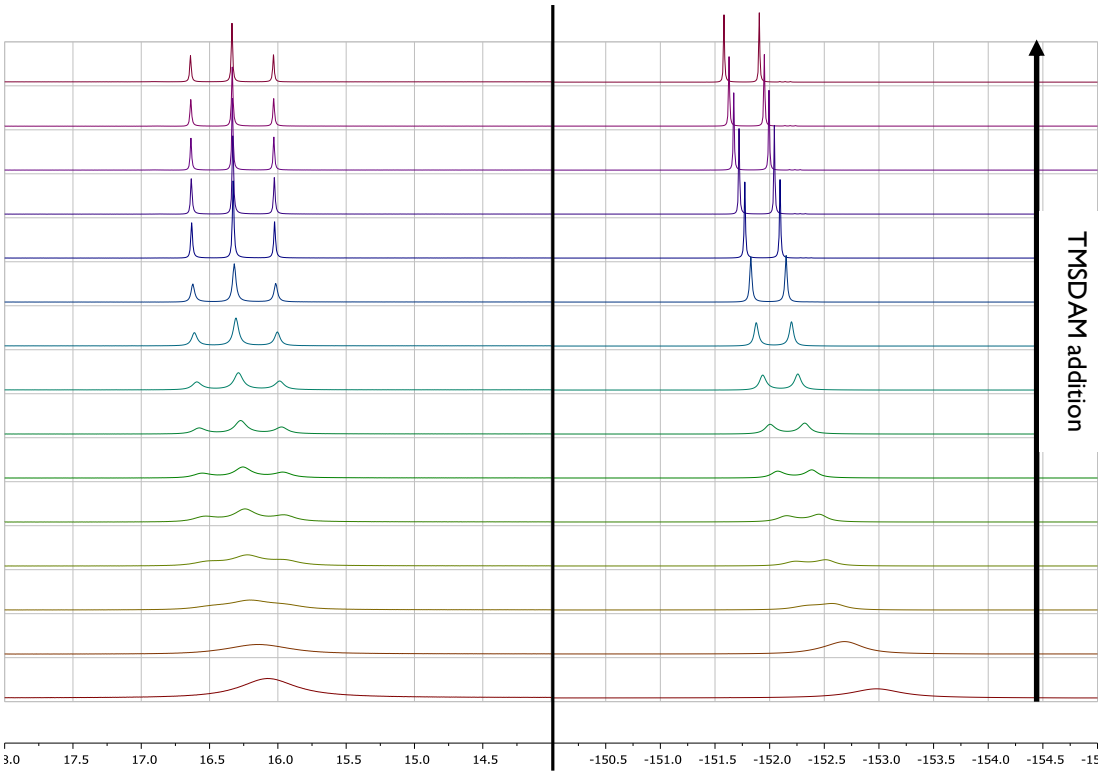

Figure 2.14 Partial ^1H (left) and ^{19}F (right) NMR spectra of reaction mixtures resulting from the addition of TMSDAM to TBABF, showing the progressive resolution of scalar coupling in bifluoride anion.

The unexpected resolution of $^{1}J_{H\text{-}F}$ couplings in both ^{1}H and ^{19}F NMR spectra must also be addressed. Control experiments demonstrated that this was not simply due to the addition of hexane (as the solvent for TMSDAM). Prior to this finding, the coupling in bifluoride anion had only been resolved at temperatures of −70 °C or below.[72] Golubev, Limbach and co-workers have investigated the scalar couplings in *n*-Bu_4N^+ $F(HF)_n^-$ salts using a combination of NMR spectroscopy (^{1}H and ^{19}F in CDF_3/CDF_2Cl at -153 °C) and *ab initio* computational methods.[83] Neither this study, nor later related reports by the same groups, suggest mechanisms for H-F exchange.[84,85] Our results are consistent with the exchange being catalysed by water; the protodesilylation of TMSDAM ultimately results in the reaction solution being dried, as traces of water are consumed in the regeneration of bifluoride. Although Limbach and Golubev make clear their efforts to dry the materials being studied, no quantification of water concentrations is given, and the method employed for drying (azeotropic distillation with dichloromethane) is not particularly efficient.

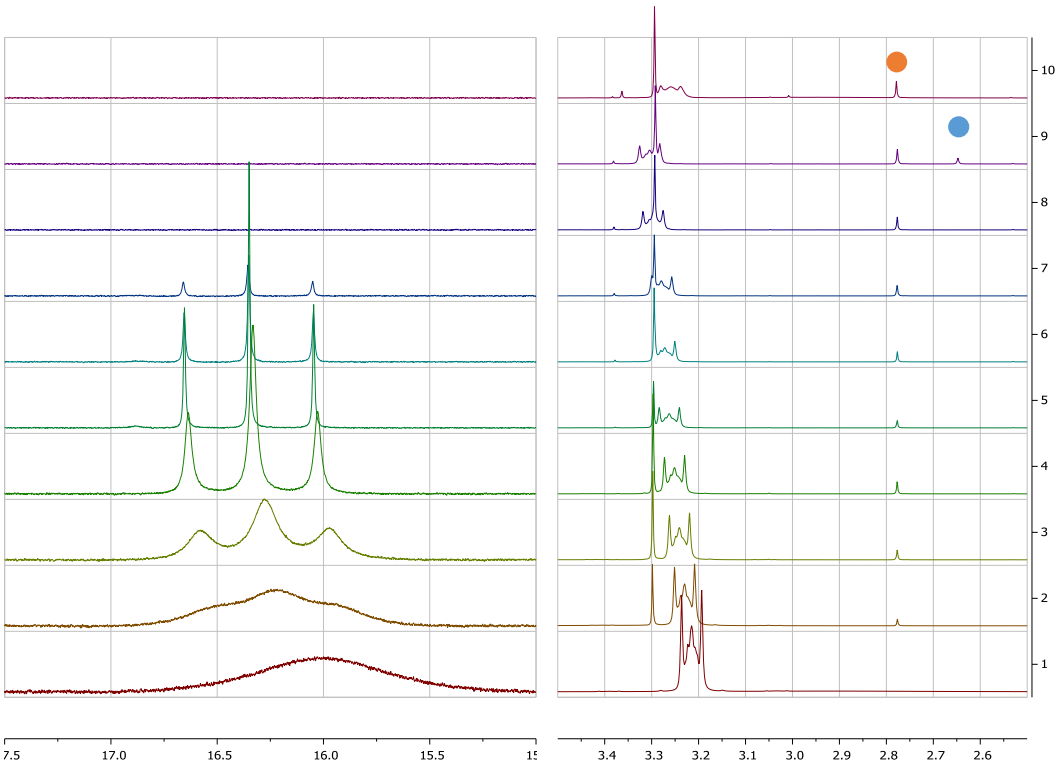

Figure 2.15 Partial ^{1}H NMR spectra showing consumption of HF_2^-, formation of diazomethane (singlet, ~3.3 ppm) and subsequent accumulation of TMSDAM (blue circle). The peak at 2.74 ppm (orange circle) is due to a catalytically-innocent impurity, (chloromethyl)trimethylsilane, present in TMSDAM solution. Intensities of left and right subspectra are not to scale.

Repeating the experiment with a much smaller amount of TBABF allowed the breakdown of bifluoride catalysis to be explored. Following approximately four turnovers, accumulation of

TMSDAM (2.65 ppm) was evident (Figure 2.15 above, spectrum nine), as was the disappearance of bifluoride (Figure 2.15, spectra eight and nine). The breakdown of catalysis was accompanied by the appearance of signals characteristic of fluorotrimethylsilane ($FSiMe_3$) in ^{1}H, ^{19}F (Figure 2.16) and ^{29}Si NMR spectra. Up until this point, three signals were observed in the upfield region of the spectrum, one of which (0.21 ppm) is readily assigned to (chloromethyl)trimethylsilane (Figure 2.15). The two that remain were thought likely to be trimethylsilanol (Me_3SiOH) and hexamethyldisiloxane ($Me_3SiOSiMe_3$). The addition of water (prior to spectrum ten, Figure 2.15) restarted catalysis, with complete consumption of the accumulated TMSDAM. However, the distribution of fluoride following the addition is not clear, with the ^{19}F NMR spectrum consisting of a broad resonance at the same chemical shift as fluorotrimethylsilane (Figure 2.16, spectrum ten, top), some 5 ppm upfield of its location at the start of the reaction. Although distant from the bifluoride peaks in earlier spectra, the mobility of the bifluoride peak in ^{19}F NMR has been noted by Lennox and Lloyd-Jones in their study of organotrifluoroborate hydrolysis (chemical shifts ranging from −139 to −180 ppm in THF/MeCN/H_2O mixtures).[70]

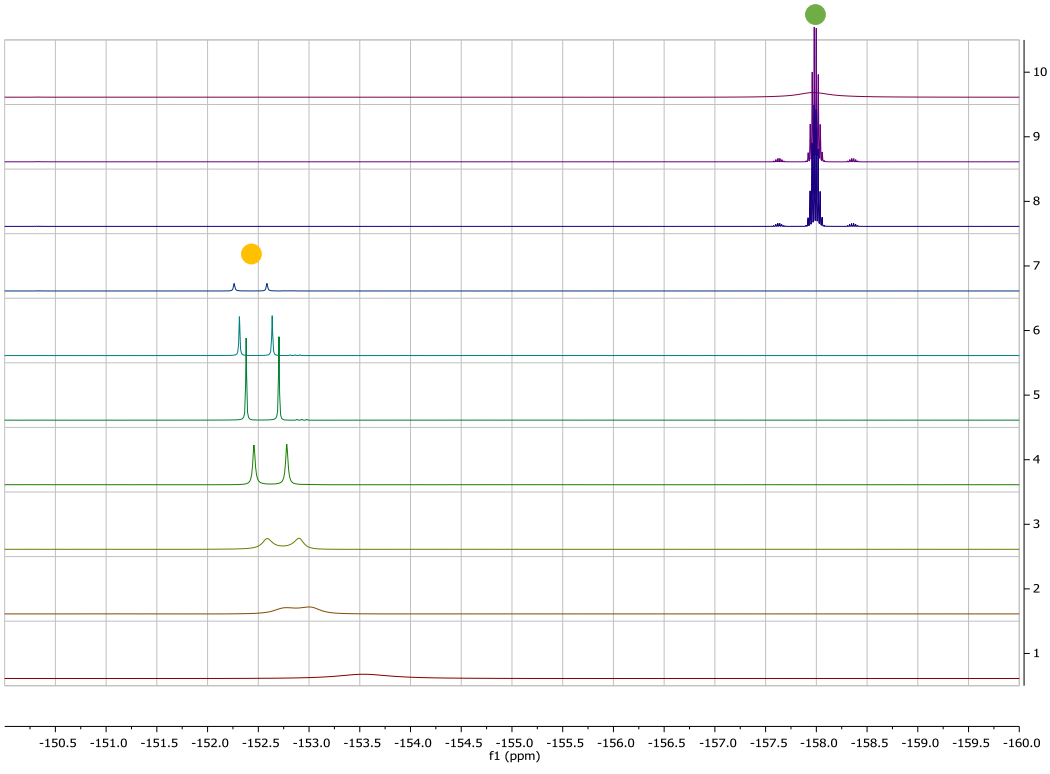

Figure 2.16 ^{19}F NMR spectra showing formation of fluorotrimethylsilane (green circle) upon exhaustion of HF_2^- (yellow circle). $^{3}J_{F\text{-}H}$ and $^{1}J_{F\text{-}Si}$ couplings of 7.5 and 274 Hz respectively can be measured from spectra eight and nine, in agreement with coupling constants measured in ^{1}H and ^{29}Si NMR spectra.

The data above are consistent with the catalytic cycle depicted below (Scheme 2.14) in which bifluoride anion reacts with TMSDAM to generate diazomethane, fluorotrimethylsilane and fluoride anion. Subsequent hydrolysis of the silyl fluoride affords the corresponding silanol and hydrogen fluoride, which recombines with fluoride to generate the hydrogen-bonded HF_2^- catalyst.

Although the broad strokes of the cycle proposed below are backed up by experiment, the details – particularly the nature of the unobserved intermediates – are open to argument. For example, mechanisms implicating the intermediacy of difluorotrimethylsilicate ($Me_3SiF_2^-$) in place of fluorotrimethylsilane and fluoride anion cannot be ruled out on the basis of the evidence in hand.

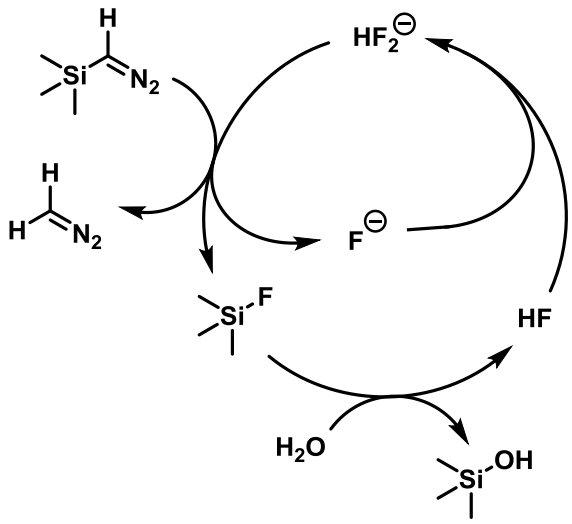

Scheme 2.14 Proposed catalytic cycle for the bifluoride-catalysed protodesilylation of TMSDAM, promoted by water.

Exploiting Unintentional Catalysis – Designed Methods for Bifluoride Regeneration

With strong evidence in hand for the "unintentional bifluoride catalysis" the possibility of deliberately effecting such a process was explored. Although the addition of exogenous water had proven effective in restarting turnover from TMSDAM to diazomethane, the impact of this on the full catalytic system was unknown, and deemed worthy of testing. It was decided to test initially the effects of water addition in reactions with stoichiometric TBABF. Given the proposed role of the tetrabutylammonium cation in stabilising the catalytically-active palladium species, and the previously demonstrated sensitivity of the catalyst to protic solvents in early

optimisation studies, it was thought that simultaneously changing the concentrations of both of these variables in the directions proposed would lead to a complete failure of catalysis. Pleasingly, carrying out the cyclopropanation reaction in the presence of two equivalents of added water had a positive effect in the later stages of the reaction. However, the addition of four equivalents led to a complete breakdown of productive catalysis due to the rapid formation of palladium black (Figure 2.17). These tests are, though, somewhat artificial; the presence of (super-)stoichiometric quantities of water from the beginning of the reaction is not necessary. However, the reaction profile from the experiment employing two equivalents of water demonstrates that the diminished selectivity for productive catalysis in the later stages of reaction is not solely due to the exhaustion of an active desilylating agent. In order to sustain protodesilylation with catalytic bifluoride, water is required in equimolar amounts to TMSDAM.[2] Given the evident sensitivity of the catalytic system to high concentrations of water, it was thought that this could be more easily achieved by the simultaneous addition of TMSDAM and water, thus allowing the temporal water concentration to remain low. However, the immiscibility of water and the hexane solution of TMSDAM does not allow for simultaneous addition of pre-hydrated TMSDAM solution with one syringe, which would represent a practically convenient method.

[2] This assumes the terminal silicon-containing product of bifluoride recycling is trimethylsilanol, Me_3SiOH. If this is prone to self-condensation under the reaction conditions (or is itself capable of effecting bifluoride recycling), as appears to be the case (*vide supra*) then only 0.5 equivalents of water relative to TMSDAM would be required.

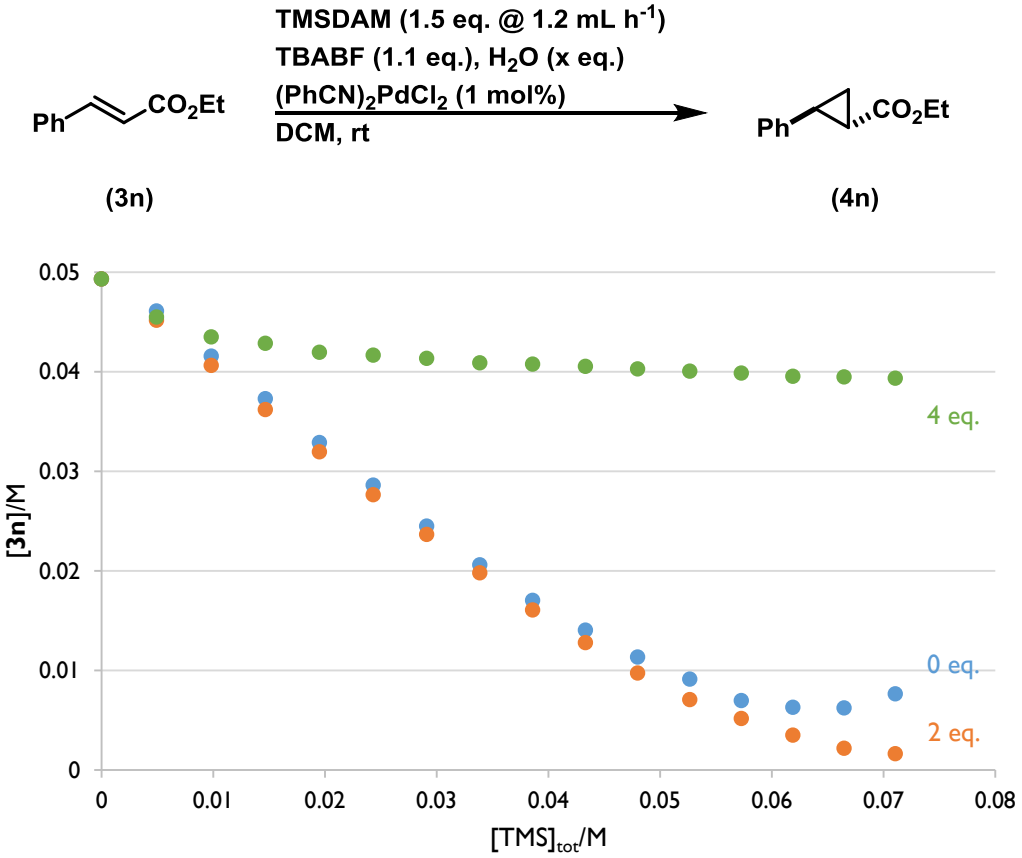

Figure 2.17 Effect of water addition on the cyclopropanation of ethyl cinnamate.

The potential for replacing water with an organic-miscible reagent was then considered. Somewhat ironically, given the very first experiments carried out in screening conditions for the protodesilylative cyclopropanation with TMSDAM (*vide supra*, Sections 2.1.1-2.1.2), alcohols were determined to be ideal candidates. The addition of 1:1, 2:1 and 4:1 solutions of EtOH:TMSDAM in hexane/DCM was found to be amenable to productive cyclopropanation catalysis (Figure 2.18). Given earlier findings relating to the importance of efficient mixing (*vide supra*, Section 2.3.1), it was thought possible that pre-dilution of the TMSDAM solution with the bulk reaction solvent (DCM) might be responsible for the improvement in reaction efficiency observed. However, an EtOH-free control reaction demonstrated this was not the case.

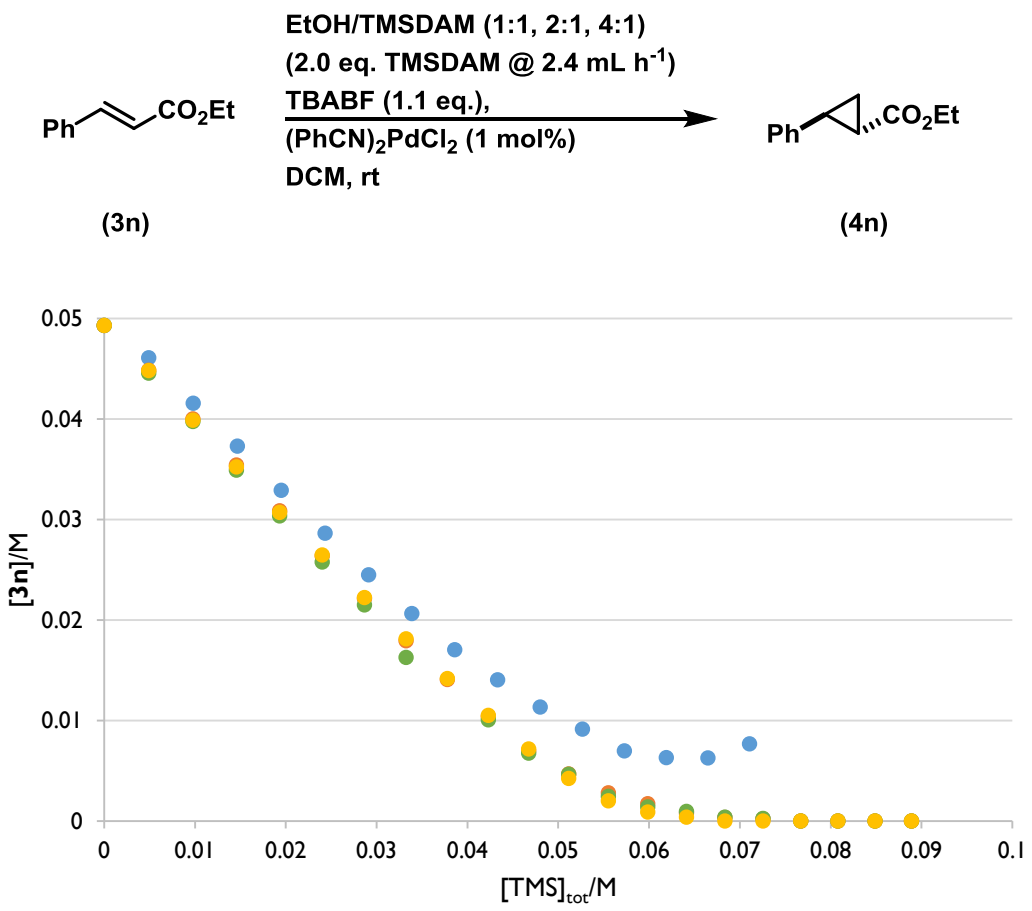

Figure 2.18 Effects of simultaneous EtOH/TMSDAM addition (1:1 – orange circles; 2:1 – green circles; 4:1 – yellow circles) on the cyclopropanation of ethyl cinnamate (**3n**), compared to an EtOH-free reaction with the same batch of TBABF (blue circles). The increased volumetric addition rate of TMSDAM relative to previous experiments (*vide supra*) reflects the dilution by half of the commercial TMSDAM/hexane solution with pre-prepared stock solutions of EtOH in DCM. The *molar* addition rate (2.16 mmol h^{-1}) is identical to earlier experiments performed at 1.2 mL h^{-1}.

With these promising results in hand, the key experiments with catalytic quantities of TBABF were undertaken. Although the addition of EtOH prior to TMSDAM proved ineffective (Figure 2.19, reactions proceeded to give only limited conversions of substrate, and the reaction mixture turned slightly green in colour prior to the formation of very fine black particulate palladium), the simultaneous addition of EtOH and TMSDAM proved highly effective with 20 mol% TBABF. Conversely, the reaction with 10 mol% TBABF gave rather poor results, lending further support to the theory that tetrabutylammonium cation plays a crucial role in the stabilisation of the palladium catalyst (Figure 2.19, data in orange).

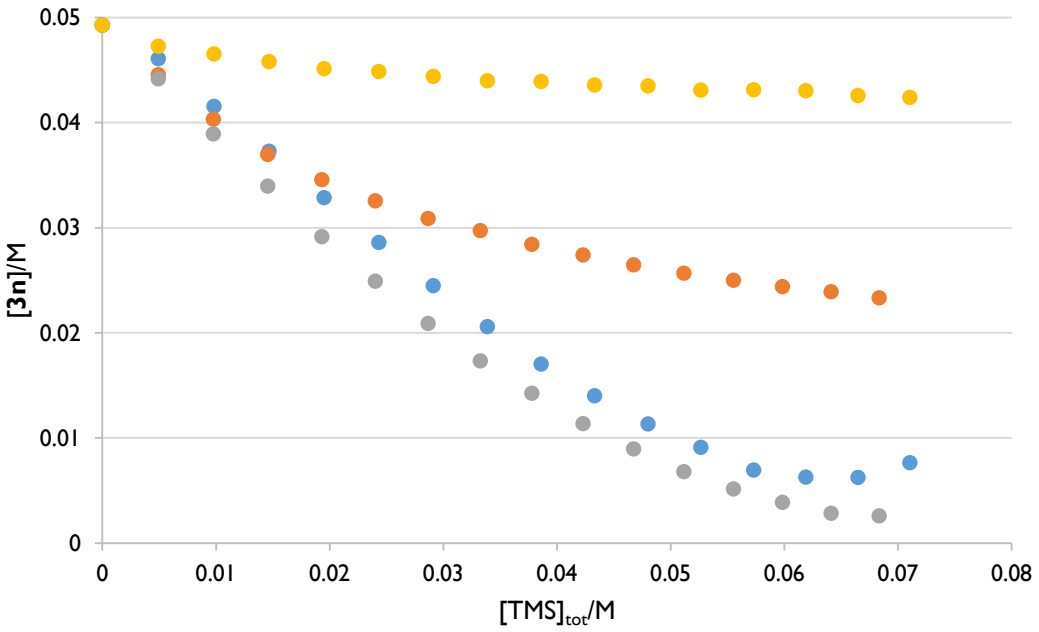

Figure 2.19 Ethanol-driven bifluoride catalysis in the cyclopropanation of ethyl cinnamate (**3n**) with (i) 17 mol% TBABF, 2 eq. EtOH added prior to TMSDAM (yellow circles), (ii) 10 mol% TBABF, 1:1 EtOH:TMSDAM (orange circles), (iii) 20 mol% TBABF, 1:1 EtOH:TMSDAM (grey circles) compared to (iv) ethanol-free reaction with 1.1 eq. TBABF (blue circles).

The 20:1 ratio of TBABF:$(PhCN)_2PdCl_2$ successfully employed above is reminiscent of the Jeffery conditions for Heck coupling,[86] which employs tetrabutylammonium salts in order to stabilise the active catalytic species. Reetz and Westermann have shown that this is due to the formation of $R_4N^+X^-$-stabilised palladium colloids by transmission electron microscopy.[87] The implication of stabilised nanoparticulate palladium in cyclopropanation catalysis would appear to be in agreement with the findings of Branchadell, Gómez, Ortuño and co-workers.[44]

Designed Bifluoride Catalysis and *In Situ* Diazomethane Generation

Following the discovery that ethanol could drive the regeneration of bifluoride, evidence was sought in support of a mechanism analogous to that proposed with water (*vide supra*, Scheme 2.14). Consequently, the *in situ* generation of diazomethane, resulting from simultaneous addition of TMSDAM and EtOH to a catalytic amount of TBABF, was re-investigated by NMR spectroscopy. As expected, complete consumption of TMSDAM was evident, as was the appearance of the characteristic singlet at 3.34 ppm previously attributed to diazomethane. Interestingly, in a number of the spectra it was possible to observe a 1:1:1 triplet slightly upfield (13 ppb) of the diazomethane singlet, with a coupling constant of 0.66 Hz (Figure 2.20). This

value (attributed to $^{2}J_{H\text{-}D}$) is in excellent agreement with the literature value for the coupling constant in monodeuterated diazomethane (**1-*d*$_1$**).[88],[3]

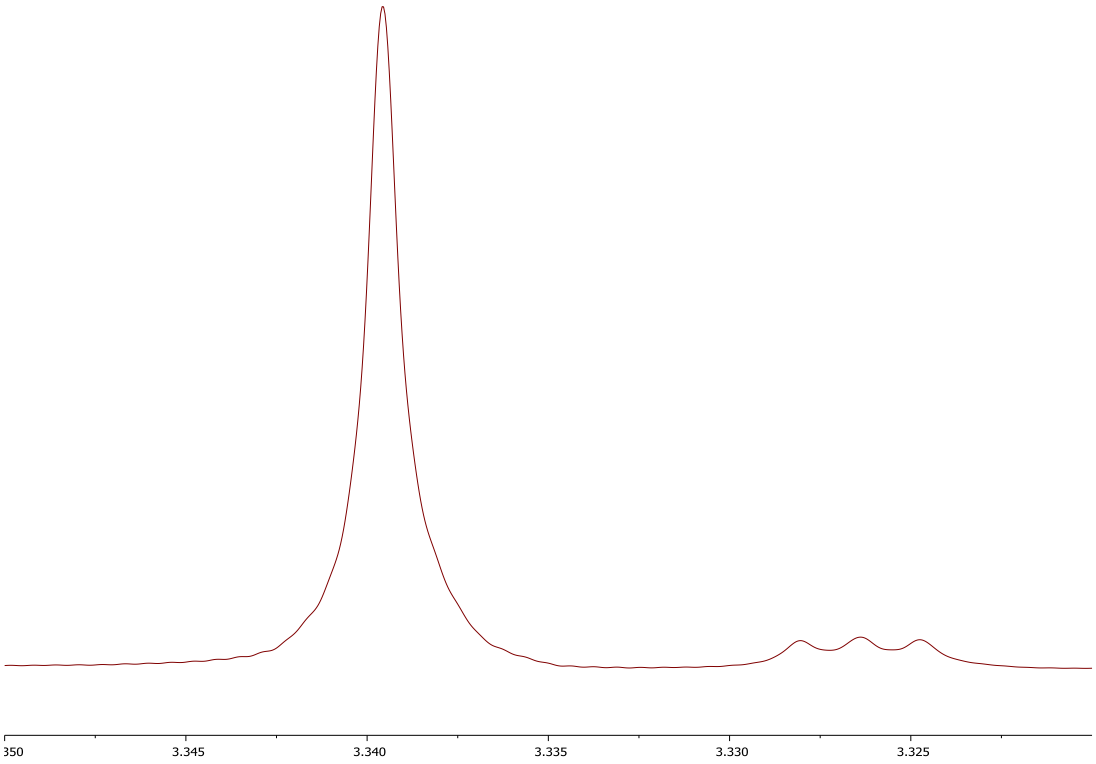

Figure 2.20 Partial ^{1}H NMR spectrum showing the presence of CH_2N_2 (**1-*h*$_2$**) and $CHDN_2$ (**1-*d*$_1$**) following the addition of three aliquots of TMSDAM/EtOH to a solution of TBABF in DCM (representing 3.6 turnovers of bifluoride). The observed deuterium incorporation (ca. 20%) arises from D_2O present in commercial DCM-d_2.

The clear involvement of D_2O (and therefore H_2O) in the bifluoride recycling (or in the H/D exchange of diazomethane), despite the presence of ethanol, prompted an investigation of the reaction under anhydrous conditions. Although the drying of the solvent is easily achieved, methods for the preparation of anhydrous TBABF remain elusive, thereby preventing an obvious means by which the necessary experiments could be undertaken. However, it was realised that by carrying out the *in situ* diazomethane generation under ethanol-free conditions, an anhydrous solution could be generated. Addition of TMSDAM/EtOH to this would demonstrate the feasibility of closing a catalytic cycle by the reaction of fluorotrimethylsilane, fluoride anion and ethanol to regenerate bifluoride (Scheme 2.15).

[3] McGarrity and Cox report $^{2}J_{H\text{-}H}$ = 4.6 Hz. Backcalculation of this (experimentally unobservable) value to the $^{2}J_{H\text{-}D}$ that was presumably measured gives a value of 0.70 Hz.

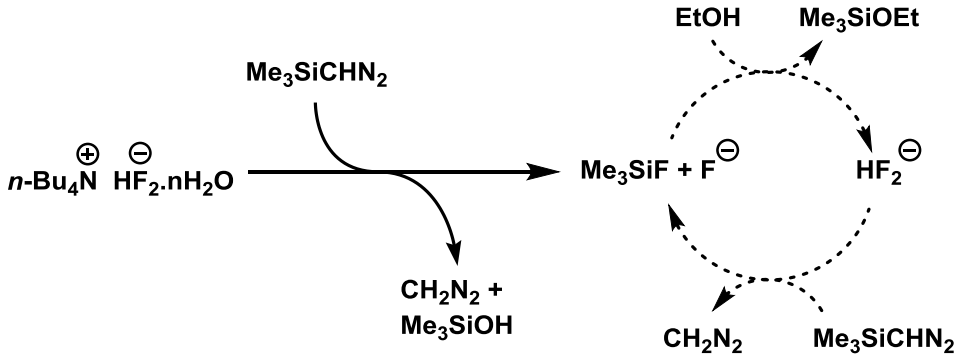

Scheme 2.15 TBABF drying can be achieved by the protodesilylation of TMSDAM, allowing the regeneration of bifluoride with EtOH (dashed arrows) to be tested under anhydrous conditions.

The reaction of ethanol-free TMSDAM with TBABF proceeded as expected. Following approximately five turnovers of bifluoride, NMR spectroscopy (^{1}H and ^{19}F) clearly showed the presence of fluorotrimethylsilane, diazomethane and a small amount of residual TMSDAM, indicative of stalled protodesilylation catalysis. Intriguingly, the subsequent addition of TMSDAM/EtOH did not result in any further turnover of TMSDAM to diazomethane (Figure 2.21). The addition of a large excess (3.9 equivalents relative to the total TMSDAM added) of ethanol also proved ineffective in restoring catalysis. Furthermore, no change was apparent in the ^{19}F spectrum – Me_3SiF was clearly unreactive towards EtOH.

The apparent inability of ethanol to regenerate bifluoride from fluorotrimethylsilane appears to argue against a catalytic cycle analogous to that proposed above (Scheme 2.14). However, given that the ability of ethanol to regenerate bifluoride had already been established (albeit in conditions where trace water may be present), this observation proved somewhat confusing. One possible explanation that was considered is that the regeneration of bifluoride under ethanolytic conditions is bifluoride-catalysed (i.e. the regeneration mechanism is autocatalytic).

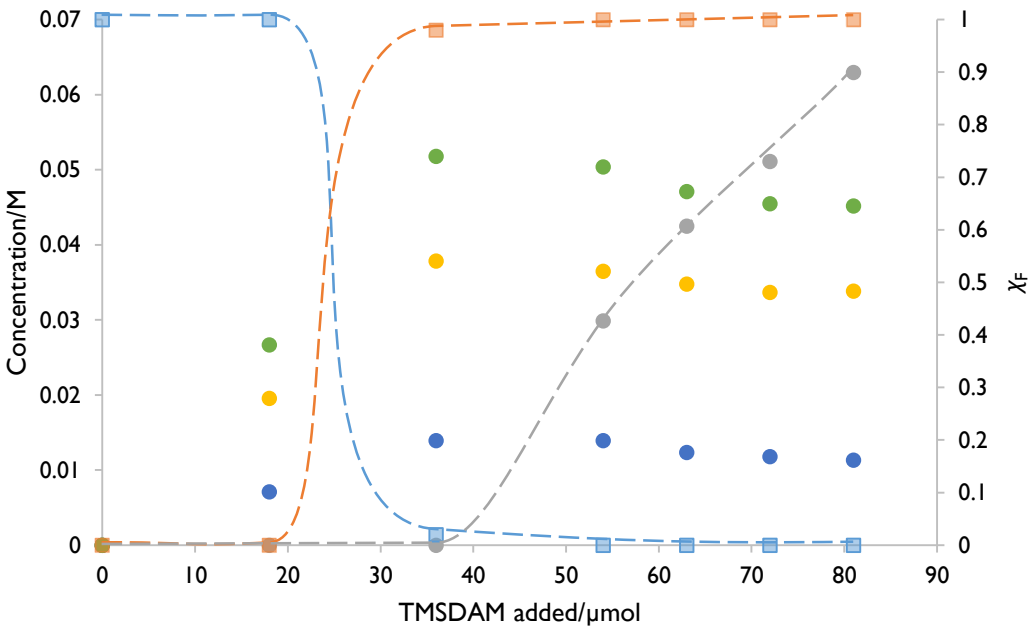

Figure 2.21 Concentrations of TMSDAM (**24**, grey circles), $C^1H_2N_2$ (**1-*h*$_2$**, yellow circles), $C^1H^2HN_2$ (**1-*d*$_1$**, dark blue circles), and CH_2N_2 (sum of the two observed isotopologues, green circles); and fluoride partitioning between HF_2^- (light blue squares) and Me_3SiF (orange squares) shown as mole fraction of exchangeable fluoride, χ_F. The first two TMSDAM additions were EtOH-free, the remainder are additions of 1:1.6 TMSDAM:EtOH. Dashed lines are intended solely as a guide to the eye.

If correct, this would explain the sustained catalysis under normal conditions (where the constant influx of ethanol maintains bifluoride concentration, and therefore regenerative turnover), and the inability to restart catalysis by the addition of ethanol once stalled. In order to test this hypothesis, the generation of diazomethane from TMSDAM and TBABF was repeated, and taken to a point at which water-promoted bifluoride catalysis stalled. Once again, the addition of ethanol proved ineffective in restarting catalysis. In accordance with the hypothesis proposed, the subsequent addition of a catalytic amount of TBABF led to complete conversion of accumulated TMSDAM into diazomethane. The ^{19}F NMR spectrum following TBABF addition consisted of only one peak (Figure 2.22), however the nature of the fluorine-containing species is unclear. Although at the same chemical shift as $FSiMe_3$, the $^3J_{F\text{-}H}$ couplings are not resolved, and satellites due to coupling to spin-dilute ^{29}Si are absent. The characteristic $^1J_{Si\text{-}F}$ coupling present in $FSiMe_3$ is also absent in the ^{29}Si NMR spectrum.

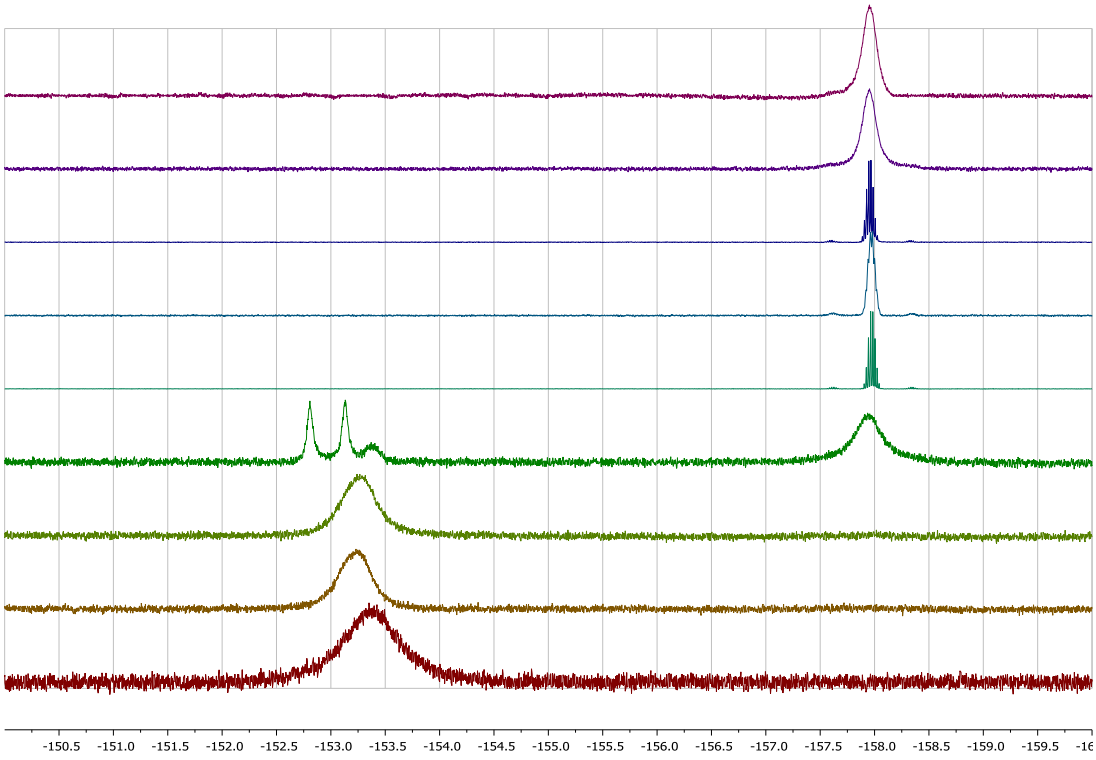

Figure 2.22 ^{19}F NMR spectra showing consumption of bifluoride and generation of fluorotrimethylsilane. Addition of fresh TBABF (second spectrum from top) results in a broad peak at -158 ppm.

The considerable solvent-dependence of the bifluoride chemical shift (*vide supra*) is such that HF_2^- cannot be ruled out on this evidence alone as the species responsible for the broad resonance observed. An alternative explanation is that the peak is due to fluorotrimethylsilane in rapid exchange, possibly with an ethanol adduct. The presence of a broad singlet at 0.25 ppm (peak width at half-height of 2.1 Hz) in the ^1H NMR spectrum suggests that the latter explanation is more likely. The chemical shifts are at least inconsistent with the presence of $Me_3SiF_2^-$.[89]

2.3.4 Unproductive Catalysis: The Origin and Nature of Side Products

Despite much discussion of the concept of unproductive catalysis in this reaction system, no evidence has thus far been presented with regard to the nature of the side products. While it has been noted that a number of potential side products (namely silylated ethylenes and cyclopropanes) are not observed, the possibility that their protodesilylated congeners are generated has not been ruled out. Given that these side products have been proposed to influence the reactivity of the catalytic system in the late stages of the reaction (*vide supra*), it was

deemed particularly important to establish unambiguously whether or not these are formed, and if possible, to probe the extent of their formation.

It is worthy of note that the question of side product formation in the palladium-catalysed cyclopropanation reaction with diazomethane has received no attention to date, despite the obvious synthetic utility of the reaction and clear evidence that the problem exists; the use of superstoichiometric diazomethane is commonplace, even to achieve less than full conversion of starting materials to the corresponding cyclopropanes. However, we are unaware of any experimental studies pertaining to the mechanistic origins of these side reactions, and only a single passing comment regarding the identities of the side products, in which the formation of ethylene and cyclopropane is noted.[29] This is in stark contrast to the numerous reports of formal carbene dimerization in reactions employing α-diazocarbonyl compounds – ethyl diazoacetate in particular.

The general procedure employed in the titration studies of cyclopropanation reactions outlined to this point has involved the evaporation of small aliquots removed from the bulk reaction mixture, followed by re-dissolution in deuterated solvent for analysis by ^{1}H NMR spectroscopy. While this technique proved entirely suitable for the determination of reaction progress with respect to the conversion of alkene substrates to cyclopropanes, the evaporation process would obviously have resulted in a loss of volatile species other than solvent. Given that the two candidate side products are considerably more volatile than the reaction solvent (ethylene (boiling point −104 °C) and cyclopropane (boiling point −33 °C)), the need for an alternative method for the analysis of the reaction mixture was evident. Reactions were scaled down by half and carried out in deuterated solvent (CD_2Cl_2). Aliquots were removed following each TMSDAM addition and diluted directly (i.e. without evaporation) with $CDCl_3$ for analysis by ^{1}H NMR spectroscopy.

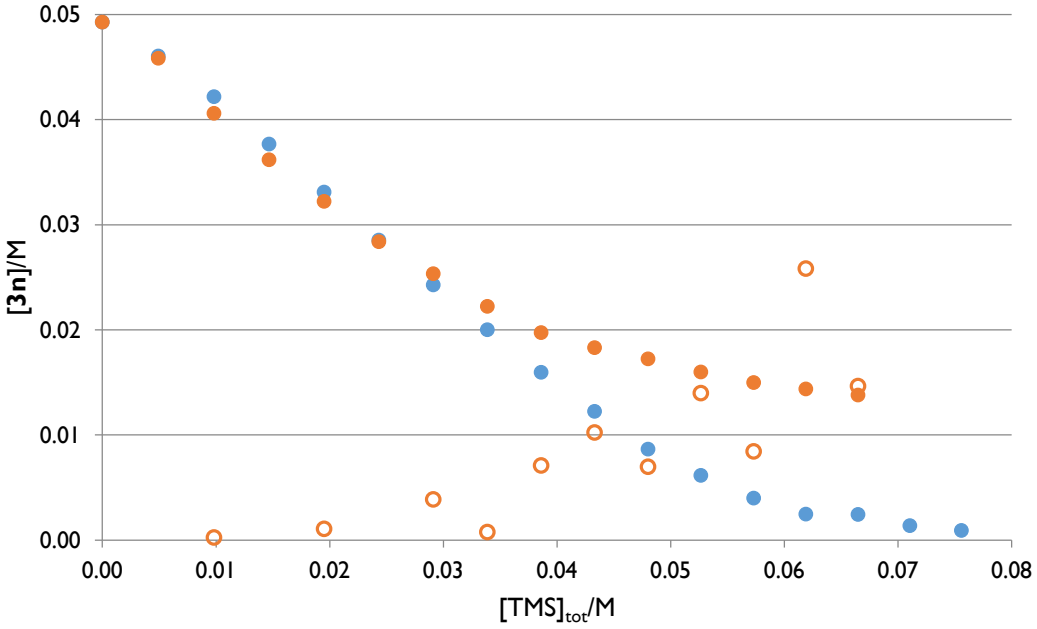

Figure 2.23 Cyclopropanation reaction of ethyl cinnamate (**3n**) in CD_2Cl_2 (solid orange circles) showing ethylene generation (empty orange circles). Also shown is ethyl cinnamate conversion in a standard run in protiated solvent for comparison (solid blue circles).

The presence of ethylene in the reaction mixture was apparent by ^{1}H NMR spectroscopy. The generation of ethylene even in the early stages of the reaction, while productive catalysis remained dominant, as well as the increased ethylene output later on, was consistent with the hypothesis outlined previously where a low-level background reaction which generates ethylene would enter autocatalytic runaway as substrate concentration diminished in concert with increased ethylene concentration (Scheme 2.12, p.51). However, this experiment does not establish the key causal link between ethylene generation and the breakdown of productive catalysis. Furthermore, the limited conversion of substrate relative to a standard run (blue circles, Figure 2.23) is noteworthy. In contrast to previous reactions employing TBABF, palladium black deposition as a fine precipitate was apparent in the reaction carried out in CD_2Cl_2. This has been attributed to the higher water concentration found in commercial CD_2Cl_2 (present as D_2O), relative to CH_2Cl_2. Earlier results (prior to the discovery of the efficacy of TBABF) had demonstrated conclusively the inability of aggregated palladium species to effect useful catalysis, while continuing to consume TMSDAM. This experiment provides good evidence that macroscopically aggregated palladium(0) species are effective catalysts for the decomposition of diazomethane to ethylene, explaining the ultimate fate of TMSDAM in numerous early experiments.

The experiment outlined above did not, however, allow us to rule in or out the presence of cyclopropane. Although it was not observed in the ^{1}H NMR spectra, the proton signal of cyclopropane (δ_H = 0.22 ppm)[90] is effectively isochronous with the considerably more intense doublet arising from fluorotrimethylsilane (δ_H = 0.23 ppm).[91]

It was realised that the EtOH-catalysed bifluoride regeneration discussed earlier (*vide supra*, pp. 65-69), could provide a convenient experimental means for studying the side product formation. Employing EtOD in place of EtOH would presumably generate DF_2^- on bifluoride recycling, and ultimately diazomethane-d_1 ($CHDN_2$). Assuming the nascent diazomethane was not subject to H/D exchange under the reaction conditions, formal dimerisation and trimerisation reactions would therefore result in 1,2-dideuteroethylene and 1,2,3-trideuterocyclopropane, while productive turnover would result in monodeuterated cyclopropanes (Scheme 2.16).

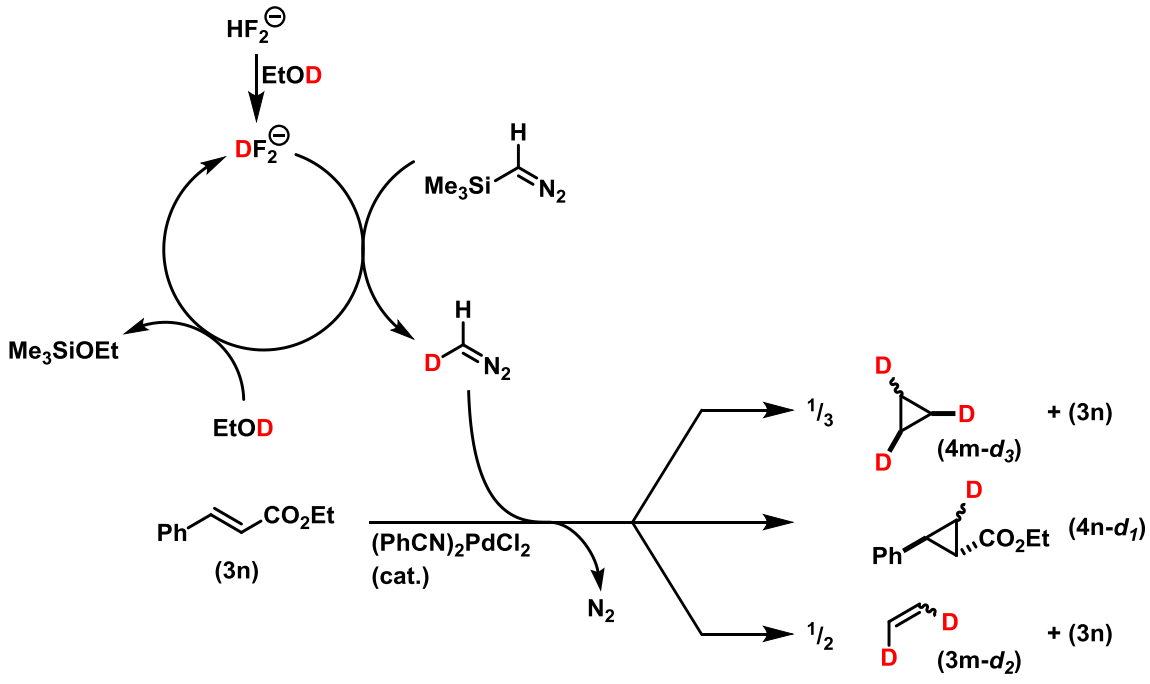

Scheme 2.16 Proposed isotopic distribution following formation of $CHDN_2$ by employing EtOD in bifluoride catalysis, allowing monitoring of product generation by ^{2}H NMR spectroscopy.

Monitoring of reactions employing EtOD and catalytic TBABF by ^{2}H NMR would therefore allow for the formation of both side-products to be tracked without the complication of overlapping NMR signals. Furthermore, it would allow for the ethylene autocatalysis hypothesis to be tested. Addition of exogenous C_2H_4 to the reaction mixture would be invisible by ^{2}H NMR

spectroscopy, but would, if the hypothesis were correct, promote the formation of isotopomeric ethylenes $C_2H_2D_2$, which would be observable, thus allowing the distinction between exogenous and endogenous ethylene to be made (Scheme 2.17). The alternative labelling strategy to achieve the same outcome would require both labelled ethylene (commercially-available, but expensive), and TMSDAM-d_9 ($(D_3C)_3SiCHN_2$, not commercially available but accessible by synthesis).

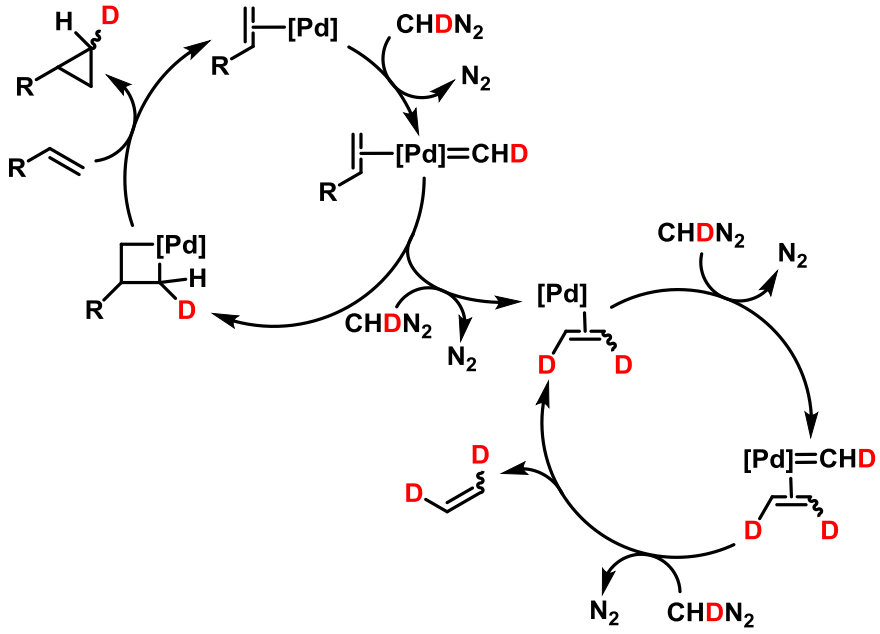

Scheme 2.17 Generation of deuterated ethylene from $CHDN_2$ (by TMSDAM deuterodesilylation, *vide supra*, Scheme 2.16) allows for the discrimination of added ethylene (C_2H_4) and that produced by catalytic turnover.

Preliminary experiments employing EtOH demonstrated that the addition of ethylene prior to TMSDAM had a marked effect on the progress of the reaction, with catalysis being considerably less efficient, resulting in just 19% of ethyl cinnamate conversion following the addition of 1.5 eq. TMSDAM. The reaction mixture in this experiment also darkened considerably following the addition of the first aliquot of TMSDAM, suggesting the formation of palladium black under the influence of ethylene, and it is believed that this is primarily responsible for the poor reactivity of this system. Consequently, the effects of adding ethylene to a reaction mixture which was demonstrably catalytically active was explored. Following the addition of 0.5 eq. TMSDAM in the usual manner, the reaction vessel was purged with *ca*. three volumes of ethylene, and the addition of TMSDAM was restarted. No palladium black formation was visible in this case, but the switch from productive to unproductive catalysis was clear (Figure 2.24).

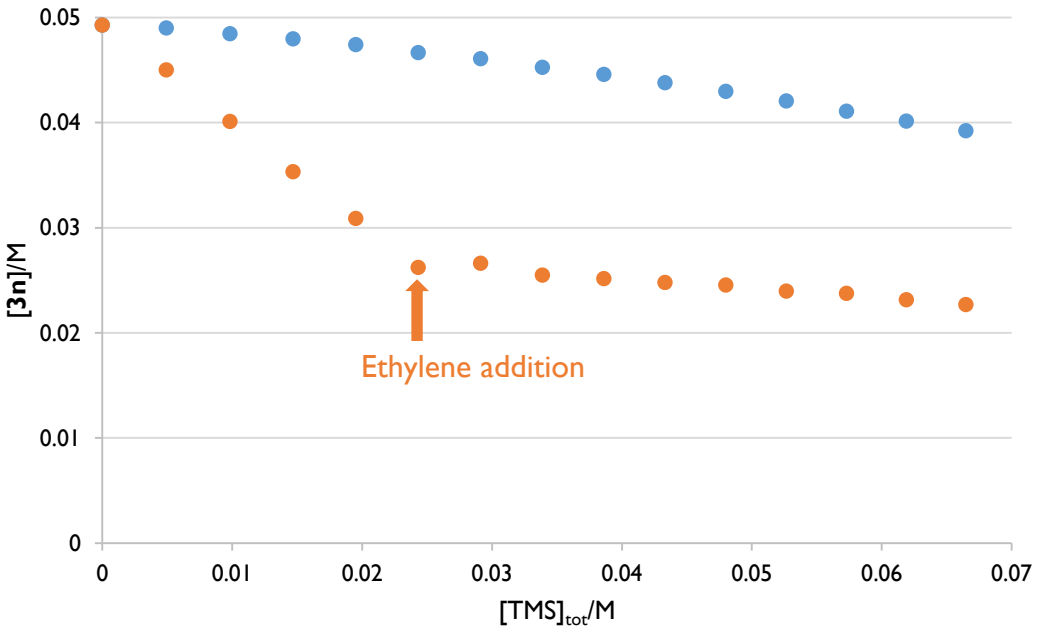

Figure 2.24 Effects of ethylene addition (i) prior to TMSDAM (blue circles), and (ii) following a period of productive catalysis (orange circles).

Although this experiment provides clear evidence for the deleterious effect of ethylene on productive catalysis, the concentration of ethylene in the system is undoubtedly higher than that which would be generated by the *ca.* 15% unproductive TMSDAM turnover (generating 7.5% ethylene). However, if the ratio of concentrations ($[C_2H_4]/[\mathbf{3n}]$) is the relevant factor in determining reaction efficiency rather than simply the ethylene concentration, then this may not represent such a bad model for the later stages of the reaction.

In order to monitor the reactions by deuterium NMR spectroscopy, as proposed above, the cyclopropanation reactions were scaled up five-fold such that larger aliquots could be taken, eliminating the need for their dilution, which would result in considerably longer acquisition times (^{2}H NMR being *ca.* 8000x less sensitive than ^{1}H for the same concentration). In the absence of ethylene purging, the formation of both diastereomeric isotopomers of **4n-*d*$_1$** was apparent, along with a species assumed on the basis of the distinctive chemical shift to be cyclopropane-d_n (Figure 2.25).

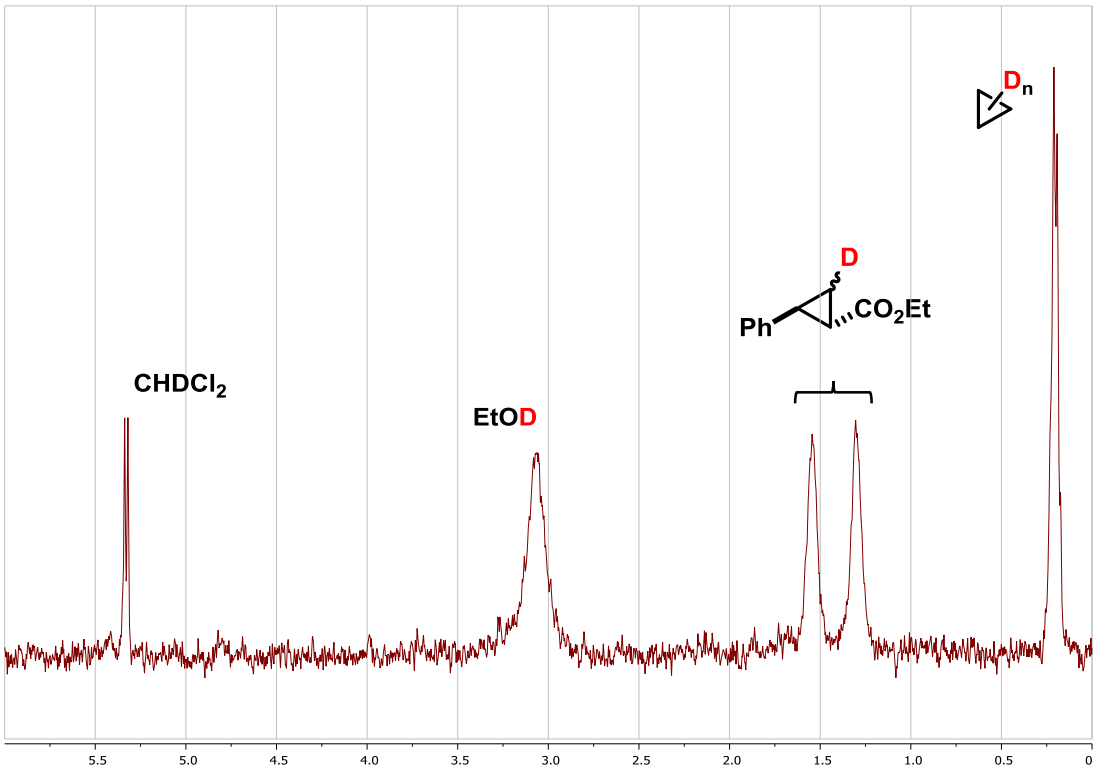

Figure 2.25 ^{2}H NMR following the addition of 1.8 eq. TMSDAM/EtOD showing the distribution of EtOD-derived products (highlighted in red).

The formation of ethyl cinnamate-derived cyclopropanes was not apparent in the earliest spectra. However, analysis of the aliquots by ^{1}H NMR spectroscopy (following evaporation and redissolution in $CDCl_3$) confirmed productive catalysis was occurring. Crucially, however, the reaction was at this point producing *non-deuterated* product, reflecting the TBABF catalyst loading (20 mol%) and adventitious water (Figure 2.26).

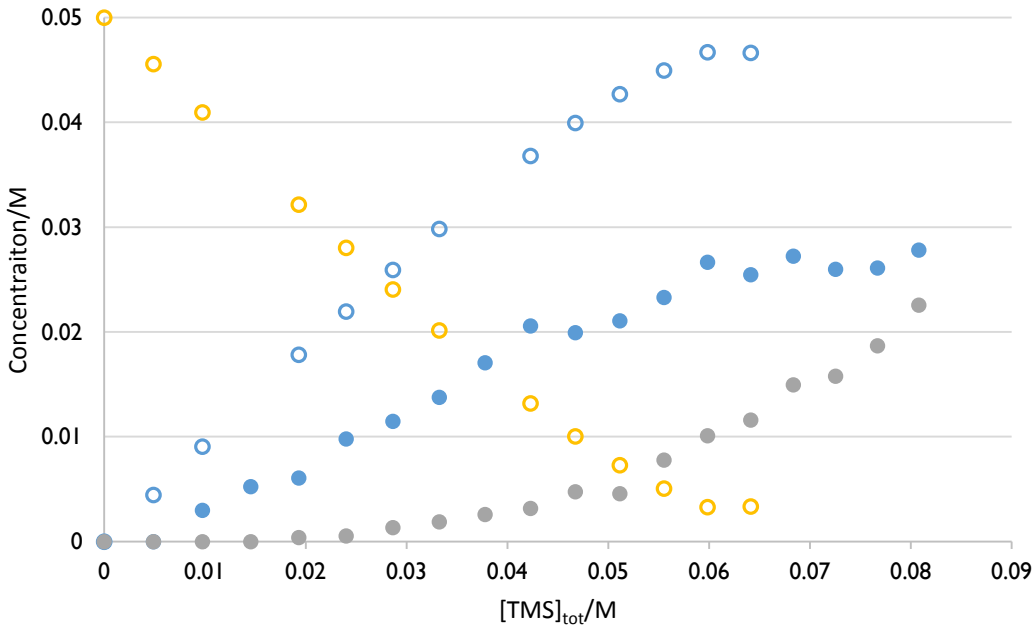

Figure 2.26 Reaction profile following additions of TMSDAM/EtOD, showing the distribution of :CHD fragments between ethyl cinnamate (affording **4n-d_1**, blue circles) and presumed formal cyclotrimerisation (grey circles), as determined by ^{2}H NMR spectroscopy. Assuming clean formation of **4m-d_3** ($C_3H_3D_3$), the cyclopropane-d_3 concentration is therefore one-third of that shown by the grey circles. Yellow and blue unfilled circles show the consumption of ethyl cinnamate and the formation of the corresponding cyclopropanes (all isotopomers), respectively, as determined by ^{1}H NMR.

The most surprising finding, however, was the complete lack of ethylene observed under the reaction conditions, in contrast to previous experiments.

Undeterred by this unexpected finding, however, the effect of ethylene addition on the catalytic system was investigated by the same method. Following five additions of TMSDAM/EtOD, to confirm the system was acting normally, the reaction vessel was purged with approximately three volumes of ethylene gas. As expected, productive catalysis stalled, becoming almost negligible. However, once again, no ethylene-d_n formation was observed, and no significant upregulation in cyclopropane-d_n generation was noted, relative to the ethylene-free system (Figure 2.27).

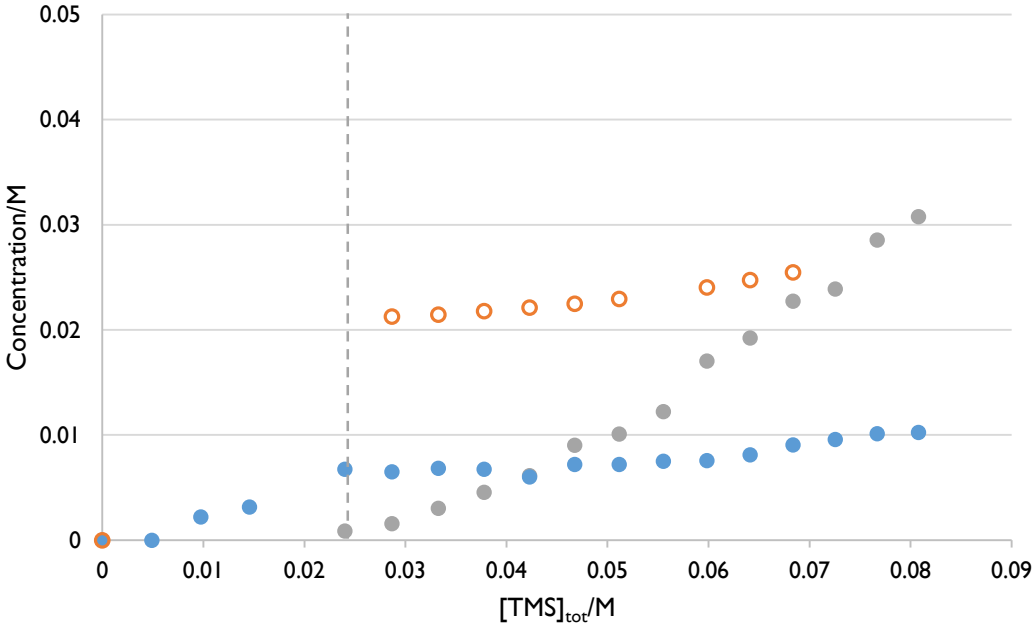

Figure 2.27 Addition of ethylene (marked with vertical dashed line) leads to the stalling of the productive cyclopropanation reaction (**4n-*d*$_1$**, blue circles; total conversion by ^{1}H NMR, unfilled orange circles). As in Figure 2.26, the grey circles denote the concentration of :CHD consumed by cyclotrimerisation to form $C_3H_3D_3$ (**4m-*d*$_3$**), the concentration of which would be one-third of that denoted by the grey circles.

The careful distillation of a number of the later aliquots, followed by ^{1}H, ^{13}C{^{1}H,^{2}H} and ^{1}H-^{13}C HSQC NMR experiments on the resulting mixture, allowed for a correlation to be established between the largely-obscured peak in the ^{1}H spectrum at 0.23 ppm, and a peak in the ^{13}C spectrum at $\delta_C = -3.24$ ppm. Both chemical shifts are indicative of cyclopropane.

One clear flaw with the experiments employing catalytic TBABF with stoichiometric EtOD is the imperfect deuteration of all products; the high desilylation catalyst loading (20 mol% TBABF), and the degree of hydration of this catalyst ensures a certain proportion of TMSDAM is subject to protodesilylation rather than deuterodesilylation, resulting in products unobservable by ^{2}H NMR. As a consequence, it is impossible to rule out ethylene formation (as $C_2{}^1H_4$) in the earliest stages of the reaction – i.e. until the medium is depleted of exchangeable protons.

To circumvent this limitation, the H/D exchange of TBABF was effected by repeated equilibration with D_2O and evaporation to yield tetrabutylammonium deuterobifluoride (n-Bu_4N^+ DF_2^-), which was subsequently employed catalytically, as above, to monitor the formation of side products by ^{2}H NMR spectroscopy.

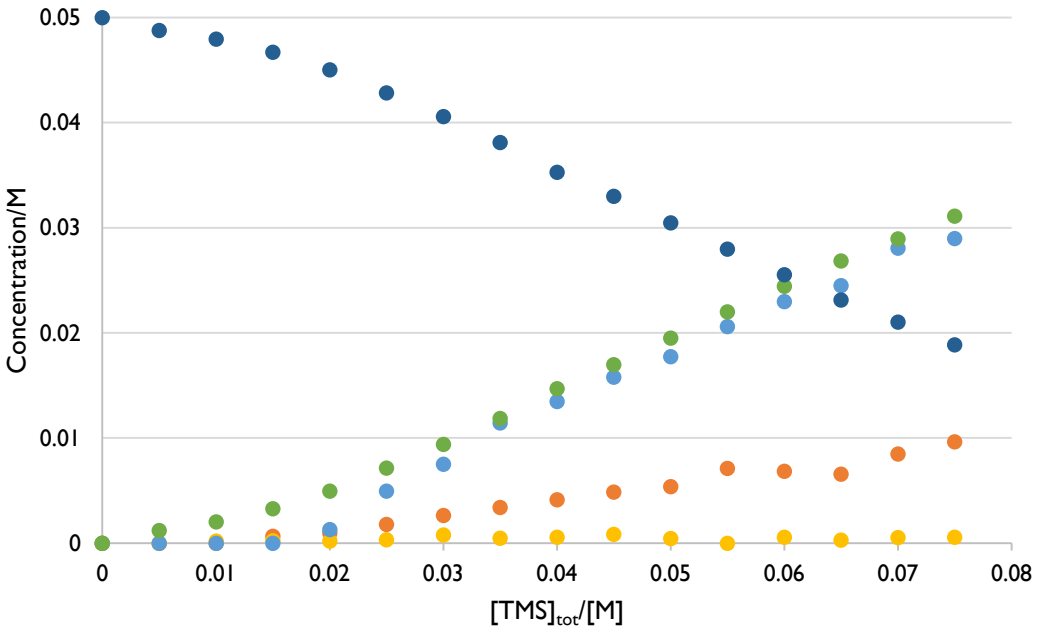

Figure 2.28 Formation of products and side products in cyclopropanation of ethyl cinnamate employing catalytic tetrabutylammonium deuterobifluoride. Formation of the two isotopomers of (**4n-d_1**) (light blue circles), cyclopropane-d_3 (orange circles) and ethylene-d_2 (yellow circles) was monitored by ^{2}H NMR, integrating against residual natural abundance $CHDCl_2$, while the formation of (**4n-d_n**, n = 0,1, both isotopologues) (green circles) and consumption of ethyl cinnamate (dark blue circles) was determined by ^{1}H NMR, following evaporation and redissolution in $CDCl_3$.

Although ethylene generation is evident (Figure 2.28), it appears to be the minor side-product, relative to the formation of cyclopropane. Although there is some scatter in the data, it appears that the majority of $C_2H_2D_2$ formation occurs in the earlier stages of the reaction, and its generation levels off, or even stops after $[TMS]_{tot} > 0.04$ M. This provides one possible explanation for our previous inability to observe ethylene by ^{2}H NMR – typically these initial turnovers are characterised by the formation of predominantly protiated product. The diminished conversion of ethyl cinnamate in this case is likely due to the increased hydration state of n-Bu_4N^+ DF_2^- relative to TBABF.

The experiments discussed above allow us to rule out an autocatalytic, ethylene-producing runaway, as we had previously hypothesised. Indeed, ethylene generation appears to represent at most only a fraction of the unproductive turnover of TMSDAM, assuming it has been correctly identified. Instead, the formal cyclotrimerisation of TMSDAM-derived methylene fragments, generating cyclopropane (C_3H_6, **4m**) accounts for the bulk of the unproductive catalysis.

The thermodynamic driving force for the formation of higher cyclic methylene oligomers (i.e. cycloalkanes) increases with ring size, at least as far as cyclohexane (as determined by DFT

calculations in Gaussian09[92] at B3LYP/6-31G(d,p), Figure 2.29), due to the relief of ring strain. As these are not observed experimentally, the kinetic barrier to further oligomerisation is presumably high. Straub's computational study found the binding of cyclopropane to (η^2-C_2H_4)Pd to be endergonic with respect to binding of a second ethylene by *ca*. 60 kJ mol^{-1}, with a low barrier (0.6 kJ mol^{-1}) to cyclopropane dissociation. (*47*) This presumably constitutes a large part of the kinetic barrier to further cyclo-oligomerisation. Consequently, it is difficult to advance any convincing arguments that would implicate cyclopropane in the deviation of the catalytic manifold from productive to unproductive catalysis. As such, we are compelled to abandon the concept that the products of side reactions are significantly influencing the late-stage efficiency of the catalytic system. If ethylene is present, it is surely at too low a concentration, relative to substrate, to have such significant effects. Even when saturated with ethylene, the catalytic system continues to promote the cyclopropanation of ethyl cinnamate, albeit inefficiently (*vide supra*, Figure 2.24). As such, the upregulation of unproductive side reactions should be seen not as a symptom of the inherent low-level inefficiency in catalysis. Instead, some other change in the system must be responsible for this rather sudden switch from largely-productive to -unproductive reactivity.

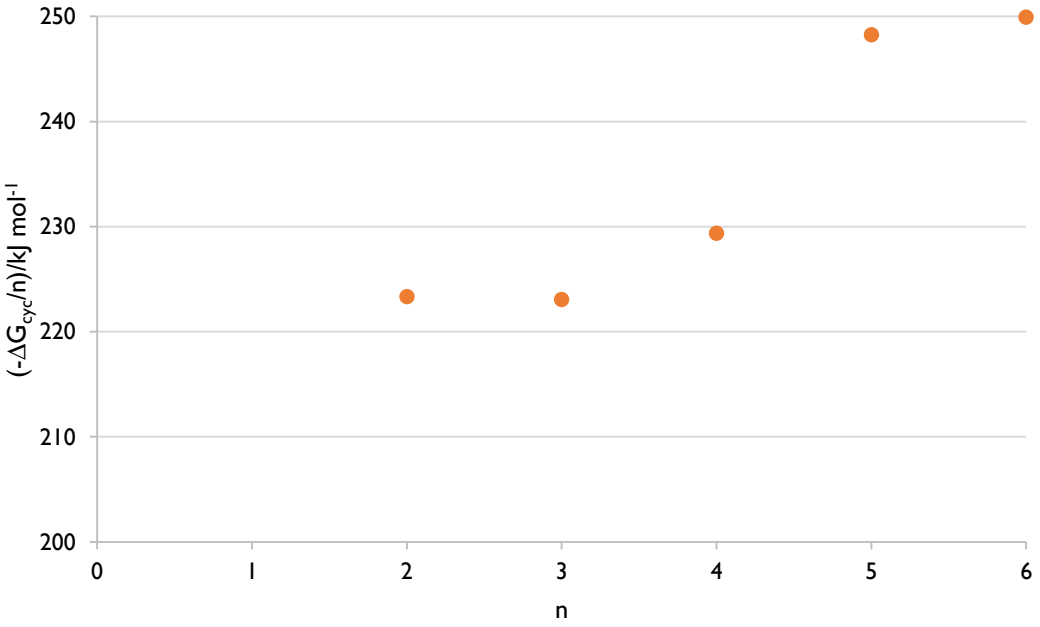

Figure 2.29 Gibbs free energy per diazomethane for cycloalkane $(CH_2)_n$ formation increases with *n* up to *n* = 6, while experimentally observed cyclo-oligomerisation stops at *n* = 3.

2.3.5 Substrate Effects

In order to better understand the factors affecting catalysis, the investigation of a number of electronically-varied substrates was carried out. A range of *meta*- and *para*-substituted styrenes were subjected to the optimal reaction conditions identified previously (Section 2.3.3). However, the addition of even small amounts of TMSDAM (*ca.* 0.2 eq.) led to a considerable darkening of the reaction mixture, indicative of catalyst degradation. The conversions were predictably disappointing – zero in the case of *m*-nitrostyrene (**3v**) – and in the case of 4-trifluoromethylstyrene (**3t**), the reaction profile exhibited considerable scatter, with no clear linear trend discernible. The outcome of the reaction with **3t** was also unchanged on slower addition (0.3 mL h^{-1}).

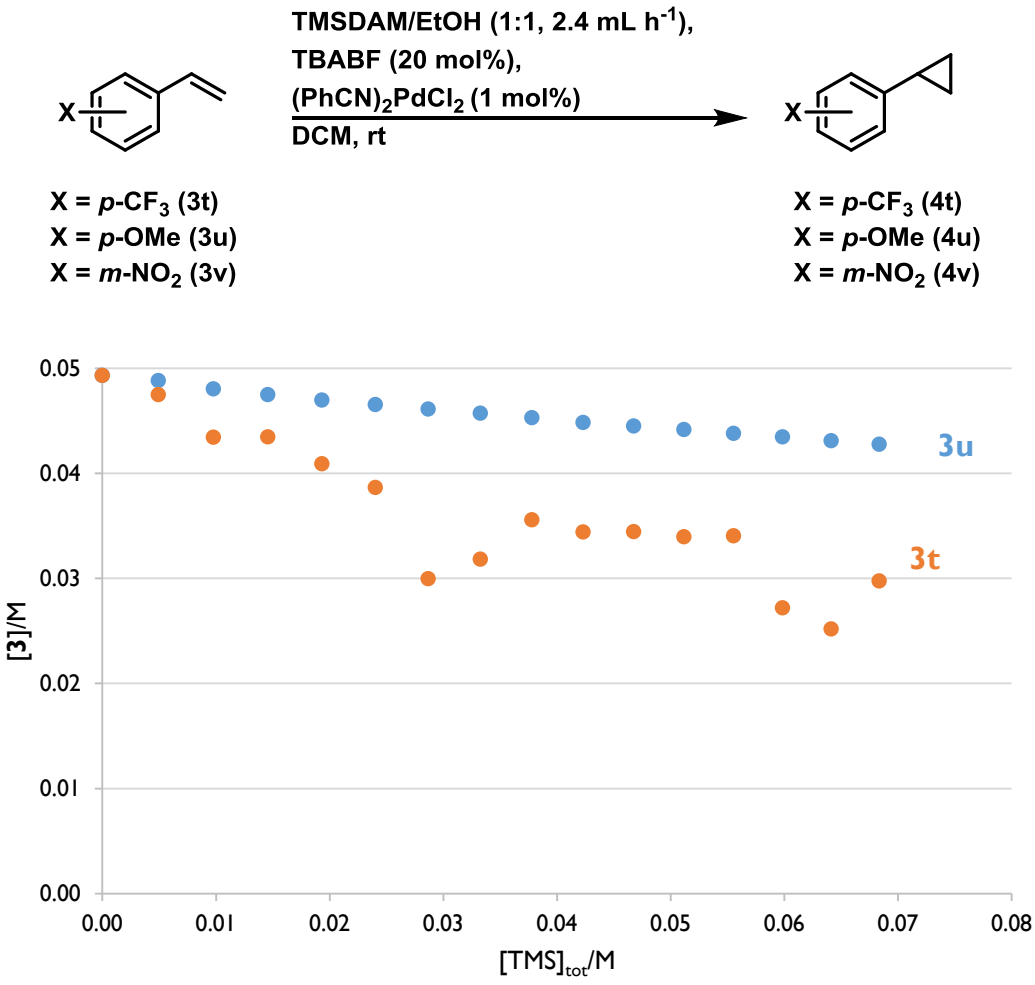

Figure 2.30 Cyclopropanation of electronically-varied styrenes under the conditions of TBABF catalysis proved ineffective.

The visually evident catalyst decomposition led us to consider the possibility that higher concentrations of tetrabutylammonium cation might prove more effective – previously palladium black deposition had proven problematic when the TBABF concentration had been reduced (*vide supra*, Figure 2.19 and associated discussion, pp. 64-65). Pleasingly, this prediction proved correct – increasing the TBABF stoichiometry (to two equivalents relative to substrate) resulted in the smooth cyclopropanation of an electronically-diverse range of styrenes (Figure 2.31).

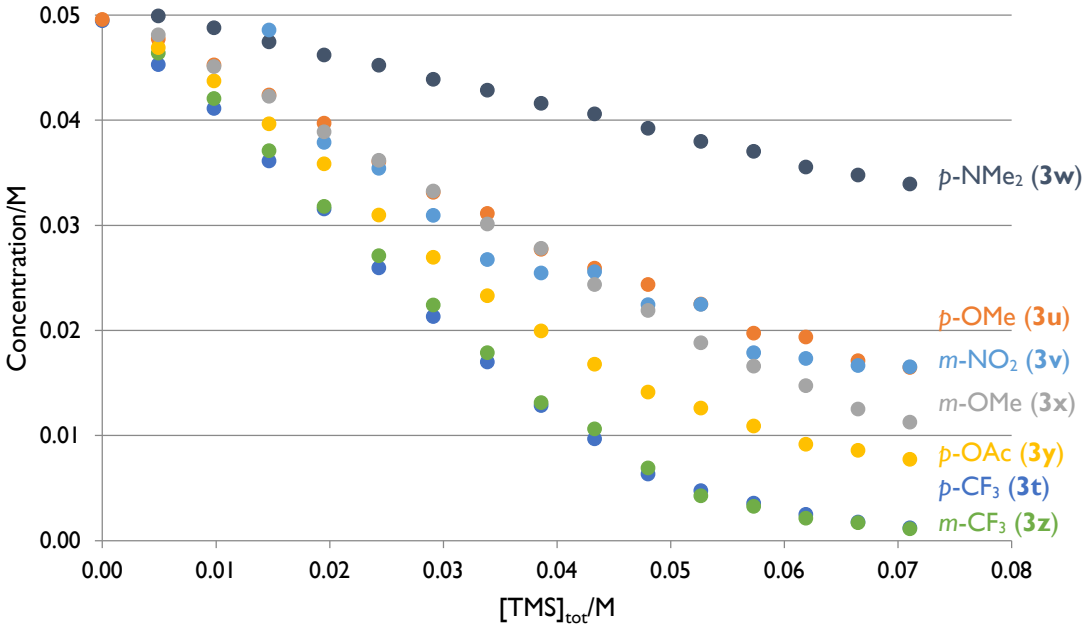

Figure 2.31 Cyclopropanation of styrenes proves effective in the presence of two equivalents of TBABF.

As with ethyl cinnamate, the reaction profiles demonstrated a degree of inefficiency even in the earliest stages of reaction – the general trend is that the reactions of more electron-deficient alkenes proceed more efficiently. As substrate concentration approaches zero, the efficiency of TMSDAM consumption drops.

From the efficiency of TMSDAM consumption in the early (linear) regime, it is possible to determine the rate of productive turnover, relative to that of unproductive catalysis. These data give positive correlations with σ, σ^+ and σ^-, however no particularly good correlations are evident (Figure 2.32).

Clearly in all cases, *m*-nitro (**3v**) lies substantially off-trend, and the correlation coefficients improve if it is excluded (Figure 2.33). The removal of *m*-nitrostyrene reveals other curious

results, most notably that the reactivity of *meta*- and *para*-methoxystyrenes (**3x** and **3u**) are surprisingly similar, despite their opposing electronic effects.

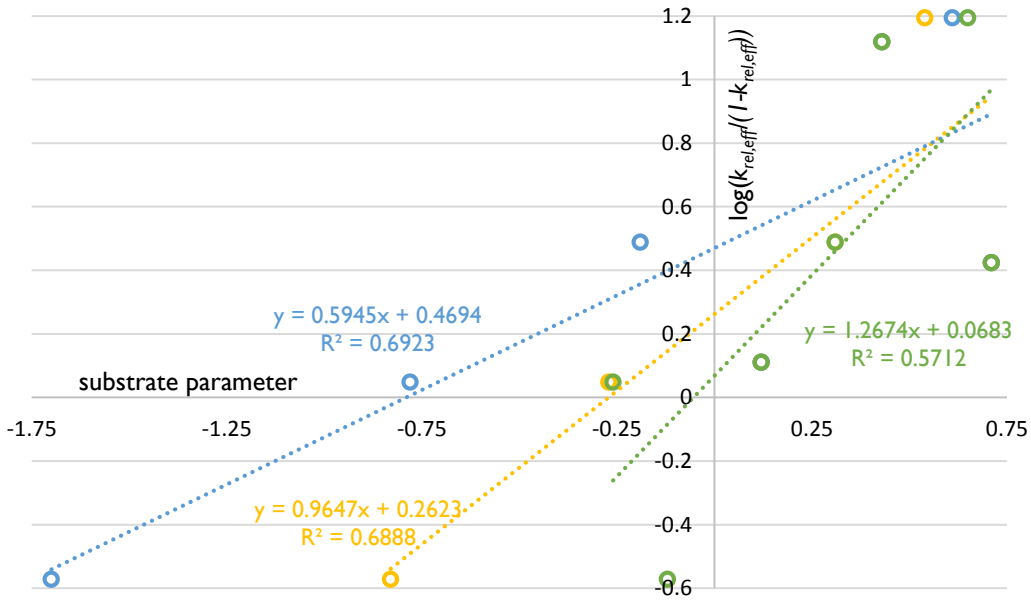

Figure 2.32 Correlations between the relative rates of efficient catalysis and various substrate parameters (σ in yellow, σ^+ in blue and σ^- in green) exhibit considerable scatter.

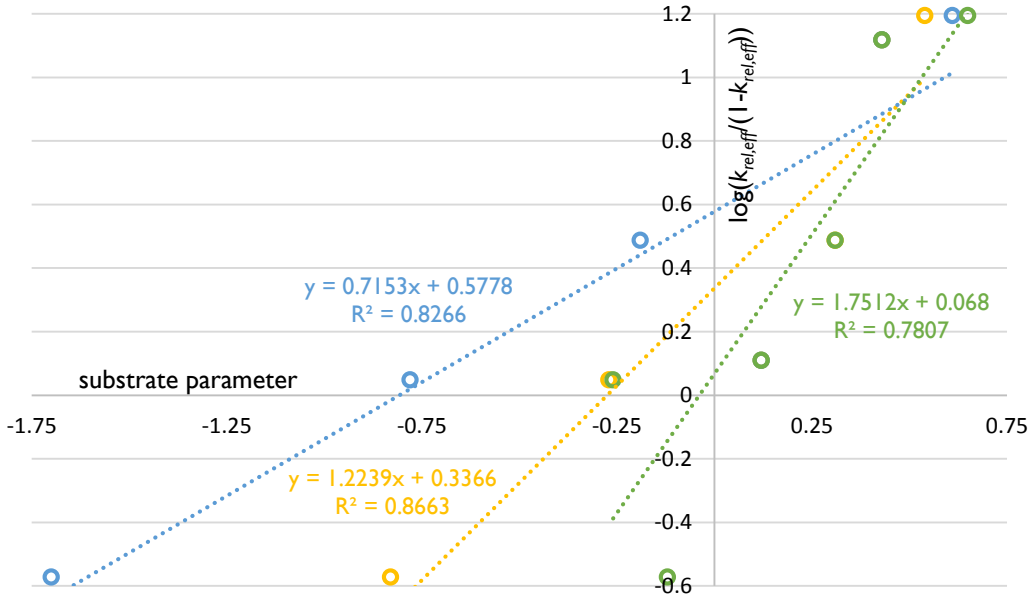

Figure 2.33 Correlations with all substrate parameters (σ in yellow, σ^+ in blue and σ^- in green) improve if *m*-nitro is excluded.

The similarities encountered with both regioisomers of the methoxy and trifluoromethyl styrenes, despite the obvious electronic differences, raised an interesting possibility. Was it possible that the efficiency of the reaction did not depend upon the electronic properties of the alkene double bond (which should provide good correlations with Hammett-type substituent constants), but rather on the electronics of the aromatic system? In an attempt to probe this possibility, geometry optimisations, frequency analyses and energy calculations were carried out by DFT methods (B3LYP/6-31G(d,p) in Gaussian 09).[92] In all cases minima were located successfully, allowing for potential correlations to be identified.

Good correlation is observed between the observed reaction efficiency and the energies of frontier molecular orbitals; once again, however, *meta*-nitrostyrene is an outlier (Figure 2.34)

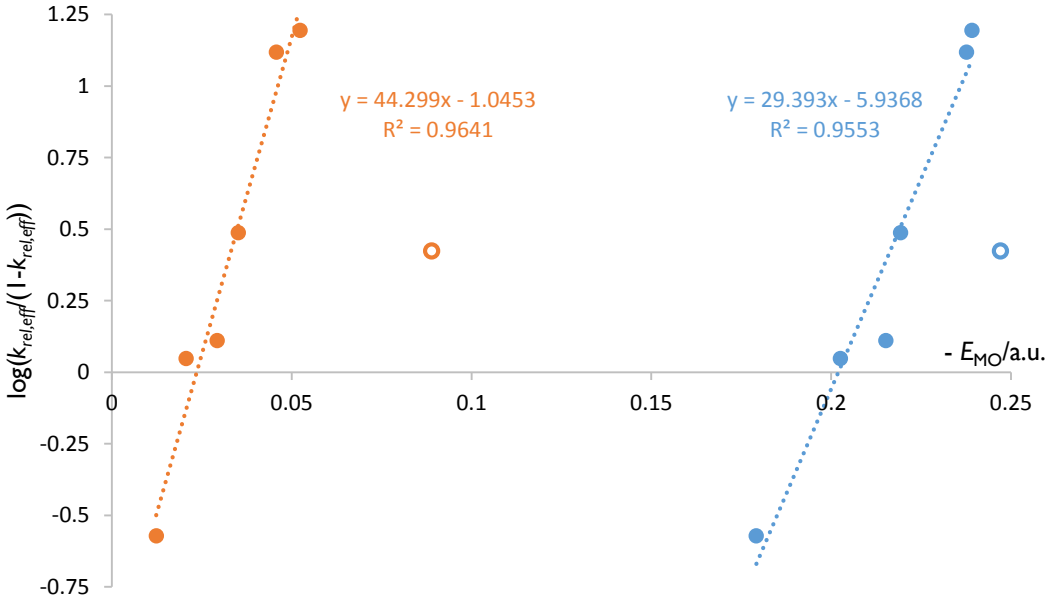

Figure 2.34 Positive correlations are observed between the relative rate of productive catalysis and the energies of the substrate HOMOs (blue circles) and LUMOs (orange circles). Substrate **3v** (meta-nitrostyrene) is marked with empty circles and is not included in the fitted lines.

Visualisation of the FMOs (Table 2.5) shows that in all cases apart from the troublesome *meta*-nitrostyrene, the LUMO has significant alkene C=C π* character. The LUMO of the *meta*-nitrostyrene appears to correspond more closely to a low-lying N=O π*-type orbital. The LUMO+1 of this structure, however, more closely resembles the lowest unoccupied orbitals common to the other examples shown (Figure 2.35). The energy of this orbital better matches

the trend shown above, but still does not allow for a good correlation ($R^2 > 0.95$) to be established (Figure 2.36).

Table 2.5 Frontier molecular orbitals from DFT calculations at B3LYP/6-31G(d,p) in Gaussian 09.

Styrene	HOMO	LUMO
p-CF_3 (**3t**)	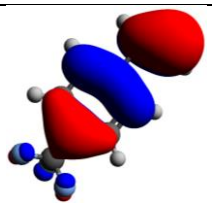	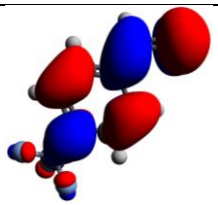
p-OMe (**3u**)	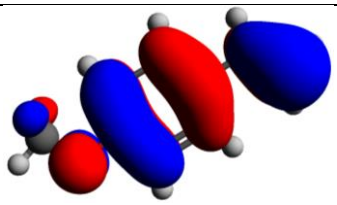	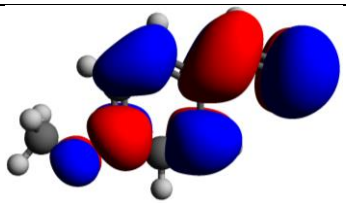
m-NO_2 (**3v**)	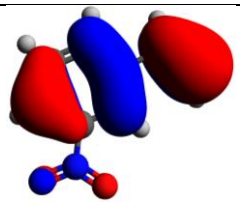	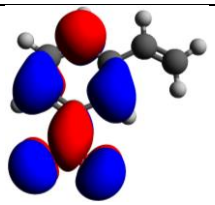
p-NMe_2 (**3w**)	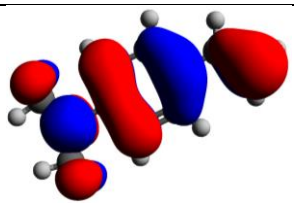	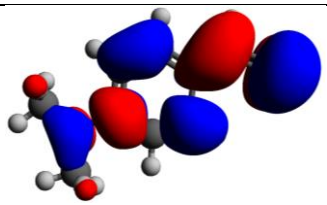
m-OMe (**3x**)	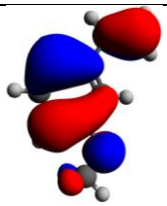	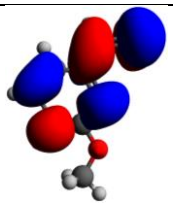
p-OAc (**3y**)	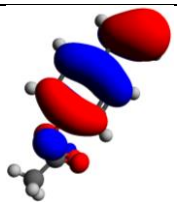	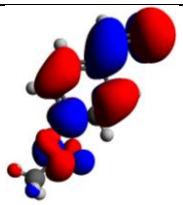
m-CF_3 (**3z**)	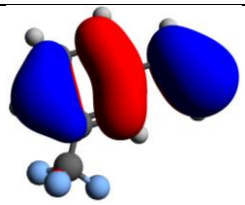	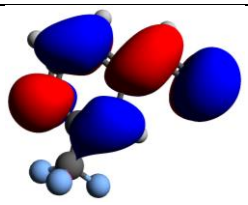

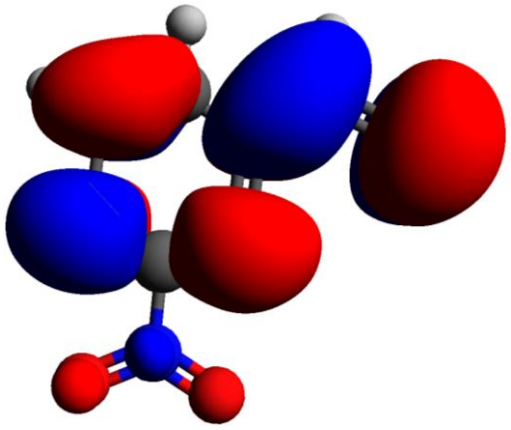

Figure 2.35 LUMO+1 of *meta*-nitrostyrene (**3v**) more closely resembles the LUMO of other styrenes (**3t**,**u**,**w-z** – see Table 2.5) than does the LUMO of **3v**, which has negligible density on the vinyl group.

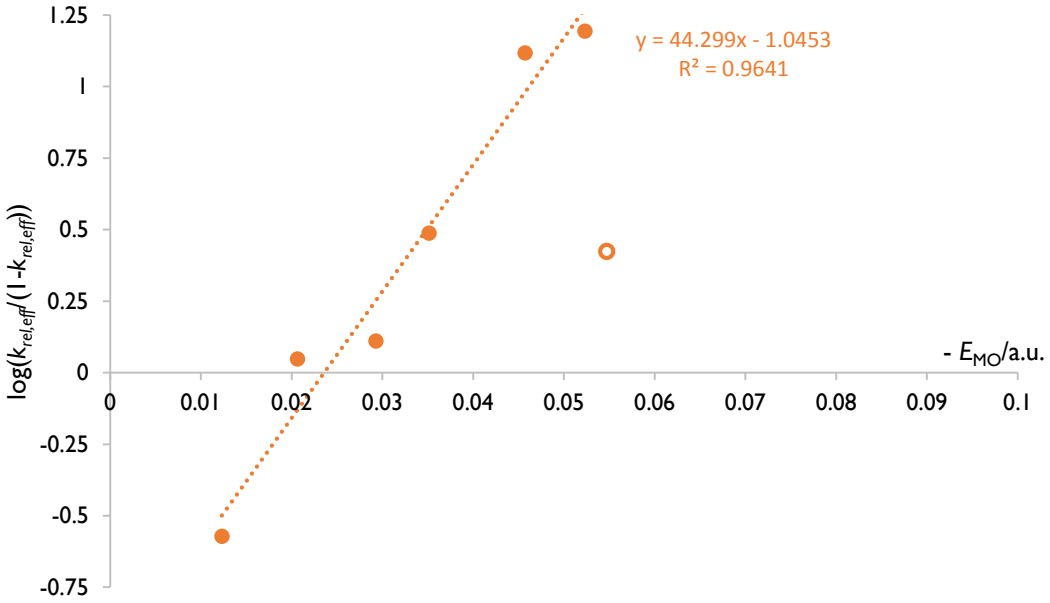

Figure 2.36 The experimentally-determined efficiency of catalysis better fits to the energy of the *meta*-nitrostyrene LUMO+1 (empty circle), but the correlation remains poor. As in Figure 2.34 above, this point has been neglected in the fitting of the straight line. Its inclusion gives a best fit line of $y = 32.613x - 0.7642$, $R^2 = 0.7165$.

In the absence of the wayward *meta*-nitrostyrene, the correlation between the efficiency of cyclopropanation ($k_{rel,eff}/(1-k_{rel,eff})$) and the energy of the substrate LUMO is rather good, and indicative of Pd(0) catalysis, as π-backbonding interactions (Pd(d)→C=C(π*)) contribute significantly to the overall stability of Pd(0)-olefin complexes.[93,94] In 2004, Stahl, Landis and co-workers reported on the mechanism of alkene substitution reactions at Pd(0) centres.[95] In

marked contrast to the prevailing mechanistic paradigm for ligand substitution reactions at transition metal centres, in which the entering ligand is considered the nucleophilic component, they found that alkene exchange in a series of (bathocuproine)Pd(0) complexes was better characterised as a "inverse-electron-demand" ligand substitution. Examination of a range of *para*-substituted β-nitrostyrenes revealed a clear thermodynamic preference for binding to electron-deficient alkenes ($\log K \propto \sigma$), while study of isodesmic alkene exchange reactions at a range of temperatures by ^{1}H NMR spectroscopy allowed for the determination of activation parameters; large negative values for $\Delta S^{\ddagger}$ (–24 to –30 kcal mol^{-1} K^{-1}) were measured. The rates of these self-exchange reactions also gave an excellent positive correlation with the Hammett substituent constants. Subsequent DFT studies on simplified model systems reveal the crucial overlap between a Pd-centred lone pair (predominantly $d_{x^2-y^2}$ in character) and the vacant π* orbital of the incoming alkene. Increasing orbital overlap along the reaction coordinate is accompanied by the transfer of negative charge from the metal to the organic fragment.

Both the enhanced rate of olefin exchange and the increased thermodynamic favourability of binding electron-deficient alkenes observed by Landis and Stahl are consistent with the mechanism proposed below (Scheme 2.18) for the palladium-catalysed cyclopropanation of alkenes with *in situ* generated diazomethane.

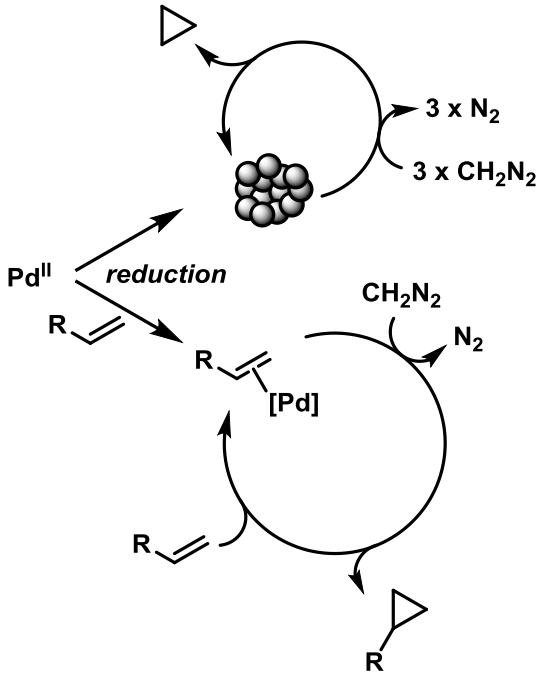

Scheme 2.18 Mechanistic hypothesis for TMSDAM partitioning between unproductive and productive catalysis.

According to this model, the reduction of palladium(II) to palladium(0) results in the formation of two markedly different catalytic species. One, likely nanoparticulate in nature, is responsible for unproductive TMSDAM consumption (top cycle), generating cyclopropane (**4m**) *via* the formal cyclotrimerisation of methylene. The other (lower cycle) engages substrate and *in situ* generated diazomethane to afford the desired products. The overall efficiency of TMSDAM consumption would then be dependent on the initial partitioning between the two palladium species, and the relative rates at which the two cycles turn over.

As stated above, the enhanced thermodynamic stability of palladium(0) complexes with electron-deficient styrenes found by Landis and Stahl would suggest that the partitioning of palladium would be most favourable (i.e. stronger preference for the lower cycle in Scheme 2.18) for these substrates. However, the electronic demands of the remainder of the lower cycle, which should exhibit some substrate-dependence, are unknown. In order to determine these, and to provide additional support for this mechanistic hypothesis, DFT calculations (B3LYP/6-31G(d,p) for C, H, N, O, F, LanL2DZ for Pd) were carried out to probe the substrate-dependence of the energy profile for the cyclopropanation reaction.

In all cases, minima on the potential energy surface were readily obtained, however attempts to locate transition states for the coordination of styrenes to palladium(0) were unsuccessful, as were all attempts to locate transition states for the coordination of diazomethane to the coordinated (styrene)Pd^0 complexes. A relaxed potential energy surface scan for the coordination of diazomethane to (3-methoxystyrene)palladium(0) also found no energy maximum for Pd-C distances of up to 3.60 Å, suggesting that diazomethane coordination occurs either without an electronic barrier, or through a very early transition state.

In all cases, the energy of styrene coordination to Pd(0) is highly exergonic, however no meaningful correlation between the strength of binding of the alkene to palladium(0) and the reaction efficiency is evident (Figure 2.37).

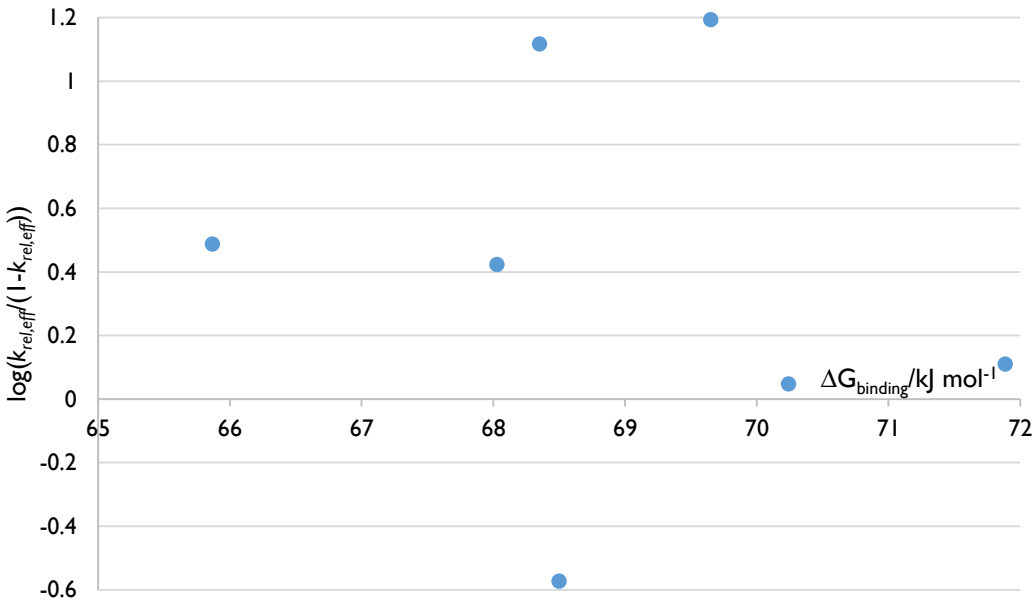

Figure 2.37 No obvious correlation is evident between the binding energy of styrenes to Pd(0) and the relative rate of productive TMSDAM consumption.

A better correlation can be identified between the efficiency of the reaction and the barrier to N_2 extrusion from (styrene)$PdCH_2N_2$ complexes (Figure 2.38).

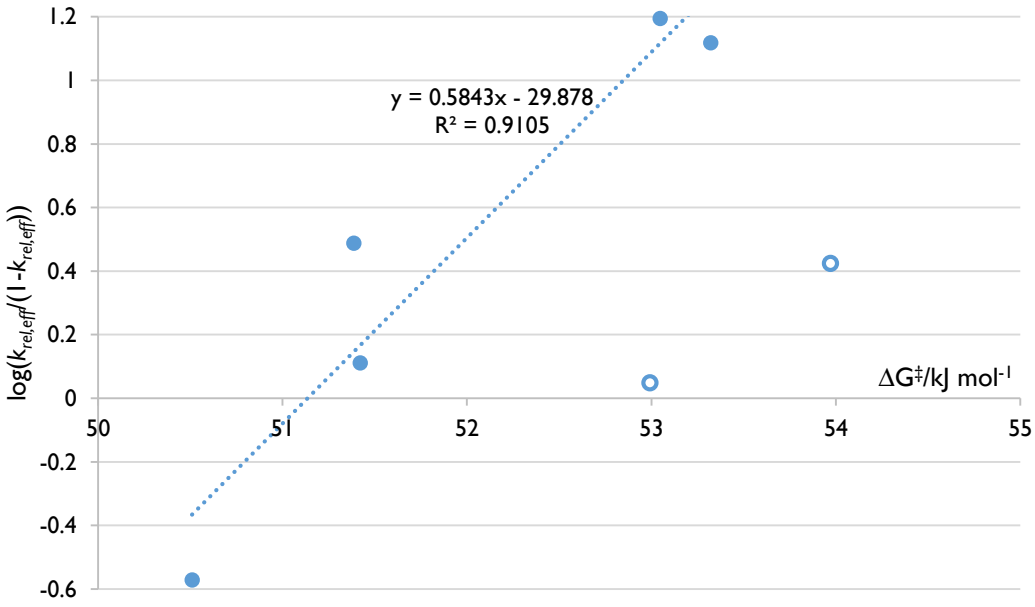

Figure 2.38 No good correlation, encompassing all substrates examined, is evident between the barrier to N_2 extrusion and the efficiency of TMSDAM consumption. The line of best fit shown does not include *p*-OMe or *m*-NO_2 (empty circles).

The positive correlation between the calculated barrier and reaction efficiency is surprising. We would expect, according to our model, that substrates which turn over fastest (i.e. those with the smallest barrier) would most successfully compete with unproductive catalysis for diazomethane, resulting in more efficient reaction. Here, the opposite correlation is evident.

This computational study is predicated on the work by Straub, who identified nitrogen extrusion as turnover-limiting in the study of the model reaction with ethylene.[47] However, the possibility that there is a change in turnover-limiting step with 'real' substrates should not be neglected. Furthermore, the likelihood for error in the calculated barrier heights, which span a relatively small range (<4 kJ mol^{-1}), must be considered. Consequently, on the basis of these computational studies alone, it seems premature to discount the proposed model. More sophisticated calculations at a higher level of theory, with additional styrene molecules in the coordination sphere of Pd and inclusive of a solvation model, may better match the experimental findings detailed above.

3 Conclusions and Future Work

3.1 Conclusions

The cyclopropanation of terminal and electron-deficient alkenes with trimethylsilyldiazomethane (TMSDAM) has been achieved for the first time in a desilylative sense. The use of tetrabutylammonium bifluoride (TBABF) was found to engender high selectivity for the non-silylated product, and, in contrast to other reagents tested, it does not promote catalyst deactivation. This process affords the products of formal [2+1] addition of methylene ($:CH_2$) across the double bond. This development can therefore be considered a safer and more convenient replacement for cyclopropanation reactions employing stoichiometric excesses of the toxic and explosive diazomethane, which instead employs commercially available, bench-stable reagents. This method is also complementary to those employing metal carbenoids, such as the Simmons-Smith reaction, giving enhanced regioselectivity in a number of cases.

Studies of reaction progress as a function of reagent addition were found to be indicative of a substrate-dependent partitioning of TMSDAM between productive and unproductive catalytic cycles, which was unaffected over a 24-fold range of addition rates.

Spectroscopic studies of the reaction between TMSDAM and TBABF demonstrate that the rapid formation of diazomethane is viable under the reaction conditions. In the active catalytic system, the nascent reagent is subject to fast capture by the reaction manifold, thus preventing its accumulation. Spectroscopic studies (^{1}H, ^{19}F NMR) also provided insight into the operation of "hidden" reactions that serve to regenerate TBABF; adventitious water present in commercial TBABF is able to hydrolyse fluorotrimethylsilane under the reaction conditions. This discovery allowed for the rational development of a catalytic cascade employing simultaneous slow addition of TMSDAM and EtOH (in place of water).

The catalytic cascade method, although not readily applicable to all alkene substrates, proved to be a valuable technique in the generation of $CHDN_2$ by bifluoride-catalysed deuterodesilylation with EtOD, which in turn allowed for the various fates of diazomethane to be monitored by ^{2}H NMR spectroscopy. The formation of cyclopropane from formal trimerisation of methylene was thereby shown to be the principal process competing with the desired cyclopropanation reaction. The previously postulated influence of ethylene on productive catalysis (resulting in an autocatalytic ethylene-generating scenario) was eliminated due to its absence from the reaction

mixture in reactions employing EtOD. It remains possible that ethylene is present transiently in solution, prior to its conversion to cyclopropane.

Cumulatively, from these results emerges a clearer picture of the mechanistic course of the palladium-catalysed cyclopropanation of alkenes with diazomethane. The efficiency of cyclopropanation correlates well with the π-acidity of the alkene substrate, consistent with a shift in partitioning between substrate-bound and -unbound palladium, with the former generating the desired product, and the latter resulting in formal carbene trimerisation. Good correlation is evident between the efficiency of TMSDAM consumption and the energies of substrate frontier molecular orbitals, but a number of questions related to this partitioning remain unanswered. The effects of tetrabutylammonium cation in stabilising palladium(0) species with respect to aggregation also appears to be important in sustaining productive catalysis; this is thought to be the reason for the ineffectiveness of the cascade catalysis conditions (employing substoichiometric TBABF) with less π-acidic substrates.

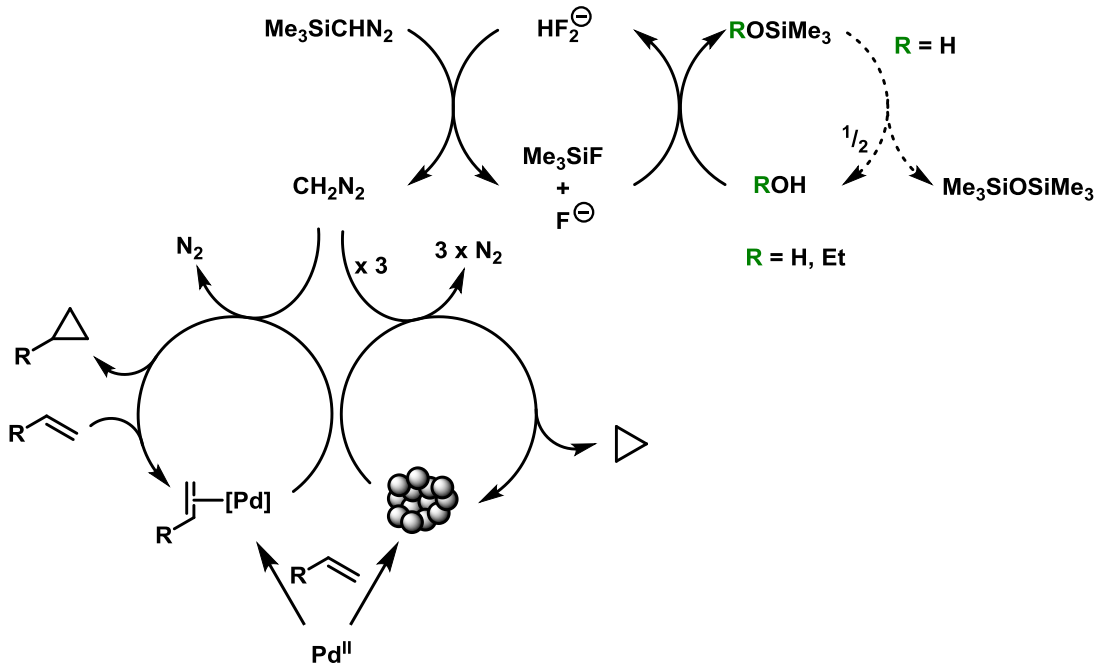

Scheme 3.1 Overview of proposed mechanisms in operation in the protodesilylative cyclopropanation of alkenes with TMSDAM.

3.2 Future Work

3.2.1 Substrate Effects in Pd-Catalysed Cyclopropanation with Diazomethane

Thus far, no coherent rationale for the efficiency of the cyclopropanation reaction as a function of the substrate is evident. Although good correlations are evident between FMO energies and the efficiency of TMSDAM consumption, *m*-nitrostyrene remains an outlier in all cases, and the similarity in the reactivity of *m*- and *p*-methoxystyrenes (despite their very different electronic demands, as exemplified by their Hammett substituent constants of 0.12 and −0.27 respectively) is as yet unexplained. One possibility is that the initial partitioning of palladium (*vide supra*, Scheme 2.18) is dependent on the electronic nature of the aromatic ring of the substrate, in a position-independent sense, for example due to stabilisation by arene-palladium π-interactions. If this is the case, it may be possible to promote the favourable partitioning of palladium, independent of substrate, by the use of an electron-deficient arene additive or solvent.

3.2.2 Protodesilylation of TMSDAM: Further Applications

The *in situ* generation of diazomethane described herein proceeds under unprecedentedly mild reaction conditions, and as such may prove useful in other transformations that conventionally employ *ex situ*-generated reagent. Although the replacement of diazomethane with TMSDAM has been reported for a number of reactions, these typically involve the use of more forcing conditions, or resort to longer reaction times. Other reactions typical of diazomethane, such as the aziridination of imines, still lack a TMSDAM variant, and may benefit from further investigation.[96]

Lithiotrimethylsilyldiazomethane (Li-TMSDAM), prepared by the deprotonation of TMSDAM by alkyllithiums, has found uses in synthesis due to its enhanced nucleophilicity. Functionalisation of this diazolithium species to afford elaborated α-silyldiazomethanes would allow access to terminal alkyldiazo compounds by application of the conditions for protodesilylative reaction. These should also be accessible directly *via* the same synthetic procedures employed for the synthesis of TMSDAM. Although these alkyldiazo compounds are

considered to be less hazardous than diazomethane, in large part due to their diminished volatility, it is clear that the ability to control the rate of addition of such species to the reaction medium can confer considerable advantages.

3.2.3 Si-Functionalised Silyldiazomethanes

The chemistry of heteroatom-substituted silyldiazomethanes ($X_nR_{2-n}SiCHN_2$) is surprisingly unexploited, with only one such example of this class of compounds having been employed in synthesis (Scheme 3.2).[97]

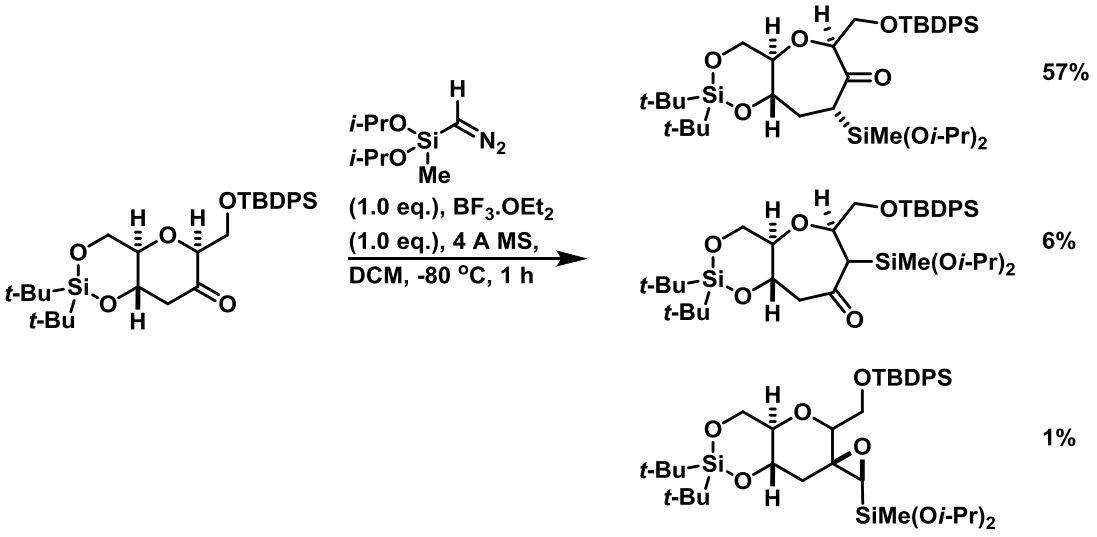

Scheme 3.2 Di(isopropoxy)methylsilyldiazomethane in synthesis: Tiffeneau-Demjanov-type ring expansion, and epoxidation.

Suitably-functionalised silanes open up access to cyclopropanols, *via* Fleming-Tamao oxidation, and a range of cross-coupling products *via* Hiyama-Denmark coupling. For example, Charette has demonstrated the efficacy of cyclopropyldi(*t*-butoxy)silanols in C-C bond forming reactions by *in situ* generation of cyclopropyltrifluorosilane.[98]

3.2.4 Isotopic Labelling

The importance of isotopic labelling in the study of reaction mechanism, biosynthetic pathways and for analytical chemistry is undeniable, and as a one-carbon synthon, diazomethane is a particularly appealing reagent for the incorporation of ^{2}H and ^{13}C labels. The deuterodesilylation of TMSDAM to generate $CHDN_2$ has been demonstrated herein, while the *in situ* formation of

CD_2N_2 was established by Lloyd-Jones and co-workers in their study of the methyl esterification reaction. In contrast, the preparation of [$^{13}C_1$]-trimethylsilyldiazomethane is unknown. Preliminary studies directed at the synthesis of this compound from ^{13}C-paraformaldehyde proved unsuccessful. More promising, however, is the synthesis of the labelled diazo reagent from $^{13}CH_3OH$. Formation of the 2,4,6-triisopropylbenzoate ester, followed by lithiation and silylation proceeds in good yield.

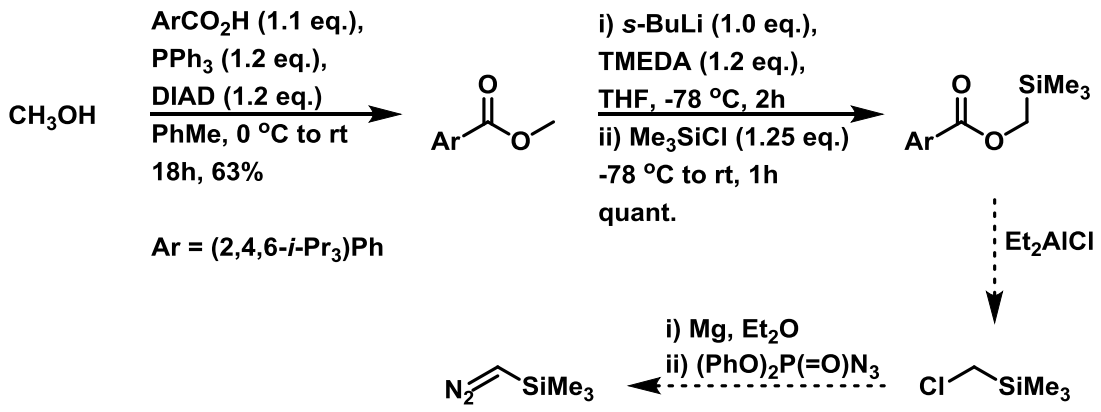

Scheme 3.3 Unoptimised preliminary studies into the synthesis of [$^{13}C_1$]-TMSDAM.

It is hoped that the cleavage of the alkyl C-O can be effected with a chloride-based Lewis acid (e.g. Et_2AlCl) to afford the corresponding silylated methyl chloride, the precursor to TMSDAM. Alternatively, reduction of the ester to afford labelled trimethylsilylmethanol, followed by an Appel reaction should allow us to intercept the same synthetic intermediate. Access to $^{13}CH_2N_2$ and [$^{13}C_1$]-TMSDAM would allow access to a wide range of labelled compounds through the synthetic transformations already known for these two important building blocks (Scheme 3.4).

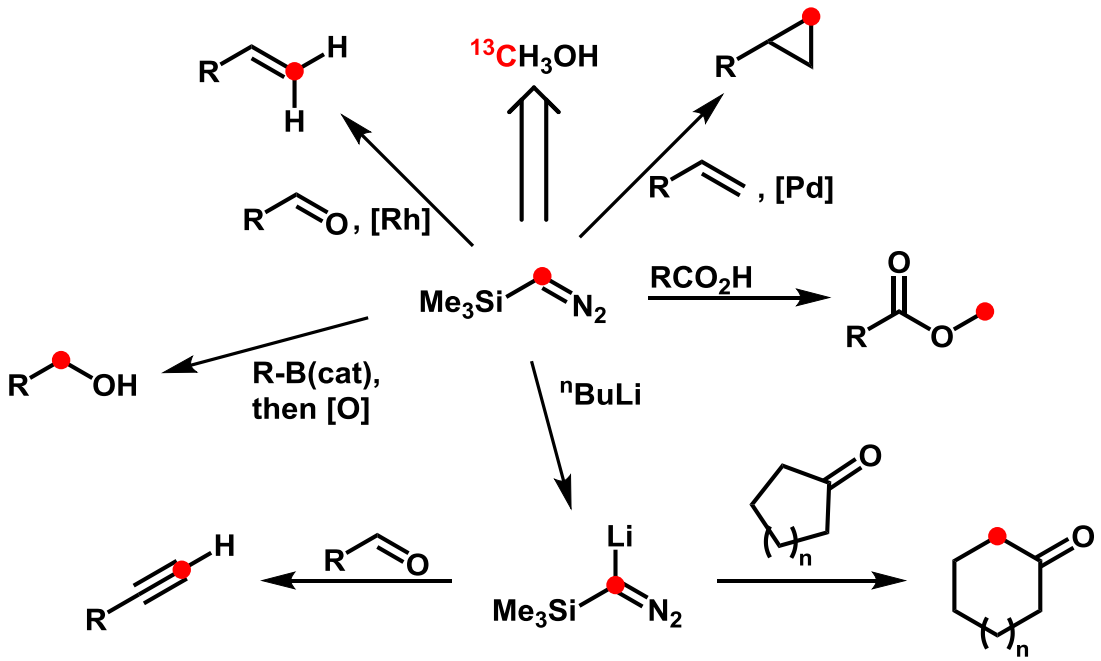

Scheme 3.4 Isotopically-labelled TMSDAM represents a versatile reagent for the synthesis of ^{13}C-labelled compounds.

3.2.5 *In Situ* Diazomethane Generation by $MeNH_2$ Diazotisation

The approach to *in situ* diazomethane synthesis demonstrated in this thesis has been predicated on the release of CH_2N_2 from a species already bearing the diazo group. This is in marked contrast to the methods typically employed for *in situ* diazomethane synthesis, which are based on the venerable base-promoted hydrolysis of *N*-methyl-*N*-nitroso compounds. A third method for diazomethane generation would involve the diazotisation of methylamine, $MeNH_2$. Very few publications exist in which this concept is explored, and none whatsoever in the context of *in situ* reagent generation. Bakke reported the use of nitrosyl chloride (NOCl) and acetic acid at low temperature (-70 °C) for the synthesis of a range of diazo compounds, including CH_2N_2.[99] Although the yields of this reaction are modest, and the conditions are not amenable to 'telescoping' with diazomethane-consuming reactions, this report provides valuable precedent for this concept, which would particularly appealing from the perspective of atom economy. Further exploration of this mechanistic paradigm for *in situ* diazomethane synthesis may prove fruitful.

4 Experimental

4.1 General Experimental Considerations

Materials and Experimental Methods

Reactions which are specified in the text below as having been carried out under nitrogen were conducted using standard Schlenk-line techniques in oven- or flame-dried glassware. Where anhydrous solvents are specified, these were obtained from Grubbs-type solvent systems (Et_2O, THF, DCM, PhMe, MeCN, hexane) at the Universities of Bristol and Edinburgh.

Reagents and materials purchased from commercial suppliers were used without further purification except where explicitly specified. Trimethylsilyldiazomethane in hexane (2M), ethylene, ethanol-*d*, ethyl cinnamate, 4-*t*-butylstyrene, 3-nitrobenzaldehyde, benzonitrile, (*S*)-4,4'-bis(phenylmethyl)-4,4',5,5'-tetrahydro-2,2'-bioxazole, potassium bifluoride, iron(II) chloride, palladium(II) chloride, palladium(II) acetate, copper(I) chloride, copper(I) iodide, platinum(II) chloride, vinylmagnesium bromide, chlorotrimethylsilane, tetrabutylammonium fluoride trihydrate and cyclohexenone were purchased from Sigma-Aldrich. 3-Trifluoromethylstyrene, 4-trifluoromethylstyrene, NaHMDS and 4-(dimethylamino)benzaldehyde were purchased from Acros Organics. Cinnamoyl chloride and triphenylphosphine were purchased from Alfa Aesar. 3-Methoxybenzaldehyde and 4-methoxybenzaldehyde were purchased from VWR International. Tetrabutylammonium bifluoride was purchased from TCI UK. 4-acetoxystyrene was purchased from Avecia. Cobalt(II) chloride and 5,10,15,20-tetraphenylporphyrin were purchased from Strem. Methyl iodide was purchased from Fisher Scientific. Potassium fluoride was purchased from Fluka. $Pd_2(dvtms)_3$ in dvtms was purchased from Umicore AG. $Pd_2(dba)_3$.dba and $[(\eta^3\text{-allyl})PdCl]_2$ were generously donated by Dr. Sophie Purser and Dr. Louise Evans, respectively.

NMR Spectroscopy

NMR spectra were acquired on Varian 400, Varian 500, JEOL Lambda 300, JEOL Eclipse 300 and JEOL Eclipse 400 spectrometers at the School of Chemistry, University of Bristol, and Bruker AVIII 400, AVIII 500 and AVIII 600 spectrometers with nitrogen or helium cryoprobes at the School of Chemistry, University of Edinburgh. Chemical shifts are quoted in parts per million (ppm). ^{1}H and ^{13}C NMR spectra are referenced to residual protiated solvent or $SiMe_4$. ^{2}H spectra were externally referenced to neat $Si(CD_3)_4$, ^{10}B and ^{11}B spectra to $BF_3{\cdot}OEt_2$ in

$CDCl_3$, ^{19}F spectra to neat $CFCl_3$, ^{29}Si spectra to 1% $SiMe_4$ in $CDCl_3$ and ^{31}P spectra to 85% aqueous H_3PO_4. The multiplicities of peaks are reported as s (singlet), d (doublet), t (triplet), q (quartet), m (multiplet), app (apparent) and combinations thereof. Assignment of signals in ^1H and ^{13}C spectra was aided by ^1H-^1H COSY, ^1H-^{13}C HSQC/HMQC where appropriate. NMR spectra were processed and analysed using MestReNova versions 7 to 10 (Mestrelab Research S. L., Santiago de Compostela, Spain).

Infrared Spectroscopy

Fourier-transform infrared spectra were recorded using a Bruker Alpha spectrometer using attenuated total reflection on a diamond window, unless otherwise specified. The intensities of absorptions are quoted as w (weak, 0-40%), m (medium, 40-70%), s (strong, 70-100%) and br (broad).

Mass Spectrometry

Mass spectrometry was carried out by Dr. Paul Gates and Mr. Paul Lawrence of the Mass Spectrometry Service, School of Chemistry, University of Bristol, and by Mr. Alan Taylor of the Mass Spectrometry Service, School of Chemistry, University of Edinburgh.

4.2 Synthesis of Metal Complexes

Bis(benzonitrile)palladium(II) chloride

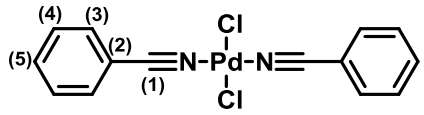

To a schlenk tube under nitrogen containing benzonitrile (15 mL, 145.6 mmol, 53 eq.) was added $PdCl_2$ (486 mg, 2.74 mmol, 1.0 eq.), and the mixture was heated to 100 °C with stirring for twenty minutes. The mixture was allowed to cool slightly (*ca*. 60 °C) and was filtered through filter paper to remove particulates. Once cooled to room temperature, the filtrate was triturated with petroleum ether (80 mL), leading to the precipitation of a bright yellow solid. The supernatant was removed, and the remaining solid was washed with additional petroleum ether (80 mL) and dried in air. Further drying under vacuum afforded the product as a bright yellow powder (900 mg, 2.33 mmol, 85%).

^{1}H NMR (300 MHz, $CDCl_3$): δ_H 7.43-7.82 (m, 10H).

MS (ESI+): $[M\text{-}Cl]^+$ requires 436.96, found 436.96.

The data are in accordance with the literature (^{1}H NMR - E. Szłyk, M. Barwiołek, *Thermochim. Acta* **2009**, *495*, 85).

(*S*)-4,4'-bis(phenylmethyl)-4,4',5,5'-tetrahydro-2,2'-bioxazole palladium(II) chloride (29.$PdCl_2$)

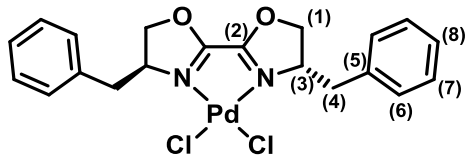

Bis(benzonitrile)palladium(II) chloride (200 mg, 0.52 mmol, 1.0 eq.) and (*S*)-4,4'-bis(phenylmethyl)-4,4',5,5'-tetrahydro-2,2'-bioxazole (167 mg, 0.52 mmol, 1.0 eq.) were dissolved in dichloromethane under air (15 mL) in a 50 mL round-bottomed flask and stirred at room temperature overnight. Hexane (15 mL) was added, the mixture cooled to 0 °C, and a yellow-orange solid precipitated. The precipitate was collected by suction filtration and dried under vacuum to afford the desired compound (193 mg, 0.41 mmol, 78%).

^{1}H NMR (400 MHz, $CDCl_3$): δ_H 3.03 (m, 2H), 3.63 (m, 2H), 4.71-4.85 (m, 6H), 7.28-7.45 (m, 10H).

$^{13}C\{^1H\}$ NMR (101 MHz, $CDCl_3$): δ_C 39.4, 64.2, 127.5, 129.0, 129.7, 134.6.

FT-IR ($\tilde{\nu}$, cm^{-1}): 3300 (w), 3064 (w), 2965 (w), 1980 (w), 1636 (m), 1514 (m), 1449 (m), 1371 (m), 1255 (s), 1149 (s), 1029 (s), 997 (m), 751 (s), 634 (s).

MS (ESI+): $[M+Na]^+$ requires 520.98, found 520.99.

(5,10,15,20-tetraphenylporphyrinato)iron(III) chloride (22)

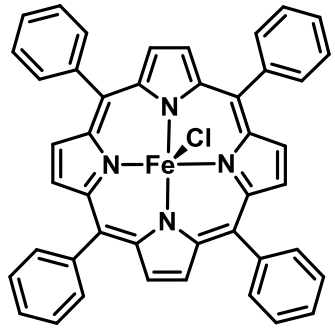

To a solution of 5,10,15,20-tetraphenylporphyrin (184.4 mg, 0.30 mmol) in chloroform (35 mL) in a 100 mL round-bottomed flask equipped with a condenser was added $FeCl_2$ (285.2 mg, 2.25 mmol) and 2,4,6-collidine (101 μL, 0.77 mmol). The resulting mixture was heated at reflux for sixteen hours. After cooling, the mixture was poured into a separating funnel containing 40 mL ice cold water and separated. The organic phase was washed with additional water (2 x 40 mL), washed with brine and evaporated *in vacuo*, to yield a very dark blue crystalline solid (202 mg, 96%).

^{1}H NMR (400 MHz, $CDCl_3$): δ_H 5.35 (br m), 6.39 (br s), 12.20 (br s), 13.36 (br s), 79.94 (br s).

$^{13}C\{^1H\}$ NMR (101 MHz, $CDCl_3$): no signals observed due to rapid relaxation.

MS (ESI+): $[M\text{-}Cl]^+$ requires 668.17, found 668.17.

UV/Vis: λ_{max}/nm 419, 509, 575.

The data are in agreement with the literature (^{1}H NMR - F. Paulat, N. Lehnert, *Inorg. Chem.* **2008**, *47*, 4963; MS – T. Gozet, L. Huynh, D. K. Bohme, *J. Mass. Spectrom.* **2010**, *45*, 35; UV/Vis – Z.-C. Sun, Y.-B. She, Y. Zhou, X.-F. Song, K. Li, *Molecules*, **2011**, *16*, 2960).

4.3 Synthesis of Fluoride Reagents

Tetrabutylammonium fluoride tetra(*t*-butanol) complex

To a solution of hexane (220 mL) and *t*-butanol (880 mL) in a 2 L round-bottomed flask was added tetrabutylammonium fluoride trihydrate (10.0 g, 31.7 mmol). The flask was fitted with a condenser and heated to 90 °C. After twenty minutes, the reaction mixture had become homogeneous, and was allowed to cool to room temperature, resulting in the precipitation of a white solid. The mixture was filtered and the solids dried under air to afford the product as a fine white crystalline solid (11.80 g, 21.1 mmol, 67%).

^{1}H NMR (300 MHz, $CDCl_3$): δ_H 1.00 (12H, t, $^{3}J_{H\text{-}H}$ = 7.3 Hz), 1.26 (36H, s), 1.45 (8H, m), 1.68 (8H, m), 3.40 (8H, m).

^{13}C{^{1}H} NMR (75 MHz, $CDCl_3$) : δ_C 13.84, 19.96, 24.36, 31.35, 59.13, 69.16.

^{19}F NMR (282 MHz, $CDCl_3$): δ_F -117.8 (s).

The data are in agreement with the literature (D. W. Kim, H.-J. Jeong, S. T. Lim, M.-H. Sohn, *Angew. Chem. Int. Ed.* **2008**, *47*, 8404).

Tetrabutylammonium bifluoride

To a solution of tetrabutylammonium bisulphate (20.37 g, 60 mmol) in chloroform (300 mL) in a 500 mL plastic bottle was added a solution of potassium bicarbonate (6.00 g, 60 mmol) in water (21 mL). The resulting biphasic mixture was mechanically stirred for ten minutes. Potassium bifluoride (4.68 g, 60 mmol) was added as a solid, and stirring was continued for one hour. Stirring was ceased, and the organic and aqueous phases were separated. The organics were evaporated under a stream of nitrogen, and redissolved in acetonitrile (60 mL). Potassium carbonate (1.20 g, 8.7 mmol) was added and the mixture stirred for ten minutes, at which point it was filtered and the filtrate was evaporated under a stream of nitrogen. The oily product was then dried to constant weight under vacuum to yield a colourless, viscous oil in yields between 80-85% (variation from run to run).

^{1}H NMR (400 MHz, $CDCl_3$): δ_H 0.89 (12H, t, $^{3}J_{H\text{-}H}$ = 7.3 Hz, 4C(1)H_3), 1.33 (8H, m, 4C(2)H_2), 1.54 (8H, m, 4C(3)H_2), 3.19 (8H, m, 4C(4)H_2).

^{13}C NMR (101 MHz, $CDCl_3$): δ_C 13.77 (4C(1)), 19.85 (4C(2)), 24.08 (4C(3)), 58.79 (4C(4)).

^{19}F NMR (376 MHz, $CDCl_3$): δ_F -156.78 (br s).

Tetrabutylammonium deuterobifluoride

To tetrabutylammonium bifluoride (600 mg, 2.13 mmol) in a plastic centrifuge tube was added D_2O (2 mL, 110 mmol). The centrifuge tube was placed under light vacuum (*ca*. 100 mbar) in a glass trap for *ca*. 90 hours, whereupon the bulk of the D_2O had evaporated. The addition of D_2O and evaporation was repeated a further two times, and the resulting oil was used directly in catalytic reactions. The mass balance suggests a 2:1 mixture of TBABF:D_2O is obtained.

4.4 Synthesis of methyl(triphenyl)phosphonium iodide

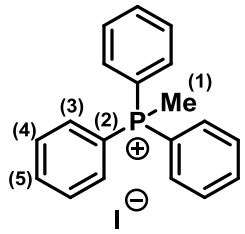

To a 500 mL round-bottomed flask equipped with a stirrer bar was added triphenylphosphine (19.65 g, 75 mmol, 1.00 eq.) and toluene (250 mL). Methyl iodide (6.20 mL, 100 mmol, 1.33 eq.) was added by syringe and the reaction was stirred for twelve hours. The resulting suspension was filtered, and the residue was dried *in vacuo* for six hours to afford the product as a white powder (29.40 g, 72.7 mmol, 97%).

^{1}H NMR (400 MHz, $CDCl_3$): δ_H 3.26 (3H, d, $^{2}J_{H\text{-}P}$ = 13.1 Hz, C(1)H_3), 7.66-7.85 (15H, m, 6C(3)H, 6C(4)H & 3C(5)H).

^{13}C{^{1}H} NMR (101 MHz, $CDCl_3$): δ_C 12.04 (d, $^{1}J_{C\text{-}P}$ = 57.0 Hz, C(1)), 119.19 (d, $^{1}J_{C\text{-}P}$ = 88.7 Hz, 3C(2)), 130.65 (d, 12.8 Hz), 133.53 (d, 10.8 Hz), 135.36 (d, $^{4}J_{C\text{-}P}$ = 3.1 Hz, 3C(5)).

^{31}P{^{1}H} NMR (162 MHz, $CDCl_3$): δ_P 21.85 (s).

FT-IR ($\tilde{\nu}$, cm^{-1}): 3047 (w), 3002 (w), 2986 (w), 2959 (w), 2934 (w), 2920 (m), 2864 (w), 2792 (w), 1586 (w), 1483 (w), 1435 (m), 1406 (w), 1337 (w), 1323 (w), 1163 (w), 1114 (s), 1072 (w), 1029 (w), 994 (w), 920 (m), 892 (m), 857 (w), 845 (w), 790 (m), 747 (s), 734 (m), 717 (s), 689 (s), 617 (w), 501 (s), 489 (s), 481 (s), 468 (m), 447 (m), 429 (m), 412 (w).

The data are in agreement with the literature (G. L. Tolnai, B. Petho, P. Králl, Z. Novák, *Adv. Synth. Catal.* **2014**, *365*, 125).

4.5 Synthesis of alkenes

Methyl cinnamate (3o)

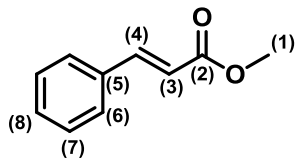

To a 250 mL round-bottomed flask was added cinnamoyl chloride (3.33 g, 20 mmol, 1.0 eq.) and ethyl acetate (100 mL).Triethylamine (2.78 mL, 20 mmol, 1.0 eq.) and methanol (0.81 mL, 20 mmol, 1.0 eq) were added, and the resulting mixture was allowed to stir for two hours. The resulting yellow suspension was filtered, the solids washed with ethyl acetate (50 mL) and the filtrate concentrated *in vacuo*. The resulting solid was dissolved in hexane (25 mL) and filtered a second time. Evaporation of the solvent afforded the product as a colourless oil (2.40 g, 14.8 mmol, 74%).

^{1}H NMR (400 MHz, $CDCl_3$): δ_H 3.81 (3H, s, C(1)H_3), 6.45 (1H, d, $^{3}J_{H\text{-}H(trans)}$ = 16.0 Hz, C(4)H), 7.40 (3H, m, 2C(7)H and C(8)H), 7.54 (2H, m, 2C(6)H), 7.70 (1H, d, $^{3}J_{H\text{-}H(trans)}$ = 16.0 Hz, C(3)H).

^{13}C NMR (101 MHz, $CDCl_3$): δ_C 51.7 (C(1)), 117.8 (C(3)), 128.1 (C(8)), 128.9 (2C(7)), 130.3 (2C(6)), 134.4 (C(5)), 144.9 (C(4)), 167.4 (C(2)).

The data are in agreement with the literature (B. Zhang, P. Feng, Y. Cui, N. Jiao, *Chem. Commun.* **2012**, *48*, 7280).

Trimethylsilylethylene (3q)

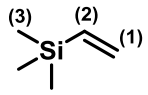

Vinylmagnesium bromide (2.5 mL, 1M in THF, 2.5 mmol, 1.0 eq.) was added to a 10 mL round-bottomed flask fitted with a condenser and heated to reflux. Chlorotrimethylsilane (0.32 mL, 2.5 mmol, 1.0 eq.) was added dropwise over two minutes, and heating was continued for a further two hours. The mixture was allowed to cool to room temperature and left to stir for seventeen hours. The product was distilled directly from the reaction mixture (60 °C) with a small amount of THF. The distillate was washed with water (10 x 0.1 mL) to remove THF, yielding a pungent, clear, colourless oil. The presence of THF in the product was evident by ^{1}H NMR spectroscopy. The yield of product was estimated to be 55% on the basis of integration of the ^{1}H NMR spectrum.

^{1}H NMR (300 MHz, $CDCl_3$): δ_H 0.01 (9H, s, 3C(3)H_3), 5.59 (1H, dd, $^{3}J_{H\text{-}H(trans)}$ = 20.0 Hz, $^{2}J_{H\text{-}H}$ = 4.0 Hz, C(1)H), 5.82 (1H, dd, $^{3}J_{H\text{-}H(cis)}$ = 15.5 Hz, $^{2}J_{H\text{-}H}$ = 4.0 Hz, C(1)H), 6.09 (1H, dd, $^{3}J_{H\text{-}H(trans)}$ = 20.0 Hz, $^{3}J_{H\text{-}H(cis)}$ = 15.5 Hz, C(2)H).

^{13}C{^{1}H} NMR (75 MHz, $CDCl_3$): δ_C -1.7 (3C(3)), 130.3 (C(2)), 140.2 (C(1)).

The data are in accordance with the literature (A. Pollex, M. Hiersemann, *Org. Lett.* **2005**, 7, 5705).

General Procedure for the Synthesis of Terminal Alkenes from Aldehydes

To a flame-dried schlenk tube equipped with a stirrer bar under a nitrogen atmosphere was added methyltriphenylphosphonium iodide (2.234 g, 5.5 mmol, 1.10 eq.) and anhydrous THF (30 mL). The resulting suspension was cooled to 0 °C, and sodium bis(trimethylsilyl)amide (2.0 M in THF, 2.75 mL, 5.5 mmol, 1.10 eq.) was added dropwise by syringe to afford a homogeneous yellow solution. The requisite aldehyde (5.0 mmol, 1.00 eq.) was then added, the reaction mixture was allowed to warm to room temperature and stirred until the reaction had reached completion (typically <18 h). Diethyl ether (10 mL) was then added to the reaction mixture under air, followed by petroleum ether (100 mL), whereupon a precipitate (triphenylphosphine oxide, $Ph_3P{=}O$) formed. The resulting slurry was filtered, and the filtrate evaporated *in vacuo*. The crude products were purified by column chromatography on silica (eluents below) to afford the desired styrenes.

4-Methoxystyrene (3u)

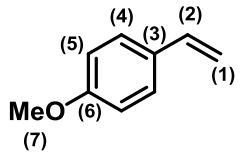

Prepared from 4-methoxybenzaldehyde.

Yield: 449 mg (3.35 mmol, 67%) as a colourless oil.

Column eluent: 1 % Et_2O in petroleum ether, $R_f = 0.10$.

^{1}H NMR (400 MHz, $CDCl_3$): δ_H 3.82 (3H, s, C(7)H_3), 5.13 (1H, dd, $^3J_{H\text{-}H(cis)}$ = 10.9 Hz, $^2J_{H\text{-}H}$ = 0.9 Hz, C(1)H), 5.61 (1H, dd, $^3J_{H\text{-}H(trans)}$ = 17.6 Hz, $^2J_{H\text{-}H}$ = 0.9 Hz, C(1)H), 6.67 (1H, dd, $^3J_{H\text{-}H(trans)}$ = 17.6 Hz, $^3J_{H\text{-}H(cis)}$ = 10.9 Hz, C(2)H), 6.87 (2H, m, 2C(5)H), 7.35 (2H, m, 2C(4)H).

^{13}C{^{1}H} NMR (101 MHz, $CDCl_3$): δ_C 55.44 (s, C(7)), 111.71 (s, C(1)), 114.04 (s, 2C(5)), 127.52 (s, 2C(4)), 130.58 (s, C(3)), 136.35 (s, C(2)), 159.50 (s, C(6)).

FT-IR ($\tilde{\nu}$, cm^{-1}): 3086 (w), 3003 (w), 2956 (w), 2934 (w), 2909 (w), 2835 (w), 1628 (m), 1605 (m), 1574 (w), 1508 (s), 1461 (w), 1442 (w), 1425 (w), 1408 (w), 1319 (w), 1301 (m), 1290 (w), 1244 (s), 1204 (w), 1173 (s), 1114 (w), 1038 (m), 1022 (m), 989 (m), 898 (m), 831 (s), 814 (m), 708 (w), 552 (w), 524 (w), 495 (w).

The data are in agreement with the literature (G. L. Tolnai, B. Petho, P. Králl, Z. Novák, *Adv. Synth. Catal.* **2014**, *365*, 125).

3-Nitrostyrene (3v)

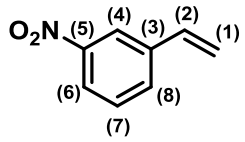

Prepared from 3-nitrobenzaldehyde.

Yield: 465 mg (3.12 mmol, 62%) as a yellow oil.

Column eluent: 5% Et_2O in petroleum ether, $R_f = 0.25$.

^{1}H NMR (400 MHz, $CDCl_3$): δ_H 5.45 (1H, d, $^3J_{H\text{-}H(cis)}$ = 10.9 Hz, C(1)H), 5.90 (1H, d, $^3J_{H\text{-}H(trans)}$ = 17.5 Hz, C(1)H), 6.77 (1H, dd, $^3J_{H\text{-}H(trans)}$ = 17.5 Hz, $^3J_{H\text{-}H(cis)}$ = 10.9 Hz, C(2)H), 7.50 (1H, t, $^3J_{H\text{-}H}$ = 7.9 Hz, C(7)H), 7.71 (1H, m, C(8)H), 8.11 (1H, ddd, $^3J_{H\text{-}H}$ = 8.1 Hz, $^4J_{H\text{-}H}$ = 2.3 Hz, $^4J_{H\text{-}H}$ = 1.0 Hz, C(6)H), 8.26 (1H, app t, 2.0 Hz, C(4)H).

^{13}C{^{1}H} NMR (101 MHz, $CDCl_3$) : δ_C 117.23 (C(1)), 121.04 (C(4)), 122.57 (C(6)), 129.59 (C(7)), 132.21 (C(8)), 134.90 (C(2)), 139.41 (C(3)) 148.78 (C(5)).

FT-IR ($\tilde{\nu}$, cm^{-1}): 3090 (w), 3014 (w), 2870 (w), 1845 (w), 1732 (w), 1633 (w), 1572 (w), 1522 (s), 1482 (w), 1436 (w), 1408 (w), 1345 (s), 1313 (m), 1287 (w), 1207 (w), 1168 (w), 1097 (w), 1086 (w), 1047 (w), 1027 (w), 988 (m), 918 (m), 898 (m), 806 (m), 793 (m), 746 (s), 698 (s), 671 (m), 638 (w), 572 (w), 542 (w), 503 (w), 458 (w), 416 (w).

The data are in agreement with the literature (S. E. Denmark, C. R. Butler, *J. Am. Chem. Soc.* **2008**, *130*, 3690).

4-(Dimethylamino)styrene (3w)

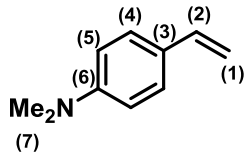

Prepared from 4-(dimethylamino)benzaldehyde.

Yield: 260 mg (1.77 mmol, 35%) as a light yellow-brown oil.

Column eluent: 5% EtOAc in petroleum ether, $R_f = 0.25$.

^{1}H NMR (400 MHz, $CDCl_3$): δ_H 2.96 (6H, s, 2C(7)H_3), 5.02 (1H, dd, $^3J_{H\text{-}H(cis)} = 10.9$ Hz, $^2J_{H\text{-}H} = 1.1$ Hz, C(1)H), 5.54 (1H, dd, $^3J_{H\text{-}H(trans)} = 17.6$ Hz, $^2J_{H\text{-}H} = 1.1$ Hz, C(1)H), 6.63 (1H, dd, $^3J_{H\text{-}H(trans)} = 17.6$ Hz, $^3J_{H\text{-}H(cis)} = 10.9$ Hz, C(2)H), 6.69 (2H, m, 2C(4)H), 7.31 (2H, m, 2C(5)H).

^{13}C{^{1}H} NMR (101 MHz, $CDCl_3$): δ_C 40.67 (s, 2C(7)), 109.50 (s, C(1)), 112.48 (s, C(4)), 126.38 (s, C(3)), 127.29 (s, C(5)), 136.75 (s, C(2)), 150.42(s, C(6)).

FT-IR ($\tilde{\nu}$, cm^{-1}): 3083 (w), 2978 (w), 2885 (w), 2799 (w), 1607 (s), 1556 (w), 1518 (s), 1479 (w), 1444 (m), 1407 (w), 1348 (m), 1326 (m), 1221 (m), 1186 (m), 1164 (m), 1127 (w), 1061 (w), 988 (m), 946 (m), 883 (m), 817 (s), 781 (w), 681 (w), 640 (w), 535 (w), 499 (m), 459 (w), 415 (w).

The data are in agreement with the literature (^{1}H, ^{13}C NMR; IR - A. Gordillo, E. de Jesús, C. López-Mardomingo, *Chem. Commun.* **2007**, 4056).

3-Methoxystyrene (3x)

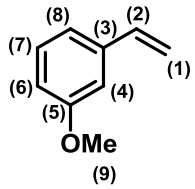

Prepared from 3-methoxybenzaldehyde.

Yield: 542 mg (4.04 mmol, 81%) as a colourless oil.

Column eluent: 5% EtOAc in petroleum ether, $R_f = 0.15$.

^{1}H NMR (400 MHz, $CDCl_3$): δ_H 3.83 (3H, s, C(9)H_3), 5.26 (1H, dd, $^3J_{H\text{-}H(cis)}$ = 10.9 Hz, $^2J_{H\text{-}H}$ = 0.9 Hz, C(1)H), 5.75 (1H, dd, $^3J_{H\text{-}H(trans)}$ = 17.6 Hz, $^2J_{H\text{-}H}$ = 0.9 Hz, C(1)H), 6.70 (1H, dd, $^3J_{H\text{-}H(trans)}$ = 17.6 Hz, $^3J_{H\text{-}H(cis)}$ = 10.9 Hz, C(2)H), 6.82 (1H, ddd, $^3J_{H\text{-}H}$ = 8.2 Hz, $^4J_{H\text{-}H}$ = 2.6 Hz, $^4J_{H\text{-}H}$ = 0.9 Hz, C(6)H), 6.96 (1H, app dd, $^4J_{H\text{-}H}$ = 2.6 Hz, $^4J_{H\text{-}H}$ = 1.6 Hz, C(4)H), 7.01 (1H, app dm, $^3J_{H\text{-}H}$ = 7.9 Hz, C(8)H), 7.25 (1H, app t, $^3J_{H\text{-}H}$ = 7.9 Hz, C(7)H).

^{13}C NMR (101 MHz, $CDCl_3$): δ_C 55.37 (s, C(9)), 111.66 (s, C(4)), 113.58 (s, C(6)), 114.27 (s, C(1)), 119.05 (s, C(8)), 129.63 (s, C(7)), 136.92 (s, C(2)), 139.18 (s, C(3)), 159.94 (s, C(5)).

FT-IR ($\tilde{\nu}$, cm^{-1}): 3087 (w), 3004 (w), 2956 (w), 2834 (w), 1598 (w), 1576 (m), 1486 (m), 1455 (w), 1434 (w), 1414 (w), 1327 (w), 1306 (w), 1285 (m), 1259 (s), 1241 (m), 1191 (w), 1152 (m), 1088 (w), 1033 (m), 989 (m), 906 (m), 873 (w), 855 (m), 781 (m), 714 (m), 667 (w), 569 (w), 540 (w), 433 (w).

The data are in agreement with the literature (S. Albert, R. Horbach, H. B. Deising, B. Siewert, R. Csuk, *Bioorg. Med. Chem.* **2011**, *19*, 5155).

4.6 Cyclopropanes

General Procedure for Monitoring Desilylative Cyclopropanation with TBABF

To a 10 mL round-bottomed flask equipped with a magnetic stirrer bar was added $(PhCN)_2PdCl_2$ (1.53 mg, 4 μmol, 1.1 mol%), tetrabutylammonium bifluoride (202.7 mg, 0.72 mmol, 2.0 eq.), the alkene substrate (0.36 mmol, 1.0 eq.). and dichloromethane (7.3 mL). The resulting mixture was magnetically stirred at 1100 rpm, and TMSDAM (20 μL, 0.036 mmol, 0.1 eq.) was added *via* 26 gauge needle submerged in the reaction solvent using a syringe pump at a rate of 1.2 mL h^{-1}. After the addition was complete (1 min), an aliquot of the reaction mixture (*ca.* 100 μL) was withdrawn by syringe and added to an NMR tube. The addition of TMSDAM and sampling was iterated to generate the desired number of data points. The NMR tubes were placed under vacuum to remove protiated solvent, and the contents were then redissolved in $CDCl_3$ for analysis by ^1H NMR spectroscopy. Due to their volatility, in the case of fluorinated substrates, the contents of the NMR tubes were diluted directly with $CDCl_3$ and data (^{19}F NMR) were acquired.

The remaining bulk solutions were subjected to filtration through a pad of silica (3-5 cm in depth) to remove tetrabutylammonium salts, which otherwise obscure ^1H NMR signals of the cyclopropane products.

Ethyl 2-phenylcyclopropanecarboxylate (4n)

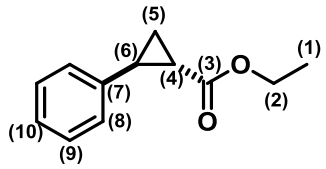

^{1}H NMR (600 MHz, $CDCl_3$): δ_H 1.28 (3H, t, $^3J_{H\text{-}H}$ = 7.1 Hz, C(1)H_3), 1.30 (partially obscured, app. 1H C(5)H), 1.60 (1H, ddd, $^3J_{H\text{-}H(cis)}$ = 9.3 Hz, $^3J_{H\text{-}H(trans)}$ = 5.3 Hz, $^2J_{H\text{-}H}$ = 4.5 Hz, C(5)H), 1.90 (1H, ddd, $^3J_{H\text{-}H(cis)}$ = 8.5 Hz, $^3J_{H\text{-}H(trans)}$ = 5.3 Hz, $^3J_{H\text{-}H(trans)}$ = 4.2 Hz, C(4)H), 2.52 (1H, ddd, $^3J_{H\text{-}H(cis)}$ = 9.3 Hz, $^3J_{H\text{-}H(trans)}$ = 6.5 Hz, $^3J_{H\text{-}H(trans)}$ = 4.2 Hz, C(6)H), 4.17 (2H, q, $^3J_{H\text{-}H}$ = 7.1 Hz, C(2)H_2), 7.10 (2H, m, 2C(8)H), 7.20 (1H, m, C(10)H), 7.28 (2H, m, 2C(9)H).

^{13}C{^{1}H} NMR (151 MHz, $CDCl_3$) : δ_C 14.41 (C(1)), 17.19 (C(5)), 24.31 (C(4)), 26.31 (C(6)), 60.84 (C(2)), 126.31 (2C(8)), 126.60 (C10), 128.60 (2C(9)), 140.27 (C(7)), 173.54 (C(3)).

The data are in agreement with the literature (Y. Chen, X. P. Zhang, *J. Org. Chem.* **2004**, *69*, 2431).

(4-*t*-butylphenyl)cyclopropane (4r)

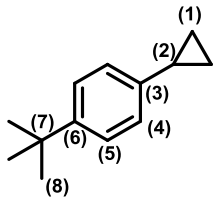

^{1}H NMR (400 MHz, $CDCl_3$): δ_H 0.68 (2H, m, 2C(1)H), 0.92 (2H, m, 2C(1)H), 1.30 (9H, s, 3C(8)H_3), 1.87 (1H, tt, $^{3}J_{H\text{-}H(cis)}$ = 8.4 Hz, $^{3}J_{H\text{-}H(trans)}$ = 5.1 Hz, C(2)H), 7.02 (2H, m, 2C(4)H), 7.29 (2H, m, 2C(5)H).

$^{13}C\{^{1}H\}$ NMR (101 MHz, $CDCl_3$) : δ_C 9.09 (2C(1)), 15.02 (C(2)), 31.55 (3C(8)), 34.46 (C(7)), 125.30 (C(5)), 125.48 (C(4)), 141.01 (C(3)), 148.35 (C(6)).

The data are in agreement with the literature (^{1}H NMR - M. Lemhadri, H. Doucet, M. Santelli, *Synth. Commun.* **2006**, *36*, 121; ^{13}C NMR - J. M. Sarria Toro, T. den Hartog, P. Chen, *Chem. Commun.* **2014**, *50*, 10608). The ^{1}H NMR data reported by Chen and co-workers does not agree with the data reported above, or that by Doucet and co-workers. It appears as if the ^{1}H NMR spectrum corresponding to (4-methylphenyl)cyclopropane has been accidentally copied in place of the correct data.

Bicyclo[4.1.0]heptan-2-one (4s)

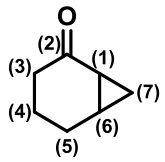

^{1}H NMR (500 MHz, $CDCl_3$): δ_H 1.08 (1H, ddd, $^{3}J_{H\text{-}H(trans)}$ = 10.0 Hz, $^{3}J_{H\text{-}H(trans)}$ = 8.1 Hz, $^{2}J_{H\text{-}H}$ = 5.3 Hz, C(7)H), 1.20 (1H, app q, $^{3}J_{H\text{-}H(cis)}$ = $^{2}J_{H\text{-}H}$ = 5.3 Hz, C(7)H), 1.56-1.78 (4H, m, C(1)H, C(4)H_2 and C(6)H), 1.86-2.00 (2H, m, C(5)H_2), 2.05 (1H, dddd, $^{2}J_{H\text{-}H}$ = 18.3 Hz, $^{3}J_{H\text{-}H}$ = 11.5 Hz, $^{3}J_{H\text{-}H}$ = 6.8 Hz, $^{4}J_{H\text{-}H}$ = 0.9 Hz, C(3)H), 2.29 (1H, ddd, $^{2}J_{H\text{-}H}$ = 18.3 Hz, $^{3}J_{H\text{-}H}$ = 5.4 Hz, $^{3}J_{H\text{-}H}$ = 3.8 Hz, C(3)H).

^{13}C{^{1}H} NMR (126 MHz, $CDCl_3$) : δ_C 10.36 (C(7)), 17.56 (C(6)), 17.94 (C(4)), 21.42 (C(5)), 25.95 (C(1)), 36.90 (C(3)), 209.38 (C(2)).

The data are in agreement with the literature (C. Rodríguez-García. J. Ibarzo, Á. Álvarez-Larena,V. Branchadell, A. Oliva, R. M. Ortuño, *Tetrahedron*, **2001**, *57*, 1025).

(4-Trifluoromethylphenyl)cyclopropane (4t)

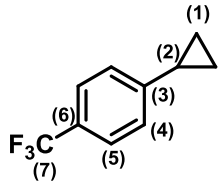

^{1}H NMR (400 MHz, $CDCl_3$): δ_H 0.75 (2H, m, 2C(1)H), 1.04 (2H, m, 2C(1)H, 1.94 (1H, tt, $^{3}J_{H\text{-}H(cis)}$ = 8.4 Hz, $^{3}J_{H\text{-}H(trans)}$ = 5.0 Hz), 7.15 (2H, m, 2C(4)H), 7.49 (2H, m, 2C(5)H).

^{13}C{^{1}H} NMR (101 MHz, $CDCl_3$) : δ_C 10.06 (s, 2C(1)), 15.55 (s, C(2)), 125.30 (q, $^{3}J_{C\text{-}F}$ = 3.7 Hz, 2C(5)), 125.89 (s, 2C(4)), 126.36 (q, $^{1}J_{C\text{-}F}$ = 271 Hz, C(7)), 127.75 (q, $^{2}J_{C\text{-}F}$ = 32.3 Hz, C(6)), 148.54 (s, C(3)).

^{19}F NMR (376 MHz, $CDCl_3$): δ_F −62.24 (s).

The data (^{1}H NMR) are in agreement with the literature (M. Lemhadri, H. Doucet, M. Santelli, *Synth. Commun.* **2006**, *36*, 121).

(4-Methoxyphenyl)cyclopropane (4u)

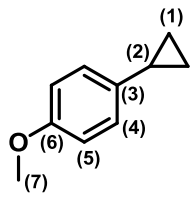

^{1}H NMR (400 MHz, $CDCl_3$): δ_H 0.62 (2H, m, 2C(1)H), 0.90 (2H, m, 2C(1)H), 1.86 (1H, tt, $^{3}J_{H\text{-}H(cis)}$ = 8.4 Hz, $^{3}J_{H\text{-}H(trans)}$ = 5.1 Hz, C(2)H), 3.78 (3H, s, C(7)H_3), 6.82 (2H, m, 2C(5)H), 7.02 (2H, m, 2C(4)H).

^{13}C{^{1}H} NMR (101 MHz, $CDCl_3$) : δ_C 8.64 (2C(1)), 14.74 (C(2)), 55.46 (C(7)), 113.90 (2C(5)), 126.98 (2C(4)), 135.85 (C(3)), 157.57 (C(6)).

The data are in agreement with the literature (G. A. Molander, P. E. Gormisky, *J. Org. Chem.* **2008**, *73*, 7481).

(3-nitrophenyl)cyclopropane (4v)

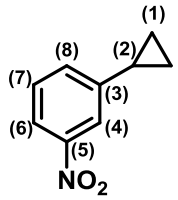

^{1}H NMR (500 MHz, $CDCl_3$): δ_H 0.78 (2H, m, 2C(1)H), 1.08 (2H, m, 2C(1)H), 2.00 (1H, tt, $^{3}J_{H\text{-}H(cis)}$ = 8.4 Hz, $^{3}J_{H\text{-}H(trans)}$ = 5.0 Hz, C(2)H), 7.40 (2H, m, C(8)H and C(6)H), 7.90 (1H, m, C(6)H), 7.99 (1H, m, C(4)H).

^{13}C{^{1}H} NMR (126 MHz, $CDCl_3$) : δ_C 10.00 (2C(1)), 15.50 (C(2)), 120.59 (C(4)), 120.60 (C(6)), 129.16 (C(7)), 132.21 (C(8)), 146.50 (C(3)), 148.63 (C(5)).

The data are in agreement with the literature (^{1}H NMR – R. C. Hahn, P. H. Howard, S.-M. Kong, G. A. Lorenzo, N. L. Miller, *J. Am. Chem. Soc.* **1969**, *91*, 3558; ^{13}C NMR – N. Inamoto, S. Masuda, W. Nakanishi, Y. Ideda, *Chem. Lett.* **1977**, 759).

(4-(dimethylamino)phenyl)cyclopropane (4w)

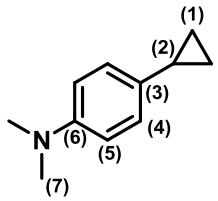

^{1}H NMR (400 MHz, $CDCl_3$): δ_H 0.60 (2H, m, 2C(1)H), 0.86 (2H, m, 2C(1)H), 1.83 (1H, tt, $^{3}J_{H\text{-}H(cis)}$ = 8.4 Hz, $^{3}J_{H\text{-}H(trans)}$ = 5.1 Hz, C(2)H), 2.90 (6H, s, 2C(7)H_3), 6.70 (2H, m, 2C(5)H), 7.00 (2H, m, 2C(4)H).

^{13}C{^{1}H} NMR (101 MHz, $CDCl_3$) : δ_C 8.23 (2C(1)), 14.59 (C(2)), 41.16 (2C(7)), 113.32 (2C(5)), 127.29 (2C(4)), 132.14 (C(3)), 149.14 (C(6)).

The data are in agreement with the literature (H. Chen, M. J. de Groot, N. P. E. Vermeulen, R. P. Hanzlik, *J. Org. Chem.* **1997**, *62*, 8227).

(3-methoxyphenyl)cyclopropane (4x)

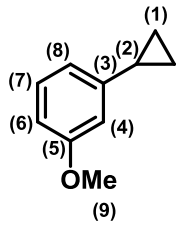

^{1}H NMR (400 MHz, $CDCl_3$): δ_H 0.70 (2H, m, 2C(1)H), 0.95 (2H, m, 2C(1)H), 1.88 (1H, tt, $^{3}J_{H\text{-}H(cis)}$ = 8.4 Hz, $^{3}J_{H\text{-}H(trans)}$ = 5.1 Hz, C(2)H), 3.79 (3H, s, C(9)H_3), 6.63 (1H, t, $^{4}J_{H\text{-}H}$ = 2.1 Hz, C(4)H), 6.69 (2H, m, C(6)H and C(8)H), 7.17 (1H, t, 7.9 Hz, C(7)H).

^{13}C{^{1}H} NMR (101 MHz, $CDCl_3$) : δ_C 9.37 (2C(1)), 15.61 (C(2)), 55.29 (C(9)), 110.74 (C(6)), 111.70 (C(4)), 118.25 (C(8)), 129.36 (C(7)), 145.91 (C(3)), 159.83 (C(5)).

The data are in agreement with the literature (J. M. Sarria Toro, T. den Hartog, P. Chen, *Chem. Commun.* **2014**, *50*, 10608).

(4-acetoxyphenyl)cyclopropane (4y)

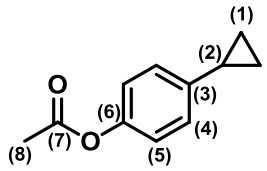

^{1}H NMR (500 MHz, $CDCl_3$): δ_H 0.67 (2H, m, 2C(1)H), 0.95 (2H, m, 2C(1)H), 1.90 (1H, m, C(2)H), 2.28 (3H, s, C(8)H_3), 6.97 (2H, m, C(4)H), 7.08 (2H, m, C(3)H).

^{13}C{^{1}H} NMR (126 MHz, $CDCl_3$) : δ_C 9.16 (2C(1)), 15.05 (C(2)), 21.22 (C(8)), 121.35 (2C(5)), 126.79 (2C(4)), 136.01 (C(3)), 148.53 (C(6)), 169.88 (C(7)).

The data are in agreement with the literature (B. W. Horrom, H. Mazdiyasni, *Org. Prep. Proced. Int.* **1992**, *24*, 696).

(3-trifluoromethylphenyl)cyclopropane (4z)

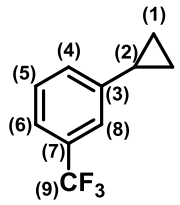

^{1}H NMR (600 MHz, $CDCl_3$): δ_H 0.74 (2H, m, 2C(1)H), 1.03 (2H, m, 2C(1)H), 1.96 (1H, tt, $^{3}J_{H\text{-}H(trans)}$ = 8.4 Hz, $^{3}J_{H\text{-}H(cis)}$ = 5.1 Hz, C(2)H), 7.24 (1H, app. d, C(4)H), 7.32 (1H, app. br s, C(8)H), 7.35 (1H, t, $^{3}J_{H\text{-}H}$ = 7.7 Hz, C(5)H), 7.40 (1H, m, C(6)H).

^{13}C{^{1}H} NMR (151 MHz, $CDCl_3$) : δ_C 9.06 (s, C(1)), 14.20 (s, C(2)), 121.72-127.18 (q, $^{1}J_{C\text{-}F}$ = 272 Hz, C(9)), 122.31 (q, $^{3}J_{C\text{-}F}$ = 3.8 Hz, C(6)), 122.68 (q, $^{3}J_{C\text{-}F}$ = 4.0 Hz, C(8)), 128.76 (s, C(5)), 129.16 (s, C(4)), 130.77 (q, $^{4}J_{C\text{-}F}$ = 32.1 Hz, C(7)), 145.17 (s, C(3)).

^{19}F NMR (470 MHz, $CDCl_3$): δ_F −62.70 (s).

MS (EI+): 117.0 ([M-CF_3]$^+$, 100%), 186.0 ([M]$^+$, 75%).

Accurate Mass (EI+): $C_{10}H_9F_3$ requires 186.06509, found 186.064561.

FT-IR ($\tilde{\nu}$, cm^{-1}): 3087 (w), 3013 (w), 1618 (w), 1596 (w), 1494 (w), 1444 (w), 1385 (w), 1368 (w), 1323 (m), 1277 (m), 1220 (w), 1160 (m), 1120 (m), 1073 (m), 1057 (m), 1021 (w), 1001 (w), 910 (m), 795 (m), 699 (s), 657 (m).

4.7 Diazomethane Generation – *In Situ* NMR Experiments

4.7.1 TBABF/TMSDAM

To a brand new 5 mm NMR tube (Norell S400) was added tetrabutylammonium bifluoride (61.76 mg, 0.22 mmol) and dichloromethane-d_2 (0.60 mL). The tube was placed into the pre-cooled (293 K) probe of a Bruker Avance III 400 MHz NMR spectrometer, and ^{1}H and ^{19}F spectra were acquired. The sample was then removed from the spectrometer, and trimethylsilyldiazomethane (10 μL of a 1.8 M solution in hexane, 0.018 mmol) was added using a syringe pump (12 mL h^{-1}, addition time 3 s), with addition through a fine (26 gauge) needle. In order to minimise the risk of explosion, the needle was **not** submerged in the solution, but rather the TMSDAM was injected down the inside of the sample tube. The tube was capped, and inverted three times prior to it being replaced in the spectrometer and ^{1}H and ^{19}F spectra being acquired. The addition-acquisition sequence was repeated an additional thirteen times. At the end of the experiment, the contents of the NMR tube were quenched with a solution of acetic acid in dichloromethane.

4.7.2 TBABF/TMSDAM/H_2O

The experiment was carried out in as detailed above (Section 4.7.1). The addition-acquisition sequence was repeated seven times. After the seventh TMSDAM addition, the absence of HF_2^- was apparent in both ^{1}H and ^{19}F NMR spectra, and following the eighth addition, the accumulation of TMSDAM was evident in the ^{1}H NMR spectrum. A ^{29}Si NMR spectrum was also acquired. Following the eighth set of spectra, the sample was removed from the spectrometer, and a small amount of water (*ca.* 10 μL) was drawn up into a flame-polished pipette and added to the NMR tube, which was then capped and cautiously shaken to disperse water droplets. The NMR tube was returned to the spectrometer and ^{1}H, ^{19}F and ^{29}Si NMR spectra were acquired. Following the acquisition of the required data, the contents of the NMR tube were quenched with a solution of acetic acid in dichloromethane.

4.7.3 TBABF/TMSDAM/EtOH

To a brand new 5 mm NMR tube (Norell S400) was added tetrabutylammonium bifluoride (2.12 mg, 7.5 μmol) and dichloromethane-d_2 (0.60 mL). The tube was placed into the pre-cooled (293 K) probe of a Bruker Avance III 400 MHz NMR spectrometer, and ^{1}H and ^{19}F spectra were acquired.

EtOH (52.5 μL, 1.45 mmol) was added to a 0.5 mL volumetric flask, and diluted to 0.5 mL with dichloromethane-d_2. 200 μL of this solution was added to 200 μL of TMSDAM solution (1.8 M in hexane, 0.36 mmol). 10μL aliquots of this solution (9.0 μmol TMSDAM) were added to the TBABF solution in the NMR tube by syringe pump (12 mL h^{-1}, addition time 3 s), with addition through a fine (26 gauge) needle. In order to minimise the risk of explosion, the needle was **not** submerged in the solution, but rather the TMSDAM/EtOH mixture was injected down the inside of the sample tube. The tube was capped, and inverted three times prior to it being replaced in the spectrometer and ^{1}H and ^{19}F spectra being acquired. The addition-acquisition sequence was repeated an additional seven times. After the final addition and acquisition of spectra, the contents of the NMR tube were quenched with a solution of acetic acid in dichloromethane.

4.8 Reaction Monitoring by ^{2}H NMR Spectroscopy

The general procedure for monitoring desilylative cyclopropanation reactions detailed above (p. 113) was used as the basis for the design of these experiments. In order to allow NMR samples (600 uL) to be taken from the reaction mixture directly without the necessity of dilutions, reactions were scaled up five-fold.

To a 50 mL, two-necked round-bottomed flask equipped with a magnetic stirrer bar was added $(PhCN)_2PdCl_2$ (7.65 mg, 20 μmol, 1.1 mol%), tetrabutylammonium bifluoride (101.3 mg, 0.072 mmol, 20 mol%), ethyl cinnamate (300 μL, 1.8 mmol, 1.0 eq.) and dichloromethane (29 mL). The flask was capped with a septum and a balloon. To the resulting solution was added a 1:1 mixture of TMSDAM:EtOD (prepared by mixing equal volumes of commercial TMSDAM in hexane with a 10.5% v/v solution of EtOD in DCM) in 200 μL portions at 12 mL h^{-1} by syringe pump. Aliquots (600 μL) were withdrawn by syringe to NMR tubes, which were capped and immediately cooled to below −5 °C to prevent loss of volatiles. The samples were kept at this temperature until NMR spectra could be acquired. The probe of the NMR instrument was pre-cooled to 2 °C, and maintained at this temperature for the acquisition of all spectra. Once removed from the instrument, samples were returned to the cold bath, and subsequently stored in a freezer (−20 °C) over the weekend.

Cyclopropane ($C_3^{1/2}H_6$)-rich aliquots (i.e. the last few taken from the reaction mixture) were combined in one bulb of a short-path distillation kit. The system was sealed, and the receiving bulb cooled to −78 °C with a dry ice/acetone bath. Distillation of volatiles was effected by gentle heating of the filled bulb with a heat gun set to 70 °C (**CAUTION:** heating a closed system carries the risk of explosion – very gentle heating is required). The distilled solution was added to an NMR tube equipped with a J Young valve and sealed to prevent the loss of volatile species.

In cases where ethylene purges were carried out, this was done following the fifth addition of TMSDAM by exchanging the partially nitrogen-inflated balloon for a balloon filled with ethylene, and piercing the septum with a needle. Approximately three volumes of ethylene (150 mL) were passed through the flask, then the needle was removed from the septum and a fresh ethylene balloon was attached to the flask to maintain ethylene saturation. The TMSDAM additions and sample withdrawal were then continued as previously described.

5 References

1. H. von Pechmann, *Ber. Dtsch. Chem. Ges.* **1894**, *27*, 1888.
2. H. von Pechmann, *Ber. Dtsch. Chem. Ges.* **1895**, *28*, 855.
3. G. W. Cowell, A. Ledwith, *Quart. Rev. Chem. Soc.* **1970**, *24*, 119.
4. E. B. LeWinn, *Am. J. Med. Sci.* **1949**, *218*, 556.
5. Y. Terao, M. Sekiya, *e-EROS Encyclopedia of Reagents for Organic Synthesis*, **2001**.
6. Sigma-Aldrich Technical Bulletin: Diazald ® and Diazomethane Generators, **2007**, www.sigmaaldrich.com/content/dam/sigma-aldrich/docs/Aldrich/Bulletin/al_techbull_al180.pdf (Accessed 3rd March 2015)
7. T. G. Archibald, J. C. Barnard, H. F. Reese, US Patent 0916648.
8. A. J. Warr, L. Proctor, UK Patent 1240134.
9. L. D. Proctor, A. J. Warr, *Org. Process Res. Dev.* **2002**, *6*, 884.
10. M. Putala, D. A. Lemenovskii, *Russ. Chem. Rev.* **1994**, *63*, 197.
11. H. Lebel, J.-F. Marcoux, C. Molinaro, *Chem. Rev.* **2003**, *103*, 977.
12. G. Bartoli, G. Bencivenni, R. Dalpozzo, *Synthesis* **2014**, *46*, 979.
13. R. K. Armstrong, *J. Org. Chem.* **1966**, *31*, 618.
14. W. Kirmse, M. Kapps, *Chem. Ber.* **1968**, *101*, 994.
15. M. Kapps, W. Kirmse, *Angew. Chem. Int. Ed. Engl.* **1969**, *8*, 75.
16. R. Paulissen, A. J. Hubert, P. Teyssie, *Tetrahedron Lett.* **1972**, *15*, 1465.
17. J. Kottwitz, H. Vorbrüggen, *Synthesis* **1975**, 636.
18. U. Mende, B. Raduchel, W. Skuballa, H. Vorbrüggen, *Tetrahedron Lett.* **1975**, *9*, 629.
19. B. Raduchel, U. Mende, G. Cleve, G.-A. Hoyer, H. Vorbrüggen, *Tetrahedron Lett.* **1975**, *16*, 633.
20. M. Suda, *Synthesis* **1981**, 714.
21. I. E. Markó, T. Giard, S. Sumida, A.-E. Gies, *Tetrahedron Lett.* **2002**, *43*, 2317.
22. M. Rubin, M. Rubina, V. Gevorgyan, *Chem. Rev.* **2007**, *107*, 3117.
23. N. Heureux, M. Marchant, N. Maulide, G. Berthon-Gelloz, C. Hermans, S. Hermant, E. Kiss, B. Leroy, P. Wasnaire, I. E. Markó, *Tetrahedron Lett.* **2005**, *46*, 79.
24. P. Fontani, B. Carboni, M. Vaultier, R. A. Carrié, *Tetrahedron Lett.* **1989**, *30*, 4815.
25. P. Fontani, B. Carboni, M. Vaultier, G. Maas, *Synthesis* **1991**, 605.
26. J. P. Hildebrand, S. P. Marsden, *Synlett* **1996**, 893.

27. G. Berthon-Gelloz, M. Marchant, B. F. Straub, I. E. Marko, *Chem. Eur. J.* **2009**, *15*, 2923.
28. Y. V. Tomilov, V. G. Bordakov, I. E. Dolgii, O. M. Nefedov, *Bull. Acad. Sci. USSR Ch.* **1984**, *33*, 533.
29. U. M. Dzhemilev, V. A. Dokichev, S. Z. Sultanov, R. I. Khusnutdinov, Y. V. Tomilov, O. M. Nefedov, G. A. Tolstikov, *Bull. Acad. Sci. USSR Ch.* **1989**, *38*, 1707.
30. K. Shimamoto, M. Ishida, H. Shinozaki, Y. Ohfune, *J. Org. Chem.* **1991**, *56*, 4167.
31. J. Pietruszka, A. Witt, *Synlett* **2003**, 91.
32. H. Abdallah, R. Grée, R. Carrié, *Tetrahedron Lett.* **1982**, *23*, 503.
33. J. Vallgårda, U. Hacksell, *Tetrahedron Lett.* **1991**, *32*, 5625.
34. J. Vallgårda, U. Appelberg, C. Ingeborg, U. Hacksell, *J. Chem. Soc. Perkin Trans. I* **1994**, 461.
35. L.-Q. Sun, K. Takaki, J. Chen, S. Bertenshaw, L. Iben, C. D. Mahle, E. Ryan, D. Wu, Q. Gao, C. Xu, *Bioorg. Med. Chem. Lett.* **2005**, *15*, 1345.
36. J. Pietruszka, M. Widenmeyer, *Synlett* **1997**, 977.
37. J. Pietruszka, J. E. Luithle, *Liebigs Ann.* **1997**, 2297.
38. J. Pietruszka, J. E. Luithle, *J. Org. Chem.* **1999**, *64*, 8287.
39. N. Ty, R. Pontikis, G. C. Chabot, E. Devillers, L. Quentin, S. Bourg, J.-C. Florent, *Bioorg. Med. Chem.* **2013**, *21*, 1357.
40. H. Nozaki, S. Moriuti, H. Takaya, R. Noyori, *Tetrahedron Lett.* **1966**, *7*, 5239.
41. S. E. Denmark, R. A. Stavenger, A.-M. Faucher, J. P. Edwards, *J. Org. Chem.* **1997**, *62*, 3375.
42. L. Canovese, F. Visentin, *Inorg. Chim. Acta* **2010**, *363*, 2375.
43. R. McCrindle, G. J. Arsenault, R. Farwaha, A. J. McAlees, D. W. Sneddon, *J. Chem. Soc. Dalton Trans.* **1989**, 761.
44. I. Illa, C. Rodríguez-García, C. Acosta-Silva, I. Favier, D. Picurelli, A. Oliva, M. Gómez, V. Branchadell, R. M. Ortuño, *Organometallics* **2007**, *26*, 3306.
45. F. Bernardi, A. Bottoni, G. P. Miscione, *Organometallics* **2001**, *20*, 2751.
46. C. Rodríguez-García, A. Oliva, R. M. Ortuño, V. Branchadell, *J. Am. Chem. Soc.* **2001**, *123*, 6157.
47. B. F. Straub, *J. Am. Chem. Soc.* **2002**, *124*, 14195.
48. H. Meerwein, DE Patent 579309.
49. S. M. Hecht, J. W. Kozarich, *Tetrahedron Lett.* **1973**, *14*, 1397.

50. O. M. Nefedov, Y. V. Tomilov, A. B. Kostitsyn, U. M. Dzhemilev, V. A. Dokitchev, *Mendeleev Commun.* **1992**, *2*, 13.
51. C. H. Oh, D. I. Park, J. H. Ryu, J.-S. Han, *Bull. Kor. Chem. Soc.* **2007**, *28*, 322.
52. I. R. Ramazanov, L. K. Dil'mukhametova, L. Khalikov, U. M. Dzhemilev, O. M. Nefedov, *Tetrahedron Lett.* **2008**, *49*, 6058.
53. A. R. Tuktarov, V. V. Korolev, L. M. Khalilov, A. G. Ibragimov, U. M. Dzhemilev, *Russ. J. Org. Chem.* **2009**, *45*, 1594.
54. L. G. Tomilova, A. V. Ivanov, I. V. Kostyuchenko, E. V. Shulishov, O. M. Nefedov, *Mendeleev Commun.* **2002**, *12*, 149.
55. Y. V. Tomilov, N. M. Tsvetkova, O. M. Nefedov, *Russ. Chem. Bull.* **1997**, *46*, 507.
56. Y. V. Tomilov, A. B. Kostitsyn, E. V. Shulishov, O. M. Nefedov, *Russ. Chem. Bull.* **1993**, *42*, 118.
57. D. Moody, Int. Patent WO/2008/040947.
58. B. Morandi, E. M. Carreira, *Science* **2012**, *335*, 1471.
59. J. R. Wolf, C. G. Hamaker, J.-P. Djukic, T. Kodadek, L. K. Woo, *J. Am. Chem. Soc.* **1995**, *117*, 9194.
60. N. Hashimoto, T. Aoyama, T. Shioiri, *Chem. Pharm. Bull.* **1981**, *29*, 1475.
61. D. Seyferth, A. W. Dow, H. Menzel, T. C. Flood, *J. Am. Chem. Soc.* **1968**, *90*, 1080.
62. E. Kühnel, D. D. P. Laffan, G. C. Lloyd-Jones, T. Martínez del Campo. I. R. Shepperson, J. L. Slaughter, *Angew. Chem. Int. Ed.* **2007**, *46*, 7075.
63. H. Lebel, V. Paquet, C. Proulx, *Angew. Chem. Int. Ed.* **2001**, *40*, 2887.
64. H. Lebel, V. Paquet, *J. Am. Chem. Soc.* **2004**, *126*, 320.
65. T. Aoyama, Y. Iwamoto, S. Nishigaki, T. Shioiri, *Chem. Pharm. Bull.* **1989**, *37*, 253.
66. P. Bergamini, O. Bortolini, E. Costa, P. G. Pringle, *Inorg. Chim. Acta* **1996**, *252*, 33.
67. G. Maas, J. Seitz, *Tetrahedron Lett.* **2001**, *42*, 6137.
68. H. Sun, S. G. DiMagno, *J. Am. Chem. Soc.* **2005**, *127*, 2050.
69. D. W. Kim, H.-J. Jeong, S. T. Lim, M.-H. Sohn, *Angew. Chem. Int. Ed.* **2008**, *47*, 8404.
70. A. J. J. Lennox, *Organotrifluoroborate Preparation, Coupling and Hydrolysis*, PhD Thesis, University of Bristol, **2012**.
71. A. J. J. Lennox, G. C. Lloyd-Jones, *J. Am. Chem. Soc.* **2012**, *134*, 7431.
72. R. K. Sharma, J. L. Fry, *J. Org. Chem.* **1983**, *48*, 2112.
73. P. Bosch, F. Camps, E. Chamorro, V. Gasol, A. Guerrero, *Tetrahedron Lett.* **1987**, *28*, 4733.

74. S. J. Brown, J. H. Clark, *J. Chem. Soc. Chem. Commun.* **1985**, 672.
75. S. J. Brown, J. H. Clark, *J. Fluorine Chem.* **1985**, *30*, 251.
76. D. Landini, H. Molinari, M. Penso, A. Rampoldi, *Synthesis* **1988**, *12*, 953.
77. A. Huang, H.-Q. Li, W. Massefski, E. Saiah, *Synlett* **2009**, *15*, 2518.
78. K.-Y. Kim, B. C. Kim, H. B. Lee, H. Shin, *J. Org. Chem.* **2008**, *73*, 8106.
79. G. K. Surya Prakash, F. Pertusati, G. A. Olah, *Synthesis* **2011**, 292.
80. R. A. Batey, T. D. Quach, *Tetrahedron Lett.* **2001**, *42*, 9099.
81. C. Martín, F. Molina, E. Alvarez, T. R. Belderrain, *Chem. Eur. J.* **2011**, *17*, 14885.
82. K. J. van der Merwe, P. S. Steyn, S. H. Eggers, *Tetrahedron Lett.* **1964**, *52*, 3923.
83. I. G. Shenderovich, S. N. Smirnov, G. S. Denisov, V. A. Gindin, N. S. Golubev, A. Dunger, R. Reibke, S. Kirpekar, O. L. Malkina, H.-H. Limbach, *Ber. Bunsen. Phys. Chem.* **1998**, *102*, 422.
84. I. G. Shenderovich, H.-H. Limbach, S. N. Smirnov, P. M. Tolstoy, G. S. Denisov, N. S. Golubev, *Phys. Chem. Chem. Phys.* **2002**, *4*, 5488.
85. I. G. Shenderovich, P. M. Tolstoy, N. S. Golubev, S. N. Smirnov, G. S. Denisov, H.-H. Limbach, *J. Am. Chem. Soc.* **2003**, *125*, 11710.
86. T. Jeffery, *Tetrahedron* **1996**, *52*, 10113.
87. M. T. Reetz, E. Westermann, *Angew. Chem. Int. Ed.* **2000**, *39*, 165.
88. J. F. McGarrity, D. P. Cox, *J. Am. Chem. Soc.* **1093**, *105*, 3961.
89. M. Henrich, A. Marhold, A. A. Kolomeitsev, N. Kalinovich, G. V. Röschenthaler, *Tetrahedron Lett.* **2003**, *44*, 5795.
90. M. Baranac-Stojanovic, M. Stojanovic, *J. Org. Chem.* **2013**, *78*, 1504.
91. M. Rohde, L. O. Müller, D. Himmel, H. Scherer, I. A. Krossing, *Chem. Eur. J.* **2014**, *20*, 1218.
92. Gaussian 09, Revision A.02, M. J. Frisch, G. W. Trucks, H. B. Schlegel, G. E. Scuseria, M. A. Robb, J. R. Cheeseman, G. Scalmani, V. Barone, B. Mennucci, G. A. Petersson, H. Nakatsuji, M. Caricato, X. Li, H. P. Hratchian, A. F. Izmaylov, J. Bloino, G. Zheng, J. L. Sonnenberg, M. Hada, M. Ehara, K. Toyota, R. Fukuda, J. Hasegawa, M. Ishida, T. Nakajima, Y. Honda, O. Kitao, H. Nakai, T. Vreven, J. A. Montgomery Jr., J. E. Peralta, F. Ogliaro, M. Bearpark, J. J. Heyd, E. Brothers, K. N. Kudin, V. N. Staroverov, R. Kobayashi, J. Normand, K. Raghavachari, A. Rendell, J. C. Burant, S. S. Iyengar, J. Tomasi, M. Cossi, N. Rega, J. M. Millam, M. Klene, J. E. Knox, J. B. Cross, V. Bakken,

C. Adamo, J. Jaramillo, R. Gomperts, R. E. Stratmann, O. Yazyev, A. J. Austin, R. Cammi, C. Pomelli, J. W. Ochterski, R. L. Martin, K. Morokuma, V. G. Zakrzewski, G. A. Voth, P. Salvador, J. J. Dannenberg, S. Dapprich, A. D. Daniels, Ö. Farkas, J. B. Foresman, J. V. Ortiz, J. Cioslowski, D. J. Fox, Gaussian Inc., Wallingford CT, 2009.

93. I. J. S. Fairlamb, *Org. Biomol. Chem.* **2008**, *6*, 3645.
94. H. Zhao, A. Ariafard, Z. Lin, *Inorg. Chim. Acta* **2006**, *359*, 3527.
95. B. V. Popp, J. L. Thorman, C. M. Morales, C. R. Landis, S. S. Stahl, *J. Am. Chem. Soc.* **2004**, *126*, 14832.
96. P. S. Branco, V. P. Raje, J. Dourado, J. Gordo, *Org. Biomol. Chem.* **2010**, *8*, 2968.
97. T. Sakai, S. Ito, Y. Furuta, Y. Mori, *Org. Lett.* **2012**, *14*, 4564.
98. L.-P. B. Beaulieu, L. B. Delvos, A. B. Charette, *Org. Lett.* **2010**, *12*, 1348.
99. J. M. Bakke, *Acta, Chem. Scand.* **1982**, *36b*, 127.

6 Appendix – Computational Chemistry

All structures were optimised in Gaussian 09 using the B3LYP DFT functional with a mixed basis set (6-31G(d,p) for H, C, N, O, F, LanL2DZ for Pd). Structures were confirmed as minima or first-order saddle points (corresponding to transition states) by frequency analysis; minima are characterised by a lack of imaginary frequencies, transition states by one imaginary frequency (shown as negative in the calculation output).

In cases where transition states could not be located, relaxed scans of the relevant potential energy hypersurface were carried out using the keyword "opt=modredundant" in the header section of the input file and specifying the variable coordinate following the molecule specification (i.e. "*x y* S *n d*" – increments the distance between atoms numbered *x* and *y* in *n* steps of *d* Å each).

6.1 Alkenes

4-trifluoromethylstyrene (3t)

```
C  4.451352   -0.580122    0.022231
C  3.529011    0.389362    0.013206
C  2.065911    0.230331   -0.004129
C  1.258090    1.380011   -0.010687
C -0.130806    1.290426   -0.027425
C -0.744192    0.037042   -0.039681
C  0.042151   -1.120651   -0.035029
C  1.427137   -1.023705   -0.018161
H  5.509199   -0.340463    0.035703
H  4.198329   -1.636036    0.016972
H  3.871099    1.423421    0.019753
H  1.729468    2.358912   -0.005160
H -0.737096    2.189547   -0.038470
C -2.242466   -0.076037    0.002895
H -0.435836   -2.094123   -0.053360
H  2.018530   -1.933297   -0.019108
F -2.702867   -0.166362    1.273908
F -2.682119   -1.176952   -0.648341
F -2.847328    0.995769   -0.556195

E(RB3LYP) =  -646.697182228     A.U.
Zero-point correction=0.138314 (Hartree/Particle)
Thermal correction to Energy=0.148679
Thermal correction to Enthalpy=0.149623
Thermal correction to Gibbs Free Energy=0.100351
```

Sum of electronic and zero-point Energies=-646.558868
Sum of electronic and thermal Energies=-646.548503
Sum of electronic and thermal Enthalpies=-646.547559
Sum of electronic and thermal Free Energies=-646.596832

4-methoxystyrene (3u)

C	3.506872	-0.778733	0.000011
O	2.715183	0.398971	-0.000001
C	1.356884	0.265276	-0.000002
C	0.624213	1.459748	0.000004
C	-0.762552	1.422404	0.000001
C	-1.472023	0.206035	-0.000006
C	-2.941757	0.232567	-0.000006
C	-3.784073	-0.808363	0.000018
C	-0.717305	-0.977258	-0.000014
C	0.675637	-0.959905	-0.000012
H	4.545074	-0.443708	0.000026
H	3.325170	-1.389256	0.893722
H	3.325196	-1.389256	-0.893707
H	1.164590	2.400540	0.000010
H	-1.317005	2.357530	0.000006
H	-3.371624	1.234125	-0.000027
H	-3.446118	-1.840487	0.000043
H	-4.857981	-0.655187	0.000014
H	-1.221906	-1.938646	-0.000024
H	1.217764	-1.898044	-0.000019

E(RB3LYP) = -424.186223135 A.U.
Zero-point correction=0.166090 (Hartree/Particle)
Thermal correction to Energy=0.175436
Thermal correction to Enthalpy=0.176381
Thermal correction to Gibbs Free Energy=0.131005
Sum of electronic and zero-point Energies=-424.020133
Sum of electronic and thermal Energies=-424.010787
Sum of electronic and thermal Enthalpies=-424.009843
Sum of electronic and thermal Free Energies=-424.055218

3-nitrostyrene (3v)

N	2.310030	-0.511551	0.000052
O	2.371807	-1.740248	0.000422
O	3.285799	0.237999	-0.000635
C	0.971594	0.107829	0.000047

C -0.147134 -0.718962 0.000013
C -1.430604 -0.154376 0.000050
C -2.596977 -1.053557 -0.000037
C -3.888583 -0.705338 -0.000287
C -1.535149 1.250097 0.000182
C -0.402223 2.059582 0.000183
C 0.873962 1.495780 0.000081
H -0.007415 -1.793290 -0.000019
H -2.349199 -2.113674 0.000113
H -4.224182 0.327334 -0.000484
H -4.666012 -1.461683 -0.000294
H -2.515135 1.715880 0.000284
H -0.511128 3.139380 0.000277
H 1.772704 2.098567 0.000062

E(RB3LYP) = -514.160842818 A.U.

Zero-point correction=0.136192 (Hartree/Particle)
Thermal correction to Energy=0.145441
Thermal correction to Enthalpy=0.146385
Thermal correction to Gibbs Free Energy=0.100553
Sum of electronic and zero-point Energies=-514.024651
Sum of electronic and thermal Energies=-514.015402
Sum of electronic and thermal Enthalpies=-514.014458
Sum of electronic and thermal Free Energies=-514.060290

4-(dimethylamino)styrene (3w)

C 4.232454 -0.556608 0.029711
C 3.292266 0.398264 0.031767
C 1.834830 0.231890 0.001025
C 1.005502 1.364633 -0.004948
C -0.380678 1.272572 -0.032920
C -1.022501 0.014845 -0.066121
C -0.191506 -1.131659 -0.045707
C 1.190083 -1.017771 -0.017202
H 5.286367 -0.300721 0.054469
H 3.995245 -1.616177 0.002872
H 3.624161 1.436515 0.057543
H 1.461094 2.351970 0.017794
H -0.962221 2.186004 -0.027540
N -2.406060 -0.094906 -0.126306
H -0.627840 -2.122859 -0.050824
H 1.781041 -1.928883 -0.003251
C -3.028482 -1.392628 0.072030
C -3.221853 1.092039 0.062240

```
H -2.697161   -2.108927   -0.688084
H -4.109988   -1.288696   -0.027472
H -2.814358   -1.825437    1.061780
H -2.993213    1.849541   -0.695707
H -3.087748    1.553861    1.053203
H -4.273653    0.824697   -0.049890
```

```
E(RB3LYP) =  -443.635098932     A.U.
Zero-point correction=0.206547 (Hartree/Particle)
Thermal correction to Energy=0.217708
Thermal correction to Enthalpy=0.218652
Thermal correction to Gibbs Free Energy=0.169296
Sum of electronic and zero-point Energies=-443.428551
Sum of electronic and thermal Energies=-443.417391
Sum of electronic and thermal Enthalpies=-443.416447
Sum of electronic and thermal Free Energies=-443.465803
```

3-methoxystyrene (3x)

```
C  1.266911    0.262633    0.000022
C  0.196270   -0.635796   -0.000244
C -1.132655   -0.171543   -0.000346
C -2.216184   -1.169637   -0.000523
C -3.535025   -0.942089    0.000744
C -1.366151    1.211986   -0.000301
C -0.293368    2.102058   -0.000039
C  1.019803    1.641786    0.000143
H  0.373179   -1.705340   -0.000329
H -1.877485   -2.205388   -0.001755
H -3.959753    0.057084    0.002174
H -4.241761   -1.765189    0.000425
H -2.381002    1.594622   -0.000587
H -0.482004    3.171802   -0.000015
H  1.863691    2.323331    0.000324
O  2.583693   -0.102918    0.000139
C  2.898477   -1.485852    0.000205
H  2.509471   -1.991068    0.893686
H  3.987765   -1.546712    0.000454
H  2.509888   -1.991062   -0.893463
```

```
E(RB3LYP) =  -424.185758152     A.U.
Zero-point correction=0.166146 (Hartree/Particle)
Thermal correction to Energy=0.175451
Thermal correction to Enthalpy=0.176395
Thermal correction to Gibbs Free Energy=0.131263
Sum of electronic and zero-point Energies=-424.019612
```

Sum of electronic and thermal Energies=-424.010307
Sum of electronic and thermal Enthalpies=-424.009363
Sum of electronic and thermal Free Energies=-424.054495

4-acetoxystyrene (3y)

C	2.944054	0.158262	0.160545
C	4.267757	-0.514459	-0.106048
O	2.789752	1.225707	0.700329
O	1.928979	-0.635666	-0.306141
C	0.586389	-0.276383	-0.186380
C	0.107188	1.021338	-0.357617
C	-1.267397	1.240486	-0.286172
C	-2.180124	0.198761	-0.053523
C	-3.616903	0.508040	0.009835
C	-4.626886	-0.341664	0.232417
C	-1.660891	-1.099179	0.106162
C	-0.294417	-1.336276	0.041392
H	4.299512	-1.489893	0.387750
H	4.389824	-0.688259	-1.179136
H	5.073839	0.117807	0.263877
H	0.789170	1.842557	-0.527713
H	-1.642972	2.252153	-0.415197
H	-3.858054	1.559166	-0.145103
H	-4.478012	-1.404412	0.398771
H	-5.653309	0.008486	0.256182
H	-2.330465	-1.934757	0.282602
H	0.107994	-2.336725	0.160804

E(RB3LYP) = -537.540472719 A.U.
Zero-point correction=0.175031 (Hartree/Particle)
Thermal correction to Energy=0.186539
Thermal correction to Enthalpy=0.187483
Thermal correction to Gibbs Free Energy=0.135541
Sum of electronic and zero-point Energies=-537.365442
Sum of electronic and thermal Energies=-537.353934
Sum of electronic and thermal Enthalpies=-537.352990
Sum of electronic and thermal Free Energies=-537.404932

3-trifluoromethylstyrene (3z)

C	0.654569	0.220957	-0.034405
C	-0.436989	-0.647583	-0.024554
C	-1.751496	-0.157482	-0.001662
C	-2.865915	-1.119846	0.000898
C	-4.175641	-0.846557	0.003085

```
C -1.935422    1.237257    0.013446
C -0.846368    2.102724    0.002845
C  0.456517    1.602487   -0.021153
H -0.264776   -1.718863   -0.044194
H -2.559586   -2.165024   -0.000009
H -4.567791    0.165967    0.002173
H -4.909590   -1.645224    0.005178
H -2.939492    1.648537    0.031452
H -1.010659    3.175885    0.010037
H  1.307635    2.274175   -0.037386
C  2.052395   -0.335966   -0.001473
F  2.123052   -1.558627   -0.574001
F  2.507861   -0.470896    1.266816
F  2.928460    0.466034   -0.647192

E(RB3LYP) =  -646.696937408     A.U.
Zero-point correction=                           0.138375
(Hartree/Particle)
Thermal correction to Energy=0.148704
Thermal correction to Enthalpy=0.149649
Thermal correction to Gibbs Free Energy=0.100556
Sum of electronic and zero-point Energies=-646.558562
Sum of electronic and thermal Energies=-646.548233
Sum of electronic and thermal Enthalpies=-646.547289
Sum of electronic and thermal Free Energies=-646.596382
```

6.2 (Alkene)Pd Complexes

(4-trifluoromethylstyrene)palladium(0) (3t.Pd)

```
C  -2.714859   -0.161189    1.543762
C  -1.807494    0.725474    0.939659
C  -0.386011    0.455920    0.635546
C   0.425092    1.515066    0.189873
C   1.773274    1.324017   -0.098630
C   2.345269    0.059934    0.055798
C   1.555899   -1.007076    0.502131
C   0.210742   -0.811395    0.785890
H  -3.590706    0.239739    2.047711
H  -2.408717   -1.151482    1.871980
H  -2.063363    1.784603    0.948335
H  -0.012647    2.502151    0.067085
H   2.380242    2.152372   -0.447745
C   3.811514   -0.148311   -0.195684
H   1.997815   -1.991417    0.616370
H  -0.386533   -1.653753    1.118869
```

```
Pd -3.117974   -0.166787   -0.542986
F   4.067147   -1.382414   -0.687439
F   4.539343   -0.026387    0.940838
F   4.307972    0.750506   -1.075100
```

```
E(RB3LYP) =  -773.443737056     A.U.
Zero-point correction=0.139166 (Hartree/Particle)
Thermal correction to Energy=0.151092
Thermal correction to Enthalpy=0.152036
Thermal correction to Gibbs Free Energy=0.097011
Sum of electronic and zero-point Energies=-773.304562
Sum of electronic and thermal Energies=-773.292636
Sum of electronic and thermal Enthalpies=-773.291692
Sum of electronic and thermal Free Energies=-773.346717
```

(4-methoxystyrene)palladium(0) (3u.Pd)

```
C  -2.062455   -0.071165    1.569095
C  -1.207353    0.791941    0.861647
C   0.213624    0.558246    0.534205
C   0.976509    1.613160   -0.005235
C   2.319111    1.457324   -0.319049
C   2.953611    0.226719   -0.099129
C   2.218109   -0.838055    0.440472
C   0.869880   -0.664747    0.747568
H  -2.933978    0.341422    2.071444
H  -1.706329   -1.017673    1.969193
H  -1.508208    1.837212    0.790492
H   0.500699    2.575238   -0.178971
H   2.900521    2.274394   -0.733730
H   2.682523   -1.800096    0.622771
H   0.319260   -1.506757    1.155647
Pd -2.552309   -0.261613   -0.489954
O   4.274367    0.166787   -0.438244
C   4.963802   -1.056694   -0.240271
H   5.987913   -0.883728   -0.574816
H   4.524375   -1.870557   -0.831613
H   4.975458   -1.349931    0.817601
```

```
E(RB3LYP) =  -550.933351812     A.U.
Zero-point correction=0.167046 (Hartree/Particle)
Thermal correction to Energy=0.177924
Thermal correction to Enthalpy=0.178868
Thermal correction to Gibbs Free Energy=0.128025
Sum of electronic and zero-point Energies=-550.766305
Sum of electronic and thermal Energies=-550.755428
```

Sum of electronic and thermal Enthalpies=-550.754484
Sum of electronic and thermal Free Energies=-550.805327

(3-nitrostyrene)palladium(0) (3v.Pd)

C	-1.832676	-0.523010	1.532353
C	-1.279153	0.663676	1.023789
C	0.110121	0.848794	0.550093
C	0.548828	2.139262	0.197294
C	1.851865	2.374057	-0.242353
C	2.762904	1.325530	-0.339247
C	2.324473	0.049736	0.017279
C	1.031835	-0.207176	0.455321
H	-2.704375	-0.465697	2.179189
H	-1.239839	-1.428220	1.637932
H	-1.793846	1.596083	1.253132
H	-0.148655	2.969538	0.270879
H	2.159424	3.380753	-0.507644
H	3.781665	1.470188	-0.674366
N	3.273526	-1.075421	-0.072610
H	0.763369	-1.223749	0.711127
Pd	-2.502582	-0.317802	-0.474002
O	4.415044	-0.828304	-0.459873
O	2.869603	-2.193857	0.244243

E(RB3LYP) = -640.906753149 A.U.
Zero-point correction=0.137039 (Hartree/Particle)
Thermal correction to Energy=0.147838
Thermal correction to Enthalpy=0.148782
Thermal correction to Gibbs Free Energy=0.097197
Sum of electronic and zero-point Energies=-640.769714
Sum of electronic and thermal Energies=-640.758915
Sum of electronic and thermal Enthalpies=-640.757971
Sum of electronic and thermal Free Energies=-640.809556

((4-dimethylamino)styrene)palladium(0) (3w.Pd)

C	-2.470909	-0.165340	1.519349
C	-1.545007	0.714645	0.929468
C	-0.124566	0.444159	0.645987
C	0.729353	1.506932	0.307271
C	2.082176	1.320698	0.048526
C	2.665988	0.036595	0.127078
C	1.806164	-1.041001	0.452823
C	0.457703	-0.835605	0.704370
H	-3.344597	0.244031	2.020953

```
H  -2.172001   -1.156773    1.851732
H  -1.796307    1.775464    0.940462
H   0.320528    2.512917    0.243342
H   2.683163    2.182876   -0.213136
H   2.193013   -2.051303    0.506530
H  -0.161779   -1.696598    0.937773
Pd -2.887775   -0.153827   -0.561762
N   4.023518   -0.160884   -0.094974
C   4.536861   -1.514203   -0.220941
C   4.820043    0.927461   -0.634529
H   4.803041    1.795971    0.033737
H   4.478710    1.258907   -1.628068
H   5.858086    0.602468   -0.721388
H   4.352066   -2.091962    0.691773
H   5.617350   -1.474141   -0.368405
H   4.094901   -2.065679   -1.065863
```

```
E(RB3LYP) =  -570.381425487     A.U.
Zero-point correction=0.207511 (Hartree/Particle)
Thermal correction to Energy=0.220217
Thermal correction to Enthalpy=0.221161
Thermal correction to Gibbs Free Energy=0.166176
Sum of electronic and zero-point Energies=-570.173915
Sum of electronic and thermal Energies=-570.161208
Sum of electronic and thermal Enthalpies=-570.160264
Sum of electronic and thermal Free Energies=-570.215249
```

(3-methoxystyrene)palladium(0) (3x.Pd)

```
C  -1.769523   -0.387488    1.573196
C  -1.124717    0.704908    0.969762
C   0.281262    0.757506    0.510321
C   0.801610    1.989747    0.066218
C   2.121683    2.084338   -0.359188
C   2.963227    0.968485   -0.354018
C   2.454482   -0.259740    0.090533
C   1.126760   -0.359321    0.517752
H  -2.644830   -0.210498    2.193290
H  -1.240769   -1.315739    1.775642
H  -1.581751    1.685944    1.097343
H   0.162279    2.868091    0.058776
H   2.511733    3.039644   -0.699478
H   3.988926    1.064406   -0.688842
O   3.176236   -1.419782    0.145034
H   0.774724   -1.330674    0.847302
Pd -2.398995   -0.323929   -0.457838
```

```
C   4.530313   -1.388109   -0.272828
H   4.908485   -2.404204   -0.148576
H   5.130200   -0.703752    0.341429
H   4.624296   -1.096181   -1.327089
```

```
E(RB3LYP) =  -550.933106367     A.U.
Zero-point correction=0.166999 (Hartree/Particle)
Thermal correction to Energy=0.177867
Thermal correction to Enthalpy=0.178811
Thermal correction to Gibbs Free Energy=0.127876
Sum of electronic and zero-point Energies=-550.766108
Sum of electronic and thermal Energies=-550.755240
Sum of electronic and thermal Enthalpies=-550.754296
Sum of electronic and thermal Free Energies=-550.805231
```

(4-acetoxystyrene)palladium(0) (3y.Pd)

```
C  -2.666156   -0.743723    1.385097
C  -1.860240    0.369980    1.092608
C  -0.440819    0.346320    0.680989
C   0.280918    1.552579    0.653981
C   1.626130    1.585020    0.297834
C   2.277353    0.400272   -0.038737
C   1.589272   -0.816680   -0.028941
C   0.245492   -0.831503    0.329541
H  -3.537106   -0.614237    2.022859
H  -2.268773   -1.755134    1.348727
H  -2.191959    1.336663    1.471187
H  -0.220991    2.479150    0.920275
H   2.180112    2.517740    0.275909
O   3.602833    0.536474   -0.453229
H   2.098429   -1.735547   -0.285890
H  -0.280956   -1.780574    0.326750
Pd -3.201835   -0.077928   -0.560401
C   4.566633   -0.375237   -0.111185
O   4.373665   -1.361930    0.555534
C   5.891112    0.053153   -0.694127
H   6.169613    1.038278   -0.308424
H   5.811879    0.139886   -1.781768
H   6.653993   -0.678973   -0.431973
```

```
E(RB3LYP) =  -664.285587294     A.U.
Zero-point correction=0.175891 (Hartree/Particle)
Thermal correction to Energy=0.188978
Thermal correction to Enthalpy=0.189922
Thermal correction to Gibbs Free Energy=0.132213
```

Sum of electronic and zero-point Energies=-664.109697
Sum of electronic and thermal Energies=-664.096609
Sum of electronic and thermal Enthalpies=-664.095665
Sum of electronic and thermal Free Energies=-664.153375

(3-trifluoromethylstyrene)palladium(0) (3z.Pd)

C	-2.103752	-0.346883	1.592993
C	-1.620625	0.802008	0.944376
C	-0.234707	1.032953	0.481784
C	0.134460	2.318422	0.047786
C	1.432340	2.593486	-0.380576
C	2.397443	1.589161	-0.386417
C	2.044387	0.305191	0.045331
C	0.749074	0.028291	0.473834
H	-2.998749	-0.271868	2.205484
H	-1.448766	-1.179867	1.836362
H	-2.210917	1.713165	1.037175
H	-0.609537	3.110927	0.052466
H	1.692712	3.596247	-0.705887
H	3.411742	1.793734	-0.710637
C	3.059252	-0.804621	-0.017266
H	0.505644	-0.975761	0.801653
Pd	-2.722368	-0.459312	-0.437091
F	4.315863	-0.351105	0.190804
F	3.059135	-1.411792	-1.227910
F	2.818286	-1.766689	0.901386

E(RB3LYP) = -773.443505401 A.U.
Zero-point correction=0.139229 (Hartree/Particle)
Thermal correction to Energy=0.151100
Thermal correction to Enthalpy=0.152045
Thermal correction to Gibbs Free Energy=0.097735
Sum of electronic and zero-point Energies=-773.304277
Sum of electronic and thermal Energies=-773.292405
Sum of electronic and thermal Enthalpies=-773.291461
Sum of electronic and thermal Free Energies=-773.345771

6.3 (Alkene)palladium(CH_2N_2) complexes

4-trifluoromethylstyrene exo complex (3t.PdCH_2N_2-exo)

C	1.661423	2.262055	-0.309657
C	0.869099	1.609572	0.630342
C	-0.472251	1.031466	0.400560
C	-1.196790	0.537006	1.499970
C	-2.468983	-0.006130	1.345691

C	-3.050613	-0.066726	0.077838
C	-2.347271	0.422943	-1.029367
C	-1.077567	0.962326	-0.869467
H	2.467881	2.908585	0.023977
H	1.323737	2.427659	-1.329238
H	1.125765	1.732236	1.681621
H	-0.750619	0.579933	2.489989
H	-3.008459	-0.387024	2.206288
C	-4.445601	-0.594765	-0.095178
C	-0.545149	1.326768	-1.741684
Pd	2.396201	0.223430	-0.150564
C	3.520312	-1.560529	-0.608916
N	4.675397	-1.587260	0.096346
H	3.728267	-1.490930	-1.677784
H	2.867311	-2.379693	-0.302724
N	5.636172	-1.590263	0.692401
H	-2.795552	0.371182	-2.016096
F	-4.774282	-1.486718	0.866730
F	-4.607736	-1.208887	-1.290071
F	-5.370197	0.394813	-0.041164

E(RB3LYP) = -922.217873542 A.U.
Zero-point correction=0.173184 (Hartree/Particle)
Thermal correction to Energy=0.189675
Thermal correction to Enthalpy=0.190620
Thermal correction to Gibbs Free Energy=0.123929
Sum of electronic and zero-point Energies=-922.044690
Sum of electronic and thermal Energies=-922.028198
Sum of electronic and thermal Enthalpies=-922.027254
Sum of electronic and thermal Free Energies=-922.093944

4-trifluoromethylstyrene endo complex (3t.PdCH_2N_2-endo)

C	1.855213	-2.110706	1.012767
C	0.985410	-1.915970	-0.056162
C	-0.343308	-1.269929	-0.006013
C	-1.144292	-1.272202	-1.162092
C	-2.409792	-0.692812	-1.169385
C	-2.909643	-0.099012	-0.008871
C	-2.130690	-0.091808	1.154644
C	-0.867772	-0.669280	1.155183
H	2.642433	-2.855249	0.933835
H	1.599863	-1.808903	2.024773
H	1.166843	-2.488023	-0.965361
H	-0.765668	-1.739875	-2.067081
H	-3.014058	-0.710904	-2.070043

H	-0.280502	-0.653216	2.067332
Pd	2.557620	-0.370180	-0.079709
C	3.835608	1.263392	-0.674180
N	3.458554	2.409308	-0.059720
H	3.692122	1.344492	-1.753057
H	4.833394	0.966507	-0.347207
N	3.128838	3.354651	0.465373
H	-2.522682	0.358869	2.060506
C	-4.249486	0.578696	-0.015275
F	-4.877662	0.463119	1.177642
F	-5.073208	0.068814	-0.958794
F	-4.142628	1.906364	-0.267773

E(RB3LYP) = -922.217856673 A.U.
Zero-point correction=0.173181 (Hartree/Particle)
Thermal correction to Energy=0.189668
Thermal correction to Enthalpy=0.190612
Thermal correction to Gibbs Free Energy=0.123794
Sum of electronic and zero-point Energies=-922.044676
Sum of electronic and thermal Energies=-922.028189
Sum of electronic and thermal Enthalpies=-922.027245
Sum of electronic and thermal Free Energies=-922.094063

4-methoxystyrene exo complex (3u.PdCH$_2$N$_2$-exo)

C	1.019803	2.268554	0.124655
C	0.213223	1.399316	0.851630
C	-1.088331	0.839505	0.433749
C	-1.867104	0.142581	1.368031
C	-3.114755	-0.395093	1.043047
C	-3.614926	-0.238495	-0.253130
C	-2.851579	0.456782	-1.206241
C	-1.615500	0.982018	-0.867301
H	1.778641	2.853337	0.636490
H	0.724542	2.640192	-0.853073
H	0.416859	1.298075	1.917185
H	-1.490818	0.016942	2.380456
H	-3.679619	-0.924248	1.801523
H	-1.043041	1.507300	-1.625450
Pd	1.862681	0.271308	-0.112244
C	3.068642	-1.357224	-0.832742
N	4.132998	-1.545756	-0.019448
H	3.395405	-1.030422	-1.821499
H	2.408288	-2.225653	-0.807906
N	5.019502	-1.692867	0.668660
H	-3.254794	0.569005	-2.207647

O	-4.817990	-0.715149	-0.690162
C	-5.630615	-1.423908	0.230151
H	-6.530203	-1.709372	-0.317658
H	-5.914005	-0.798662	1.087024
H	-5.131295	-2.329335	0.599508

E(RB3LYP) = -699.707015090 A.U.
Zero-point correction=0.201008 (Hartree/Particle)
Thermal correction to Energy=0.216453
Thermal correction to Enthalpy=0.217397
Thermal correction to Gibbs Free Energy=0.154582
Sum of electronic and zero-point Energies=-699.506007
Sum of electronic and thermal Energies=-699.490562
Sum of electronic and thermal Enthalpies=-699.489618
Sum of electronic and thermal Free Energies=-699.552433

4-methoxystyrene endo complex (3u.PdCH$_2$N$_2$-endo)

C	1.191300	-2.186402	0.852875
C	0.300535	-1.814287	-0.148838
C	-0.962269	-1.066684	0.017207
C	-1.840053	-0.952495	-1.069663
C	-3.058387	-0.275788	-0.973840
C	-3.426658	0.309402	0.241358
C	-2.562682	0.206487	1.344809
C	-1.357273	-0.466375	1.231475
H	1.902634	-2.986467	0.667390
H	1.004870	-1.960730	1.899287
H	0.395746	-2.312877	-1.113271
H	-1.567041	-1.406777	-2.019160
H	-3.702903	-0.215691	-1.842941
H	-0.704864	-0.522900	2.097216
Pd	2.030349	-0.425340	-0.117801
C	3.399549	1.136110	-0.676136
N	3.087172	2.284472	-0.032863
H	3.265099	1.251462	-1.752978
H	4.373928	0.767449	-0.350723
N	2.814732	3.237619	0.513119
H	-2.863725	0.667071	2.280319
O	-4.588037	0.994245	0.459458
C	-5.495497	1.132721	-0.620821
H	-6.340885	1.704563	-0.234599
H	-5.853316	0.158221	-0.978305
H	-5.045999	1.677557	-1.461411

E(RB3LYP) = -699.706946324 A.U.
Zero-point correction=0.200953 (Hartree/Particle)
Thermal correction to Energy=0.216429
Thermal correction to Enthalpy=0.217374
Thermal correction to Gibbs Free Energy=0.154294
Sum of electronic and zero-point Energies=-699.505994
Sum of electronic and thermal Energies=-699.490517
Sum of electronic and thermal Enthalpies=-699.489573
Sum of electronic and thermal Free Energies=-699.552653

3-nitrostyrene exo complex (3v.PdCH$_2$N$_2$-exo)

C	-0.774287	0.484192	2.118873
C	-0.275219	1.317229	1.121676
C	0.999649	1.141655	0.392483
C	1.454518	2.169267	-0.454859
C	2.656271	2.061922	-1.156068
C	3.446036	0.922341	-1.031808
C	2.991436	-0.092797	-0.188839
C	1.798935	-0.007156	0.517907
H	-1.536286	0.856745	2.797269
H	-0.224777	-0.385799	2.468834
H	-0.707746	2.311936	1.026308
H	0.851675	3.067253	-0.561380
H	2.979477	2.873104	-1.801149
H	4.383430	0.804594	-1.559472
H	1.506677	-0.837576	1.147037
Pd	-1.790267	-0.040505	0.275313
C	-3.036168	-1.171207	-1.078828
N	-4.304063	-0.696956	-1.069097
H	-3.007401	-2.189592	-0.688088
H	-2.582395	-1.025402	-2.060622
N	-5.357000	-0.286567	-1.044106
N	3.810618	-1.309585	-0.042497
O	4.866972	-1.365094	-0.671815
O	3.392495	-2.199025	0.698510

E(RB3LYP) = -789.681187262 A.U.
Zero-point correction=0.171055 (Hartree/Particle)
Thermal correction to Energy=0.186451
Thermal correction to Enthalpy=0.187395
Thermal correction to Gibbs Free Energy=0.123191
Sum of electronic and zero-point Energies=-789.510132
Sum of electronic and thermal Energies=-789.494737
Sum of electronic and thermal Enthalpies=-789.493792
Sum of electronic and thermal Free Energies=-789.557997

3-nitrostyrene endo complex (3v.PdCH$_2$N$_2$-endo)

C	-0.918161	-1.437156	-1.787903
C	-0.355918	-1.828878	-0.576348
C	0.896981	-1.314488	0.017748
C	1.400099	-1.915696	1.186892
C	2.583723	-1.479760	1.783392
C	3.307378	-0.427976	1.228094
C	2.806495	0.161752	0.066780
C	1.630648	-0.255843	-0.543324
H	-1.643522	-2.083096	-2.274546
H	-0.443770	-0.702138	-2.432288
H	-0.708744	-2.757704	-0.130187
H	0.848577	-2.739770	1.631872
H	2.945043	-1.965093	2.684777
H	4.229312	-0.064110	1.662447
H	1.302269	0.252716	-1.440095
Pd	-1.991952	-0.399035	-0.215726
C	-3.504081	0.829631	0.714721
N	-3.077839	2.110521	0.825442
H	-4.358204	0.770940	0.038193
H	-3.650428	0.391529	1.703546
N	-2.702648	3.173395	0.906300
N	3.557019	1.276021	-0.540250
O	4.597563	1.631190	0.013030
O	3.101255	1.786716	-1.563168

E(RB3LYP) = -789.681058117 A.U.
Zero-point correction=0.171057 (Hartree/Particle)
Thermal correction to Energy=0.186440
Thermal correction to Enthalpy=0.187384
Thermal correction to Gibbs Free Energy=0.123466
Sum of electronic and zero-point Energies=-789.510001
Sum of electronic and thermal Energies=-789.494619
Sum of electronic and thermal Enthalpies=-789.493674
Sum of electronic and thermal Free Energies=-789.557592

4-dimethylaminostyrene exo complex (3w.PdCH$_2$N$_2$-exo)

C	1.375900	2.283148	0.069230
C	0.595944	1.451809	0.866404
C	-0.730054	0.894050	0.540592
C	-1.460783	0.219975	1.532400
C	-2.724029	-0.309825	1.295227
C	-3.330937	-0.198412	0.024822
C	-2.604781	0.493299	-0.974436

C	-1.344337	1.014478	-0.718979
H	2.168611	2.872590	0.520798
H	1.034917	2.625997	-0.904193
H	0.858764	1.379610	1.921551
H	-1.028857	0.113744	2.525076
H	-3.237366	-0.808592	2.108132
H	-0.825472	1.528273	-1.522887
Pd	2.182150	0.265087	-0.146084
C	3.310741	-1.415171	-0.864977
N	4.405985	-1.602770	-0.094077
H	3.599125	-1.126578	-1.877383
H	2.631612	-2.265245	-0.781372
N	5.320203	-1.751413	0.557224
H	-3.027197	0.627068	-1.962872
N	-4.580386	-0.753088	-0.238165
C	-5.380663	-1.247192	0.868858
H	-6.306515	-1.673291	0.478543
H	-5.642471	-0.462945	1.597440
H	-4.855085	-2.043817	1.407039
C	-5.270640	-0.397014	-1.466206
H	-4.684405	-0.687623	-2.345022
H	-5.485916	0.680778	-1.544380
H	-6.217418	-0.937935	-1.513104

E(RB3LYP) = -719.154524996 A.U.
Zero-point correction=0.241363 (Hartree/Particle)
Thermal correction to Energy=0.258674
Thermal correction to Enthalpy=0.259618
Thermal correction to Gibbs Free Energy=0.192403
Sum of electronic and zero-point Energies=-718.913162
Sum of electronic and thermal Energies=-718.895851
Sum of electronic and thermal Enthalpies=-718.894907
Sum of electronic and thermal Free Energies=-718.962122

4-dimethylaminostyrene endo complex (3w.PdCH$_2$N$_2$-endo)

C	1.556471	-2.069223	1.093089
C	0.699143	-1.865931	0.016380
C	-0.604957	-1.177837	0.031231
C	-1.427151	-1.225799	-1.106283
C	-2.675916	-0.616123	-1.148304
C	-3.173512	0.095852	-0.034658
C	-2.355072	0.134342	1.120077
C	-1.111275	-0.480216	1.142741
H	2.316427	-2.843573	1.034771
H	1.305328	-1.735871	2.096377

H	0.873468	-2.462297	-0.879284
H	-1.080736	-1.765367	-1.985050
H	-3.263847	-0.700353	-2.054072
H	-0.519573	-0.413401	2.050976
Pd	2.359077	-0.385340	-0.038059
C	3.668643	1.172984	-0.723751
N	3.275410	2.365215	-0.220811
H	3.562801	1.160461	-1.809912
H	4.648750	0.895194	-0.332122
N	2.937438	3.357167	0.207929
H	-2.691812	0.649249	2.011632
N	-4.406458	0.739809	-0.072224
C	-5.305055	0.482671	-1.184007
H	-6.207549	1.084009	-1.061373
H	-5.604115	-0.575002	-1.261820
H	-4.845089	0.772570	-2.135455
C	-4.978250	1.251838	1.161190
H	-4.322914	2.003002	1.616101
H	-5.163406	0.465895	1.910867
H	-5.928429	1.740447	0.938605

E(RB3LYP) = -719.154483866 A.U.
Zero-point correction=0.241274 (Hartree/Particle)
Thermal correction to Energy=0.258620
Thermal correction to Enthalpy=0.259564
Thermal correction to Gibbs Free Energy=0.192167
Sum of electronic and zero-point Energies=-718.913210
Sum of electronic and thermal Energies=-718.895864
Sum of electronic and thermal Enthalpies=-718.894920
Sum of electronic and thermal Free Energies=-718.962317

3-methoxystyrene exo complex (3x.PdCH$_2$N$_2$-exo)

C	-0.648110	0.917755	2.005704
C	-0.118594	1.441396	0.831629
C	1.147215	1.045023	0.173960
C	1.557588	1.743824	-0.979071
C	2.746524	1.412401	-1.618329
C	3.563493	0.385821	-1.135912
C	3.164744	-0.310446	0.013100
C	1.969392	0.020455	0.659300
H	-1.398487	1.478876	2.555146
H	-0.133532	0.146220	2.572254
H	-0.527799	2.384078	0.470339
H	0.935686	2.546087	-1.366183
H	3.052391	1.958852	-2.506344

H	4.487039	0.144604	-1.647933
O	3.877311	-1.329069	0.584374
H	1.702750	-0.544181	1.546043
Pd	-1.690709	-0.034736	0.345817
C	5.101955	-1.710471	-0.018009
H	5.497560	-2.525221	0.590907
H	5.825977	-0.885009	-0.027822
H	4.956415	-2.068242	-1.045937
C	-2.959684	-1.386194	-0.748148
N	-4.162745	-0.813497	-0.981474
H	-3.066584	-2.245193	-0.083479
H	-2.432392	-1.567428	-1.686158
N	-5.164689	-0.322278	-1.169778

E(RB3LYP) = -699.706645497 A.U.
Zero-point correction=0.200797 (Hartree/Particle)
Thermal correction to Energy=0.216297
Thermal correction to Enthalpy=0.217241
Thermal correction to Gibbs Free Energy=0.153999
Sum of electronic and zero-point Energies=-699.505848
Sum of electronic and thermal Energies=-699.490349
Sum of electronic and thermal Enthalpies=-699.489405
Sum of electronic and thermal Free Energies=-699.552647

3-methoxystyrene endo complex (3x.PdCH$_2$N$_2$-endo)

C	-0.816077	-1.700148	-1.574540
C	-0.199808	-1.839877	-0.335920
C	1.051576	-1.188517	0.111851
C	1.585919	-1.539208	1.367779
C	2.767562	-0.960992	1.817273
C	3.454625	-0.024796	1.039275
C	2.931857	0.325696	-0.212998
C	1.743377	-0.253638	-0.668332
H	-1.534725	-2.445518	-1.903857
H	-0.391651	-1.080738	-2.359888
H	-0.511960	-2.675240	0.290121
H	1.066373	-2.267425	1.984332
H	3.169776	-1.239755	2.787454
H	4.374110	0.413476	1.407754
O	3.510758	1.223973	-1.067069
H	1.374991	0.049871	-1.642088
Pd	-1.886115	-0.419965	-0.173732
C	4.720249	1.844998	-0.667807
H	5.002833	2.510222	-1.485553
H	5.521516	1.111391	-0.507998

H	4.591368	2.436659	0.248203
C	-3.385479	0.893188	0.638520
N	-2.986219	2.182073	0.539549
H	-4.267875	0.717124	0.021084
H	-3.465906	0.596480	1.685747
N	-2.638983	3.255042	0.447923

E(RB3LYP) = -699.706614602 A.U.
Zero-point correction=0.200854 (Hartree/Particle)
Thermal correction to Energy=0.216335
Thermal correction to Enthalpy=0.217279
Thermal correction to Gibbs Free Energy=0.154268
Sum of electronic and zero-point Energies=-699.505760
Sum of electronic and thermal Energies=-699.490280
Sum of electronic and thermal Enthalpies=-699.489336
Sum of electronic and thermal Free Energies=-699.552347

4-acetoxystyrene exo complex (3y.PdCH$_2$N$_2$-exo)

C	1.632113	2.230236	-0.256635
C	0.920811	1.529477	0.711695
C	-0.416436	0.917507	0.557125
C	-1.066235	0.403644	1.692701
C	-2.333767	-0.165953	1.607824
C	-2.977140	-0.230245	0.374190
C	-2.359019	0.265940	-0.776746
C	-1.092841	0.832921	-0.674289
H	2.439978	2.891452	0.043175
H	1.225016	2.410815	-1.247958
H	1.243106	1.633277	1.747070
H	-0.569452	0.454283	2.658075
H	-2.831890	-0.563818	2.485933
O	-4.210683	-0.885164	0.365394
H	-2.864202	0.220225	-1.732217
H	-0.619225	1.210787	-1.574625
Pd	2.448785	0.211997	-0.196435
C	-5.265813	-0.422494	-0.374824
O	-5.235640	0.558174	-1.076877
C	-6.457035	-1.326707	-0.170156
H	-6.729819	-1.354862	0.888858
H	-6.207166	-2.349001	-0.469141
H	-7.294787	-0.958961	-0.761515
H	2.954024	-2.376097	-0.446467
N	5.729389	-1.570501	0.517734
N	4.755134	-1.562289	-0.057333

C	3.585515	-1.534895	-0.737367
H	3.768306	-1.421122	-1.807230

E(RB3LYP) = -813.059265951 A.U.
Zero-point correction=0.209823 (Hartree/Particle)
Thermal correction to Energy=0.227510
Thermal correction to Enthalpy=0.228454
Thermal correction to Gibbs Free Energy=0.158645
Sum of electronic and zero-point Energies=-812.849443
Sum of electronic and thermal Energies=-812.831756
Sum of electronic and thermal Enthalpies=-812.830812
Sum of electronic and thermal Free Energies=-812.900621

4-acetoxystyrene endo complex (3y.PdCH$_2$N$_2$-endo)

H	-4.939443	0.952827	0.191252
N	-3.563485	2.420233	0.092077
C	-3.969917	1.235609	0.604442
H	-3.897652	1.244871	1.693475
N	-3.211418	3.401844	-0.346494
C	-1.803051	-1.998070	-1.141134
C	-1.029865	-1.864322	0.007611
C	0.294045	-1.215074	0.113757
C	1.026574	-1.351659	1.305456
C	2.288149	-0.780945	1.451255
C	2.841486	-0.058792	0.396748
C	2.138850	0.103032	-0.800398
C	0.880043	-0.474472	-0.929962
H	-2.585872	-2.750696	-1.175715
H	-1.463808	-1.633307	-2.106845
H	-1.282615	-2.495634	0.859057
H	0.600410	-1.917793	2.129607
H	2.850593	-0.886392	2.373222
O	4.075323	0.543293	0.653008
H	2.573571	0.660703	-1.619109
H	0.339704	-0.337851	-1.861159
Pd	-2.632571	-0.339204	-0.002677
C	5.072289	0.566873	-0.285585
O	4.985610	0.095039	-1.392546
C	6.281489	1.267978	0.284290
H	6.628076	0.748482	1.182447
H	6.018730	2.288173	0.579334
H	7.072890	1.287842	-0.464072

E(RB3LYP) = -813.059238577 A.U.
Zero-point correction=0.209841 (Hartree/Particle)

Thermal correction to Energy=0.227512
Thermal correction to Enthalpy=0.228456
Thermal correction to Gibbs Free Energy=0.158805
Sum of electronic and zero-point Energies=-812.849397
Sum of electronic and thermal Energies=-812.831727
Sum of electronic and thermal Enthalpies=-812.830782
Sum of electronic and thermal Free Energies=-812.900434

3-trifluoromethylstyrene exo complex (3z.PdCH$_2$N$_2$-exo)

C	-1.075212	0.827698	2.059077
C	-0.626240	1.548097	0.956346
C	0.660196	1.362657	0.249767
C	1.061852	2.317933	-0.700148
C	2.272815	2.198648	-1.381070
C	3.115232	1.118062	-1.131574
C	2.728134	0.159416	-0.187656
C	1.520362	0.277577	0.494786
H	-1.865835	1.236429	2.681603
H	-0.469776	0.053902	2.523494
H	-1.125665	2.488533	0.728005
H	0.413835	3.167499	-0.900032
H	2.561894	2.954198	-2.105594
H	4.062009	1.018403	-1.650744
H	1.246584	-0.481005	1.218787
Pd	-2.043586	-0.013355	0.305658
C	-3.193994	-1.379915	-0.903734
N	-4.481994	-0.972808	-0.986939
H	-3.128233	-2.331434	-0.373580
H	-2.718792	-1.346931	-1.885623
N	-5.553979	-0.617389	-1.043581
C	3.596673	-1.047980	0.039857
F	4.909111	-0.761983	-0.117497
F	3.307940	-2.041647	-0.835253
F	3.440933	-1.563818	1.279769

E(RB3LYP) = -922.217619873 A.U.
Zero-point correction=0.173175 (Hartree/Particle)
Thermal correction to Energy=0.189665
Thermal correction to Enthalpy=0.190610
Thermal correction to Gibbs Free Energy=0.123779
Sum of electronic and zero-point Energies=-922.044444
Sum of electronic and thermal Energies=-922.027954
Sum of electronic and thermal Enthalpies=-922.027010
Sum of electronic and thermal Free Energies=-922.093841

3-trifluoromethylstyrene endo complex (3z.PdCH$_2$N$_2$-endo)

C	1.855213	-2.110706	1.012767
C	0.985410	-1.915970	-0.056162
C	-0.343308	-1.269929	-0.006013
C	-1.144292	-1.272202	-1.162092
C	-2.409792	-0.692812	-1.169385
C	-2.909643	-0.099012	-0.008871
C	-2.130690	-0.091808	1.154644
C	-0.867772	-0.669280	1.155183
H	2.642433	-2.855249	0.933835
H	1.599863	-1.808903	2.024773
H	1.166843	-2.488023	-0.965361
H	-0.765668	-1.739875	-2.067081
H	-3.014058	-0.710904	-2.070043
H	-0.280502	-0.653216	2.067332
Pd	2.557620	-0.370180	-0.079709
C	3.835608	1.263392	-0.674180
N	3.458554	2.409308	-0.059720
H	3.692122	1.344492	-1.753057
H	4.833394	0.966507	-0.347207
N	3.128838	3.354651	0.465373
H	-2.522682	0.358869	2.060506
C	-4.249486	0.578696	-0.015275
F	-4.877662	0.463119	1.177642
F	-5.073208	0.068814	-0.958794
F	-4.142628	1.906364	-0.267773

E(RB3LYP) = -922.217856673 A.U.
Zero-point correction=0.173181 (Hartree/Particle)
Thermal correction to Energy=0.189668
Thermal correction to Enthalpy=0.190612
Thermal correction to Gibbs Free Energy=0.123794
Sum of electronic and zero-point Energies=-922.044676
Sum of electronic and thermal Energies=-922.028189
Sum of electronic and thermal Enthalpies=-922.027245
Sum of electronic and thermal Free Energies=-922.094063

6.4 Transition states for nitrogen extrusion

4-trifluoromethylstyrene exo TS (3t.PdCH$_2$-N$_2$-exoTS)

C	1.623780	2.316936	-0.279143
C	0.841668	1.647919	0.646654
C	-0.490308	1.051036	0.413340
C	-1.197662	0.522855	1.507321

C	-2.463042	-0.035104	1.349864
C	-3.051971	-0.076174	0.084727
C	-2.364175	0.446383	-1.016919
C	-1.101293	1.000968	-0.853963
H	2.447041	2.939962	0.057958
H	1.299136	2.481771	-1.302024
H	1.114237	1.734492	1.697700
H	-0.744099	0.549382	2.494430
H	-2.990818	-0.442989	2.205184
C	-4.441148	-0.620538	-0.090806
H	-0.580216	1.391532	-1.721664
Pd	2.412072	0.254282	-0.151401
C	3.257547	-1.426848	-0.817221
N	4.840101	-1.798521	0.092574
H	3.750140	-1.479354	-1.795343
H	2.837348	-2.415331	-0.596327
N	5.676704	-1.673167	0.813756
H	-2.818430	0.408347	-2.001449
F	-4.753877	-1.529901	0.859379
F	-4.599034	-1.219062	-1.293687
F	-5.376831	0.357009	-0.019186

E(RB3LYP) = -922.194605704 A.U.
Zero-point correction=0.170739 (Hartree/Particle)
Thermal correction to Energy=0.187524
Thermal correction to Enthalpy=0.188468
Thermal correction to Gibbs Free Energy=0.120880
Sum of electronic and zero-point Energies=-922.023867
Sum of electronic and thermal Energies=-922.007082
Sum of electronic and thermal Enthalpies=-922.006138
Sum of electronic and thermal Free Energies=-922.073726

Imaginary vibration: -378.2428 cm^{-1}

4-trifluoromethylstyrene endo TS (3t.PdCH$_2$-N$_2$-endoTS)

C	1.817956	-2.177528	0.982756
C	0.952509	-1.966914	-0.077685
C	-0.366853	-1.303651	-0.020367
C	-1.150458	-1.250617	-1.187124
C	-2.406617	-0.652293	-1.188777
C	-2.912144	-0.092991	-0.013225
C	-2.149632	-0.139093	1.159405
C	-0.895714	-0.737020	1.155263
H	2.629149	-2.891810	0.885206
H	1.572449	-1.882570	1.998929

H	1.148029	-2.498197	-1.007364
H	-0.765386	-1.688956	-2.103784
H	-2.999225	-0.627914	-2.096952
H	-0.322699	-0.765655	2.076115
Pd	2.525024	-0.363354	-0.063609
C	3.951581	0.902728	-0.654054
N	3.622949	2.635209	-0.073631
H	4.045741	1.213506	-1.701643
H	4.955043	0.889475	-0.213156
N	3.104320	3.475683	0.437028
H	-2.546817	0.284870	2.075632
C	-4.242859	0.604348	-0.014313
F	-4.874070	0.484939	1.176126
F	-5.070959	0.114776	-0.964431
F	-4.115515	1.931783	-0.254142

E(RB3LYP) = -922.194684573 A.U.
Zero-point correction=0.170765 (Hartree/Particle)
Thermal correction to Energy=0.187548
Thermal correction to Enthalpy=0.188493
Thermal correction to Gibbs Free Energy=0.120826
Sum of electronic and zero-point Energies=-922.023919
Sum of electronic and thermal Energies=-922.007136
Sum of electronic and thermal Enthalpies=-922.006192
Sum of electronic and thermal Free Energies=-922.073858

Imaginary vibration: -387.6309 cm^{-1}

4-methoxystyrene exo TS (3u.PdCH$_2$-N$_2$-exoTS)

C	0.976337	2.312552	0.098396
C	0.174573	1.459262	0.835700
C	-1.114177	0.869342	0.425250
C	-1.872720	0.160436	1.366772
C	-3.110408	-0.403051	1.050064
C	-3.619629	-0.260842	-0.244697
C	-2.875477	0.446340	-1.204508
C	-1.649018	0.997902	-0.873621
H	1.751839	2.889673	0.593752
H	0.700535	2.651051	-0.895776
H	0.390945	1.359416	1.898981
H	-1.487673	0.044532	2.376950
H	-3.660480	-0.941572	1.812657
H	-1.091855	1.532900	-1.636281
Pd	1.876937	0.293418	-0.097306
C	2.798491	-1.247673	-0.961401

N	4.322982	-1.737119	-0.046000
H	3.337563	-1.131840	-1.909598
H	2.384517	-2.262873	-0.931203
N	5.110521	-1.712643	0.739888
H	-3.285977	0.546437	-2.204125
O	-4.814259	-0.761924	-0.673483
C	-5.608685	-1.485519	0.252057
H	-6.504999	-1.788804	-0.291333
H	-5.899837	-0.864402	1.109170
H	-5.089827	-2.380502	0.619440

E(RB3LYP) = -699.684505019 A.U.
Zero-point correction=0.198689 (Hartree/Particle)
Thermal correction to Energy=0.214375
Thermal correction to Enthalpy=0.215319
Thermal correction to Gibbs Free Energy=0.152036
Sum of electronic and zero-point Energies=-699.485816
Sum of electronic and thermal Energies=-699.470130
Sum of electronic and thermal Enthalpies=-699.469186
Sum of electronic and thermal Free Energies=-699.532469

Imaginary vibration: -395.9559 cm^{-1}

4-methoxystyrene endo TS (3u.PdCH$_2$-N$_2$-endoTS)

C	1.132617	-2.265543	0.778188
C	0.247930	-1.858089	-0.205606
C	-1.001673	-1.097034	-0.016210
C	-1.835733	-0.865344	-1.119475
C	-3.039774	-0.168397	-1.006226
C	-3.437769	0.319341	0.243123
C	-2.617950	0.097721	1.362581
C	-1.425939	-0.595527	1.232493
H	1.870240	-3.030863	0.559114
H	0.955002	-2.071600	1.832250
H	0.362584	-2.291016	-1.198049
H	-1.537093	-1.240513	-2.095248
H	-3.650937	-0.015833	-1.887910
H	-0.811613	-0.749412	2.114085
Pd	1.982922	-0.412440	-0.095830
C	3.485642	0.759726	-0.682286
N	3.352897	2.464764	-0.020952
H	3.569647	1.101643	-1.721180
H	4.500293	0.621521	-0.290091
N	2.925927	3.315424	0.556548
H	-2.942905	0.481923	2.324088

O -4.589021   1.011731   0.480259
C -5.454781   1.268611   -0.613442
H -6.298909   1.826993   -0.205727
H -5.822921   0.338841   -1.066405
H -4.962789   1.872626   -1.386836

E(RB3LYP) = -699.684676886   A.U.
Zero-point correction=0.198676 (Hartree/Particle)
Thermal correction to Energy=0.214393
Thermal correction to Enthalpy=0.215338
Thermal correction to Gibbs Free Energy=0.151734
Sum of electronic and zero-point Energies=-699.486001
Sum of electronic and thermal Energies=-699.470284
Sum of electronic and thermal Enthalpies=-699.469339
Sum of electronic and thermal Free Energies=-699.532943

Imaginary vibration: -406.8262 cm^{-1}

3-nitrostyrene exo TS (3v.PdCH$_2$-N$_2$-exoTS)

C -0.722037   0.446064   2.166204
C -0.240882   1.293901   1.183255
C   1.011765   1.130898   0.414621
C   1.418227   2.155844   -0.459330
C   2.598740   2.061346   -1.196896
C   3.413153   0.938035   -1.081969
C   3.006229   -0.073438   -0.211280
C   1.835273   -0.000460   0.532084
H -1.494453   0.791816   2.846849
H -0.185192   -0.444345   2.479613
H -0.692838   2.280959   1.096214
H   0.793975   3.039652   -0.559769
H   2.885751   2.868779   -1.863252
H   4.335740   0.830343   -1.637300
H   1.581260   -0.826041   1.183779
Pd -1.808551   -0.050814   0.308531
C -2.745724   -1.255430   -0.978821
N -4.521535   -0.736382   -1.228764
H -3.032505   -2.278051   -0.707194
H -2.535893   -1.236914   -2.054923
N -5.458826   -0.151188   -1.109823
N   3.855101   -1.270892   -0.072379
O   4.889015   -1.316718   -0.738256
O   3.481715   -2.153289   0.699894

E(RB3LYP) = -789.657748977   A.U.
Zero-point correction=0.168630 (Hartree/Particle)

Thermal correction to Energy=0.184290
Thermal correction to Enthalpy=0.185234
Thermal correction to Gibbs Free Energy=0.120797
Sum of electronic and zero-point Energies=-789.489119
Sum of electronic and thermal Energies=-789.473459
Sum of electronic and thermal Enthalpies=-789.472515
Sum of electronic and thermal Free Energies=-789.536952

Imaginary vibration: -375.1335 cm^{-1}

3-nitrostyrene endo TS (3v.PdCH_2-N_2-endoTS)

C	-0.870954	-1.546420	-1.747571
C	-0.314081	-1.886627	-0.526128
C	0.919692	-1.324783	0.063605
C	1.397922	-1.849155	1.279363
C	2.562255	-1.365522	1.875843
C	3.288721	-0.340644	1.274836
C	2.811597	0.173285	0.069029
C	1.655394	-0.293680	-0.543332
H	-1.615900	-2.192855	-2.200211
H	-0.410264	-0.823199	-2.414357
H	-0.680725	-2.782460	-0.028808
H	0.841846	-2.649200	1.760610
H	2.905990	-1.790922	2.813512
H	4.196387	0.058655	1.708309
H	1.347924	0.155131	-1.478733
Pd	-1.965187	-0.401826	-0.208882
C	-3.591147	0.525181	0.487909
N	-3.255985	2.323580	0.840500
H	-4.443640	0.760049	-0.159712
H	-3.973405	0.344301	1.499796
N	-2.695780	3.280790	0.911467
N	3.566840	1.256624	-0.586908
O	4.589361	1.655932	-0.030817
O	3.131701	1.697532	-1.650255

E(RB3LYP) = -789.657732878 A.U.
Zero-point correction=0.168635 (Hartree/Particle)
Thermal correction to Energy=0.184305
Thermal correction to Enthalpy=0.185249
Thermal correction to Gibbs Free Energy=0.120698
Sum of electronic and zero-point Energies=-789.489098
Sum of electronic and thermal Energies=-789.473428
Sum of electronic and thermal Enthalpies=-789.472484
Sum of electronic and thermal Free Energies=-789.537035

Imaginary vibration: -381.5341 cm^{-1}

4-(dimethylamino)styrene endo TS (3w.PdCH$_2$-N$_2$-endoTS)

C	1.503535	-2.188119	0.970297
C	0.651577	-1.920472	-0.088305
C	-0.640467	-1.216294	-0.034199
C	-1.426040	-1.120173	-1.195275
C	-2.661563	-0.485686	-1.205096
C	-3.182275	0.107630	-0.032489
C	-2.400882	0.000697	1.143771
C	-1.169588	-0.638001	1.134101
H	2.291143	-2.926148	0.857557
H	1.258032	-1.914274	1.992560
H	0.846015	-2.428391	-1.031776
H	-1.058761	-1.562608	-2.118433
H	-3.221879	-0.455371	-2.131433
H	-0.608872	-0.689029	2.062726
Pd	2.304793	-0.368602	-0.017091
C	3.793082	0.810010	-0.625290
N	3.541884	2.561994	-0.189513
H	3.943756	1.025982	-1.690298
H	4.779765	0.765488	-0.148743
N	3.028869	3.446091	0.253694
H	-2.757839	0.418801	2.076896
N	-4.401215	0.772406	-0.033732
C	-5.260983	0.683258	-1.201167
H	-6.155735	1.284853	-1.033436
H	-5.577050	-0.348110	-1.423867
H	-4.759617	1.080987	-2.090976
C	-4.992270	1.185565	1.227429
H	-4.331704	1.875562	1.764750
H	-5.213809	0.339075	1.896386
H	-5.925440	1.714921	1.028489

E(RB3LYP) = -719.132656925 A.U.
Zero-point correction=0.239098 (Hartree/Particle)
Thermal correction to Energy=0.256678
Thermal correction to Enthalpy=0.257622
Thermal correction to Gibbs Free Energy=0.189578
Sum of electronic and zero-point Energies=-718.893559
Sum of electronic and thermal Energies=-718.875979
Sum of electronic and thermal Enthalpies=-718.875035
Sum of electronic and thermal Free Energies=-718.943079

Imaginary vibration: -416.0277 cm^{-1}

3-methoxystyrene exo TS (3x.PdCH$_2$-N$_2$-exoTS)

C	-0.608454	-1.216875	-1.879181
C	-0.074921	-1.578391	-0.655323
C	1.180104	-1.082479	-0.048681
C	1.610030	-1.645769	1.168804
C	2.793277	-1.219999	1.761214
C	3.582239	-0.230934	1.167096
C	3.162352	0.330982	-0.046214
C	1.972814	-0.095124	-0.645628
H	-1.377364	-1.831522	-2.338319
H	-0.116790	-0.507643	-2.538016
H	-0.489909	-2.456558	-0.162054
H	1.008593	-2.416109	1.643100
H	3.115810	-1.661243	2.700214
H	4.501157	0.085979	1.645338
O	3.845666	1.300699	-0.726000
H	1.686462	0.369181	-1.582853
Pd	-1.704400	-0.052135	-0.343180
C	5.059761	1.779165	-0.172960
H	5.430072	2.536003	-0.866489
H	5.807467	0.980522	-0.079776
H	4.905024	2.239332	0.811842
C	-2.650202	1.516470	0.443828
N	-4.374763	1.098308	0.960788
H	-2.981695	2.357521	-0.177011
H	-2.388094	1.910448	1.433237
N	-5.286046	0.479465	1.117400

E(RB3LYP) = -699.683940773
Zero-point correction=0.198573 (Hartree/Particle)
Thermal correction to Energy=0.214297
Thermal correction to Enthalpy=0.215241
Thermal correction to Gibbs Free Energy=0.151609
Sum of electronic and zero-point Energies=-699.485368
Sum of electronic and thermal Energies=-699.469644
Sum of electronic and thermal Enthalpies=-699.468700
Sum of electronic and thermal Free Energies=-699.532332

Imaginary vibration: -391.6498 cm^{-1}

3-methoxystyrene endo TS (3x.PdCH$_2$-N$_2$-endoTS)

C	-0.748909	-1.793789	-1.528518
C	-0.137866	-1.888593	-0.290491
C	1.092633	-1.193957	0.146624

C	1.607022	-1.472891	1.428571
C	2.768200	-0.850201	1.870788
C	3.451901	0.061041	1.060627
C	2.948244	0.341032	-0.216761
C	1.780325	-0.284022	-0.665961
H	-1.486826	-2.531745	-1.826481
H	-0.338155	-1.188187	-2.331357
H	-0.461900	-2.686215	0.375645
H	1.087831	-2.179010	2.070280
H	3.156322	-1.072825	2.860853
H	4.355312	0.535066	1.424721
O	3.526145	1.207485	-1.102123
H	1.428351	-0.036916	-1.661484
Pd	-1.838529	-0.416805	-0.176037
C	4.711233	1.878142	-0.708231
H	4.995229	2.509870	-1.551500
H	5.526269	1.173627	-0.496219
H	4.546697	2.509583	0.174721
C	-3.485297	0.512817	0.459317
N	-3.268585	2.336007	0.558695
H	-4.376670	0.594342	-0.173823
H	-3.817798	0.433618	1.501619
N	-2.756616	3.320343	0.471578

E(RB3LYP) = -699.684083866 A.U.
Zero-point correction=0.198538 (Hartree/Particle)
Thermal correction to Energy=0.214291
Thermal correction to Enthalpy=0.215235
Thermal correction to Gibbs Free Energy=0.151322
Sum of electronic and zero-point Energies=-699.485545
Sum of electronic and thermal Energies=-699.469793
Sum of electronic and thermal Enthalpies=-699.468849
Sum of electronic and thermal Free Energies=-699.532762

Imaginary vibration: -402.8060 cm^{-1}

4-acetoxystyrene exo TS (3y.PdCH_2-N_2-exoTS)

C	1.598329	2.272593	-0.281170
C	0.890348	1.588217	0.690824
C	-0.436292	0.954025	0.544946
C	-1.070734	0.434634	1.686126
C	-2.330373	-0.152531	1.609796
C	-2.979420	-0.229017	0.379493
C	-2.375096	0.272440	-0.776566
C	-1.116654	0.857657	-0.682689

H	2.423506	2.918546	0.004429
H	1.209490	2.422443	-1.283782
H	1.224957	1.688043	1.722824
H	-0.568297	0.493235	2.647994
H	-2.817948	-0.555519	2.491352
O	-4.203314	-0.899648	0.380354
H	-2.884666	0.216589	-1.729021
H	-0.653920	1.240048	-1.586711
Pd	2.465972	0.234575	-0.188743
C	-5.267738	-0.457983	-0.360958
O	-5.253126	0.518246	-1.069344
C	-6.444272	-1.378587	-0.146989
H	-6.710558	-1.408096	0.913601
H	-6.180954	-2.397827	-0.444938
H	-7.290478	-1.024777	-0.734765
H	2.909609	-2.434116	-0.602749
N	5.809539	-1.613001	0.611890
N	4.934471	-1.771679	-0.056246
C	3.301740	-1.444347	-0.866072
H	3.728965	-1.507667	-1.874097

E(RB3LYP) = -813.036453689 A.U.
Zero-point correction=0.207448 (Hartree/Particle)
Thermal correction to Energy=0.225392
Thermal correction to Enthalpy=0.226336
Thermal correction to Gibbs Free Energy=0.155890
Sum of electronic and zero-point Energies=-812.829005
Sum of electronic and thermal Energies=-812.811062
Sum of electronic and thermal Enthalpies=-812.810118
Sum of electronic and thermal Free Energies=-812.880564

Imaginary vibration: -388.3491 cm^{-1}

4-acetoxystyrene endo TS (3y.PdCH$_2$-N$_2$-endoTS)

H	-5.044616	0.885198	-0.004298
N	-3.743657	2.648509	0.074471
C	-4.080653	0.892099	0.517964
H	-4.269282	1.131600	1.571627
N	-3.193084	3.519787	-0.344899
C	-1.774627	-2.108421	-1.048824
C	-1.002139	-1.917878	0.083982
C	0.312970	-1.249079	0.158198
C	1.011312	-1.256662	1.378347
C	2.262068	-0.659661	1.500349
C	2.839035	-0.038861	0.393981

C	2.170303	-0.006622	-0.832669
C	0.921549	-0.611023	-0.938564
H	-2.585490	-2.829634	-1.035178
H	-1.447177	-1.788620	-2.033920
H	-1.272856	-2.473424	0.980243
H	0.565455	-1.740355	2.243375
H	2.798783	-0.664993	2.443303
O	4.058820	0.596711	0.627686
H	2.623326	0.469945	-1.691230
H	0.411873	-0.579772	-1.896148
Pd	-2.595895	-0.326319	-0.021575
C	5.073769	0.579799	-0.292627
O	5.016809	0.037249	-1.368563
C	6.258382	1.338228	0.254113
H	6.594242	0.885522	1.191605
H	5.972194	2.370731	0.475411
H	7.065052	1.323225	-0.477850

E(RB3LYP) = -813.036594312 A.U.
Zero-point correction=0.207462 (Hartree/Particle)
Thermal correction to Energy=0.225410
Thermal correction to Enthalpy=0.226355
Thermal correction to Gibbs Free Energy=0.155732
Sum of electronic and zero-point Energies=-812.829132
Sum of electronic and thermal Energies=-812.811184
Sum of electronic and thermal Enthalpies=-812.810240
Sum of electronic and thermal Free Energies=-812.880862

Imaginary vibration: -399.1078 cm^{-1}

3-trifluoromethylstyrene exo TS (3z.PdCH_2-N_2-exoTS)

C	-1.029454	0.882819	2.077972
C	-0.590713	1.578063	0.964412
C	0.676526	1.367685	0.231990
C	1.048920	2.287295	-0.763023
C	2.243453	2.145696	-1.468116
C	3.095800	1.078409	-1.196497
C	2.736817	0.155461	-0.207072
C	1.545485	0.295718	0.499363
H	-1.830693	1.289322	2.688139
H	-0.439908	0.097039	2.540285
H	-1.103739	2.504611	0.710077
H	0.391638	3.125212	-0.980521
H	2.511533	2.872773	-2.228761
H	4.030495	0.962279	-1.733987

H	1.293670	-0.434663	1.259263
Pd	-2.064997	0.003138	0.333064
C	-2.898662	-1.449329	-0.752007
N	-4.691196	-1.095957	-1.105681
H	-3.125297	-2.431957	-0.321602
H	-2.662626	-1.591581	-1.813392
N	-5.663562	-0.557067	-1.094611
C	3.620628	-1.035980	0.046658
F	4.928899	-0.734609	-0.117008
F	3.345776	-2.050807	-0.807269
F	3.471471	-1.525833	1.297558

E(RB3LYP) = -922.194396729 A.U.
Zero-point correction=0.170756 (Hartree/Particle)
Thermal correction to Energy=0.187524
Thermal correction to Enthalpy=0.188468
Thermal correction to Gibbs Free Energy=0.120944
Sum of electronic and zero-point Energies=-922.023640
Sum of electronic and thermal Energies=-922.006873
Sum of electronic and thermal Enthalpies=-922.005928
Sum of electronic and thermal Free Energies=-922.073453

Imaginary vibration: -381.0000 cm^{-1}

3-trifluoromethylstyrene endo TS (3z.PdCH$_2$-N$_2$-endoTS)

C	-1.180781	-1.575279	-1.757478
C	-0.687182	-1.961214	-0.522725
C	0.567654	-1.501176	0.108900
C	0.977905	-2.089153	1.317915
C	2.161611	-1.703458	1.945186
C	2.966152	-0.717190	1.379660
C	2.569641	-0.123584	0.175539
C	1.389055	-0.508225	-0.453681
H	-1.961764	-2.159405	-2.233504
H	-0.645760	-0.889392	-2.408069
H	-1.140308	-2.826128	-0.041807
H	0.357960	-2.861133	1.766279
H	2.459216	-2.177341	2.875742
H	3.893033	-0.415129	1.854988
H	1.112361	-0.033527	-1.387632
Pd	-2.227878	-0.349135	-0.244989
C	-3.798637	0.679452	0.433332
N	-3.352098	2.433335	0.839029
H	-4.616953	0.985394	-0.228752
H	-4.219258	0.497621	1.429797

N	-2.722949	3.343790	0.946191
C	3.406438	0.982298	-0.409586
F	3.190071	1.142269	-1.733942
F	4.728490	0.752269	-0.240171
F	3.141220	2.172634	0.178952

E(RB3LYP) = -922.194488089 A.U.
Zero-point correction=0.170843 (Hartree/Particle)
Thermal correction to Energy=0.187580
Thermal correction to Enthalpy=0.188524
Thermal correction to Gibbs Free Energy=0.121295
Sum of electronic and zero-point Energies=-922.023645
Sum of electronic and thermal Energies=-922.006908
Sum of electronic and thermal Enthalpies=-922.005964
Sum of electronic and thermal Free Energies=-922.073193

Imaginary vibration: -388.6555 cm^{-1}

6.5 (Styrene)palladium methylidene complexes

(4-methoxystyrene)palladium methylidene (3u.PdCH$_2$)

C	1.995391	1.847070	-0.253246
C	0.990921	1.499759	0.631936
C	-0.342256	0.997997	0.279894
C	-1.199383	0.545739	1.303012
C	-2.472091	0.049068	1.034522
C	-2.922963	-0.015457	-0.291010
C	-2.083410	0.421477	-1.329958
C	-0.820316	0.914494	-1.050997
H	2.909511	2.293048	0.121503
H	1.827423	1.945530	-1.320720
H	1.169656	1.643460	1.695406
H	-0.858600	0.593980	2.333904
H	-3.097091	-0.283455	1.854564
H	-0.198527	1.257020	-1.871327
Pd	2.009127	-0.408434	0.028506
C	3.431621	-1.651138	-0.241357
H	3.945502	-2.175731	0.578228
H	4.049367	-1.749388	-1.145577
H	-2.450698	0.362502	-2.349110
O	-4.142920	-0.478366	-0.673806
C	-5.033284	-0.949447	0.327935
H	-5.932868	-1.272105	-0.197832
H	-5.295755	-0.156850	1.039997
H	-4.609774	-1.800500	0.875732

E(RB3LYP) = -590.176129290 A.U.
Zero-point correction=0.190574 (Hartree/Particle)
Thermal correction to Energy=0.203788
Thermal correction to Enthalpy=0.204732
Thermal correction to Gibbs Free Energy=0.148863
Sum of electronic and zero-point Energies=-589.985555
Sum of electronic and thermal Energies=-589.972341
Sum of electronic and thermal Enthalpies=-589.971397
Sum of electronic and thermal Free Energies=-590.027266

(3-nitrostyrene)palladium methylidene (3v.PdCH$_2$)

C	-1.615414	-0.046732	1.902556
C	-1.023540	1.038587	1.278156
C	0.301172	1.048366	0.639981
C	0.736046	2.214598	-0.028404
C	1.972636	2.269329	-0.666568
C	2.816846	1.159442	-0.666236
C	2.381490	0.008003	-0.012813
C	1.153933	-0.073440	0.633149
H	-2.541684	0.090175	2.448975
H	-1.076462	-0.964357	2.116123
H	-1.530577	1.999735	1.315247
H	0.088174	3.086718	-0.035652
H	2.282380	3.180764	-1.167791
H	3.784027	1.167086	-1.151928
H	0.890236	-0.997781	1.129742
Pd	-2.040904	-0.202023	-0.299632
C	-3.473036	-1.142504	-1.149249
H	-3.788530	-2.172976	-0.934794
H	-4.276496	-0.648947	-1.715843
N	3.264273	-1.174430	0.003654
O	4.347092	-1.082745	-0.572231
O	2.865387	-2.177288	0.593477

E(RB3LYP) = -680.146167972 A.U.
Zero-point correction=0.160407 (Hartree/Particle)
Thermal correction to Energy=0.173599
Thermal correction to Enthalpy=0.174543
Thermal correction to Gibbs Free Energy=0.117584
Sum of electronic and zero-point Energies=-679.985761
Sum of electronic and thermal Energies=-679.972569
Sum of electronic and thermal Enthalpies=-679.971625
Sum of electronic and thermal Free Energies=-680.028584

(4-acetoxystyrene)palladium methylidene (3y.PdCH$_2$)

C	2.533659	1.526145	-1.051461
C	1.690355	1.612471	0.042285
C	0.313275	1.108088	0.117843
C	-0.380381	1.189767	1.345188
C	-1.677516	0.712389	1.472314
C	-2.312311	0.129963	0.372854
C	-1.651938	0.015849	-0.853144
C	-0.353215	0.502491	-0.970500
H	3.497885	2.020799	-1.024422
H	2.187547	1.225899	-2.035218
H	2.041700	2.143624	0.924097
H	0.109895	1.642889	2.202315
H	-2.210918	0.777028	2.414748
O	-3.581535	-0.380880	0.624145
H	-2.146981	-0.430512	-1.704011
H	0.143102	0.423015	-1.931641
Pd	2.602151	-0.441251	0.067730
C	-4.585294	-0.351267	-0.312053
O	-4.476350	0.116875	-1.417890
C	-5.825033	-0.987571	0.264629
H	-6.125604	-0.467136	1.178476
H	-5.619012	-2.027643	0.534735
H	-6.626894	-0.945773	-0.471479
H	4.613691	-1.973072	0.950380
C	3.986028	-1.756088	0.073078
H	4.473949	-2.192952	-0.809801

E(RB3LYP) = -703.527153352 A.U.
Zero-point correction=0.199294 (Hartree/Particle)
Thermal correction to Energy=0.214748
Thermal correction to Enthalpy=0.215693
Thermal correction to Gibbs Free Energy=0.152760
Sum of electronic and zero-point Energies=-703.327859
Sum of electronic and thermal Energies=-703.312405
Sum of electronic and thermal Enthalpies=-703.311461
Sum of electronic and thermal Free Energies=-703.374393

(3-trifluoromethylstyrene)palladium methylidene (3z.PdCH$_2$)

C	-1.881108	0.091852	1.930437
C	-1.377701	1.165596	1.216498
C	-0.060028	1.231575	0.568014
C	0.269916	2.369026	-0.200579
C	1.495487	2.467838	-0.850897

```
C   2.424291    1.429783   -0.763820
C   2.109414    0.292419   -0.015382
C   0.885816    0.188597    0.644050
H  -2.823166    0.193894    2.457043
H  -1.269188   -0.754715    2.224689
H  -1.968142    2.077462    1.166926
H  -0.448234    3.181256   -0.272648
H   1.731241    3.356919   -1.427540
H   3.383998    1.501091   -1.262997
H   0.681025   -0.695359    1.236406
Pd -2.239699   -0.292238   -0.263855
C  -3.560544   -1.413663   -1.069869
H  -3.794010   -2.450841   -0.791459
H  -4.388101   -1.031145   -1.685770
C   3.075626   -0.862034    0.040312
F   4.352877   -0.457309   -0.134650
F   2.815139   -1.775030   -0.922547
F   3.013509   -1.512275    1.223875

E(RB3LYP) =  -812.683800221     A.U.
Zero-point correction=0.162614 (Hartree/Particle)
Thermal correction to Energy=0.176868
Thermal correction to Enthalpy=0.177812
Thermal correction to Gibbs Free Energy=0.118141
Sum of electronic and zero-point Energies=-812.521186
Sum of electronic and thermal Energies=-812.506932
Sum of electronic and thermal Enthalpies=-812.505988
Sum of electronic and thermal Free Energies=-812.565659
```